Sustainable Cellulose Solubilization, Regeneration and Derivatization in a DBU-CO$_2$ Switchable Solvent System

M.Sc. Kelechukwu Nnabuike Onwukamike

February 2019

This thesis was performed as a co-tutelle project between Karlsruhe Institute of Technology, Germany and University of Bordeaux, France.

Supervisors:

Prof. Dr. M.A.R Meier (Karlsruhe Institute of Technology, Germany)

Prof. H. Cramail (University of Bordeaux, France)

Prof. S. Grelier (University of Bordeaux, France)

Dr. E. Grau (University of Bordeaux, France)

Sustainable Cellulose Solubilization, Regeneration and Derivatization in a DBU-CO$_2$ Switchable Solvent System

Zur Erlangung des akademischen Grades eines

DOKTORS DER NATURWISSENSCHAFTEN

(Dr. rer. nat.)

KIT-Fakultät für Chemie und Biowissenschaften

Karlsruher Institut für Technologie (KIT)

genehmigte

DISSERTATION

von

M.Sc. Kelechukwu Nnabuike Onwukamike

aus

Enugu, Nigeria

Dekan: Prof. Dr. Reinhard Fischer

Referent: Prof. Dr. Michael. A. R. Meier

Korreferent: Dr. François Jérôme

Tag der mündlichen Prüfung: 4th Feb. 2019

My darling wife Nneka and our Lovely sons

Chukwuemerie and Chukwuebuka.

Hiermit erkläre ich wahrheitsgemäß, dass ich die vorliegende Arbeit selbstständig angefertigt und keine anderen als die angegebenen Quellen und Hilfsmittel benutzt sowie die wörtlich oder inhaltlich übernommenen Stellen als solche kenntlich gemacht und die Satzung des Karlsruher Instituts für Technologie (KIT) zur Sicherung guter wissenschaftlicher Praxis in der jeweils gültigen Fassung beachtet habe. Des Weiteren erkläre ich, dass ich mich derzeit in keinem laufenden Promotionsverfahren befinde, und auch keine vorausgegangenen Promotionsversuche unternommen habe.

---------------------------   -------------------------------

    Ort, Datum   Unterschrift

Acknowledgement

It is said that a journey of a thousand miles start with a single step, so was my PhD research journey. As this episode in my life gradually comes to an end I will like to acknowledge all those that made this journey successful in one way or another.

Without the funding of the European Union, this project would not have been possible, for this I am very grateful to them.

Next, I will like to appreciate the immeasurable contribution of my supervisors: Mike, Henri, Stéphane and Etienne. Without their constant willingness to listen and guide me when necessary, this work would not have been successfully completed. In this regard I thank Mike immensely for his time, attention, guidance, and encouragement. I remember walking up to his office after six months of starting my PhD with a broken spirit as I had just discovered the presumed successful modification on cellulose was merely a co-precipitated side-product! He said „Kenny a failed reaction is not a failed life, you have time and it is good we noticed this now and not latter ". I did not only leave his office more cheerful but even more determined, the outcome was a series of publications within the next two years! Mike gave me every possible opportunity and was keen to listen to every suggestion I had at all times. His promptness at responding to emails despite his very tight schedule is worth mentioning. Mike, I am very grateful...Danke Schön. I am equally very grateful to Henri; I also owe the success of this project to him. I remember sitting in his office just after I was accepted into the program, despite his very tight schedule (then as the director of LCPO), he advised me on how best to go about the PhD program. As a student who always aim to make straight A's in my courses, without being familiar to failure per say, his advice that being a good student does not translate to being a good researcher, because a good researcher will not quit over failed reactions but will rather exploit all possible alternatives. This advice has stayed with me ever since and am thankful for that. Etienne gave me all the support especially in setting up the CO_2 reactors, working with high pressure CO_2 and many other technical aspects of my project. I am thankful to Stéphane for his assistance especially with new possible modification routes for cellulose. In all, I was indeed the most „luckiest" doctoral student for being blessed with four amazing supervisors ☺

Abstract

As the most abundant source of carbon in our planet, without any competition with food or feed supplies, cellulose is a viable alternative to replace the widely used and unsustainable fossil-based polymers. However, the majority of researchers working on this fascinating biopolymer fail to incorporate sustainability considerations during cellulose chemical transformation to make materials. The consequence is a shift of the "environmental burden" to other stages of the process cycle. Therefore, to ensure sustainability, both the renewability feature of cellulose as well as sustainability considerations concerning its transformation processes are necessary. This implies to consider the solvent, the reactants, the derivatization process and the wastes produced as well as an evaluation of the suitability of the resultant products, for which relevant properties have to be obtained to compete with existing alternatives. This thesis is therefore divided into three main parts (solubilization, regeneration and derivatization of cellulose), and addresses the various concerns of sustainability during cellulose transformation with an end-goal of making processable materials.

In the first part of the thesis, a sustainable solvent system for cellulose was investigated. In this regard, a detailed optimization study of the DBU-CO_2 switchable solvent system was performed using *in-situ* infrared spectroscopy. Upon optimization, up to 8 wt.% cellulose could be dissolve within 15 min at 30 °C using low CO_2 pressure (2-5 bar). What makes this solvent system sustainable, when compared to other classical cellulose solvents, includes: easier recyclability by simple release of the CO_2 pressure, fast and mild solubilization and lower cost compared to ionic liquids. Finally, by successfully trapping the formed *in-situ* cellulose carbonate using an electrophile, a clearer understanding of this solvent system was established.

The successful optimization of a sustainable solvent system for cellulose led to the second part of the thesis: the regeneration of cellulose. Here, the general solubilization and coagulation ways followed by freeze-drying was adopted to prepare cellulose aerogels. Various processing conditions such as cellulose concentration, coagulating solvent and super base, were investigated on their effect of the aerogels properties (density, morphology, pore size). The obtained results showed aerogels with densities between 0.05 and 1.2 g/cm^3, porosities between 92 and 97 % and pore sizes between

1.1 and 4.5 µm. In addition, from scanning electron microscopy (SEM), open large macroporous inter-connected cellulose networks were observed.

The derivatization of cellulose to make thermally processable materials is covered in the third part of the thesis. This part is divided into two sub-parts; transesterification and multicomponent reaction modification. In the first sub-part, and keeping in mind the principles of Green Chemistry, the unique nature of the studied DBU-CO_2 switchable solvent system (ability to switch polarity) allowed for a direct use of high oleic sunflower oil in the transesterification of cellulose. This approach is more sustainable than the more common use of activated acid derivatives (i.e. anhydrides or acid chlorides), that are not only toxic, but equally need to be pre-synthesized. A degree of substitution (DS) of 1.59 was achieved and the obtained fatty acid cellulose esters (FACEs) could be processed into films showing good mechanical and thermal properties (elastic modulus up to 478 MPa, maximum stress of 22 MPa, thermal degradation up to 368 °C). In the second sub-part, multicomponent reactions (MCRs) were employed to synthesize multifunctional processable cellulose-based materials. MCRs, which are one pot reactions and generally highly atom economic as well as efficient, avoid the purifications in between steps. The first attempt of using cellulose directly alongside CO_2 in an Ugi five component reaction was unsuccessful. However, an indirect approach using succinylated cellulose and applying the Ugi four component reaction was successful. In this case, high molecular weight modified celluloses (193-242 KDa) were obtained and showed T_g values between 99 and 116 °C. Interestingly, their T_g values could be tuned by simply changing any of the components.

Finally, in perspective and to expand the scope of multicomponent reactions, the Passerini four component reaction was introduced. The key in this approach was the *in situ* generated carbonate anion in the CO_2 switchable solvent system, allowing the direct incorporation of CO_2 into the synthesized compounds. This approach, which can be seen as a way of trapping CO_2 into making valuable compounds, also allows the use of a diverse class of alcohols (primary, secondary, aromatic, allylic) directly. As many carbohydrates contain hydroxyl groups, this reaction could open new routes for their valorization in the future.

Key words: Cellulose, Sustainability, Homogeneous modification, CO_2-switchable solvent, Regeneration, Derivatization, Transesterification, Multicomponent reactions.

Zusammenfassung

Als Kohlenstoffquelle mit der größten Verfügbarkeit auf unserem Planeten, ohne Konkurrenz zur Lebens- und Futtermittelversorgung, stellt Cellulose eine interessante Alternative dar, um die vielfältig genutzten, nicht-nachhaltigen Polymere auf Erdölbasis zu ersetzen. Die Mehrheit der Forscher, die mit diesem faszinierenden Biopolymer arbeiten, vernachlässigt allerdings Überlegungen zur Nachhaltigkeit in die chemische Modifizierung von Cellulose bei der Herstellung von Materialien zu integrieren. Die Konsequenz dessen ist eine Verlagerung der Umweltbelastung auf andere Abschnitte des Prozess-Zyklus. Um Nachhaltigkeit sicherzustellen, sind deshalb sowohl der erneuerbare Aspekt von Cellulose als auch Überlegungen zur Nachhaltigkeit im Reaktionsprozess wichtig. Dies beinhaltet die Berücksichtigung des Lösungsmittels, die Reaktanden, des Derivatisierungsprozesses, die produzierten Abfälle sowie eine Beurteilung der Nachhaltigkeit der resultierenden Produkte, die relevante Eigenschaften aufweisen müssen um mit bestehenden Alternativen konkurrieren zu können. Diese Arbeit ist deshalb in drei Teile gegliedert (Löslichkeit, Rückgewinnung und Derivatisierung von Cellulose) und befasst sich mit den verschiedenen Aspekten der Nachhaltigkeit während der Umsetzung von Cellulose mit dem Ziel, verarbeitbare Materialien herzustellen.

Im ersten Teil der Arbeit wurde ein nachhaltiges Lösungsmittelsystem für Cellulose untersucht. In diesem Zusammenhang wurde eine detaillierte Optimierungsstudie des DBU-CO_2 schaltbaren Lösungsmittelsystems mittels *in-situ* Infrarot Spektroskopie durchgeführt. Nach der Optimierung konnten bis zu 8 Gew.-% Cellulose innerhalb von 15 min. bei 30°C und einem niedrigen CO_2-Druck (2-5 bar) gelöst werden. Verglichen mit klassischen Lösungsmitteln für Cellulose weist dieses Lösungsmittelsystem verschiedene nachhaltige Aspekte auf: Einfaches Recycling durch entfernen des CO_2-Drucks, schnelles und mildes Auflösen und geringere Kosten als ionische Flüssigkeiten. Durch erfolgreiches Abfangen des *in-situ* gebildeten Cellulose-Carbonats mit einem Elektrophil, konnte schließlich ein besseres Verständnis dieses Lösungsmittelsystems erreicht werden.

Die erfolgreiche Optimierung eines Lösungsmittelsystems für Cellulose führte zum zweiten Teil der Arbeit: der Regenerierung von Cellulose. Hier wurde der bereits mit

anderen Systemen beschriebene Weg von Lösen und Ausfällen, gefolgt von Gefriertrocknen übernommen, um Cellulose-Aerogele herzustellen. Verschiedene Bedingungen bei der Verarbeitung wie die Cellulose-Konzentration, Lösungsmittel zum Ausfällen und die Superbase und deren Effekt auf die Eigenschaften der Aerogele (Dichte, Morphologie und Porengröße) wurden untersucht. So wurden Aerogele mit einer Dichte von 0.05-1.20 g/cm^3, Porositäten zwischen 92 und 97% und Porengrößen zwischen 1.1 und 4.5 µm erhalten. Zusätzlich wurden im Rasterelektronenmikroskop offene große und makroporöse, miteinander verbundene Cellulose-Netzwerke beobachtet.

Die Derivatisierung von Cellulose zur Herstellung von thermisch verarbeitbaren Materialien wird im dritten Teil der Arbeit behandelt. Dieser Teil ist in die zwei Kapitel Umesterung und Modifizierung durch Multikomponenten-Reaktionen unterteilt. Im ersten Kapitel, und unter Berücksichtigung der Prinzipien der Nachhaltigen Chemie, ermöglichte die einzigartige Natur des DBU-CO_2 schaltbaren Lösungsmittelsystems (Möglichkeit zur Änderung der Polarität) den direkten Einsatz von Sonnenblumenöl mit hohem Ölsäuregehalt in der Umesterung von Cellulose. Dieser Ansatz ist nachhaltiger als der übliche Einsatz von aktivierten Säurederivaten (z.B. Anhydride oder Säurechloride), die nicht nur giftig sind, sondern gleichermaßen im Voraus synthetisiert werden müssen. Es wurde ein Substitutionsgrad von 1.59 erreicht und die erhaltenen Fettsäure-Cellulose-Ester (FACEs) konnten zu Filmen mit guten mechanischen und thermischen Eigenschaften verarbeitet werden (E-Module von bis zu 478 MPa, maximale Spannung von 22 MPa, Zersetzungstemperaturen bis zu 368°C). Im zweiten Kapitel wurden Multikomponenten-Reaktionen (MCRs) eingesetzt, um multifunktionale, verarbeitbare Materialien auf Cellulosebasis zu synthetisieren. MCRs sind Eintopfreaktionen, weisen üblicherweise eine hohe Atomökonomie und Effizienz auf und benötigen keine Aufreinigung zwischen den Syntheseschritten. Der erste Ansatz, Cellulose direkt mit CO_2 in einer Ugi Fünfkomponenten-Reaktion umzusetzen, war nicht erfolgreich. Ein indirekter Ansatz unter Verwendung von mit Bernsteinsäureanhydrid modifizierter Cellulose in der Ugi Vierkomponenten-Reaktion war jedoch erfolgreich. In diesem Fall wurden modifizierte Cellulosederivate mit hohem Molekulargewicht (193-242 kDa) erhalten, diese zeigten hohe T_g-Werte zwischen 99 und 116°C. Die T_g-Werte konnten durch einen einfachen Austausch der einzelnen Komponenten verändert werden.

Um den Anwendungsbereich der Multikomponenten-Reaktionen zu erweitern, wurde anschließend die Passerini Vierkomponenten-Reaktion eingeführt. Der Schlüsselschritt in diesem Ansatz war das *in-situ* gebildete Carbonat-Ion im CO_2 schaltbaren Lösungsmittelsystem, das die direkte Einführung von CO_2 in die synthetisierte Verbindung ermöglichte. Dieser Ansatz, der eine Möglichkeit zur Fixierung von CO_2 zur Herstellung nützlicher Verbindungen darstellt, ermöglicht auch den direkten Einsatz von verschiedenen Alkoholen (primär, sekundär, aromatisch, allylisch). Da viele Kohlenhydrate Hydroxygruppen enthalten, könnte diese Reaktion in der Zukunft neue Möglichkeiten für deren Modifikation eröffnen.

Schlüsselwörter: Cellulose, Nachhaltigkeit, homogene Modifizierung, CO_2 schaltbare Lösungsmittel, Rückgewinnung, Derivatisierung, Umesterung, Multikomponenten-Reaktionen.

Résumé Français

Source de carbone la plus abondante du règne végétal et non concurrentielle de la chaîne alimentaire, la cellulose est une alternative aux ressources fossiles crédible pour le développement de nouveaux matériaux polymères. Néanmoins, à ce jour, les nombreux travaux décrits dans la littérature et visant la valorisation et la modification chimique de ce biopolymère fascinant ne répondent pas suffisamment, ou tout au moins que très partiellement, aux critères de durabilité. Pour répondre à ces critères de développement durable, le caractère renouvelable de la cellulose et les concepts de procédés propres et de chimie 'verte', doivent être réellement pris en compte. Ceci implique un choix réfléchi des solvants et réactifs utilisés, une maîtrise des procédés de modification chimique et bien évidemment une évaluation de la pertinence des produits formés, pour lesquels les propriétés obtenues doivent être innovantes et supérieures aux matériaux polymères existants. Cette thèse se divise en trois parties principales, à savoir la solubilisation, la régénération et la modification chimique de la cellulose. Tout au long de ce travail, une attention particulière a été porté sur la durabilité de sa transformation chimique pour viser l'élaboration de matériaux cellulosiques processables et aux propriétés innovantes.

Dans la première partie de la thèse, un système composé d'un catalyseur organique nucléophile (DBU) et de CO_2 a permis la dissolution rapide de la cellulose dans le DMSO. Une étude détaillée visant à optimiser le système DMSO-DBU-CO_2 a été réalisée grâce à un suivi par spectroscopie infrarouge *in situ*. Ainsi, jusqu'à 8 % massique de cellulose ont pu être dissous en 15 minutes à 30 °C sous une faible pression de CO_2 (2-5 bars). L'originalité de ce système commutable (fixation-relargage réversible du CO_2), par comparaison aux autres solvants classiques de la cellulose, inclut une recyclabilité plus facile par simple dépressurisation du CO_2 et une solubilisation rapide et douce, à plus bas coût, en comparaison aux systèmes utilisant les liquides ioniques. La mise en évidence de la création de fonctions carbonate par réaction avec différents composés électrophiles tels les halogénures d'alkyle a permis d'avoir une connaissance approfondie de ce système.

L'optimisation réussie d'un système 'propre' permettant la dissolution de la cellulose nous a conduit à étudier sa régénération. Dans cet objectif, des aérogels de cellulose

ont été préparés par un procédé de solubilisation, coagulation et lyophilisation. Différents paramètres ont été examinés tels la concentration en cellulose, le solvant de coagulation ou encore la nature et concentration en super-base (DBU-CO$_2$), sur les propriétés des aérogels (densité, morphologie, taille des pores). Les résultats obtenus démontrent que des aérogels avec une densité entre 0.05 et 1,2 g/cm^3, des porosités entre 92 et 97 % et des tailles de pore entre 1,1 et 4,5 µm ont été obtenus. Enfin, l'analyse des aérogels par microscopie électronique à balayage (SEM), a révélé la formation de réseaux de cellulose interconnectés et macroporeux.

La modification chimique de la cellulose pour l'élaboration de matériaux processables aux propriétés innovantes fait l'objet de la troisième partie de la thèse. Cette partie est divisée en deux sous-parties: la dérivatisation de la cellulose par réaction de transestérification d'une part, et par réaction multi-composants, d'autre part. Dans la première sous-partie et gardant à l'esprit les principes de la chimie verte, la nature unique du système commutable DBU-CO$_2$ amenant un changement d'hydrophilie du squelette cellulosique a permis l'utilisation directe de l'huile de tournesol pour la transestérification de la cellulose. Cette approche est beaucoup plus durable que l'utilisation, plus classique, d'acides activés tels les anhydrides ou les chlorures acides, souvent toxiques. Ainsi un degré de substitution (DS), par les acides gras de 1,59 a été obtenu permettant l'élaboration de films cellulosiques présentant de bonnes propriétés mécaniques et thermiques (module d'élasticité jusqu'à 478 MPa, contrainte à la rupture de 22 MPa, température de dégradation thermique jusqu'à 368 °C). Dans la deuxième sous-partie, des réactions multi-composants 'one pot', efficaces et économes en atomes ont été réalisées en une seule étape, pour élaborer des matériaux cellulosique processables et multifonctionnels. La première tentative visant la modification de la cellulose directement dans le CO$_2$ par réaction de Ugi à cinq composants a échoué. Cependant, une approche indirecte utilisant la cellulose préalablement modifiée par réaction avec l'anhydride succinique a permis de réaliser avec succès la réaction de Ugi à quatre composants. Dans ce cas, les celluloses ainsi modifiées ont une masse molaire qui varient entre 190 et 250 kDa et présentent des valeurs de T$_g$ entre 99 et 116 °C. De façon intéressante, les valeurs de T$_g$ ont pu être ajustées en changeant simplement la nature des composants utilisés.

Enfin, dans la perspective d'étendre la portée des réactions multi-composants sur ce type de squelette cellulosique, la réaction de Passerini à quatre composants a été

réalisée. La clé dans cette approche est la formation *in situ* de la fonction carbonate qui permet l'incorporation directe du CO_2 dans les composés synthétisés. Cette approche, que l'on peut voir comme une façon de piéger le CO_2 pour la synthèse de composés à haute valeur ajoutée, peut être étendue à l'utilisation directe d'une large gamme d'alcools (primaire, secondaire, aromatique, allylique). Puisque la plupart des carbohydrates contiennent des fonctions hydroxyle, cette réaction laisse entrevoir de nouvelles voies de valorisation pour ces substrats.

Mots clés: Cellulose, durabilité, modification en milieu homogène, solvant commutable au CO_2, régénération, dérivatisaton, transestérification, réactions multi-composants

Table of Contents

1. Introduction: Sustainability in today's society

The industrial revolution at the beginning of the 18th century led to in a "new" world characterized by many inventions and rapid global development. During this period, the place of crude oil as a reliable source of raw material started taking shape. Crude oil was used about 4000 years ago mainly for water-proofing boats and in construction.[1] However, the works of the Scottish chemist James Young, who distilled paraffin oil from coal and oil shales, marked the beginning of the crude oil refining process.[2] Subsequent development of this technology eventually led to addressing various material demands from crude oil. With the invention of the internal combustion engine, the first wide application of refined crude oil was then to power these engines. But crude oil showed to be worth more than that. As they are essentially made of hydrocarbons of various molecular weights, development of cracking and reforming technology allowed for preparation of new compounds such as ethylene, propylene and benzene. Development of efficient catalysts and polymerization methods allowed for polymerization of these monomers. The resulting polymers, now referred to as plastics, have become one of the largest ever man-made materials (about 8,300 million metric tons until 2015), only outweighed by cement and steel used in construction.[3] However, with an annual production of 322 million metric tons as of 2015, (322 billion litre; 1kg plastic = 1 litre), plastics are produced in higher volume than steel with an annual production of 1,623 million tons (203 billion litres; 8kg steel = 1 litre).[4] Some common names include polyethylene (PE), polypropylene (PP), polystyrene (PS), polyvinyl chloride (PVC) and polyethylene terephthalate (PET). What makes these polymers attractive are their light weight, corrosion resistant, tuneable properties, good mechanical and thermal properties and above all a comparative cheap source from crude oil. Today, we are living in what is termed the "plastic" age as their versatility has allowed them to find their way into every aspect of our lives.[5,6] It is almost inconceivable that the plastics we see today were barely nowhere to be found before the 1940`s. In 1941, the global plastic production was less than 1 million tons, this increased to 15 million tons in 1964 and as of 2015, the number stands at 322 million tons.[4,6,7] But what is it about crude oil and plastics that makes the society more concerned today? Some of these issues/challenges can be summarized as follows:

1. *Source.* To begin with, crude oil, coal or gas are not sustainable; they will eventually be depleted or fail to meet their increasing demand in the future if no substitute is developed.

2. *Location.* Their region-specific locations cause prices to be unstable and unreliable. Regional conflicts led to serious energy crises as was the case in 1973 which saw the price of oil increased from $3 to $12 (300 % increased) within few months.[7]

3. *Pollution concern.* This can be divided into two parts;

a. *Extraction.* The process of crude oil extraction/exploration led to serious environmental degradation. Personally coming from Nigeria, where the production produces almost two million barrels of crude oil per day, I have witnessed first-hand the extend of environmental pollution and it is unimaginable. In 2011, the United Nations Environment Program (UNEP), released its environmental report of Ogoniland (part of oil producing community in Nigeria). In their report, they estimated that up to 30 years of serious efforts will be required with up to $1bn (1 billion US dollars) to mitigate this problem.[8]

b. *Usage.* The resulting products (plastics for example) are mostly made for one-time usage and are not biodegradable (accumulation in the environment leads to both land and ocean pollutions that are visible today). The World Economy forum (WEF) postulated in their recent study that with the increasing global plastic production, they might be more plastics in the ocean than fish by 2050 (today the ratio between plastic to fish stands at 1:5).[9] Another pollution concern from crude oil stems from their extensive usage in power generation for both industrial and commercial usage, as well as transport (automobile, trains and airplanes) that annually releases billion metric tons of CO_2. The role of CO_2 in global warming is now well established.[10–12]

These challenges/concerns are summarized in **Figure 1**.
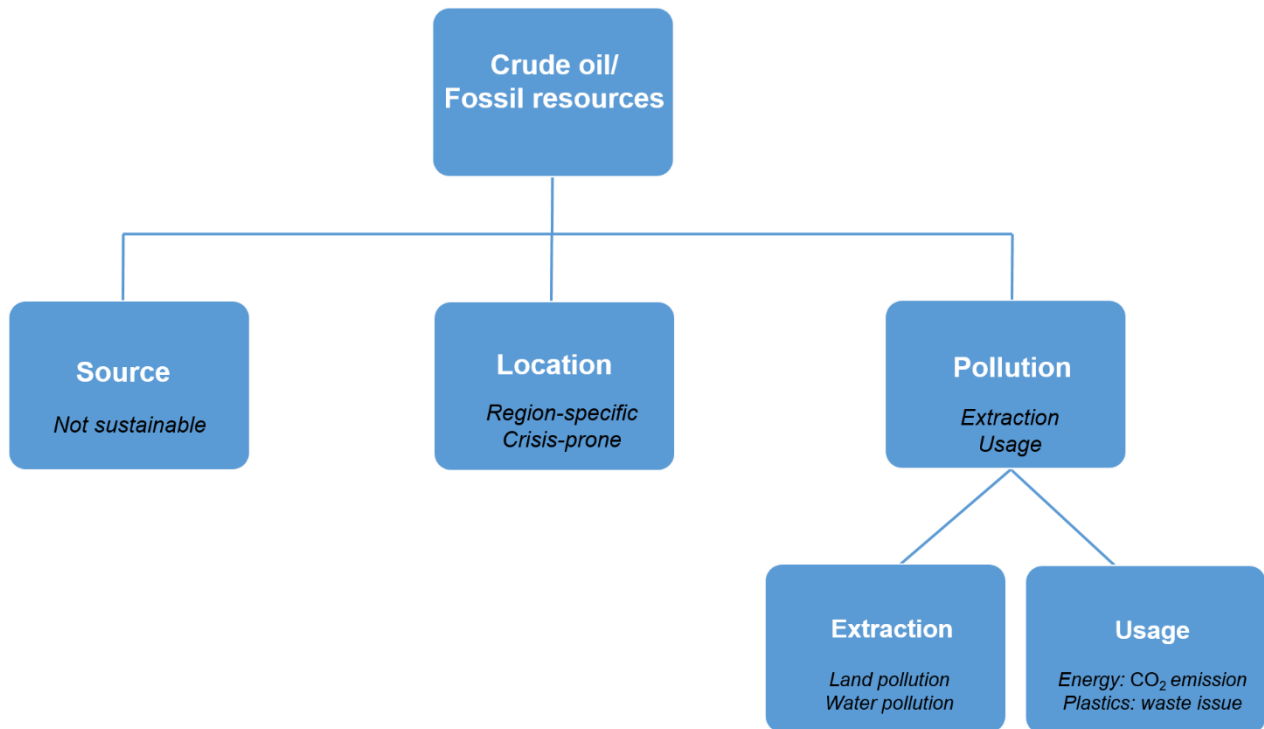
Figure 1: Summary of crude oil/fossil resources global challenges/concerns.

There is obviously no magical wand that can address all these challenges. The closest to this is **Sustainability**. This term, first used in the 1987 report of the World Commission on Environment and Development, is defined as *"meeting the needs of the present generation without compromising the ability of future generations to meet their own needs"*.[13] By its definition, sustainability considers not only the source of the raw material but its entire transformation to ensure that both the raw material source and their usage do not leave a degraded environment for the future generation. In addition, sustainability also considers the end-of-life of the materials; their re-usability, recycling or safest disposal to ensure the overall safety of the environment. Therefore, an ideal sustainable society will use sustainable raw materials (renewable), employ safe transformation processes to make safe materials, that can be re-used, recycled, or biodegraded (it is also important to consider the resulting metabolites after biodegradation to ensure their non-toxicity to the environment) after usage. These conditions (ideal), which are obviously hard to meet, require a gradual but steady move in the right direction. Therefore, in the past decades, different methodologies and governmental regulations have been developed and enforced to move towards sustainability. More recently, in 2015, the World leaders met in Paris to sign an agreement on climate change with the aim at cutting the global CO_2 release.[14] In

addition, the European Union banned in May 2018 the use of single-use plastics such as plastic cotton buds, straws, cutlery and plates with effect from 2021.[15] With respect to methodologies, scientists have continued to promote sustainability-driven goals, some of which are discussed in the following paragraphs.

Rogers Sheldon introduced the concept of the Environmental factor (E-factor) to address the amount of waste generated mostly in the pharmaceutical industries.[16,17] This concept is now being applied in various fields where zero waste remains the target (E-factor of zero). Also important in the direction of sustainability are the Twelve Principles of Green Chemistry developed by Anastas and Warner in the late 1990s,[18] as well as the Twelve Principles of Green Engineering by Anastas and Zimmerman in 2003.[19] At the centre of these principles is the concept of design. Through careful design, waste can be minimized, derivatization avoided, biodegradable materials produced and renewable raw materials used.

The use of renewable resources will address the first challenge (non-sustainable crude oil), and eventually the issue of accumulation (for biodegradable materials). Care must be taken at this point as the use of renewable resources does not necessarily make the material biodegradable. As an example, polyethylene is non-biodegradable whether it was obtained from crude oil or renewable sources. Interestingly, nature has blessed us with enormous abundance of various resources (biomass), which are, compared to fossil-based materials, highly functionalized. Biomass has an annual production of over 170 billion tons.[20] Examples include cellulose, hemicellulose, lignin, terpenes, triglycerides, proteins, alginate and chitin.[21,22] Carbohydrates are leading this group of biomass accounting for 75 % of the total number.[20] Produced by plants during the process of photosynthesis, carbohydrates are the most abundant material in our planet.

To address our material need from carbohydrates, care should be taken as some are very important as food or feed (for example starch). Therefore, cellulose, which does not compete as food or feed, is a viable alternative for making materials. In addition, as cellulose accounts for 35-50 % of the total biomass,[23–25] it is the most abundant organic polymer in our planet. However, as most cellulose is obtained from trees, care must be taken again to ensure sustainably grown forests, not only because trees play an important role in keeping the CO_2 level within check. Cellulose indeed played a key

role in the development of the field of polymer science as well as a key industrial raw material.[26] Over the years, much works has been reported on the chemical modification of cellulose to make various materials. However, what is lacking in most of these reports, is a consideration of the sustainability aspect during such chemical transformation. Therefore, the focus of this thesis is not only on the use of cellulose to make materials, but a consideration of the entire transformation process to improve sustainability.

2. Theoretical background

2.1. Introduction

Cellulose, the most abundant organic polymer in nature, was first isolated in 1837 thanks to the French chemist Anselm Payen.[27,28] As reported, after treating various plant tissues with acids and ammonia followed by an extraction using ether, water and alcohol, a resistant fibrous solid remained. By elemental analysis, he obtained the molecular formula $C_6H_{10}O_5$.[27] Subsequently the name "cellulose" was coined in 1839 to describe this plant constituent material.[29] Cellulose, as we know today, is the main component of the plant cell walls measuring up to 1 µm in native plants and offering strength to the cell walls.[30] Cellulose, along with hemicellulose and lignin, is the most widespread produced organic polymers by plants (lignocellulose). Through the process of photosynthesis, plants are able to convert CO_2 from the atmosphere using solar energy from the sun and water to make carbohydrates that serve as its primary energy storage and also for structural use (**Scheme 1**).

$$6\ CO_2\ +\ 6\ H_2O\ \xrightarrow{\text{sunlight}}\ C_6H_{12}O_6\ +\ 6\ O_2$$

Scheme 1: Photosynthesis reaction

Apart from plants, cellulose is equally produced by some bacteria such as *Acetobacter xylinum (*now renamed, *Gluconacetobacter xylinus*) as well as green algae (*Valonia* species) in very pure form without the associated lignin as in wood cellulose.[31–33] Depending on the source of cellulose, their degree of polymerization (DP) ranges from 300 to 15,000.[26,34]

2.2. Occurrence, structure and basic chemistry

2.2.1 Occurrence

Lignocellulose is the main source of cellulose. Lignocellulose is found not only in wood but other types of biomass such as cotton and agricultural wastes. The percentage of cellulose with respect to hemicellulose, lignin and extractives in various biomass sources are summarized in **Table 1**.

Table 1: Various biomass sources and composition for lignocellulose, adapted from Khalil *et al.*[35]

Source	Composition (%)			
	Cellulose	Hemicellulose	Lignin	Extract
Hardwood	43-47	25-35	16-24	2-8
Softwood	40-44	25-29	25-31	1-5
Bagasse	40	30	20	10
Corn cobs	45	35	15	5
Corn stalks	35	25	35	5
Cotton	95	2	1	0.4
Flax (retted)	71	21	2	6
Flax (unretted)	63	12	3	13
Hemp	70	22	6	2
Jute	71	14	13	2
Kenaf	36	21	18	2
Wheat straw	30	50	15	5

The percentage of cellulose not only varies between different types of biomass, but also within similar family of wood for instance. In hardwoods such as poplar, its composition ranges between 51 and 53 %, whereas this number is slightly higher in eucalyptus (54 %). Within softwoods, the composition varies between 42 and 50 % in pine and lies around 45 % in spruce.[36]

2.2.2 Structure and basic chemistry

Cellulose is a polysaccharide consisting of repeating units of smaller monomers (monosaccharides). Structurally, cellulose is a linear homopolymer consisting of β-1,4 linked D-glucopyranose units.[26] The structural elucidation of cellulose was pioneered by the works of Staudinger, who found that the repeating D-glucose units were linked covalently *via* glycosidic bonds.[37] This glycosidic bonds occur between the hydroxyl groups of C1 and C4 of the next repeating unit. The obtained $^4C_1$ chair conformation[38] typical of C-6 membered pyranose molecules has the C2, C3 and C5 carbons and the oxygen atom within the plane of the molecule, while the C4 and C1 carbon atoms stay above and below the plane respectively. The hydroxymethyl side group (CH_2OH) is arranged in a *trans-gauche (tg)* position relative to the O5-C5 and C4-C5 bonds.[26] In order to keep the preferred bond angle between the acetal bridges, a 180° rotation in the plane after every second anhydroglucose unit (AGU) is observed.[26] This leads to

the repeating unit in cellulose being cellobiose (disaccharide; two glucose units) as opposed to starch, in which the repeating units are glucose units. The general structure of cellulose is shown in **Scheme 2**.
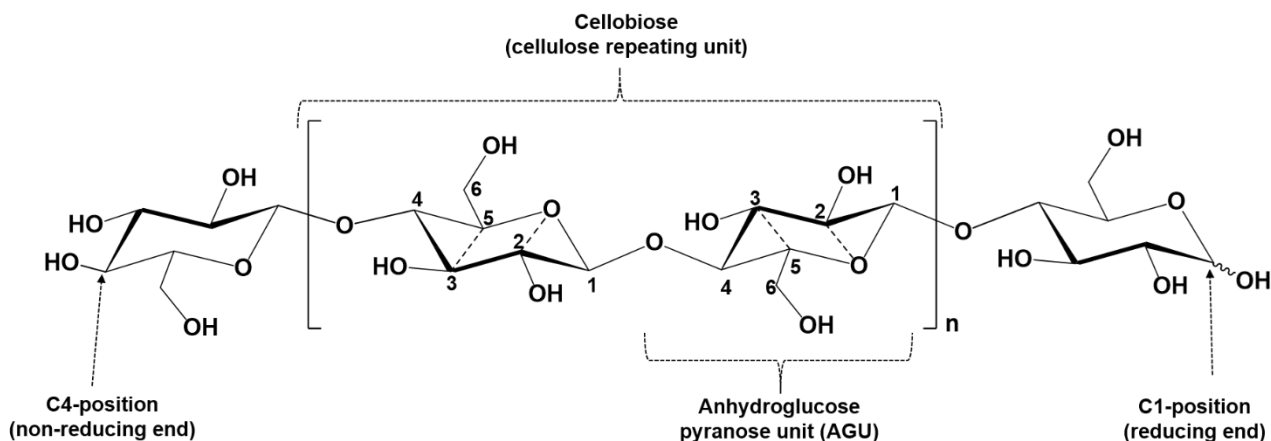
Scheme 2: Structure of cellulose; where **n** represents the repeating units in cellulose and not the degree of polymerization.

This supposedly slight difference has a tremendous impact on the properties of cellulose compared to starch. For instance, while starch can easily be solubilized in common solvents, cellulose cannot. Although, it is worth mentioning that this observed difference is also related to the fact that whereas cellulose is a complete linear homopolymer, starch consist of both linear (amylose; 1,4-α glycosidic linkage) and branched (amylopectin; 1,6-α glycosidic linkage) segments.[39,40]

A closer look into the structure of cellulose shows the presence of three hydroxyl groups at C2, C3 and C6 positions. These three hydroxyl groups, which show different reactivity are classified as primary (C6 position) and secondary (C2, C3 positions). During chemical modification, the term degree of substitution (DS) is used to describe how many of these hydroxyl groups have been replaced per AGU. Therefore, a DS of 1.0 means one of the hydroxyl group is substituted on average, while a DS of 3.0 means a complete substitution of all three hydroxyl groups. Depending on the type of reaction, regioselective substitution to a particular position can be achieved.[41] Studies have shown that such regioselective substitution can play an important role on the properties of the obtained material.[41–43] Other interesting features presented by cellulose include the different reactivity of its chain-ends. On one end of the polymer is the so-called reducing end and typically assigned on C1 position (anomeric carbon). At this end, the hemiacetal is in equilibrium with its corresponding aldehyde, therefore

both α- and β- conformations are possible leading to a non-fixed stereochemistry at this carbon (signified by a wavy bond),[26] as illustrated in **Scheme 2**. On the other end of the polymer is the so-called non-reducing end (typically assigned to C4 position). Due to the uniqueness of the reducing end, selective modification such as reductive amination can be carried out at this position. In one study, reductive amination with an azido-functional amine followed by click reaction allowed for the preparation of a fully bio-based cellulose oligomer-based amphiphilic molecule.[44]

Cellulose is a semi-crystalline polymer meaning, it consists of both highly ordered (crystalline) and a less ordered (amorphous) regions.[34] Partial dissolution of the amorphous regions leads to an increase in crystallinity as seen in microcrystalline (MCC), nanofibrillated cellulose (NFC) and cellulose nanocrystals (CNC).[35,45–49] These different types of cellulose are interesting for various applications.[34,47,50] In regards to their crystal structures, cellulose exist in different allomorphs, which include: cellulose I (Iα and Iβ), cellulose II, cellulose III, and cellulose IV.[51] However, the most common in nature are cellulose Iα and Iβ, with the ratio between both depending on the cellulose source.[52,53] For instance, cellulose Iα is found mostly in lower organisms like bacteria[54] and algae,[55] whereas cellulose Iβ dominates in higher plants. Cellulose II is the most thermodynamically stable form of cellulose and can be obtained from cellulose I through two approaches: regeneration (solubilization followed by re-crystallization) and mercerization (aqueous sodium hydroxide treatment).[26] Cellulose III can be obtained from cellulose I or II *via* treatment with liquid ammonia, whereas subsequent heat treatment of cellulose III leads to formation of cellulose IV.[51,56] The interconversion between these different allomorphs of cellulose is represented in **Scheme 3**.
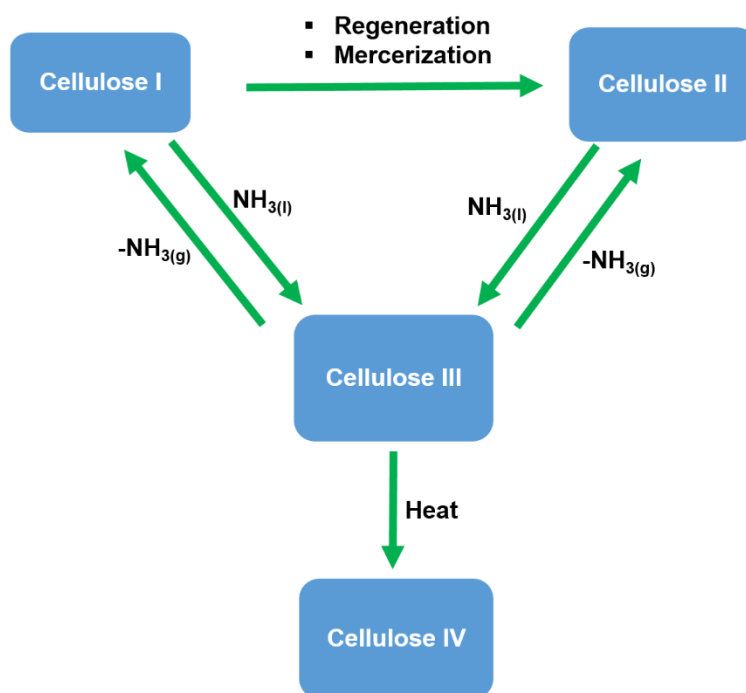
Scheme 3: Interconversion between different allomorphs of cellulose crystal structures, adapted from O'Sullivan.[51]

Langan and co-workers employed the use of synchrotron X-ray and neutron fiber diffraction experiments to study in detail the crystal structure of cellulose I (Iα and Iβ).[57,58] From the obtained crystal lattice results, cellulose Iα was found to have a triclinic unit cell, whereas Iβ has the monoclinic unit cell. In both allotropes, the cellulose chains are arranged in a "parallel" configuration.[53] Cellulose II on the other hand has a monoclinic crystal structure with two "anti-parallel" arranged chains in the unit cell.[26,59] The *inter-* and *intra-*molecular hydrogen bonding between the cellulose chains are responsible for their hierarchical supramolecular arrangement. A consensus of reports in the literature agrees that this bonding is dominated by a more defined O3-H···O5-H bond, in addition to the less defined O2-H···O6-H bond.[34,57] In **Scheme 4**, the O3-H···O5 intramolecular hydrogen bonding is represented by a purple dashed bond, while the O-H2···O6-H and H-O2···H6-O intramolecular and intermolecular hydrogen bonding are is represented by a green and red dash bond respectively.
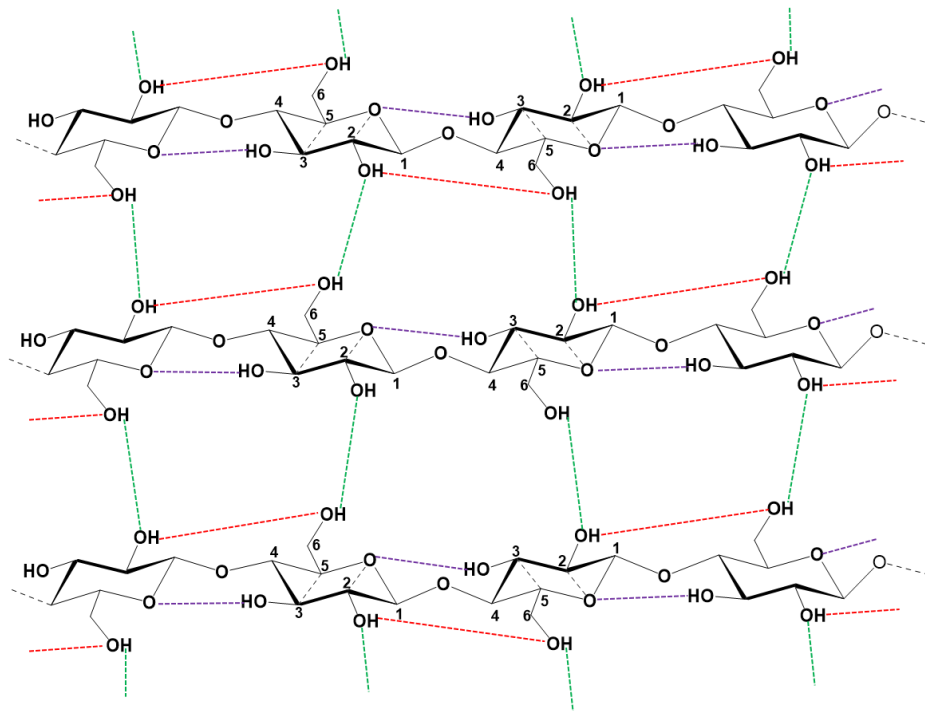
Scheme 4: *Intra-* and *inter-* molecular hydrogen bonding in cellulose I structure. O3-H···O5 intramolecular (purple), O-H2···O6-H intramolecular (red) and H-O2···H6-O intermolecular (green) hydrogen bonds.

2.3 Isolation process for cellulose: the pulping process

The most common source of cellulose fibres is from wood and cotton. Cotton offers the advantage that the cellulose fibres are almost pure (see **Table 1**), thereby largely simplifying the purification process. The very high land and water demand for growing cotton has made wood a preferred choice for obtaining cellulose fibres in recent times. However, isolating cellulose fibres from wood that also contains lignin and hemicellulose is not trivial and involves many steps. The annual production of paper (including cardboard, graphic and hygienic paper) amounts to about 350 x 10^6 tons.[30] The process of isolating cellulose fibre from wood is called pulping. Though many variations exist, the goal is always to isolate the cellulose fibres from the other wood constituents and at the same time avoiding breakage of the fibres. Pulping can be achieved through mechanical or chemical approaches.

2.3.1. Mechanical pulping

Mechanical pulping involves the disintegration of the wood using mechanical energy. This mechanical energy can be provided by grinding the wood with a rotating stone or by placing the wood between two metal discs.[60,61] The yield of mechanical pulping is

usually above 90 % and the obtained pulps are referred to as mechanical pulp (MP) or thermomechanical pulp (TMP).[30] However, through this method, most of the lignin is not removed, affecting the overall property of the resulting paper such as low light stability as well as the color. Therefore, MP are mostly employed for lower paper prints such as newspaper.[30] A slight variation of mechanical pulping exists: chemothermomechanical pulping (CTMP), whereby chemicals such as Na_2SO_3/Na_2CO_3 or NaOH are added to reduce the high energy demand during mechanical wood disintegration.[30]

2.3.2. Chemical pulping

Chemical pulping for instance *Kraft* (German word for strength) or sulphate pulping, is the most dominant process for production of paper grade and textile grade cellulose fibers.[60,61] The first step of the Kraft pulping involves chopping of the wood into smaller pieces (wood chips) to increase their surface area and allow effective chemical treatment. Next, the wood chips are treated at 150-170 °C between 1.5-2 h under pressure (7-10 bar) using a combination of Na_2S and NaOH ("white liquor"), with the OH^- and HS^- anions being the active species. This alkaline condition ensures the breakage of the aryl-linkages found between the lignin and the cellulose fibres, thereby leading to the removal of most of the lignin through subsequent washing steps.[30,35] However, since there are no specific lignin removal solvents, some of the cellulose as well as hemicellulose are lost during the washing step. The remaining lignin in the final pulp is referred to as the kappa number and is very important in classifying the pulp.[35] In another variant called Pre-Hydrolysis Kraft (PHK), for the preparation of dissolving pulp, a pre-hydrolysis step is involved. At this stage, the wood chips are first pre-treated with steam at 140-170 °C or with dilute acids at 110-120 °C. This step leads to about 20 % decrease in the wood mass mainly due to the removal of extractives, most of the hemicellulose in softwoods as well as part of the lignin in hardwoods.[30] Another variation of chemical pulping called sulphite pulping involves the use of sulphurous acid (H_2SO_3) with HSO_3^- being the active ions for the de-lignifying process.[60] More recently developed chemical pulping (organosolv) employs the use of organic solvents such as methanol, ethanol, butanol, ethylene glycol, acetone and peracetic acid (CH_3CO_3H) for lignin removal under pressure and temperatures between 140 and 220 °C.[60–62]

The final step of the chemical pulping process involves bleaching. This is done to remove residual lignin and also improve the brightness of the cellulose fibers (improve ageing property of resulting paper). This can be achieved *via* totally chlorine free (TCF) or elemental free chlorine process (EFC) bleaching.[30] Examples of bleaching agents include chlorine dioxide (ClO_2), hypochlorite (ClO^-), hydrogen peroxides (H_2O_2) and ozone (O_3) and are applied depending on the bleaching process.[60,61] In the ECF bleaching, chlorine dioxide is used followed by an alkaline extraction in the presence of oxygen or hydrogen peroxide. The TCF bleaching uses ozone, oxygen, and hydrogen peroxide under alkaline environment to generate hydroperoxide ions that are able to attack the lignin structure leading to their removal.[30]

2.4 Cellulose as a key industrial raw material: historical perspective

Cellulose has been used for thousands of years, mostly in the form of wood and cotton to address energy and clothing demands.[26] After the isolation of cellulose by Anselm Payen, cellulose became a key raw material in the developing chemical industry. The first cellulose derivative, cellulose nitrate, was accidentally discovered by the German-Swiss chemist, Christian Friedrich Schoenbein in 1845 after cleaning a spill of sulphuric acid and nitric acid using his wife's cotton apron.[63,64] It was later discovered that cellulose nitrate with high nitrogen content could be used as an explosive (guncotton).[65] Upon treating this cellulose derivative with camphor, John Wesley Hyatt produced the first man made plastic in 1865 (Celluloid)[66]. At this time, the increasing price of silk (natural fiber from silk worm) for clothing challenged many scientists to seek for alternatives (artificial silk fibers). By dissolving cellulose nitrates in ether or alcohols followed by extruding *via* holes in a spinneret, Count Louis-Marie-Hilaire Bernigaud (Comte de Chardonnet) created the first artificial silk called Chardonnet silk.[67] Though he went on to set up a company in 1892 on his invention, the resulting materials were flammable. Addressing the flammability challenge of the Chardonnet silk was a cumulative effort. First, the Swiss chemist, Matthias Edward Schweizer realized in 1857 that it was possible to solubilize cotton directly in a mixture of copper salts and ammonia (cuprammonium solution).[68] Later on, the French chemist Louis-Henri Despeissis reported for the first time a spinning of cellulose fibers from this solution with a subsequent recovery of pure cellulose fiber in a water bath containing

dilute sulphuric acid.[69] With some improvements on his spinning process by Dr. Edmund Thiele, the second artificial silk was made and marketed under the name Bemberg silk in 1908. The Bemberg silk went on to achieve commercial success only to be out-performed by the viscose fiber.

The success story of the viscose fiber starts with the patent of three British chemists in 1891: Charles Cross, Edward Beaver and Clayton Beadle. In their patent, they described a process of solubilizing cellulose (both cotton and wood pulp) by treating with carbon disulphide in alkaline media.[70] The obtained solution (*viscose*) could then be coagulated in an ammonium sulphate bath and then converted back to pure cellulose by treating with dilute acid. Following this new cellulose solubilization approach, German scientists working for Donnermarck in 1905 developed a dilute sulphuric acid bath containing salts (the Mueller spinbath), which allowed the collection of pure cellulose fibers from viscose.[71] Till date the viscose process, also referred to as the xanthate process, remains the most important route for obtaining cellulose fibers. Peak annual production of cellulose viscose fibers reached 3.8 million tons in 1973 with a decline ever since as the cheaper alternative of synthetic polyester fibers from petroleum became available, coupled with stricter environmental rules in Europe and the United states. Despite the huge environmental concern of the viscose process (volatile and toxic CS_2, high amounts of toxic salt wastes), less toxic alternative technologies such as Carbacell (uses cellulose carbamate formed from reaction between cellulose and urea or ammonia),[72–75] Lyocell (uses direct solubilization of cellulose in *N*-methyl morpholine *N*-oxide solvent),[76] Ioncell (uses imidazolium based ionic liquids to directly solubilize cellulose)[77] or Ioncell-F (uses 1,5-diazabicyclo[4.3.0]non-5ene/acetate to solubilize cellulose)[78] have not been able to successfully replace the viscose process. Though it is worth mentioning that some of these technologies are still at their early stages and with the increasing global interest towards sustainability, such environmentally-friendly processes will become attractive.

The process of shaping cellulose into fibers do not chemically modify the polymer, and are thus referred to as regeneration. For other applications, the need to chemically modify cellulose becomes necessary. During the same time of developing the artificial silk, many cellulose derivatives were developed. Chemical modification of cellulose occurs mainly through a substitution of one of its hydroxyl groups either by a heterogeneous or homogeneous approach. The difference between these two

approaches depends on whether the cellulose needs to be first completely solubilized or not. Whereas complete cellulose solubilization is required in the homogeneous approach, only swelling of the polymer is needed for the heterogeneous counterpart. Most industrially relevant cellulose derivatives include cellulose esters (e.g. cellulose acetate) and ethers.

Cellulose acetate, which is today one of the most important commercial derivatives of cellulose (900,000 tons annual production),[79] was first reported in 1865 by Paul Schützenberger by heating cellulose in a sealed glass containing acetic anhydride.[80] The patent for this process was applied in 1894 by Cross and Bevan.[81] The success story of cellulose acetate (triacetate; DS = 3) was initially limited by the need for high quality cotton linters and excess (5-6 times) of acetic acid and acetic anhydride. However, a breakthrough occurred between 1904 and 1905 when Miles[82] and Eichengün *et al*.[83] reported on how to make cellulose diacetate (CDA; DS = 2) that could be solubilized in acetone and ethyl acetate. The first widespread applications of CDA was as lacquers for aeroplane wings (made with heavy rubber tissues at this time) marketed under the trade name "Cellit" by F. Bayer & Co.[84,85] After the first world war, the decrease demand for CDA drove the producers to seek for new applications. This way, CDA found its way into the textile market thanks to the success of the Dreyfus brothers who developed a spinning process[86] and Clavel who developed a faster dying route.[87] Today, the market share of cellulose acetate textiles has been largely replaced by polyesters and other synthetic fibres. Most market share of cellulose acetate today is as membrane filters in cigarettes (almost 600,000 metric tons) and also as film for photographic display applications.[85]

Cellulose ethers, another commercially relevant cellulose derivative, was first reported by Suida in 1905 by reaction of cellulose using dimethyl sulfate.[88] The first patent was applied by Henry Dreyfus in 1912.[89] By 1935, various cellulose ethers such as methyl, ethyl and benzyl derivatives were already commercial as thermoplastics and for other applications.[90,91] Today, the most commercial cellulose ethers or their functional derivatives include: carboxyl methyl cellulose (300,000 tons per year), methyl cellulose (150,000 tons per year) and hydroxyl ethyl cellulose (50,000 tons per year).[79] A more detailed description of their synthesis and applications are discussed in **Chapter 2.5.5.**

2.5 Relevance of sustainability during homogeneous cellulose modification: the future in perspective.

This chapter is adapted from the following literature:

K.N. Onwukamike, S. Grelier, E. Grau, H. Cramail, M.A.R. Meier, Critical Review on Sustainable Homogeneous Cellulose Modification: Why Renewability is not enough, *ACS Sustainable. Chem. Eng.* **2019**, 7(2), 1826.

With kind permission from the American Chemical Society (ACS), copyright © 2019.

https://pubs.acs.org/doi/10.1021/acssuschemeng.8b04990

Notice: Further re-use of this material should be directed to the American Chemical Society (ACS).
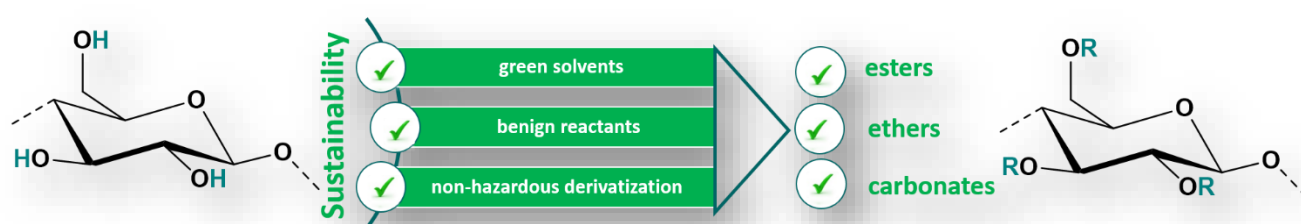
2.5.1 Abstract

As we passed the 20th anniversary of the publication of the Twelve Principles of Green Chemistry, the sustainable modification of cellulose, being the most abundant bio-based polymer, is certainly worth considering. Many researchers work on an efficient valorization of this renewable resource due to its manifold and promising application possibilities, but very often the use of non-sustainable approaches (i.e. solvents, reactants and modification approaches) only addresses the renewability aspect of cellulose, while neglecting most or all of the other principles of Green Chemistry. In this chapter, the use of E-factors together with basic toxicity information have been employed to compare between various approaches for homogeneous cellulose modification. This approach, though simple and certainly not overarching, can provide quick and useful first sustainability assessment. Therefore, in order to achieve a truly sustainable modification of cellulose, its renewability combined with mild and efficient

reaction protocols is crucial in order to obtain sustainable materials that are capable of reducing the overall negative impact of today's fossil-based polymeric materials.

2.5.2 Introduction

The importance of cellulose as a key raw material has been presented in **Chapter 2.4**, though its importance over the last century has been largely diminished by cheaper crude oil-derived polymers. However, in recent times, an increasing awareness of the environmental impact of fossil fuels has led to an increased interest in renewable resources such as cellulose. Coupled with having good mechanical and thermal properties, cellulose is also biodegradable, biocompatible, does not compete with food supply.[26] However, despite its abundance, it suffers from insolubility in common solvents, including water. Furthermore, the absence of any thermal transition makes it non-processable. Both characteristics, which can be attributed to the strong *intra-* and *inter*-molecular hydrogen bonds,[26] prevent a sustainable use. Thus, only solvents capable of interrupting these hydrogen bonds are capable of solubilizing cellulose. However, most of these "cellulose solvents" [i.e. *N,N*-dimethylacetamide-lithium chloride (DMAc-LiCl),[92] dimethyl sulfoxide-tetrabutyl ammonium fluoride (DMSO-TBAF),[93] or *N*-methylmorpholine-*N*-oxide (NMMO)[94] are either toxic (Acute toxicity $LD_{50, rat}$, DMAc = 4300 mg/kg, LiCl = 526 mg/kg), harmful (TBAF causes severe skin burn and eye damage), thermally unstable (NMMO),[95,96] and/or difficult to recycle and therefore not sustainable.

One way to introduce solubility as well as processability to cellulose is through chemical modification of its three hydroxyl groups (per anhydroglucose unit, AGU).[97] Such modifications, homogeneous or heterogeneous, have been investigated over the past years. Via the heterogeneous route, cellulose modifications such as esterification (cellulose esters; acetates),[98] etherification (cellulose ethers; carboxyl methyl cellulose, methyl cellulose),[99,100] silylation (silyl cellulose),[101,102] phosphorylation (cellulose phosphates),[103] and nitration (nitrocellulose)[104] are more common. The resulting cellulose derivatives cover a wide range of applications, including textile applications, cigarette filters, transparent film support in optical displays (cellulose acetates),[105,106] cosmetics, pharmaceutical applications (carboxyl methyl cellulose, methyl cellulose),[99,100] and biomedical/orthopedic applications (cellulose phosphates).[103] Nitrocellulose of lower nitrogen contents are used as protective

coatings, while higher nitrogen content samples find applications as explosives and propellants.[104]

Heterogeneous modifications are widely employed in industry since complete cellulose solubilization is not required, thus making the process much easier to apply.[107] These processes typically use over-stoichiometric amounts of reactants as well as acids or bases for the activation of the cellulose, thereby generating large amounts of waste. In addition, control over the degree of substitution (DS) of the resulting modified cellulose is absent or difficult to achieve. In line with the Twelve Principles of Green Chemistry, which encourage the use of catalysis over stoichiometric reactants as well as avoidance of waste,[18,108] homogeneous approaches are a promising option offering the use of less reactants and resulting in a better control of the DS and therefore of the obtained material properties. However, overcoming the poor solubility of cellulose is a prerequisite. Thus, in order to keep the overall process of cellulose transformation as sustainable as possible, identifying green solvents for its solubilization and subsequent functionalization becomes a necessity.

2.5.3 Towards green solvents for cellulose

Identifying the criteria for a solvent to be considered green is usually not trivial and cannot be generalized. Notwithstanding, most researchers agree that a solvent for cellulose should (i) offer a low vapor pressure to enable easy recycling and re-use, (ii) be non-toxic, and (iii) if possible, be bio-derived.[109] Furthermore, if these conditions are fulfilled, the energy requirement (time and temperature) of the solubilization process is equally important as it has an inherent carbon footprint. However, finding a solvent that meets all these criteria is not easy. Thus, a more general definition for a green solvent is one that leaves the least negative environmental and health footprint.[110] An easy tool, which can be employed to evaluate the synthetic process of the solvent is the Environmental factor (E-factor) and was developed in the late 1980's by Sheldon and co-workers.[17] It evaluates the amount of waste generated by the process, thereby aiding early decision making between alternative processes. An ideal sustainable process should have an E-factor of zero (no generation of waste). Also closely related to the E-factor is the atom economy developed by Trost, allowing the evaluation of the synthetic process by calculating how many atoms of the starting materials end up in the desired product.[111] However, in order to further consider the

environmental, safety and health aspects of these solvents, the ESH (environmental, health and safety) green metrics seem more useful. They can be employed to choose between different solvents.[112] Fischer *et al.* successfully applied this approach in combination with a life cycle analysis (LCA) to 26 organic solvents in order to identify those with the least environmental, safety and health concerns.[110] In their report, the potential solvent effects were classified into three categories with three sub-categories as follows: i) safety hazards (release potential, fire/explosion, reaction/decomposition), ii) health hazards (acute toxicity, irritation, chronic toxicity), iii) environmental hazards (persistency, air hazard, water hazard). For each subclass, an index between 1 and 0 was calculated, thereby giving an overall between 0 and 9 for each solvent. In this way, they showed that simple alcohols, such as methanol and ethanol with an overall score of ~2.5 were the greenest choices, followed by ethyl acetate with an overall score of ~3.0. The alkanes (heptane and hexane) and tetrahydrofuran had overall scores of ~4.0. On the high side were acetic acid (~4.5), dioxane (~5.0) and formaldehyde (~5.5), which were the least green solvents. Furthermore, when the EHS approach was combined with an LCA assessment, solvents such as THF and cyclohexanone with high cumulative energy demand (CED) for their synthesis coupled with their low environmental credit value from possible incineration makes them the least green solvents.[110] However, a discrepancy between what researchers perceive as green solvents compared to what class of solvents they work with, seems to persist. This became obvious in 2011, when Jessop conducted a survey among researches working in the field of green solvents. In this survey, the researchers were asked to choose what class of solvents would have the highest impact on an overall decrease in environmental damage.[113] To his surprise, while the majority of the researchers chose mostly CO_2 and water as solvents, this contradicted the mostly employed ionic liquid solvents as reported in 2010.[113] As many researchers mostly evaluate the success of a reaction based on yield, conversion and selectivity, a less green solvent will easily be chosen if it meets these criteria compared to a greener alternative. Hence, while a greener solvent might be interesting, there is the need to evaluate the entire process in order to avoid an "environmental burden shift" further down in the process cycle. Therefore, sustainability assessments are necessary, as they take into consideration the entire process. To fully describe the sustainability of a process, a life cycle assessment (LCA) is advised. However, it takes a considerable amount of time and the absence of data also makes its implementation challenging, at least in

everyday academic laboratory work. However, by critically evaluating a given process, it is possible to identify better options (i.e. solvent, reactant and functionalization method), which will make the process more sustainable. The latter approach will be applied in this section on selected chemical modification procedures reported for cellulose. Therefore, not only the greenness of the solvent; but rather the entire process during cellulose transformation will be considered in order to identify more sustainable alternatives.

2.5.4 Methodology

As mentioned in **Chapter 2.5.3**, LCA analysis is necessary to fully assess the sustainability of a given process, thereby allowing for an accurate comparison of different procedures. However, the lack of necessary data makes their application very difficult and time consuming. This is most likely also the reason that so far no comparative study investigating the sustainability between different cellulose modification protocols is available. In this regard and to be able to at least choose between alternative options in an everyday laboratory work situation, the use of E-factors is encouraged as a simple but very meaningful metric for a first basic evaluation.

The E-factor can be calculated from eq.1 as follows.[17]

$$E - factor = \frac{\text{Weight of raw materials} - \text{Weight of desired product}}{\text{Weight of desired product}} \dots\dots\dots\dots\dots\dots\dots\dots\dots\dots\dots \text{eq.1}$$

In addition, the toxicity data of the used chemicals have been included to guide the selection of certain processes. In this way, admittedly a very basic, yet meaningful first assessment of the procedure can be performed quickly. The goal here is to encourage researchers working on this very interesting biopolymer to consider not only the renewability aspect, but also the entire transformation process to promote sustainability. In this regard, E-factors will be employed to compare the various homogeneous cellulose modifications and also address toxicity issues where necessary.

In order to avoid any misunderstanding, it is important to explicitly mention the limitations of this approach: In this chapter, the use of E-factors combined with toxicity information is used in order to compare the sustainability between different homogeneous cellulose modification procedures, but please be reminded that

E-factors report *how* much waste is generated during a chemical transformation, but not the *type* of waste. Generally, solvents often contribute most to the E-factor. To overcame this limitation, a comparison was made between E-factors for procedures that reported a solvent recovery, thus pointing out the importance of using recyclable solvents. Most importantly, E-factors do not consider the toxicity of the reactants, products, or waste. To overcome this limitation, available toxicity information of some of the reactants have been included. Despite these limitations, E-factors offer an easy, yet reliable first-step in accessing the sustainability. More thorough comparisons would require comprehensive LCA calculations, but these are not available and cannot be simply obtained from the reported literature data. At the end, the goal is to challenge other researchers working on this interesting biopolymer to include at least basic sustainability considerations, as introduced here, in their future research.

Estimation of E-Factor from selected reports

Approximations:

100 % yield is considered for all reports to avoid the limitation from the absence of this data in some of these reports as well as to estimate the lowest possible E-factor possible through the given process.

1. Hindi and Abohassan.[98]

Heterogeneous approach

Raw materials: Cellulose (cotton fiber) = 2 g, glacial acetic acid = 36.75 g, 98 % H_2SO_4 = 0.74 g, acetic anhydride (9 eq. per AGU) = 10.8 g

Total raw materials: 50.29 g

Obtained DS: 2.86

Average molecular weight of cellulose acetate repeating unit: [162 + (42 x 2.86)] = 282.1 g/mol

Expected product for 2 g cellulose = 3.48 g

$$\mathrm{E-factor} = \frac{50.29 \ - 3.48}{3.48} = \ 13.5$$

Total solvent (glacial acetic acid) weight = 36.75 g

$$\text{Solvent contribution to E} - \text{factor} = \frac{\text{weight of solvent}}{\text{total weight of raw material}} \text{ x E} - \text{factor}$$

$$\dots = \frac{36.75}{50.29} \text{ x } 13.5 \ = \ 9.9 \ (73 \ \%)$$

2. Liu *et al.*[114]

Heterogeneous approach

Raw materials: Cellulose pulp = 0.5 g, DMSO = 11.0 g, DBU = 1.53 g, isopropenyl acetate (16 eq. per AGU) = 4.56 g

Total raw materials: 17.59 g

Obtained DS: 3.0

Average molecular weight of cellulose acetate repeating unit: [162 + (42 x 3.0)] = 288.0 g/mol

Expected product for 0.5 g cellulose = 0.89 g

$$\text{E} - \text{factor} = \frac{17.59 \ - 0.89}{0.89} = \ 18.9$$

Total solvent (DMSO) weight = 11.0 g

$$\text{Solvent contribution to E} - \text{factor} = \frac{11.0}{17.59} \text{ x } 18.9 \ = \ 11.8 \ (63 \ \%)$$

3. Guo *et al.*[115]

Homogeneous approach

Raw materials: Cellulose (MCC) = 0.4 g, $[Amim]^{+}[Cl^{-}]$ = 10.0 g, acetic anhydride (5 eq. per AGU) = 1.26 g

Total raw materials: 11.66 g

Obtained DS: 2.74

Average molecular weight of cellulose acetate repeating unit: [162 + (42 x 2.74)] = 277.1 g/mol

Expected product for 0.4 g cellulose = 0.68 g

$$\text{E} - \text{factor} = \frac{11.66 \ - 0.68}{0.68} = 16.1$$

Total solvent recovered (100 %) weight = 10.0 g

$$E - \text{factor after solvent recovery} = \frac{1.66 - 0.68}{0.68} = 1.4 \ (91 \ \% \ \text{decrease})$$

4. Heinze and Barthel.[116]

Homogeneous approach

a). Using acetic anhydride

Raw materials: Cellulose (MCC) = 0.5 g, $[C_4mim]^+[Cl^-]$ = 4.5 g, acetic anhydride (10 eq. per AGU) = 2.52 g

Total raw materials: 7.53 g

Obtained DS: 3.0

Average molecular weight of cellulose acetate repeating unit: [162 + (42 x 3.0)] = 288.0 g/mol

Expected product for 0.5 g cellulose = 0.89 g

$$E - \text{factor} = \frac{7.53 - 0.89}{0.89} = 7.5$$

Total solvent recovered (100 %) weight = 4.5 g

$$E - \text{factor after solvent recovery} = \frac{3.03 - 0.89}{0.89} = 2.4 \ (68 \ \% \ \text{decrease})$$

b). Using acetyl chloride

Raw materials: Cellulose (MCC) = 0.5 g, $[C_4mim]^+[Cl^-]$ = 4.5 g, acetyl chloride (5 eq. per AGU) = 1.20 g

Total raw materials: 6.20 g

Obtained DS: 3.0

Average molecular weight of cellulose acetate repeating unit: [162 + (42 x 3.0)] =

288.0 g/mol

Expected product for 0.5 g cellulose = 0.89 g

$$E - factor = \frac{6.20 - 0.89}{0.89} = 6.0$$

Total solvent recovered (100 %) weight = 4.5 g

$$E - factor\ after\ solvent\ recovery = \frac{1.7 - 0.89}{0.89} = 0.9\ (85\ \%\ decrease)$$

c). Using lauroyl chloride

Raw materials: Cellulose (MCC) = 0.5 g, $[C_4mim]^+[Cl^-]$ = 4.5 g, lauroyl chloride (3 eq. per AGU) = 2.02 g

Total raw materials: 7.02 g

Obtained DS: 1.54

Average molecular weight of cellulose laurate repeating unit: [162 + (182.17 x 1.54)]

= 442.5 g/mol

Expected product for 0.5 g cellulose = 1.37 g

$$E - factor = \frac{7.02 - 1.37}{1.37} = 4.1$$

Total solvent recovered (100 %) weight = 4.5 g

$$E - factor\ after\ solvent\ recovery = \frac{2.52 - 1.37}{1.37} = 0.8\ (80\ \%\ decrease)$$

5. Kilpeläinen *et al.*[117]

Homogeneous approach

a). Using acetic anhydride

Raw materials: Cellulose (PHK pulp) = 0.5 g, $[DBNH]^+OAc^-$ = 10 g, acetic anhydride (3 eq. per AGU) = 0.76 g, 0.1 mol DBN = 0.67 g

Total raw materials: 11.93 g

Obtained DS: 2.80

Average molecular weight of cellulose acetate repeating unit: [162 + (42 x 2.8)]

= 279.6 g/mol

Expected product for 0.5 g cellulose = 0.86 g

$$E - factor = \frac{11.93 - 0.86}{0.86} = 12.9$$

Total solvent recovered (80 %) weight = 8.0 g

$$E - factor\ after\ solvent\ recovery = \frac{3.93 - 0.86}{0.86} = 3.6\ (72\ \%\ decrease)$$

b). Using vinyl acetate

Raw materials: Cellulose (PHK pulp) = 0.5 g, [DBNH]+OAc- = 10 g, vinyl acetate (3 eq. per AGU) = 0.8 g

Total raw materials: 11.3 g

Obtained DS: 1.58

Average molecular weight of cellulose acetate repeating unit: [162 + (42 x 1.58)] =

228.4 g/mol

Expected product for 0.5 g cellulose = 0.70 g

$$E - factor = \frac{11.93 - 0.7}{0.7} = 15.1$$

Total solvent recovered (80 %) weight = 8.0 g

$$E - factor\ after\ solvent\ recovery = \frac{3.3 - 0.7}{0.7} = 4.1\ (75\ \%\ decrease)$$

c). Using vinyl propionate

Raw materials: Cellulose (PHK pulp) = 0.5 g, [DBNH]+OAc- = 10 g, vinyl propionate (3 eq. per AGU) = 0.93 g

Total raw materials: 11.43 g

Obtained DS: 1.34

Average molecular weight of cellulose propionate repeating unit: [162 + (56 x 1.34)]

= 237.0 g/mol

Expected product for 0.5 g cellulose = 0.73 g

$$E-\text{factor} = \frac{11.43 - 0.73}{0.73} = 14.7$$

Total solvent recovered (80 %) weight = 8.0 g

$$E-\text{factor after solvent recovery} = \frac{3.43 - 0.73}{0.73} = 3.7 \ (75 \ \% \ \text{decrease})$$

d). Using isopropenyl acetate

Raw materials: Cellulose (PHK pulp) = 0.5 g, [DBNH]+OAc- = 10 g, isopropenyl acetate (3 eq. per AGU) = 0.93g

Total raw materials: 11.43 g

Obtained DS: 2.97

Average molecular weight of cellulose acetate repeating unit: [162 + (42 x 2.97)] =

286.7 g/mol

Expected product for 0.5 g cellulose = 0.89 g

$$E-\text{factor} = \frac{11.43 - 0.89}{0.89} = 11.8$$

Effect of solvent recovery on E-factor

Total solvent recovered (80 %) weight = 8.0 g

$$E-\text{factor after solvent recovery} = \frac{3.43 - 0.89}{0.89} = 2.9 \ (75 \ \% \ \text{decrease})$$

6. Xie and Liu *et al.*[118]

Homogeneous approach

Raw materials: Cellulose (MCC) = 1.3 g, DMSO = 14.4 g, DBU = 7 g, methanol (1.5 g), acetic anhydride (3.6 eq. per AGU) = 2.86

Total raw materials: 27.06 g

Obtained DS: 2.94

Average molecular weight of cellulose acetate repeating unit: [162 + (42 x 2.94)] =

285.5 g/mol

Expected product for 1.3 g cellulose = 2.29 g

$$E - factor = \frac{22.06 - 2.29}{2.29} = 10.8$$

Total solvent recovered (DMSO = 92 %, DBU = 91 %) weight = 19.62 g

$$E - factor\ after\ solvent\ recovery = \frac{7.44 - 2.29}{2.29} = 2.2\ (80\ \%\ decrease)$$

7. Xie *et al.*[119]

Homogeneous approach

Raw materials: Cellulose (pulp) = 0.4 g, DMSO = 6.1 g, DBU = 1.2 g, acetic anhydride (5 eq. per AGU) = 1.3 g

Total raw materials: 9.0 g

Obtained DS: 2.89

Average molecular weight of cellulose acetate repeating unit: [162 + (42 x 2.89)]

= 283.4 g/mol

Expected product for 0.4 g cellulose = 0.7 g

$$E - factor = \frac{9.0 - 0.7}{0.7} = 11.9$$

Total solvent recovered (DMSO = 93 %, DBU = 91 %) weight = 6.76 g

$$E - factor\ after\ solvent\ recovery = \frac{2.24 - 0.7}{0.7} = 2.2\ (82\ \%\ decrease)$$

8. Meier and Cramail *et al.*[120]

Homogenous approach

Raw materials: Cellulose (MCC) = 0.25 g, DMSO = 5.5 g, DBU = 0.7 g, High oleic sunflower oil (3 eq. per AGU) = 4.0 g

Total raw materials: 9.75 g

Obtained DS: 1.54

Average molecular weight of fatty acid cellulose ester (FACE) repeating unit: [162 + (799 x 1.59)] = 1432.4 g/mol

Expected product for 0.25 g cellulose = 2.21 g

$$E - factor = \frac{9.75 - 2.21}{2.21} = 3.4$$

2.5.5 Homogeneous cellulose modification

Many reports exist on the homogeneous modification of cellulose, mainly describing esterification/transesterification, alkoxycarbonylation and etherification approaches. Generally, the advantages of a homogeneous modification are a better control over the degree of substitution and regioselectivity (both in terms of primary vs. secondary OH-groups as well as in terms of a homogeneous functional group distribution along the polymer chain), leading to more defined cellulose derivatives with improved and tuneable material properties. However, even a basic sustainability assessment is usually not incorporated in most of these studies. Considering that the utilization of renewable resources is not enough to ensure sustainability,[121] in this chapter, a critical assessment will be made regarding recent reports on the modification of cellulose that have the potential to increase sustainability. In this regard, selected examples of reports on homogeneous cellulose modification will be discussed in terms of the solvent used and its recycling/re-usability, the type of derivatization agent and its equivalents employed. The focus thereby is on new developments using ionic liquids as well as CO_2 switchable solvent systems. In addition, the choice of chemical modification route employed is essential to ensure an overall sustainability of the process. In essence, in reviewing these reports, the principles of Green Chemistry as proposed by Anastas and Warner[18] will be highlighted and discussed. Moreover, E-factors are estimated from reported synthesis protocols (see **Chapter 2.5.4**) and used for quantitative comparison herein. A general overview of reports on homogeneous cellulose modification is shown in **Scheme 5**, focusing on ionic liquids and CO_2 switchable solvents systems.
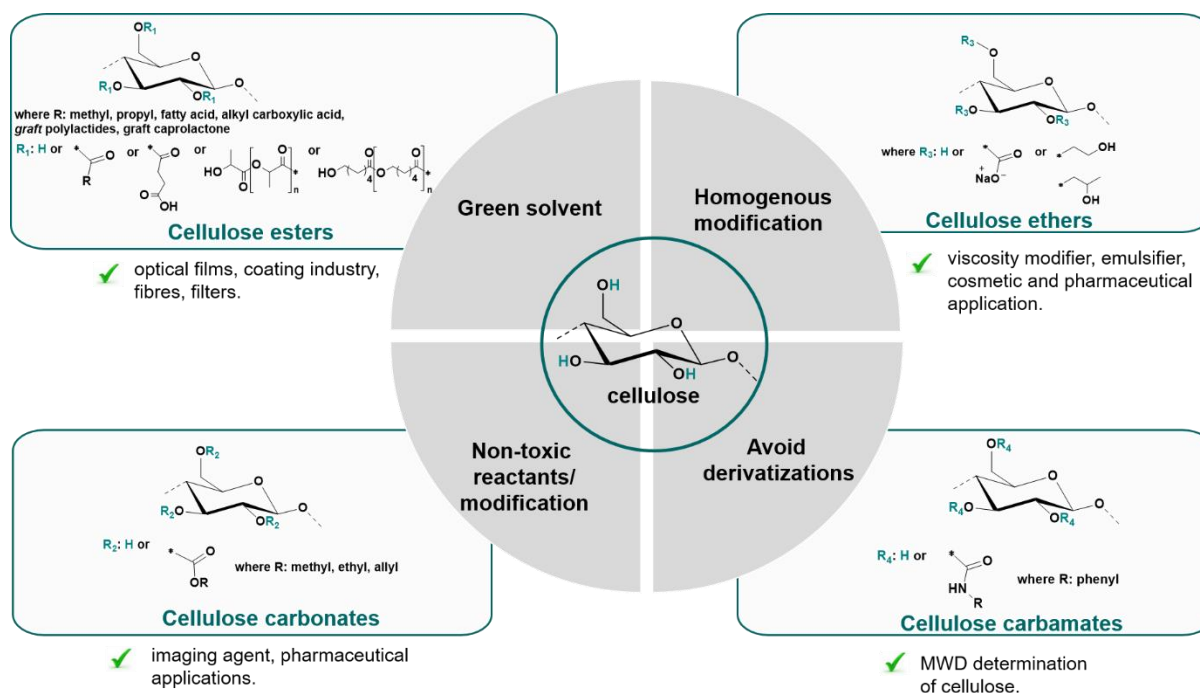
Scheme 5: Cellulose derivatives *via* homogeneous modification in ionic liquids or CO_2 switchable solvent systems.

Esterification and Transesterification

Cellulose esters are among the most important and common forms of cellulose derivatives. Cellulose esters such as cellulose acetate (CA), cellulose acetate propionate (CAP) and cellulose acetate butyrate (CAB) have long been a key player in the coating industry, where they improve cold-crack resistance, act as stable carriers of metallic pigments as well as improve polishability.[106] Furthermore, cellulose esters are employed as stable and safe excipients in the pharmaceutical industries, where they aid in controlled drug release.[106] Cellulose triacetate (CTA) finds application as a transparent film support for light-sensitive emulsions used in optical displays.[26,106] In addition, cellulose acetates (CA) are widely employed as cigarette filters,[122] as well as in textile manufacture.[105]

Typically, cellulose esters such as cellulose acetates are synthesized industrially *via* (initially) heterogeneous approaches using activated acid derivatives (acetic anhydride) in acetic acid as solvent.[107,123] Using the data provided from such an approach reported by Hindi and Abohassan,[98] an E-factor of 13.5 was estimated for the process, with the solvent (glacial acetic acid) accounting to 73 % of this amount (see **Chapter 2.5.4** for calculation). This clearly shows that solvents contribute significantly to the waste generated during chemical synthesis. Therefore, identifying

recyclable and re-usable solvents is paramount to ensure sustainability. Notwithstanding, this approach is considered more attractive for the industry compared to homogeneous routes, as it avoids the challenge of solubilizing the cellulose. However, this comes with concerns such as the over-stoichiometric use of derivatization agent and the use of sulphuric acid as catalyst to activate the cellulose hydroxyl groups, leading to generation of waste. Furthermore, an inhomogeneous distribution of the functional groups along the cellulose chain as well as hydrolysis of the polymeric chains are unavoidable with this approach. Liu and co-workers reported another method for heterogeneous acetylation of cellulose in DMSO.[114] Herein, DBU was used quantitatively (3 eq. per AGU of cellulose). A DS of 3.0 was reached after 12 h for a reaction performed at 110 °C. However, an excess (16 eq. per AGU of cellulose) of an activated acid derivative (isopropenyl acetate; acute oral toxicity $LD_{50, rat}$ = 3,000 mg/kg) was employed. The calculated E-factor of this process is rather high (18.9), thereby generating even more waste than the typical heterogeneous approach (see **Table 3** for comparison). On the other hand, homogeneous acetylation of cellulose has been reported in classic cellulose solvents such as DMAC-LiCl,[92] and TBAF-DMSO,[93] but their toxicity and difficult recyclability make them non-sustainable (see general considerations in **Chapter 2.5.3**). Therefore, the greener cellulose solvents, such as ionic liquids and the more recently reported CO_2 switchable solvent system, will be the focus of the current discussion.

Ionic liquids are a class of solvents defined as molten salts with melting points below 100 °C.[124,125] They are a broad class of solvents and typically consist of a relatively large acidic cation and a smaller basic anion. Graenacher had earlier reported the use of molten salts (alkyl pyrimidinium chlorides) for solubilizing cellulose.[126] However, since the melting point of such salts is above 100 °C, they are not classified as "ionic liquids" as currently defined. Ionic liquids did not gain much interest as cellulose solvents until the report of Rogers *et al.*, where cellulose solubilization was demonstrated in the ionic liquid 1-*N*-butyl-3-methylimidazolium chloride [C_4mim]$^+$[Cl$^-$] without any derivatization.[77] Due to their very low vapour pressure and possible recyclability, ionic liquids have been promoted as green solvents for cellulose.[127,128] Mikkola *et al.* reported a comprehensive review on the application of ionic liquids for cellulose solubilization.[129] Their review addressed the relationship between the structure of ionic liquids and their solubilization capacity towards cellulose,

lignocellulose and lignin. The groups of El Seoud and Heinze reviewed the application of ionic liquids for carbohydrate modification such as simple sugars, cyclodextrin, starch, cellulose and chitin/chitosan.[130] In addition, Heinze and Liebert reviewed the applications of ionic liquids based on imidazolium, pyridinium and ammonium cations for the homogeneous modification of cellulose, such as esterification, etherification and carbanilation.[131] Furthermore, cellulose blend preparation, in addition to typical chemical modifications routes for cellulose such as esterification, etherification, sulfation, silylation, or *grafting from* approaches, have been well covered in the review by Mercerryes and co-workers.[132] Generally, the most employed ionic liquids for cellulose modification consist of dialkyl imidazolium cations along with acetate or halogenide anions. A comparison of their dissolution ability, alongside some of their basic characteristics is summarized in **Table 2**.

Table 2: Names and dissolution ability of frequently employed ionic liquids for cellulose solubilization.

Name	Melting point (°C)	Cellulose type dissolution ability	Challenge
1-*N*-ethyl-3-methylimidazolium acetate	< -20	a) Eucalyptus pulp (DP 569), 13.5 wt. %, 85 °C, 1-3 h.[133] b) Avicel PH 101 (DP 398) 8 wt.%, 100 °C, 15min-1 h.[134]	not inert, easily contaminated *via* the acetate anion.[135]
1-*N*-butyl-3 methylimidazolium chloride	70-73	a) Dissolving pulp (DP 650) 10 wt.%, 100 °C, 25 wt.% (microwave heating, 2-5 s pulses at 70 °C).[77] b) Eucalyptus pulp (DP 569) 13.6 wt.%, 85 °C, 1-3 h.[133] c) Avicel (DP 286) 18 wt.%, 80 °C, 12 h.[116]	slightly toxic;[136] $[C_4mim]^+$ cation reacts with reducing end of the cellulose.[137]
1-*N*-allyl-3-methylimidazolium chloride	49-50	Dissolving pulp (DP 650) 5 wt.%; 80 °C and 30 min, 15 wt.%; 100 °C above 1 h.[138]	contains reactive allylic function.[131]
1-*N*-ethyl-3-methylimidazolium chloride	80	a) Avicel PH 101 (DP 398) 10-14 wt.%, 100 °C, 15 min to 2 h.[134] b) Avicel (DP 286) 12 wt.% , 80 °C, 12 h.[116]	possible proton abstraction at the C2-position of the $[C_2mim]^+$ cation under basic reaction conditions.[131]
1-*N*-butyl-3-methylimidazolium acetate	< -20	a) Eucalyptus pulp (DP 569), 13.5 wt. %, 85 °C, 1-3 h.[133] b) Avicel PH 101 (DP 398) 12 wt.%, 100 °C, 15 min to 1 h.[134]	non inert, $[C_4mim]^+$ cation reacts with reducing end of the cellulose.[139]
1-*N*-butyl-3-methylimidazolium bromide	77	Avicel PH 101 (DP 398) 2-3 wt.%, 100 °C, 15 min to 1 h.[134]	$[C_4mim]^+$ cation reacts with reducing end of the cellulose.[137]

Despite their wide success as cellulose solvents, it is worth noting that ionic liquids are not without limitations.[135] Among these is their non-inertness (especially those with acetate anion such as $[C_2mim]^+[OAc^-]$),[135,139] or corrosiveness and slight toxicity as in the case of $[C_4mim]^+Cl^-$ (oral acute toxicity $LD_{50, \, rat}$ = 50-300 mg/kg).[136] The non-inertness as well as the usually promoted "non-volatility" of ionic liquids makes their

recovery difficult. Nonetheless, some reports have demonstrated the recovery and re-use of ionic liquids. BASF, which have a patent for [C$_2$mim]$^+$[OAc]$^-$, reported the recovery of over 95 % of the ionic liquid *via* high vacuum (1 mbar) distillation after application for cellulose fibre spinning.[140] However, no information about the purity of the recovered ionic liquid nor how many times it could be re-used was provided. From a sustainability point of view, the large carbon footprint of their synthesis[130] can only be justified if they can be recycled and re-used repeatedly. In addition, a careful choice of ionic liquids is necessary to avoid any possible side reaction that will make their recovery more problematic. Typically, cellulose solubilized in ionic liquid results in viscous solutions that might be challenging for subsequent modification approaches. Thus, DMSO, which is usually considered as a benign solvent,[141] with a relatively undetectable toxicity (acute oral toxicity LD$_{50,\text{rat}}$ = 40,000 mg/kg) is usually added (10 to 20 w/w) to reduce the viscosity.

Ionic liquids have been employed for the homogeneous acetylation of cellulose. Guo *et al.* investigated the acetylation of cellulose in the ionic liquid 1-*N*-allyl-3-methylimidazolium chloride ([Amim]$^+$[Cl$^-$]) using acetic anhydride.[142] A maximum DS of 2.74 was achieved using 5 eq. of the reactant/AGU of cellulose at 80 °C within 23 h. A good control of the DS was equally demonstrated by the variation of cellulose concentration, reactant equivalents and reaction temperature. Using data provided by the authors, an E-factor of 16.1 was estimated (see **Chapter 2.5.4**). Finally, the authors reported a recovery of the ionic liquid by distilling off the residual water after product isolation. Considering the recovery of the ionic liquid (high purity and quantitative recovery), the estimated E-factor is significantly reduced to 1.4 (91 % waste reduction due to IL recovery). This further shows the importance of using recyclable/re-usable solvents for waste minimization. According to their report, no observable difference was noticed when the recovered ionic liquid was used for new cellulose solubilization and subsequent acetylation. While this report addressed some important sustainability concerns by the use of ionic liquids (low vapour pressure solvents) and a demonstration of their recovery and re-use, the use of activated acids such as acetic anhydride is not encouraged due to their instability. Furthermore, acetic acid as side product could promote hydrolysis of the cellulose backbone. Although the reaction was reported to occur in the absence of a catalyst, subsequent studies have shown that possible impurities of imidazole and 1-methylimidazole in such ionic liquids

could act as a basic catalyst.[139] The purity of ionic liquids has been highlighted as one of its inherent challenges.[136] Reports on different batches of ionic liquids from the same manufacturer revealed a different cellulose solubilization capability and reactivity behaviour.[143] In a similar approach, Barthel and Heinze reported on the acetylation of cellulose in the ionic liquids 1-*N*-butyl-3-methylimidazolium chloride ([C_4mim]$^+$[Cl$^-$]), 1-*N*-ethyl-3-methylimidazolium chloride ([C_2mim]$^+$[Cl$^-$]), 1-*N*-butyldimethylimidazolium chloride ([C_4dmim]$^+$[Cl$^-$]) and 1-*N*-allyl-2,3-dimethylimidazolium bromide ([Admim]$^+$[Br$^-$]).[116] Cellulose (microcrystalline cellulose, sulphite spruce pulp and cotton linters) was solubilized in these ionic liquids at 80 °C for up to 12 h. The acetylation was performed using acetic anhydride or acetyl chloride in the presence or absence of pyridine at 80 °C. Cellulose solubilization was achieved within 2 h at 80 °C in [C_4mim]$^+$[Cl$^-$]. The authors reported a DS value of 3.0 within 30 min when acetyl chloride was used. From the experimental data provided, E-factors of 6.0 and 7.5 were estimated for reactions performed using acetyl chloride and acetic anhydride, respectively (see calculation in **Chapter 2.5.4**). This value shows much preference for acetyl chloride with regards to waste minimization during the modification, neglecting the type of waste formed. In addition, a maximum DS value of 1.54 was reached when fatty acid chlorides, such as lauroyl chloride, were employed (estimated E-factor = 4.1). The recovery of the ionic liquids was equally demonstrated (quantitative) by distilling off the water after product isolation. Thus, the E-factor was significantly reduced to 0.9 (reduction of 85%), 2.4 (68%) and 0.8 (80%) for acetic anhydride, acetyl chloride and lauroyl chloride, respectively. As reported, no loss in efficiency for subsequent cellulose solubilization was observed. However, care must be taken to ensure complete water removal from the recovered ionic liquid. Therefore, freeze-drying was proposed by the authors. Furthermore, the authors reported a degradation of the ionic liquids ([C_2mim]$^+$[Cl$^-$], [Admim]$^+$[Br$^-$], [C_4dmim]$^+$[Cl]) and the cellulose polymer backbone when acetyl chloride was utilized. This undesirable observation might be due to the formation of HCl as side product when acetyl chloride is used. This not only reduces the recovery yield of the ionic liquids, but also the sustainability of the process.

In 2010, MacFarlane *et al.* demonstrated the concept of distillable ionic liquids for biopolymer processing.[144] Herein, tannin extraction was achieved from certain plant species using *N,N*-dimethylammonium-*N',N'*-dimethylcarbamate (DIMCARB), which was formed by the reaction of dimethylamine and CO_2. The as-reported distillable ionic liquid reported by MacFarlane *et al.* was not able to solubilize cellulose. Therefore, an adaption of such distillable IL for cellulose solubilization was reported by Kilpeläinen *et al.*[145] In their work, they showed that a 1:1 molar ratio of an organic super base (1,1,3,3-tetramethylguadinine, TMG) with carboxylic acids such as formic, acetic or propionic acid results in an acid-base conjugate type ionic liquid that was capable of solubilizing cellulose. In the case of TMG in combination with acetic acid, the resulting $[TMGH]^+[CO_2CH_3]^-$ was capable of solubilizing 5 wt.% MCC (microcrystalline cellulose) within 10 min. at 100 °C. However, higher weight concentration (up to 10 wt.%) required much longer solubilization times (up to 20 h) at the same temperature. More interesting, this report demonstrates the recycling of this ionic liquid with high purity (over 99 %) and a recovery of over 99 % by distillation between 100-200 °C and 1.0 mm Hg (1.33 mbar) pressure. As demonstrated, above a given temperature, the formed acid-base conjugate ionic liquid dissociates, allowing the species to be recovered as a mixture as depicted in **Scheme 6**.
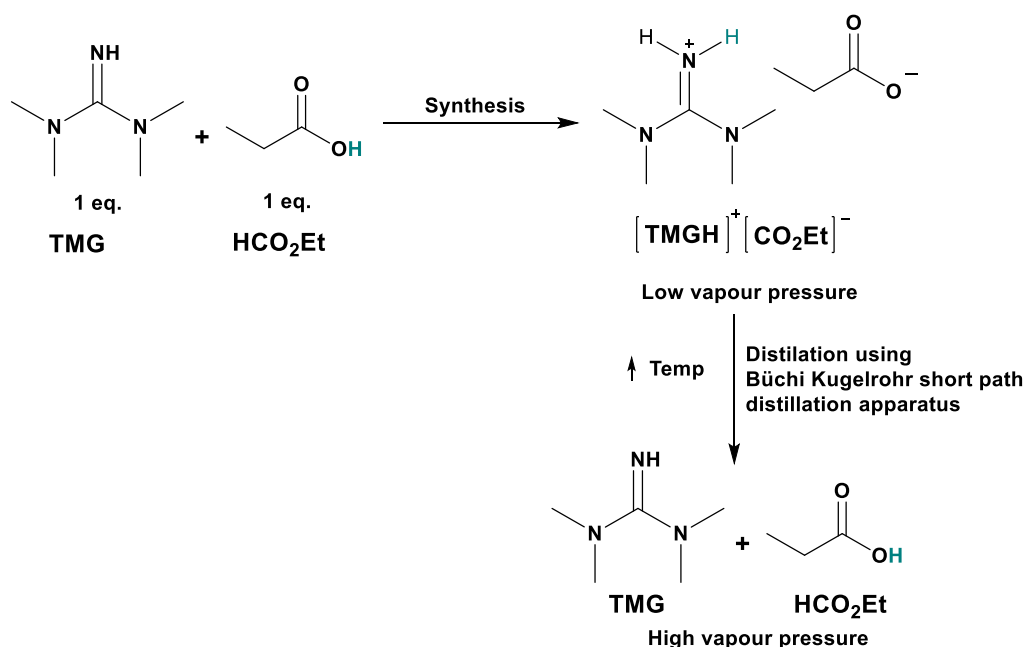
Scheme 6: Concept of a distillable ionic liquid from TMG and propanoic acid, adapted from Kilpeläinen *et al.*[145]

By applying different conditions (varying the high vacuum and temperature), this mixture could be separated into the pure starting materials. While this property is desirable for ionic liquid recovery, it also raises the question concerning the volatility of such an "ionic liquid" and its constituents (high vapour pressure). This is because low vapour pressure is considered as a key property for green solvents, a property typical for classic ionic liquids. Furthermore, care must be taken when considering such ionic-liquid systems as the required high vacuum for recycling is quite energy demanding.

In order to predict the right acid-base conjugates capable of solubilizing cellulose, Kilpeläinen and co-workers screened a series of organic bases with acetic and propionic acid. Results showed that only combinations containing super bases were capable of solubilizing cellulose.[146] Furthermore, it was discovered that a minimum proton affinity of the super base (240 kcal mol^{-1}) was required to ensure cellulose solubility.[146] Finally, from their report, both the acidity of the cation as well as the basicity of the anion were necessary for cellulose solubility.

The same authors subsequently reported the acetylation of cellulose (eucalyptus pre-hydrolysis Kraft pulp, PHK) in a similar acid-base conjugated ionic liquid.[117] In this case, the ionic liquid was formed by a 1:1 molar combination of the organic super base 1,5-diazabicyclo[4.3.0]non-5-ene (DBN) and acetic acid, resulting in the formation of [DBNH]$^+$[OAc]$^-$. Acetylation was carried out after cellulose solubilization at 70 °C for 0.5-1 h using activated acids (acetic anhydride, propionic anhydride), vinyl esters (vinyl propionate, vinyl acetate) and isopropenyl acetate. For all investigated acetylating agents, 3 eq. per AGU were employed. When using acetic anhydride, acetic acid was formed as side product, thus requiring a slight excess of the base to trap this acid and prevent possible cellulose hydrolysis. Acetone and acetaldehyde were the observed side products when isopropenyl acetate and vinyl acetate or propionate were employed, respectively. These side products could be easily removed. As reported by the authors, no extra catalyst was required compared to similar reports on acetylation of cellulose in ionic liquids that required pyridine, K_2CO_3,[147–149] or NaOH[150] as catalyst. This was attributed to the excess of the base utilized in the ionic liquid, which can act as a catalyst for the acetylation reaction. For the studies with acetic anhydride or isopropenyl acetate, a DS close to 3.0 was achieved.

For the four different acetylating agents employed, E-factors of 15.1, 14.7, 12.9 and 11.8 were estimated for vinyl acetate, vinyl propionate, acetic anhydride and isopropenyl acetate, respectively (see calculation in **Chapter 2.5.4**). These values also correlate nicely with the observed DS values as well as the reactivity of these acetylating agents (see **Table 3** for comparison). However, in case of the vinyl esters (vinyl acetate and vinyl propionate), a maximum DS of 1.58 and 1.34 was reached and could not be improved by longer reaction time, higher temperature or excess of the reactant. Finally, the recovery of the ionic liquid was demonstrated (80 % reported).[117] Thus, the estimated E-factors decreased to 3.7 (reduction of 75 %), 3.7 (75 %), 3.6 (72 %) and 2.9 (75 %) for vinyl acetate, vinyl propionate, acetic anhydride and isopropenyl acetate, respectively. The authors observed the hydrolysis of DBN during the ionic liquid recovery. To minimize this hydrolysis, they proposed the use of *n*-butanol to trap remaining water molecules before distillation. Their work addresses sustainability in many aspects from the choice of solvent, its recovery and mild acetylation conditions. However, the authors observed a decrease of the original molecular weight of the cellulose pulp (up to 1/3 decreased after esterification), which could be caused by the released acetic acid. Furthermore, the use of the highly reactive (activated) vinyl esters or isopropenyl acetate (toxic, expensive) could also lead to such degradation. In addition, these acetylating agents need to be synthesized before use, thereby increasing the carbon footprint of the entire process. For instance, vinyl acetates are typically synthesized by reacting acetylene (toxic and difficult to handle gas) with acetic acid in the gas or liquid phase using zinc or mercury catalysts.[151] However, even though this process has been broadly replaced by a gas phase reaction between ethylene (difficult to handle, toxic), acetic acid and oxygen, a metal catalyst is still needed (palladium; rare metal, expensive, toxic).[151] The use of metal catalysts as well as the special reactors required for such gas phase reactions comes with an overall negative impact regarding sustainability. Thus, improving the sustainability of esterification/transesterification processes on cellulose could be achieved *via* a direct use of simple alkyl esters that are easier to produce and to handle.

It is important to note that the acetylation of cellulose in salt melts (eutectic mixture of KSCN, NaSCN and LiSCN·H_2O) has also been reported.[152] However, in such "solvents", a very large excess of the derivatization agent (50-100 equivalents/AGU)

was required to achieve a DS of 2.4 after 3 h at 130 °C. Such excess of reagents makes the process unsustainable and not practicable.

CO_2 switchable solvent systems are a recent class of cellulose solvents. Jessop *et al.* introduced the concept of utilizing CO_2 as a switch in the presence of an organic super base such as 1,8-diazabicyclo[5.4.0]undec-7-ene (DBU) to change the solvents polarity.[153] This is of course also closely related to the above mentioned concept of distillable ILs introduced by MacFarlane.[144] However, the groups of Jerome[154] and Xie[155] simultaneously and independently introduced the application of Jessop's concept for cellulose solubilization. A closer look into their reports points out two classes of such CO_2 switchable cellulose solvents: a derivative and a non-derivative system. In the derivative approach, as shown by Jerome *et al.,*[154] cellulose could be solubilized by first transforming it into an *in-situ* formed cellulose carbonate in the presence of a super base (examples include DBN, DBU, and TMG), which thus becomes soluble in DMSO. On the other hand, Xie *et al.*[155] described the so-called non-derivative approach, where, instead of using cellulose directly, simple alcohols such as methanol, hexanol or ethylene glycol are used. In this case, the so-called CO_2 switchable solvent is prepared first by the reaction of the alcohol in the presence of a super base and DMSO. The formed solvent is then used for solubilizing cellulose. These two approaches are shown in **Scheme 7**.

Derivative approach
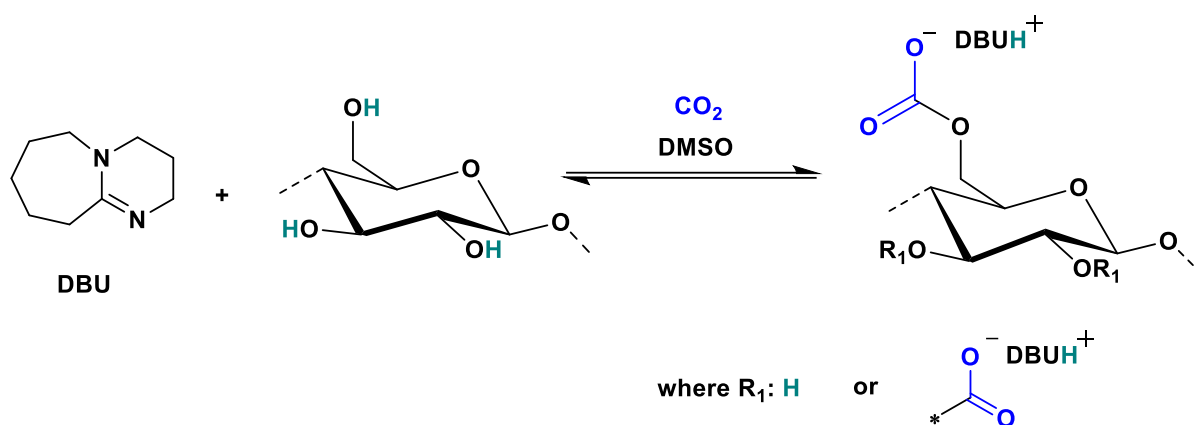
Non-derivative approach
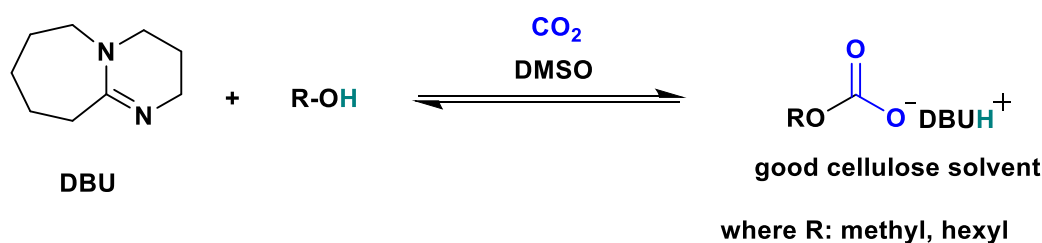
Scheme 7: Derivative (top) and non-derivative (bottom) approach of CO_2 switchable solvent system, adapted from Jerome *et al.*[154] and Xie *et al.*[155]

In both approaches, the cellulose could be regenerated by simply releasing the CO_2 pressure, also allowing the recovery of the solvent for new solubilization. Furthermore, the relatively low cost of the entire solvent system compared to traditional ionic liquids and the lower toxicity compared to DMAC-LiCl (oral acute toxicity $LD_{50,rat}$ DMAc = 4,300 mg/kg, LiCl = 526 mg/kg, DMSO = 40,000 mg/kg, DBU < 683 mg/kg) makes these solvents highly interesting and also more sustainable. It is important to point out that DBU itself is slightly toxic, however it accounts for less than 10 mol.% (with respect to DMSO) in the solvent system. In many cases, the so-called non-derivative approach employing the use of simpler alcohols is not necessary. The extra step and component involved in this approach generates more waste and side reactions become unavoidable. A detailed study of the derivative CO_2 solvent system using DBU as super base has been previously described (**Chapter 4**). In this optimized solvent system, complete cellulose solubilization (up to 8 wt.%) was achieved at 30 °C within 10-15 min under low CO_2 pressure (2-5 bar).[156] Furthermore, the presence of the *in-situ* formed cellulose carbonate anion was unambiguously proven by trapping it with electrophiles and by *in situ* IR spectroscopy.[156] The fast solubilization time and milder

conditions could pave a way for a wide spread utilization for various homogeneous modification approaches of cellulose.

The utilization of this solvent system for homogeneous cellulose modification has been reported. In this regard, the groups of Xie and Liu employed the non-derivative CO_2 switchable solvent system for the acylation of cellulose with acetic anhydride (5 eq. per AGU) under mild conditions.[118] Herein, the non-derivative cellulose solvent was formed by the reaction between methanol, DBU and CO_2. High DS values (2.94) of cellulose acetates could be reached using acetic anhydride. The E-factor for this process was estimated to be is 10.8 (see **Chapter 2.5.4**). Furthermore, other types of cellulose esters such as cellulose butyrate and propionate, could be equally synthesized. Interestingly and opposed to other solvent systems, such as ionic liquids or DMAC-LiCl, where a catalyst was necessary for such modifications, the authors showed that the acylation in this solvent system required no extra catalyst. This was attributed to the dual role of DBU, which is part of the solvent system and equally acts as an organocatalyst for the acylation step. It is also important to mention the demonstration of recovery of the solvent system, which is an important consideration for sustainability. This was achieved *via* vacuum distillation to separate the DMSO (92 % recovery) followed by basic extraction of the DBU (91 % recovery) using ethyl acetate. Considering the recovered solvent system (DMSO and DBU), the E-factor decreases to 2.2 (reduction of 80 %). The recovered DMSO and DBU could be re-used for new solubilization and subsequent acylation of cellulose. However, a slight drawback of this procedure was the observed side reaction between methanol and acetic anhydride, leading to the formation of methyl acetate. Even though this side product could be isolated with a yield of 82 %, it undermines the entire process since a higher equivalent of both methanol and acetic anhydride will be required to account for this loss. As mentioned earlier, the use of such non-derivative CO_2 solvent systems is thus not advisable for the modification of cellulose. As the derivative approach directly utilizes the cellulose, such undesirable side reaction can be completely avoided, thus offering an improved sustainability. The same authors also reported a fast and mild esterification of cellulose pulp (cotton) using acetic anhydride.[119] This time, the derivative CO_2 switchable solvent approach was utilized.[119] The estimated E-factor for this approach is 11.9, which is slightly higher than that reported for the non-derivative approach (10.8, before solvent recovery consideration). However, this

difference is mainly due to the higher equivalents of the acetic anhydride employed (5 eq. per AGU) compared to the previous case (3.6 eq. per AGU). From own experiments, working with the derivative approach, much less equivalence (3 eq. per AGU) could give similar DS. As in previous examples, no extra catalyst was required in this approach. Furthermore, a good control over the DS for the obtained cellulose esters was demonstrated by simply varying reaction parameters such as reaction time, temperature and equivalents of the acetylating agent. More so, a good recovery of the solvent system (DMSO, 93 % and DBU, 91 %) was demonstrated, leading to a decrease in the estimated E-factor to 2.2 (reduction of 82 %).

In the up to now discussed literature reports, activated acids such as acetyl chlorides, acetic anhydride or vinyl acetate, are frequently employed for the acetylation of cellulose. Some of these reactants are toxic (acetyl chloride) and require considerable synthesis effort for their production, but they are also unstable and difficult to handle compared to simple alkyl esters. Furthermore, as can be seen in some of these reports, the associated side products such as HCl or acetic acid could lead to polymer degradation and require additional base for neutralization, leading to additional waste. Therefore, in line with the Principles of Green Chemistry, the use of more benign reactants is encouraged. In this regard, the groups of Meier and Barner-Kowollik employed the use of methyl esters for the synthesis of various cellulose esters, such as cellulose butyrate and cellulose benzoates, using catalytic amounts of 1,5,7-triazabicyclo[4.4.0]dec-5-ene (TBD).[157] Although the reaction was performed in a traditional ionic liquid [C$_4$mim]$^+$[Cl$^-$], the authors demonstrated its recovery and re-use. Furthermore, the sustainability of this process could be improved by directly utilizing plant oils instead of fatty acid methyl esters (FAMEs). This approach avoids the associated derivatization steps along with the waste involved in synthesizing FAMEs from plant oils. In this light, a direct transesterification of cellulose using plant oils (high oleic sunflower oil) in the derivative DBU-CO$_2$ switchable solvent system was demonstrated (details in **Chapter 6.1**), leading to fully renewable cellulose esters in a sustainable approach.[120] A DS of 1.59 was achieved after 24 h at 115 °C when 3 equivalents of plant oil per AGU of cellulose were utilized. The calculated E-factor for this approach is 3.4, which is low compared to previous procedures (see **Table 3**) and has the additional advantage that no pre-derivatization is necessary, something not considered in the herein reported E-factors. In addition, no additional catalyst was

required as the DBU utilized in the solvent system also acted as an organocatalyst for the transesterification process. Finally, this approach was successfully transferred to different cellulose types such as microcrystalline cellulose (MCC), filter paper and cellulose pulp.

For a better comparison between the different reports discussed on cellulose esters synthesis, the estimated E-factor are shown in **Table 3** and already discussed throughout. For the purpose of simplicity and comparability, the yield of each of these reports was considered as 100% (to estimate the lowest possible E-factor, and to overcome the absence of the yield information data in some of the reports.

Table 3: Comparison between various approaches for the synthesis of cellulose esters including estimated E-factors.

Derivatization method	Acetylating agent, equivalents per AGU	Solvent	Reaction conditions	Obtained DS	[a]E-factor	Ref.
Heterogeneous	Acetic anhydride, 9	Glacial acetic acid, H_2SO_4 cat.	50-60 °C, 1-3 h	2.86	13.5	[98]
Heterogeneous	Isopropenyl acetate, 16	DMSO, DBU cat.	110 °C, 12h	2.99	18.9	[114]
Homogeneous	Acetic anhydride, 5	[Amim]+Cl-	80 °C, 23h	2.74	16.1	[142]
Homogeneous	a. Acetic anhydride, 10	[C4mim]+Cl-, 2.5 mol.% pyridine.	80 °C, 2 h	3.00	7.5	[116]
	b. Acetyl chloride, 5	[C4mim]+Cl-	80 °C, 2 h	3.00	6.0	
	c. Lauroyl chloride, 3	[C4mim]+Cl-	80 °C, 2 h	1.54	4.1	
Homogeneous	a. Acetic acid, 3	[DBNH]+OAc-	70 °C, 0.5-2 h	2.80	12.9	[117]
	b. Vinyl acetate, 3	[DBNH]+OAc-	70 °C, 0.5-2 h	1.58	15.1	
	c. Vinyl propionate, 3	[DBNH]+OAc-	70 °C, 0.5-2 h	1.34	14.7	
	d. Isopropenyl acetate, 3	[DBNH]+OAc-	70 °C, 0.5-2 h	2.97	11.8	
Homogeneous	Acetic anhydride, 3.6	MeOH-DBU-CO_2-DMSO	80 °C, 3 h	2.94	10.8	[118]
Homogeneous	Acetic anhydride, 5	DBU-CO_2-DMSO	80 °C, 5 h	2.89	11.9	[119]
Homogeneous	High oleic sunflower oil, 3	DBU-CO_2-DMSO	115 °C, 24 h	1.59	3.4	[120]

[a] calculated from experimental data of the respective references (see **Chapter 2.5.4** for details); yield for all reports considered as 100 %.

Furthermore, the solvents used during the product isolation step were not considered (to avoid complicating the calculation and inconsistencies), although this is very important for the overall sustainability of any process. As can be seen from **Table 3**, E-factor calculations could be a quick assessment tool to not only choose between the greener solvent during cellulose modification, but also the best process that takes into account the entire transformation process with the aim of minimizing waste. The calculations also clearly reveal that the employed equivalents of the reactants and the solvent itself contribute most to the E-factors. Thus, these two parameters are the most critical ones to consider in order to achieve a sustainable cellulose modification.

Functional cellulose esters

Ring opening polymerization (ROP) in a *"grafting from"* approach is a possibility to obtain functional cellulose esters. This can be achieved by using bio-derived and sustainable reactants such as lactide or ε-caprolactone. Lactide can be obtain from lactic acid (2-hydroxy propanoic acid) and is derived from sour milk or through fermentation of carbohydrates (starch or simple sugars),[158] whereas ε-caprolactone is derived from caproic acid (hexanoic acid). Industrially, it is synthesized from cyclohexanone via Baeyer-Villiger oxidation with peracetic acid. Interestingly, ε-caprolactones can also be derived from renewable resources. In this regard, the group of Heeres reported the synthesis of ε-caprolactone starting from 5-hydroxylmethylfurfural (HMF), which can be obtained from lignocellulosic biomass.[159] In a similar manner, Meier *et al.*, reported the synthesis of a series of ε-caprolactones modified at the β-position starting from 1,4-cyclohexadiene (CHD), which is a by-product from the self-metathesis of poly-unsaturated fatty acid derivatives.[160] Furthermore, Hillmyer and co-workers reported on the synthesis of modified ε-caprolactones starting from carvone which is found in spearmint (*Mentha spicata*) and caraway oils (*Carum carvi*).[161] Furthermore, the groups of Hillmyer and Dauenhauer recently reported a technical and economic viability study on the synthesis of methyl-ε-caprolactone from para-cresol derived from lignin.[162] Their approach involved two steps, starting with the hydrogenation of para-cresol to 4-methyl cyclohexanone followed by a Baeyer-Villiger oxidation to the corresponding methyl-ε-caprolactone with purity of 99.9 %. The Baeyer-Villiger oxidation was identified as the key step to achieve an economically viable product.[162]

The groups of Xie and Liu employed the DBU-CO_2 switchable solvent system for grafting of L-lactide (10 eq. per AGU) from cellulose via ROP.[163] In this report, no additional catalyst was required as the DBU again played a dual role: as part of the solvent system and equally as an organocatalyst during the ROP. A higher grafting density was obtained compared to previous reports in different solvents such as DMAC-LiCl[164] or [Amim]$^+$[Cl]$^-$.[165] Furthermore, their approach offers advantages as a lower temperature (80 °C compared to 130 °C) is employed and no additional catalyst is required.[165] Generally, the amount of catalyst, toxicity as well as possible recyclability are important to assess overall sustainability. Here, where DBU played a dual role as catalyst and part of the solvent system, consider that it is more toxic (oral acute toxicity $LD_{50,rat}$ < 683 mg/kg) than tin(II) 2-ethylhexanoate (oral acute toxicity $LD_{50,rat}$ 3,400 mg/kg), but can be easily recycled. The obtained cellulose-*g*-poly(L-lactide) reported by Liu and co-workers showed tunable T_g properties. In a similar fashion, the same authors reported on the ROP of *ε*-caprolactone (15 eq. per AGU) from cellulose in the DBU-CO_2 switchable solvent system.[166] As in the previous report, no need for any extra catalyst was required. In addition, the authors reported a high molecular substitution value (MS_{PCL} = 8.01) and grafting efficiency (84.9 %) compared to similar experiments in traditional ionic liquids.[115] Furthermore, the synthesized cellulose-*g*-PCL showed T_g values between -35 °C and -53 °C, thereby addressing the non-processability challenge of native cellulose. However, in these reports, the authors did not report any study on the recovery of the solvent system (DBU and DMSO), which is an important consideration from a sustainable point of view.

Succinylation of cellulose is another approach for obtaining functional cellulose materials bearing a pendant carboxylic acid group. In this case, succinic anhydride (which is bio-derived from sugars)[167] can be utilized. Many studies have reported the succinylation of cellulose in various solvents such as ionic liquids [C₄mim]$^+$[Cl$^-$],[168] DMAC-LiCl,[169] TBAF-DMSO[170] and tetrabutylammonium acetate-dimethyl sulfoxide (TBAA-DMSO).[171] In most of these reports, a catalyst such as 4-(dimethylamino) pyridine (DMAP)[168] or triethylamine[169] was required alongside high temperatures (100 °C) to achieve a high DS (up to 2.34). Unfortunately, no solvent recovery was described. A more sustainable approach for the succinylation of cellulose in the CO_2-DBU switchable solvent system was recently described.[172] The easy solubilization

step (30 min at 50 °C), mild reaction conditions (room temperature, 30 min), low succinic anhydride equivalents (4.5 eq. per AGU of cellulose) in combination with the absence of an additional catalyst and the demonstration of the solvent recovery (DBU, 56 % and DMSO > 90 %) makes this approach more sustainable. Interestingly, a high DS of 2.60 was achieved in this report, despite the milder reaction conditions employed without additional catalyst. Thus, this report clearly shows that sustainability principles can be fulfilled in the course of renewable resource utilization without compromising the results (here, the DS).

Alkoxycarbonylation

Cellulose carbonates are a very important class of material with potential application as imaging agents or for drug delivery.[173] However, early reports on the synthesis of cellulose carbonates employed toxic chloroformates. In addition, these chlorofomates are usually derived from phosgene, which is a toxic reagent and highly reactive reactant itself. Moreover, the use of such reagents goes along with the production of high amounts of salt waste. Thus, from a sustainable point of view, their use is not encouraged. In this regard, King *et al.* reported on using dialkylcarbonates, such as diethyl carbonate (DEC) and dimethyl carbonate (DMC), for the modification of cellulose.[174] Generally, various dialkyl carbonates can be obtained from the reaction between at least potentially renewable DMC,[175] and alcohols in the presence of catalytic amounts of TBD.[176] In their report, King *et al.* employed the two ionic liquids; 1-*N*-ethyl-3-methyl imidazolium acetate ($[C_2mim]^+[OAc]^-$) and trioctylphosphonium acetate ($[P_{8881}]^+[OAc]^-$). As with most reports utilizing ionic liquids, DMSO was added as a co-solvent to reduce the viscosity of the resulting solubilized cellulose. However, they noticed a reaction of the acetate anion of the ionic liquid with the DMC leading to the formation of methyl acetate, thus making the ionic liquid recovery very challenging. However, by using a milder recovery procedure, they were able to minimize this side reaction. Hence, while this study demonstrated the use of a more sustainable reagent for the synthesis of cellulose carbonate, it also brings to light the challenge faced by ionic liquids due to their non-inertness in some cellulose modification reactions.

As pointed out in the previous work by King *et al.*,[174] ionic liquids containing the acetate anion are more prone to contamination in the course of most reactions. One way to avoid this is to use their chloride counterparts, such as 1-*N*-butyl-3-methyl imidazolium

chloride ([C$_4$mim]$^+$[Cl$^-$]) or 1-*N*-allyl-3-methyl imidazolium chloride ([Amim]$^+$[Cl$^-$]). This has been demonstrated by Söyler and Meier.[177] In this case, diallyl carbonate was employed for the modification of cellulose in [C$_4$mim]$^+$[Cl$^-$] in the presence of DMSO as co-solvent (10 w/w.% DMSO). The obtained allyl-functional cellulose carbonate was obtained with a DS of 1.3. Utilizing the allylic functionality, a post modification *via* thiol-ene addition was achieved.[177] Interestingly, no reaction between the ionic liquid and DAC was observed, thus leading to the recovery of the ionic liquid (100 %). In this case, the resulting mixture containing ionic liquid, DMSO, unreacted DAC and allyl alcohol were separated *via* fractional distillation (200-10 mbar, 80-110 °C). Upon isolation of the lower boiling point constituents, the ionic liquid was recovered quantitatively, and was re-used for new modifications. However, it is worth mentioning that [C$_4$mim]$^+$[Cl$^-$] is slightly acidic, corrosive and shows some toxicity.[136] Therefore, its recovery after usage is strongly advised to avoid a release to the environment or other alternatives should be considered in the future.

Etherification

Carboxyl methylcellulose (CMC) is among the commercially most used derivatives of cellulose ethers and finds application as viscosity modifiers and emulsion stabilizers.[178] Heinze *et al.*, demonstrated the carboxymethylation of cellulose in the ionic liquid 1-*N*-butyl-3-methyl imidazolium chloride ([C$_4$mim]$^+$[Cl$^-$]) in the presence of DMSO as co-solvent.[179] A DS of 0.43 was reached when 1.0 equivalent of the reactant per AGU was used. Higher equivalents did not improve the DS value. The authors demonstrated the recovery and re-use of the ionic liquid. However, it is important to note that the use of sodium chloroacetate (from toxic chloroacetic acid, oral acute toxicity $LD_{50,rat}$ = 55 mg/kg) for the carboxymethylation is not sustainable. Furthermore, the use of stoichiometric amounts of NaOH in this reaction required an acidic work-up for neutralization, which further generates waste and thus further reduces the sustainability of the process.

Quaternary ammonium electrolytes (QAEs) in the presence of molecular solvents such as DMSO have also been reported for cellulose solubilization.[180] However, as mentioned earlier and using TBAF/DMSO as an example, the majority are considered toxic due to the presence of the halogen counter-ion. However, Heinze and his group reported a less toxic variant where the halogens are replaced by a carboxylate anion

(e.g. formate).[181] In this case, QAEs such as [CH$_3$N(CH$_2$CH$_3$)$_3$]$^+$[HCOO]$^-$ were obtained by quaternization of tertiary amines using benign dialkyl carbonate reagents. The efficiency of this solvent system was demonstrated for the homogeneous carboxymethylation of cellulose using sodium chloroacetate. A water soluble CMC with a DS of 1.55 was obtained.[181] Furthermore, an attempt to recover the solvent was reported. However, only the cation could be recovered, as the carboxylate anion was exchanged by the chloride ion from NaCl formed as side product, thus preventing full recovery. As in the previous examples, the use of sodium chloroacetate is not sustainable, just as the use of inorganic sodium salts, which generate salt wastes. Thus, the replacement of sodium chloroacetate as well as an organic basic catalyst that can potentially be recovered might improve the sustainability of this process. Moreover, cellulose succinates (previously described) might be suitable replacements for CMC, at least in some applications.

Hydroxyalkylation is another approach to obtain cellulose ethers. Such cellulose ethers find application in the paint and pharmaceutical industries as well as in the material construction industries.[178] By slowing down the cement hydration, they lead to improved mechanical properties.[182,183] Heinze *et al.* reported the hydroxyalkylation of cellulose using ethylene and propylene oxides.[184] The reaction was carried out in the ionic liquid [C$_2$mim]$^+$[OAc]$^-$. In this case, the basic acetate anion was able to catalyze the reaction, thereby preventing the use of any extra inorganic base catalyst and a high molecular degree of substitution (MS) of 2.79 was reached. However, since ethylene (LC$_{50,rat}$ = 72 mg/kg) or propylene (LD$_{50,rat}$ = 380 mg/kg) oxides are highly toxic, replacing them in the future should be considered.

Carbanilation

Cellulose carbamates are prepared *via* carbinilation reactions. Such derivatives are important for SEC analysis in order to obtain the molecular weight distribution (MWD) of cellulose as native cellulose is not soluble in common SEC solvents.[185] Typically, the reaction is quantitative and a DS of 3.0 can be achieved easily, as shown by Heinze *et al.* in the ionic liquid [C$_4$mim]$^+$[Cl$^-$].[116] However, this process employs the use of toxic isocyanates (i.e. phenyl isocyanate), which are usually derived from toxic phosgene. Even though a phosgene-free route for the synthesis of isocyanates has been reported by Knölker *et al.*,[186] the toxicity of the isocyanates is still worth being

taken into consideration. To obtain cellulose derivatives with interesting properties, the developments in the synthesis of so-called NIPUs (non-isocyanate polyurethanes),[187,188] should also be considered in the future.

2.5.6 Perspective: future of homogeneous cellulose modification and sustainability

Recently, and celebrating the 20th anniversary since the first publication of the Twelve Principles of Green Chemistry, Anastas *et al.* published a detailed review highlighting the progress in the field.[189] As pointed out in their work, researchers working in the field of green chemistry are advised to avoid an "environmental burden shifting". To address this, the Twelve Principles are not to be considered in isolation, but rather a careful evaluation of the entire transformation process is necessary. In this regard, while the use of cellulose as a raw material meets the 7th principle of green chemistry, which aims at promoting the use of renewable resources, avoiding an "environmental burden shifting" is important and also all other principles have to be taken into account. Since "design" can be seen as the centre around which the Twelve Principles of Green Chemistry rotate, achieving sustainable cellulose modification can be realized by a careful process design. Therefore, four important questions can be proposed that are worth being addressed before a new cellulose modification protocol is established in order to ensure sustainability.

1. The type of solvent to be used needs to be carefully considered. As special solvents are required for cellulose solubilization, important properties including toxicity, recyclability/re-usability, bio-derived, required temperature, and solubilization time need to be taken into account. In this way, a comparison among various solvents can be made in order to choose the greenest option.

2. The choice of the derivatization agent (reactant) needs to be considered. In this regard, toxicity, source, equivalents required, possible side reactions, easy separation from desired product as well as their stability are very important.

3. The choice of the functionalization method. Herein, considerations on the use of catalysts, atom efficiency, yield, absence of protection groups or pre-derivatization steps, milder reaction conditions and easy recovery of the product are necessary.

4. Finally, the properties of the obtained modified cellulose are equally important. Toxicity, biodegradability (to what type of products) and stability are important to consider.

Most importantly, desirable properties for useful applications have to be achieved in order to be able to replace existing, less sustainable alternatives. In addition, these sustainably derived cellulose materials also need to be evaluated for their economic viability in future to compete with existing counterparts. Thus, through design, the entire process should be put into perspective, thereby achieving sustainable cellulose-based materials. This design approach for cellulose modification is summarized in **Scheme 8**. In addition, the Principles of Green Chemistry that are being addressed by employing these suggestions are highlighted. In summary, careful consideration of the entire transformation process of cellulose is necessary to ensure sustainability.
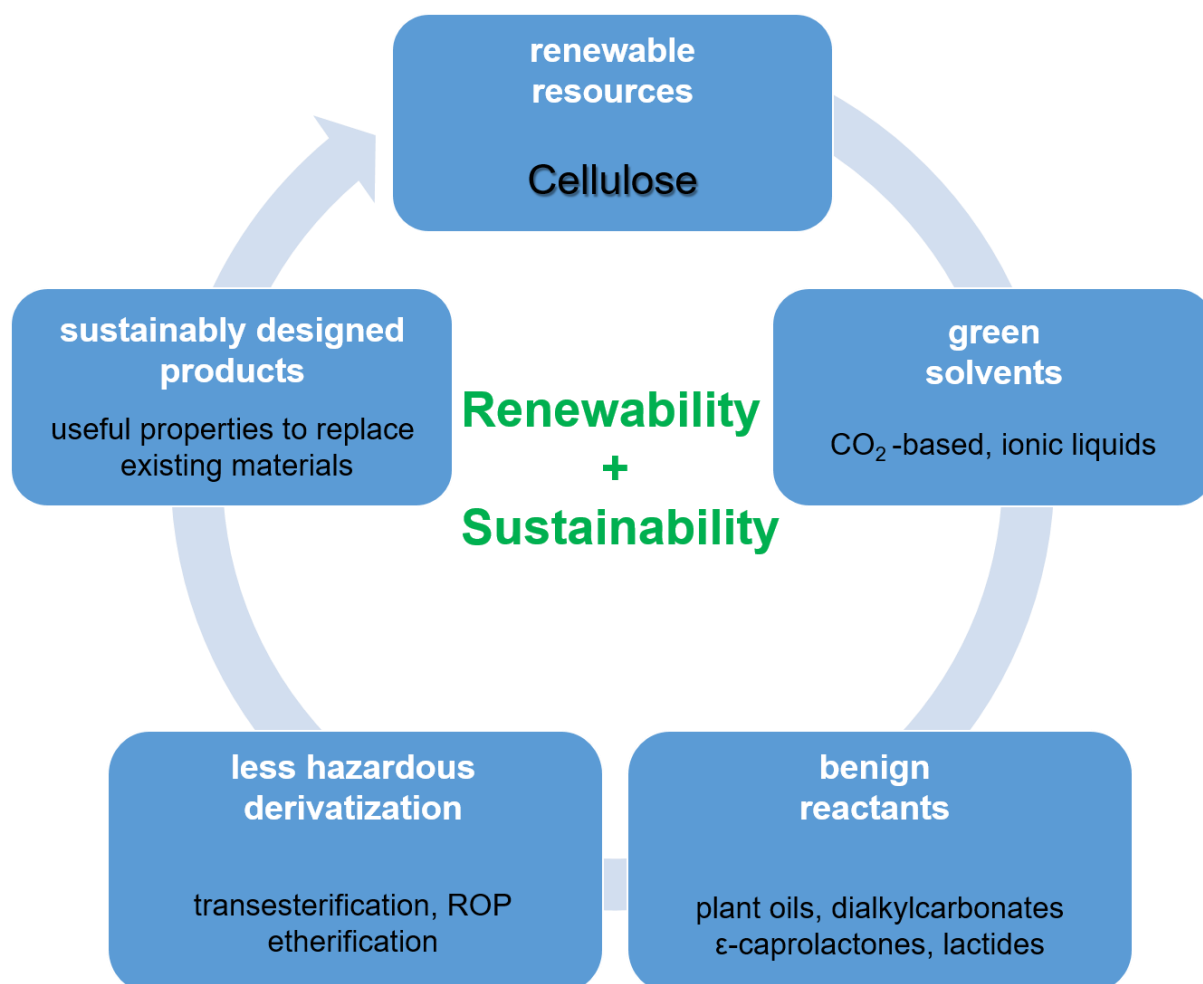
Scheme 8: Design approach towards sustainable cellulose modification

2.5.7 Conclusions

As the most abundant bio-based polymer, cellulose holds great potential as a viable alternative to replace non-sustainable fossil-derived resources. However, despite its renewability, there is a need for sustainability issues to be taken into consideration during chemical transformation in order to produce materials of interest. In line with the Twelve Principles of Green Chemistry, the design of cellulose-based materials will address environmental challenges if its transformation avoids the use of toxic reactants or solvents as well as harsh reaction conditions. Thus, at the beginning of any intended chemical transformation of cellulose, the issue of sustainability is worth considering. While quantitative approaches such as LCA are difficult to apply due to their time demand and a lack of sufficient data, simpler green metrics such as the E-factor, EHS (environmental, health and safety) and atom economy can be employed to evaluate solvents, reactants and functionalization approaches during cellulose transformation.

In this chapter, the use of E-factors along with toxicity information was employed to compare between various homogeneous cellulose modification reports. This simple approach is able to give a fast first sustainability assessment and guide between alternatives, but can of course not replace deeper analysis. As one of the primary goals of modification of cellulose is to make processable thermoplastic materials that will replace their non-sustainable fossil-based counterparts, ensuring sustainability in their entire transformation is of utmost importance and necessity.

2.6 Multicomponent reactions: literature survey

2.6.1 Introduction

Multicomponent reactions (MCRs) are defined as reactions involving more than two starting materials, while forming products in which most of the atoms of the starting materials are incorporated.[190] The synthesis of α-amino-nitriles from an aldehyde, ammonia and hydrogen cyanide in 1850 by Strecker is one the first report of MCRs.[191] Today, a large variety of different types of MCRs exist.[192] What makes MCRs very interesting are their one pot approach, which avoids separation and purification between steps as obtainable in classical organic synthesis. Consequently, MCRs lead to waste reduction, energy minimization and avoid derivatization, which are all important aspects of sustainability.[193–195] Furthermore, as most or all of the atoms of the starting materials are incorporated in the final product, MCRs are highly atom economic reactions.[196] Other interesting aspects of MCRs are their high yields and efficiency.[197] Therefore, MCRs have found applications in high throughput synthesis,[198] as well as in combinatorial chemistry,[199–201] allowing the synthesis and screening of compound libraries. In addition, MCRs are very useful for the synthesis of heterocycles.[202–204]

In 2011, Meier and co-workers reported the application of MCRs in polymer synthesis for the first time.[205] In this case, bi-functional carboxylic acids and aldehydes as well as different mono-functional isocyanides were employed as monomers and high molecular weight polymers were obtained upon Passerini three component reaction (P-3CR) polymerization.[205] In another approach, the same group employed the P-3CR for the synthesis of acrylate monomers which, after free radical polymerization, resulted in thermoresponsive polymers.[206] MCRs have also shown to be very useful for developing sequence-defined macromolecules.[207,208] Such molecules have potential for catalyst and data storage applications.[209,210] Star-shaped polymers, synthesized *via* P-3CR were shown to be able to self-assembled into defined micelles and was used for drug release applications.[211,212] Recently, the Ugi 4-CR with perfluorinated acid components was employed for the synthesis of a library of molecular keys that were applied for molecular cryptography.[213]

In 2000, MCRs were classified into three types depending on their reaction mechanism by Ugi and Dömling.[214] The three classes of reactions include: Type I reactions in which the intermediate as well as the final step to the desired product consist of equilibrium reaction pathways. This class of reaction results in mixtures between the desired product and starting material/ intermediate products that are difficult to isolate. Type II reactions involve an irreversible last step with equilibrium intermediate steps. The irreversibility of the final step in this type of reactions led to higher yields by shifting equilibrium more to the product side. This last irreversible step could be associated to an exothermic reaction, cyclization, or loss of smaller molecules (e.g. water). Type III reactions consist entirely of irreversible intermediate reaction pathways; examples of such reactions are found in biochemical or enzymatic reactions. This classification is represented in **Figure 2**.
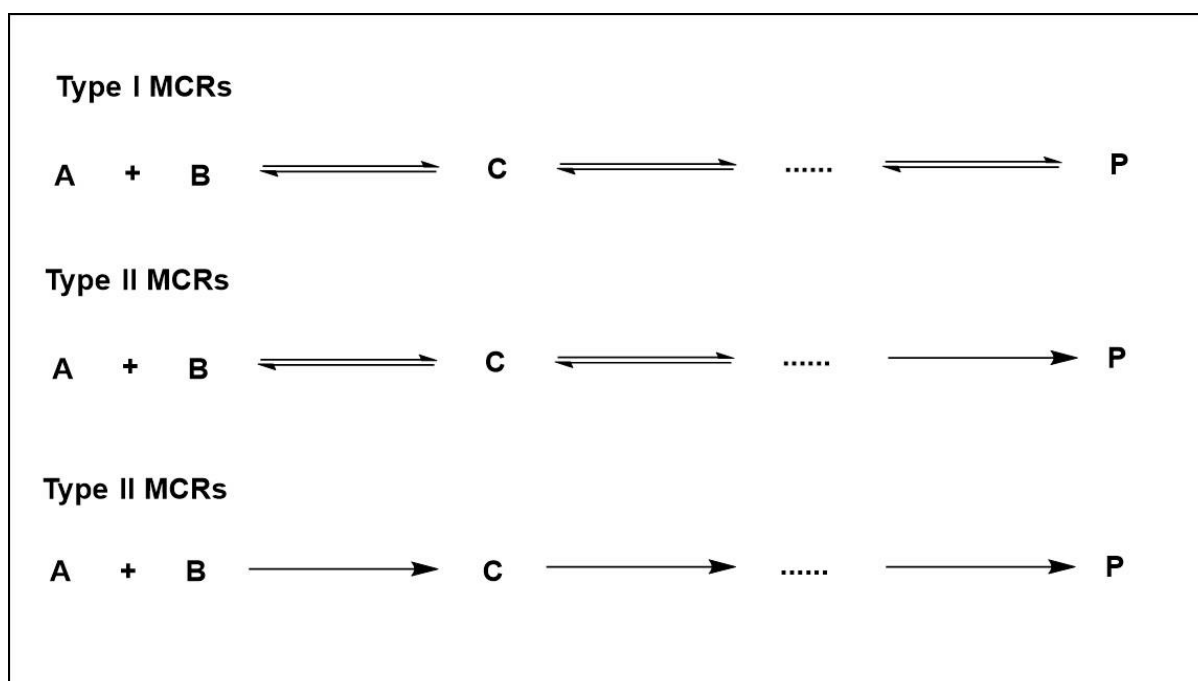
Figure 2: Types of multicomponent reactions, adapted from Ugi and Dömling.[214]

2.6.2 Variations and historical development of multicomponent reactions

2.6.2.1 Non-isocyanide based MCRs

As previously mentioned, Strecker's synthesis of α-amino-nitriles in 1850 started the development of the field of MCRs.[191] The reaction involves a direct coupling between three components, namely an aldehyde, a cyanide and ammonium chloride as shown in **Scheme 9**.
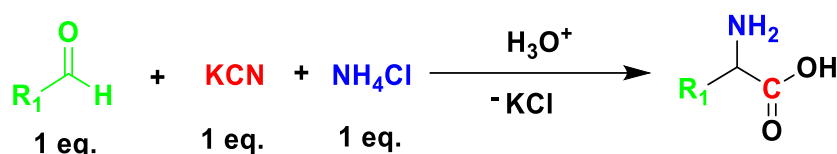
Scheme 9: Strecker synthesis of α-amino nitriles.[191]

In 1881, Arthur Aldolf Hantzsch reported the synthesis of 1,4 dihydropyridine (DHP) from a one pot reaction between an aldehyde (1 eq.), β-keto ester such as acetoacetate (2 eq.) and a nitrogen source such as ammonia or ammonium acetate (1 eq.).[215] This reaction, which is today referred to as the Hantzsch dihydropyridine reaction, is illustrated in **Scheme 10**
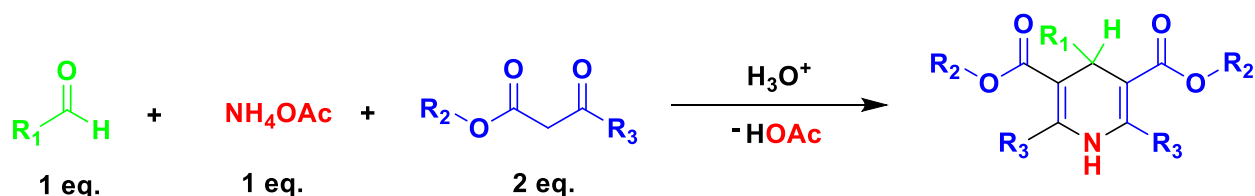
Scheme 10: Hantzsch synthesis of 1,4 dihydropyridine (DHP).[215]

Some DHP have found medicinal applications due to their pharmacological properties.[216,217] Subsequent oxidation of DHP leads to formation of the corresponding aromatic pyridine derivative.[218]

In 1893, Pietro Biginelli reported the one pot synthesis of 3,4-dihydropyrimidin-2-(1*H*)-one (DHPM) from the reaction between an aromatic aldehyde (benzaldehyde), urea and ethyl acetoacetate under acidic conditions.[219] This reaction is now referred to as the Biginelli reaction and is shown in **Scheme 11**.
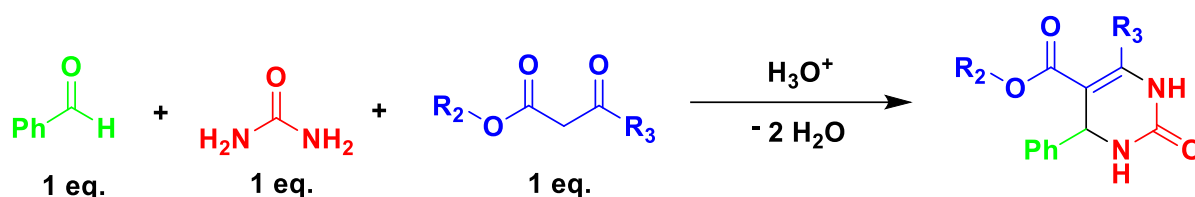
Scheme 11: The Biginelli synthesis of 3,4-dihydropyrimidin-2-(1*H*)-one (DHPM).[219]

The Biginelli reaction is a good example of a sustainable MCR, as the use of isocyanides are avoided and all the reactants can be bio-based. Due to their therapeutic and pharmacological properties such as antiviral, antitumor, and antibacterial, most DHPMs find applications in medicinal fields.[220–222]

In 1912, Carl Mannich reported the synthesis of β-amino carbonyl compounds (also called Mannich bases).[223] The reaction involves the amino-alkylation of an acidic proton next to a carbonyl function by formaldehyde and ammonia (or primary/secondary amines). This is illustrated in **Scheme 12**.
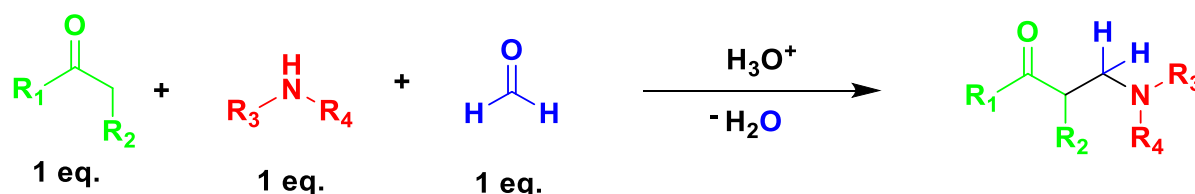
Scheme 12: Mannich synthesis of β-amino carbonyl compounds.[223]

2.6.2.2 Isocyanide-based multicomponent reactions (IMCRs)

This class of MCRs are based on isocyanides that play a pivotal role in their mechanism. Prominent examples of IMCRs are the Passerini three component reaction (P-3CR)[224] and Ugi four component reaction (Ugi 4-CR).[225] As isocyanides play a key role in this class of MCRs, a closer look into their chemistry and synthesis is first discussed.

Chemistry and synthesis of isocyanides

Isocyanides are a unique class of compounds, in which the same carbon atom is able to act both as a nucleophile and an electrophile. It is also the only class of compounds with a formally stable divalent carbon.[214] This unique property is based on the two resonance structures of isocyanides shown in **Scheme 13**.

$$\overset{|}{C}=N-R \longleftrightarrow \overset{\ominus}{\underset{|}{C}}\equiv\overset{\oplus}{N}-R$$
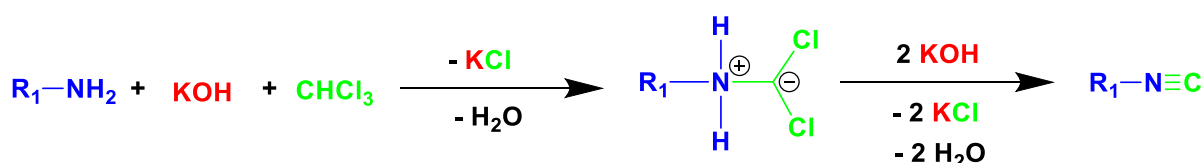
Scheme 13: Resonance structures of isocyanide.

One of the resonance structures shows a formally divalent carbon, having similar reactivity as a carbene. In the other resonance structure, the carbon atom is negatively charged and therefore can act as a nucleophile, while the nitrogen atom shows α-acidity property. After a nucleophilic attack, the same carbon atom is able to act as an electrophile (α-addition); this represents a key step in the mechanism of IMCRs.[214] Whereas isocyanides show strong stability under basic conditions, they are easily hydrolyzed to their corresponding formamides in acidic conditions.[226] They have a characteristic unpleasant smell especially those with low molecular weights.[227]

The reaction between allyl iodide and silver cyanide by Lieke in 1859 was the first isocyanide synthesis reported.[228] The unpleasant smelling liquid he obtained (allyl isocyanide) was not characteristic of his expected allyl cyanide (allyl nitrile) product (see **Scheme 14**).

$$\text{allyl—I} + \text{AgCN} \longrightarrow \text{allyl—NC} + \text{AgI}$$
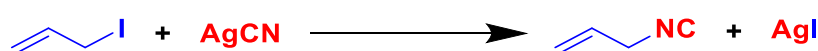
Scheme 14: Lieke route for isocyanide synthesis.[228]

Further elaboration of the isocyanide chemistry was done almost ten years later by Gautier[226] and Hofmann.[229,230] Hofmann for example reported the synthesis of isocyanides from the reaction between a primary amine, chloroform and potassium hydroxide[230] (**Scheme 15**).

$$R_1-NH_2 + KOH + CHCl_3 \xrightarrow[- H_2O]{- KCl} R_1-\overset{H}{\underset{H}{\overset{\oplus}{N}}}-\overset{Cl}{\underset{Cl}{\overset{\ominus}{C}}} \xrightarrow[\substack{- 2\ KCl \\ - 2\ H_2O}]{2\ KOH} R_1-N\equiv C$$

Scheme 15: Hofmann route for isocyanide synthesis.[230]

In the first step of the reaction, a reactive dichlorocarbene is formed from reaction between chloroform and potassium hydroxide. This reactive carbene is then attacked by the primary amine resulting in the formation of an ionic intermediate. Upon elimination of potassium chloride and water, the desired isocyanide is obtained. This approach led to only moderate yields.

In 1958, Ugi reported a much more effective synthesis of isocyanides from dehydration of *N*-formamide using phosgene as dehydrating agent and a base.[231] This is illustrated in **Scheme 16**.
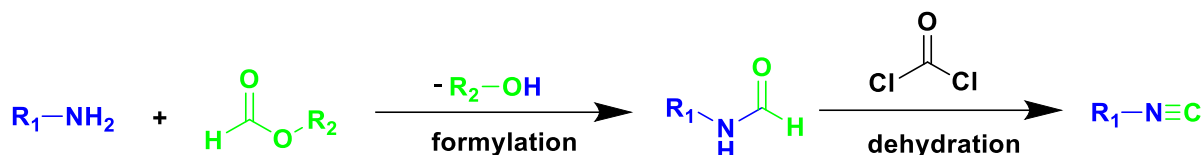
Scheme 16: Ugi route for isocyanide synthesis.[231]

This approach, which is currently the method of choice for isocyanide synthesis, has seen various variations mostly replacing the toxic phosgene as dehydrating agent. Examples include the use of less toxic phosgene analogues such as diphosgene,[232] and triphosgene.[233] However, in laboratory synthesis, the less toxic phosphorous (V)oxychloride ($POCl_3$) is used instead.

The first naturally occurring isocyanide (xanthocillin) (see structure in **Figure 3**) was discovered and isolated from the fungus, *Penicillium notatum* by Rothe in 1950.[234]
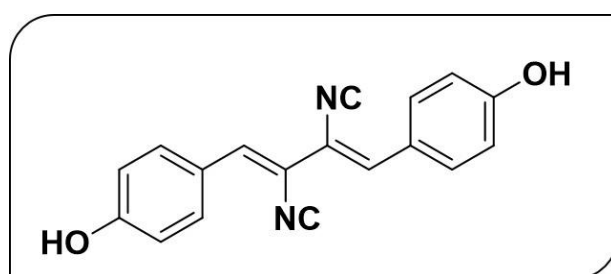
Figure 3: Structure of first isolated natural occurring isocyanide (xanthocillin).[234]

The second natural occurring isocyanide (trichoviridine, also called dermadin) was isolated in 1976 from *Trichoderma spp.*[235] Other naturally occurring isocyanides based on terpenes have been also isolated mostly from marine sponges.[227,236] Most of these naturally occurring isocyanides show strong antibiotic and fungicidal properties, thus finding medicinal applications.[227]

The Passerini three component reaction (P-3CR)

The P-3CR, the first reported IMCRs was discovered in 1921 by Mario Passerini.[224] The reaction describes the reaction between a carboxylic acid, carbonyl component (aldehyde or ketone) and an isocyanide, forming α-acyloxyl-amides. This is illustrated in **Scheme 17**.
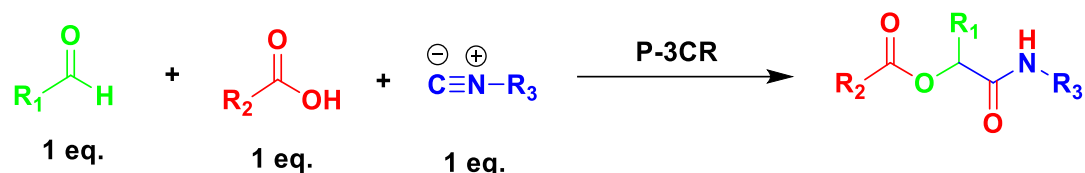
Scheme 17: General reaction scheme for the Passerini 3-CR.

The generally accepted mechanism of the P-3CR was proposed by Passerini, and later confirmed from kinetics study separately by Baker & Stanonis in 1951[237] and Ugi & Meyr in 1961.[238] The mechanism (see **Scheme 18**) starts with an intra-molecular *hydrogen* bonding activation of the carbonyl component by the carboxylic acid forming **1**. Next, the activated carbonyl carbon is attacked by the negatively charged carbon atom of the isocyanide (α-addition). Subsequent electron shift towards the positively charged nitrogen of the isocyanide leads to an electrophilic character of the isocyanide carbon atom as seen in the intermediate **2**. This causes a nucleophilic attack on this carbon by the carboxylic anion (the isocyanide carbon acting as an electrophile). In the next steps, the intermediate **3** undergoes an acyl transfer followed by an intra-molecular rearrangement to form the P-3CR (α-acyloxyl-amide) product **4**
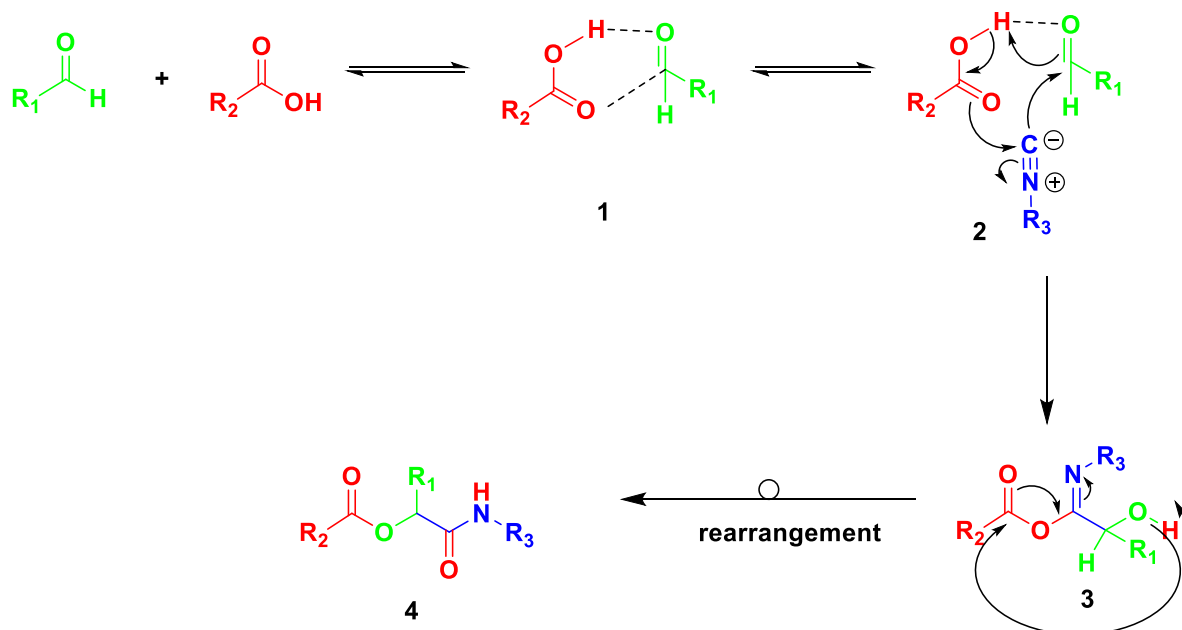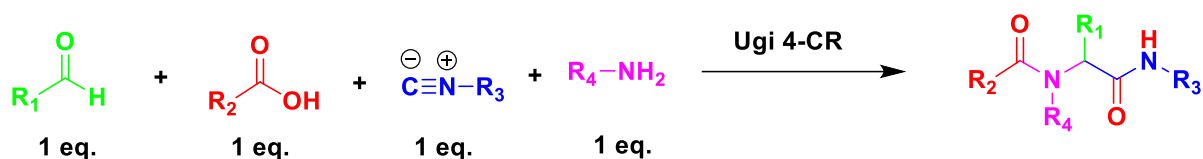
Scheme 18: Generally accepted mechanism for Passerini 3-CR.[224,237,238]

The P-3CR is an example of a 100% atom economic reaction as all the atoms of the starting components are incorporated in the final P-3CR product.

The Ugi four component reaction (Ugi 4-CR)

The Ugi four component reaction (Ugi 4-CR) was developed by Ivar Ugi in 1960 and involves a carboxylic acid, carbonyl component (aldehyde or ketone), an isocyanide and an amine as components, leading to the formation of a *bis*-amide (α-amino acylamide).[225] The general scheme of the Ugi 4-CR is shown in **Scheme 19** below.

Scheme 19: General reaction scheme for the Ugi 4-CR.

The generally accepted mechanism of the Ugi 4-CR (see **Scheme 20**) proceeds by the formation of an imine (Schiff base) **5**, from reaction between the carbonyl and amine components with a loss of water molecule. In the next step, the imine is protonated by the carboxylic acid component forming an iminium ion. This activated carbonyl specie undergoes a nucleophilic attacked by the negative charged carbon atom of the isocyanide. The electronic shift towards the positively charged nitrogen atom of the isocyanide also leads to a nucleophilic attack on the same carbon atom of

the isocyanide (acting as an electrophile) by the carboxylic acid anion (α-addition). The resulting intermediate **6**, undergoes Mumm rearrangement to the desired Ugi 4-CR product **7** (*bis*-amide).
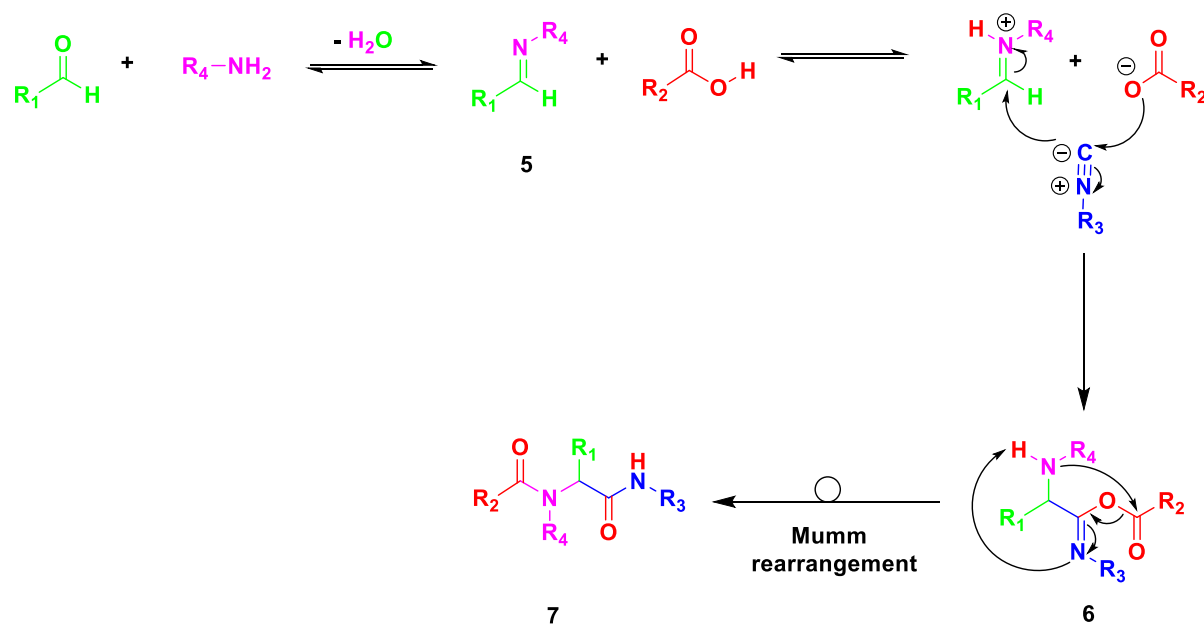
**Scheme 20**: Mechanism for the Ugi 4-CR.[225,239]

3. Aim and objectives

As the most abundant organic polymer in nature, cellulose, can indeed be a viable and sustainable replacement for petroleum-derived polymers. However, previous studies on this polymer often only considered its renewability, neglecting mostly other aspect of Green Chemistry during their transformation to make materials. This basically shifts the environmental burden to other stages of the life cycle thereby defeating the purpose of utilizing such a renewable polymer in the first place. In this regard, the aim of this thesis is to make processable materials from cellulose in a sustainable fashion. In order to reach this aim, the flowing objectives were set:

To develop or optimize a sustainable solvent system for cellulose solubilization. Sustainability in this regard considers the energy requirement (time and temperature) for the solubilization process, ability to recycle and re-use the solvent and was thus a target, which was realized by a detailed and optimization study of the $DBU-CO_2$ switchable solvent system.

To develop a sustainable regeneration protocol for cellulose. Herein, consideration is given to mildness of the cellulose solubilization process, recycle and re-use of the solvent. Therefore, the study of a straightforward approach for the preparation of cellulose aerogels from the $DBU-CO_2$ switchable solvent system will be presented.

To develop sustainable derivatization procedure for making processable cellulose-based materials. In the first instance, consideration is given to use of renewable reactant, mild derivatization protocols without need for pre-functionalization or protecting groups. Therefore, the study of transesterification of cellulose using plant oil (high oleic sunflower oil) in the $DBU-CO_2$ switchable solvent was established. Furthermore, an atom-efficient multicomponent reaction (Ugi four component reaction) was investigated for modifying cellulose. In this case, the need to design tuneable cellulose-based advanced materials were targeted and reported.
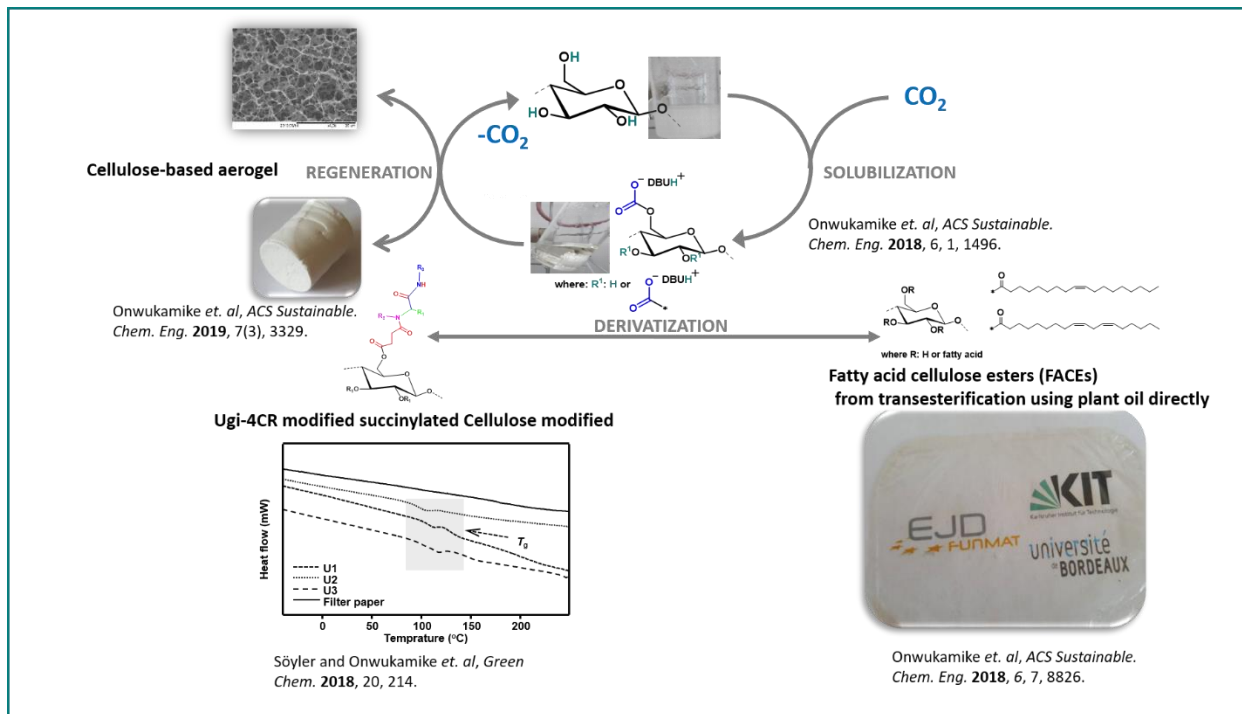
Graphical summary of thesis

# 4. Results: Sustainable cellulose solubilization

This chapter and the associated parts in the experimental section are adapted from the following literature:

K.N. Onwukamike, T. Tassaing, S. Grelier, E. Grau, H. Cramail, M.A.R. Meier, Detailed understanding of the DBU-CO_2 Switchable Solvent System for Cellulose Solubilization and Derivatization, *ACS Sustainable. Chem. Eng.* 2018, 6, 1, 1496.
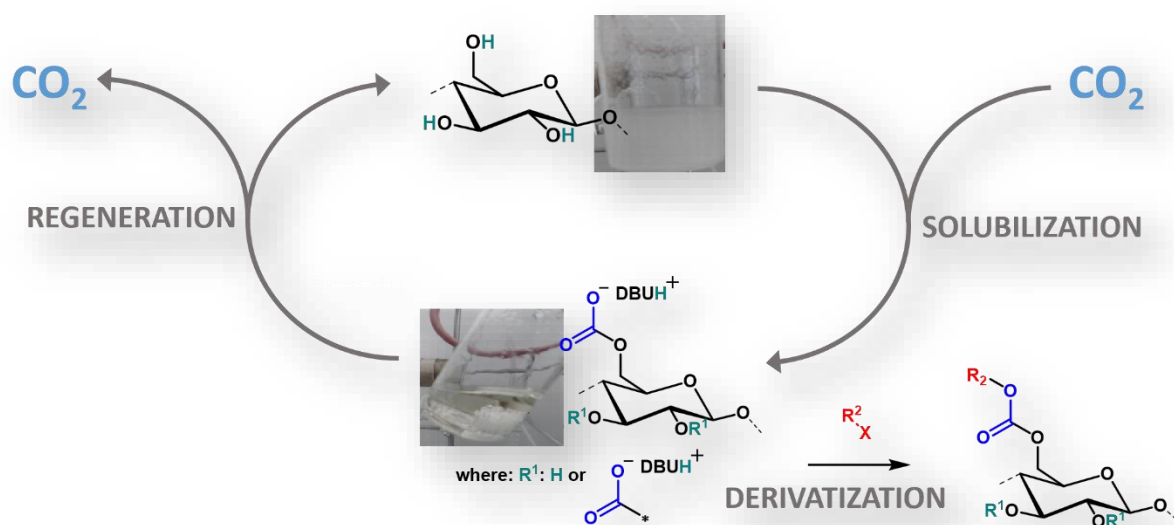
4.1 Abstract

As shown in the (**Chapter 2.5**), solubilizing cellulose is a major challenge limiting its wide spread application. More so, because most reported solvents are either toxic, expensive or difficult to recycle, a need to develop a sustainable alternative is important. In this regard, with this chapter, an optimization study of the DBU-CO_2 switchable solvent system for cellulose solubilization is presented. The optimization was achieved *via* online infrared spectroscopy (ATR-IR). By varying temperature, CO_2 pressure and time, cellulose dissolution was achieved within 10 to 15 min at 30 °C. Compared to traditionally used ionic liquids, the presented system is cheaper, easier to recycle and enables a very fast cellulose solubilization under mild conditions. The efficiency of the optimized conditions was further confirmed by an X-ray diffraction (XRD) experiment, showing the typical transformation of cellulose I to II upon regeneration. In addition, the existence of the *in-situ* formed cellulose carbonate anions was proven by trapping them with benzyl bromide and methyl iodide as electrophiles, leading to the successful synthesis of the benzyl- and methyl- cellulose carbonate respectively. In addition, the utilization of CO_2 as a renewable building block for cellulose derivatization in this approach is interesting from a sustainability point of view. The synthesized cellulose carbonates were characterized by ATR-IR, ^{1}H NMR and ^{13}C NMR spectroscopy. A degree of substitution (DS) value of 1.06, achieved for the cellulose-benzyl-carbonate was determined by ^{31}P NMR analysis. This study thus provides a deep insight into the possibilities of the reviewed switchable solvent system and offers unprecedented possibilities for novel derivatization protocols of cellulose.

4.2 Introduction

In recent years, the academic interest in renewable resources steadily increased owing to the depletion of non-sustainable fossil resources, as well as the realized need for more sustainable approaches, especially for polymeric materials. As the most abundant bio-based organic polymer, cellulose has received considerable attention in this regard. Although it has been employed as a key raw material in the chemical industry for over a century (see **Chapter 2.4**), its vast potential is seriously limited due to a solubility issue.[26] The insolubility of cellulose in most common solvents can be

attributed to its crystallinity caused by strong *intra-* and *inter*-molecular hydrogen bonds.[26,240] Only solvents capable of disrupting or breaking these *H*-bonds are able to solubilize cellulose.[240] During the last decades, various solvents have been investigated for this purpose. Examples include *N,N*-dimethylacetamide-lithium chloride (DMAc-LiCl),[92] *N*-methylmorpholine *N*-oxide (NMMO),[94] and dimethyl sulfoxide-tetrabutyl ammonium fluoride (DMSO-TBAF).[93] These solvents suffer from several drawbacks such as difficult recovery and toxicity. As described in **Chapter 2.5**, sustainability consideration is very important during cellulose modification, therefore the need for a green solvent is necessary. In this regard, solvents showing a low vapor pressure and high recyclability are desirable. In this context, in 2002, Rogers *et al.*, showed the potential of ionic liquids, such as 1-*N*-butyl-3-methylimidazolium chloride ($[C_4mim]^+[Cl^-]$), as a green solvent for cellulose solubilization.[77] After their publication, an extensive research interest in the field of ionic liquids for cellulose chemistry can be observed.[129] Despite the huge potential of ionic liquids, the disadvantages consequential to their chemical and physical properties are also noteworthy. Notably, are their high cost and easy contamination in some reactions, which makes their recovery difficult in many cases.[136] The basic characteristics of common ionic liquids used for cellulose solubilization alongside their limitations is presented in **Table 2** (**Chapter 2.5.5**) Furthermore, high temperatures (>70 °C) and long reaction times (>8 hours) are usually required for complete cellulose dissolution, with lower reaction time achieved *via* microwave irradiation.[77]

In 2005, Jessop and his group described the concept of a CO_2 switchable system as a solvent capable of being transformed from a "non-ionic" to an "ionic" state by application of CO_2, with the possibility to revert to its initial "non-ionic" state by CO_2 removal.[153] This idea was simultaneously applied by Xie *et al.*[155] and Jerome *et al.*,[154] for the purpose of cellulose solubilization. Here, in the presence of a super base and CO_2 with dimethyl sulfoxide (DMSO) as co-solvent, cellulose could be solubilized by a "non-derivative approach" (wherein an alcohol carbonate-DMSO system is formed, which is a good solvent for cellulose) or a "derivative approach" (whereby cellulose is directly transformed into a DMSO-soluble carbonate in the presence of CO_2). The two proposed mechanisms for this solvent system are shown in **Scheme 7** (**Chapter 2.5.5**). These authors independently showed complete cellulose solubilization in this solvent system within 1-3 h at temperatures ranging from 50 to 60 °C and CO_2

pressures ranging between 2 and 8 bar. In order to achieve shorter reaction times (below 30 min) at temperatures ranging between 40 °C to 60 °C, Nanta *et al.* showed that CO_2 pressures above 50 bar are required.[241] Wang *et al.* succeeded to achieve cellulose solubilization at 30 °C using a CO_2 pressure below 10 bar, but longer reaction times between 1 and 5 h were required.[242] Compared to typical ionic liquids, the CO_2 switchable solvent system is more advantageous, since it can be recycled more easily and needs a lower temperature and time for cellulose solubilization. Recently, various modifications of cellulose demonstrated the potential of this solvent system for the synthetic purposes, as shown in **Chapter 2.5.5**. Furthermore, the versatility of this solvent system has been confirmed to possess a high potential for reversible CO_2 capture application.[243] However, still absent in the literature are studies describing an optimization of not only the temperature and reaction time, but also the lowering of the required CO_2 pressure. Such an optimization would lead to an increase in sustainability of the solvent system, as less energy will be required during the process, and more importantly, the need for special equipment withstanding high pressures will become obsolete.

Moreover, the proposed mechanism *in* the "derivative" approach occurs *via* cellulose pre-modification into its carbonate anion upon reacting with CO_2 in the presence of a super base. Until today, the conclusive presence of this *in-situ* carbonate intermediate is yet to be proven beyond results from FT-IR and NMR measurements. The validity of such methods is limited due to the reaction of adventitious water (present in super bases and in cellulose) with CO_2.[244] Hence, conclusive proof would be the isolation of the carbonate intermediate. Such evidence would also lead to novel approaches for cellulose derivatization.

Therefore, in the first part of this chapter, an optimization study of the CO_2 switchable solvent system is described. In this case,1,8-diazabicyclo [5.4.0]-undec-7-ene (DBU) was used as the super base and the influence of the reaction time, temperature and CO_2 pressures on the cellulose solubilization was investigated. In addition, a comparison of other super bases (7-methyl-1,5,7-triazabicyclo[4.4.0]dec-5-ene; MTBD, and 1,1,3,3-tetramethylguanidine; TMG) during a heating and cooling cycle is included. Finally, a conclusive evidence on the existence of the *in-situ* generated cellulose carbonate is provided by trapping using electrophiles.

4.3 Results and Discussions

4.3.1 Heating and cooling cycle effect on carbonate stability

The effect of a heating and cooling cycle on the stability of the *in-situ* carbonate formed during the cellulose solubilization (see **Scheme 7**), was investigated using three super bases (DBU, MTBD and TMG). 20 bar of CO_2 pressure were applied, the temperature was increased from 30 °C to 80 °C and then decreased from 80 °C to 30 °C. Using DBU as an example, during the measurement, 3 wt.% of cellulose, DBU (3 eq. per AGU of cellulose) and 1 mL of DMSO were first agitated for a few minutes at room temperature and then transferred to the ATR cell. Next, 20 bar of CO_2 were applied and the temperature was increased from 30 to 80 °C in 10 °C steps followed by a cooling back to 30 °C, while monitoring the intensity of C=O symmetric absorbance band (1665 cm^{-1}) of the *in-situ* carbonate. At each temperature (30 to 80 °C), two measurements were recorded; first after the set temperature has been stabilized and the second after 3 min. The mean value of both measurements was then calculated. The characteristic C=O of the *in-situ* formed carbonate anion with an absorbance peak at 1665 cm^{-1} was followed by *in situ* ATR-IR and plotted as a function of temperature in **Figure 4**
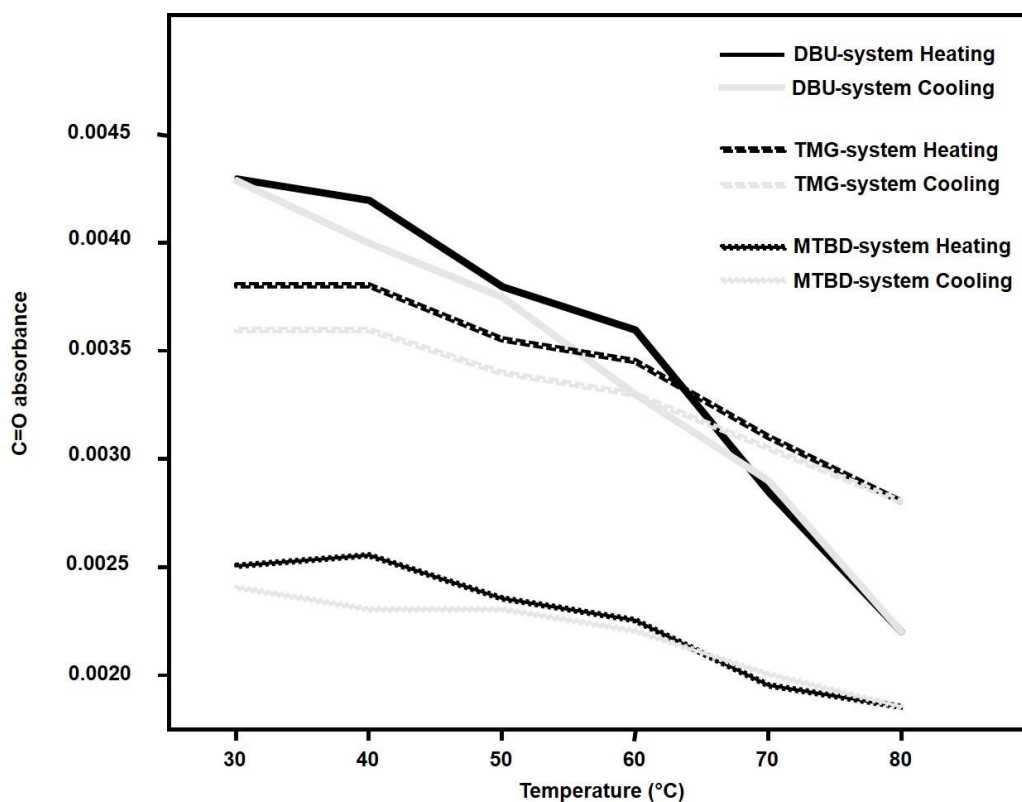
Figure 4: Change of C=O absorbance (from in situ formed carbonate anion) during a temperature cycle study on cellulose solubilization using DBU, MTBD and TMG as super bases.

For all the investigated super bases, the intensity of the C=O absorbance band of the formed carbonate decreased, as temperature was increased from 30 °C to 80 °C. Interestingly, as the system was cooled to the starting temperature, the intensity of the C=O absorbance band increased again reaching its respective initial value. This can be explained if we consider the results reported by Heldebrant *et al.,* who indicated that the reaction between CO_2 and a super base in the presence of a proton donor (alcohols), in this case cellulose, are exothermic.[245] In addition, the dissolution of cellulose in the ionic liquid, $[C_2mim]^+[OAc^-]$ has equally been confirmed to be exothermic.[246] Following Le Chatelier´s principle, increasing the temperature will shift the equilibrium to the starting reactants in an exothermic reaction at equilibrium. This explains the reason why at higher temperatures, less carbonate formation occurred. In addition, the recovery of the initial C=O intensity upon cooling confirms the thermal reversibility of the solvent system. Furthermore, for the DBU-CO_2 system, the lowest reaction temperature (30 °C), showed almost a double fold carbonate formation than at 60 °C. Compared to the other super bases, DBU exhibits the highest efficiency in the generation of the *in-situ* carbonate, but less stability with temperature compared to MTBD or TMG. To verify whether this property was inherent of this class of solvent

system, a model experiment using octanol was carried out and similar results were obtained (see **Figure 42** in the experimental section). Thus, these two series of experiments suggest that this reversibility tendency with temperature is an inherent property of the CO_2 switchable solvent system.

4.3.2 Temperature and CO_2 pressure optimization

In situ ATR-IR analysis was used to monitor the carbonate formation during cellulose solubilization as well as the protonation of DBU. As depicted in **Figure 5a** and **b**, the decreasing absorbance of the C=N band of DBU (1614 cm^{-1}; peak assigned by measuring the ATR-IR spectra of neat DBU) over the solubilization time was associated with a corresponding increase of the C=O peak (1665 cm^{-1}) of the *in-situ* formed carbonate similar to the value of 1667 cm^{-1} reported for the same absorption band.[242] Furthermore, an increase of the protonated DBU (C=NH$^+$) peak at 1639 cm^{-1} (assigned by carrying out a model reaction whereby neat DBU was protonated using dilute hydrochloric acid and the disappearance of the typical DBU (C=N) absorption band at 1614 cm^{-1} was associated by an increase in an absorption band at 1639 cm^{-1}) was observed. The obtained peak at 1639 cm^{-1} is very close to previous reported value (1644 cm^{-1}).[244] Equally, from **Figure 5b**, the absorbance intensity values stabilize after 15 min. This is considered the optimal time for the solubilization of cellulose, above which no significant change is observed. In addition, it is worth noting that the C=N absorption band peak of DBU (1614 cm^{-1}) does not decrease to zero, implying the availability of un-protonated DBU which might act as a catalyst for subsequent modification of cellulose in the solvent system. A visual proof of the dissolution of 3 wt.% of microcrystalline (MCC) can be seen in **Figure 5c**. The cloudy solution consisting of MCC, DMSO and DBU is shown on the left before application of CO_2. Applying 5 bar of CO_2 for 10 to 15 min at 30 °C led to a clear solution as seen on the right of **Figure 5c**.
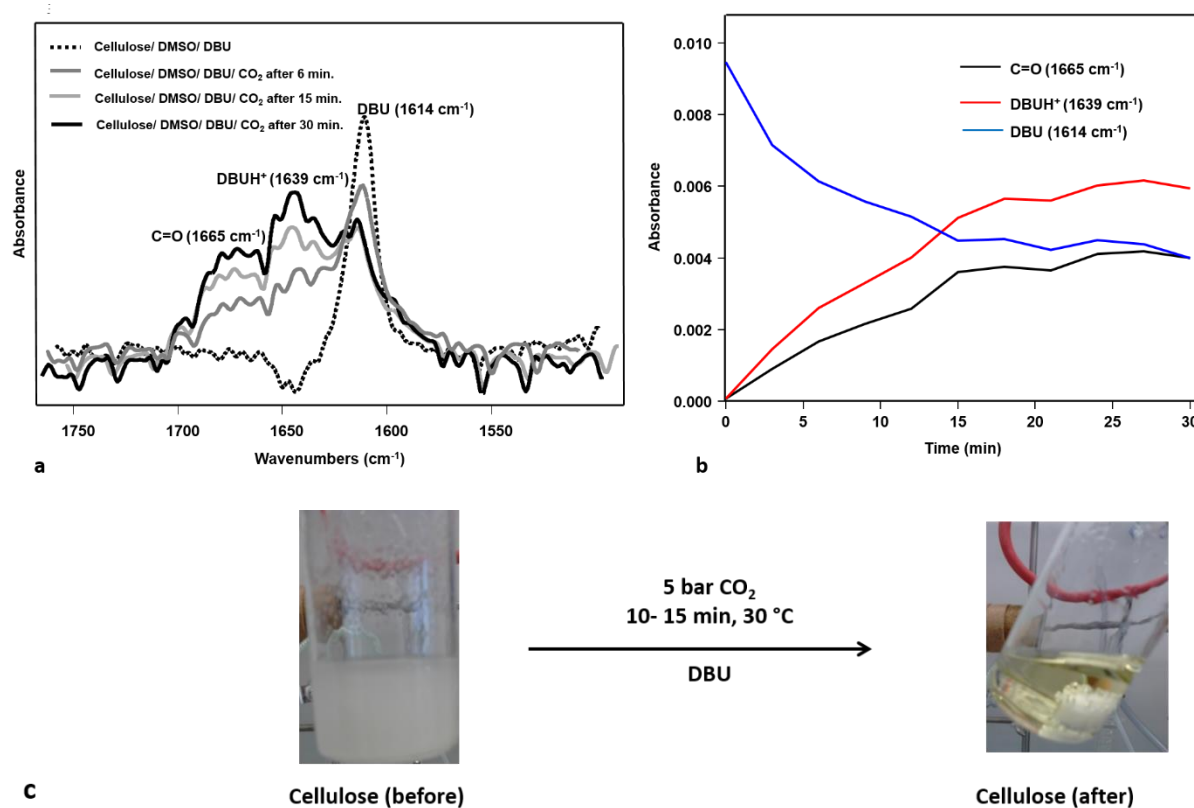
Figure 5: **a**) ATR-IR proof of *in-situ* carbonate formation during cellulose solubilization in DBU-CO_2 solvent, **b**): ATR-IR showing evolution of C=O, DBU (C=N) and DBUH$^+$ (C=NH$^+$) as function of time; **c**): Visual proof for solubilization of cellulose (3 wt.% MCC, 30 °C, 5 bar CO_2, 10 to 15 min).

The effect of different temperatures (from 30 °C to 60 °C) was investigated while keeping the CO_2 pressure constant. The measurements were recorded over a period of 30 min. The result of the experiment performed at 5 bar is presented in **Figure 6**. Based on the results, the highest carbonate formation was observed at the lowest temperature of 30 °C. The investigation on the effect of temperature at different CO_2 pressures (10, 20, 40 bar) are provided in the experimental section (**Figure 43**-**Figure 45**). The results also showed that independent of which CO_2 pressure was investigated, increasing the temperature led to a decrease in the carbonate formation, as seen by the intensity decrease of the symmetric C=O stretching vibration band at 1665 cm^{-1}. This can be attributed to the shift of the equilibrium to the starting reactants as temperature is increased, typical of an exothermic reaction at equilibrium. Thus, the optimal temperature for the maximum carbonate formed was obtained at 30 °C. In addition, carbonate saturation was observed after ~15 min of reaction time (**Figure 6**).
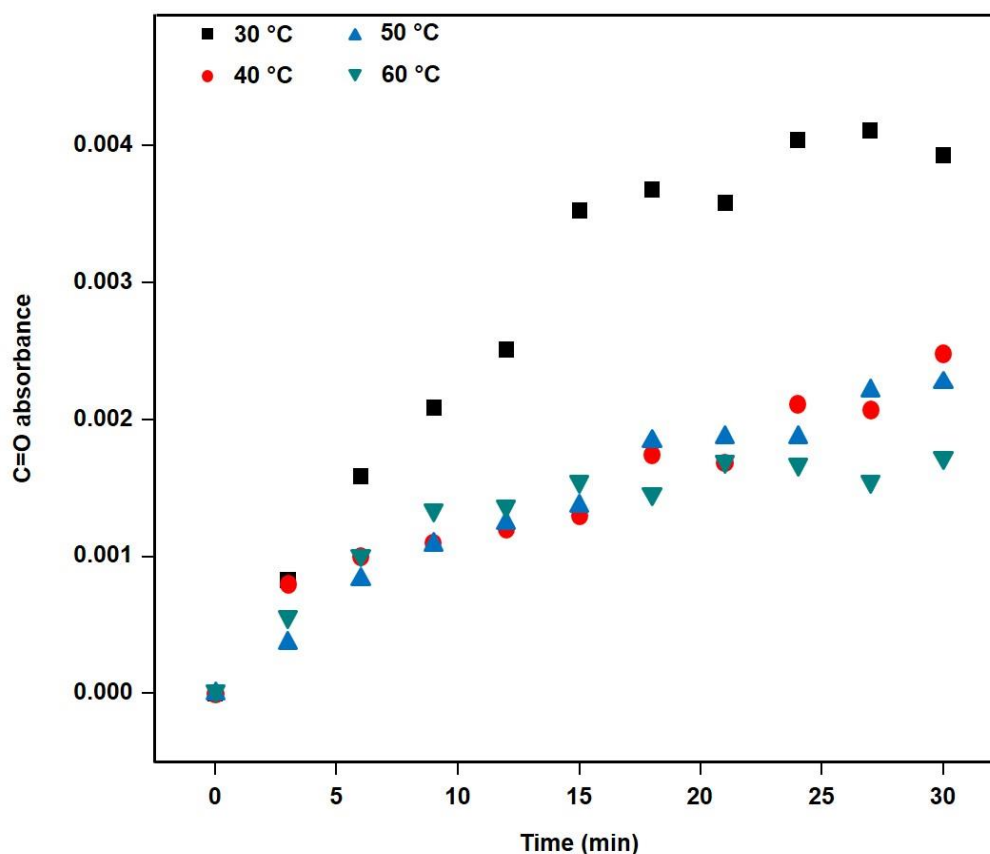
Figure 6: Optimization study *via* online *in-situ* ATR-IR measurement: effect of temperature at 5 bar of CO_2, 3 wt.% MCC.

Furthermore, the effect of CO_2 pressure was investigated by increase from 5 to 40 bar while keeping the temperature constant. The results from experiments at 30 °C are presented in **Figure 7**, and showed that higher CO_2 pressures resulted in an increase in carbonate formation. In addition, pressures above 20 bar led to an increase in the solubilization kinetics, as evidenced by the rapid attainment of the maximum intensity of the C=O band in 10 min, whereas at 40 bar, the maximum intensity was reached within 5 min (**Figure 7**). Thus, above 20 bar, it was possible to solubilize cellulose in less than 10 min at 30 °C. However, such CO_2 pressures are not very practicable. On the other hand, for CO_2 pressures below 20 bar, the solubilization was slower but still completed within 15 min. The results on investigations at different temperatures (40, 50, 60 °C) are provided in the experimental section (**Figure 46**-**Figure 48**). At all investigated temperatures, the general trend of increasing CO_2 pressure with an associated increase in carbonate formation was observed.
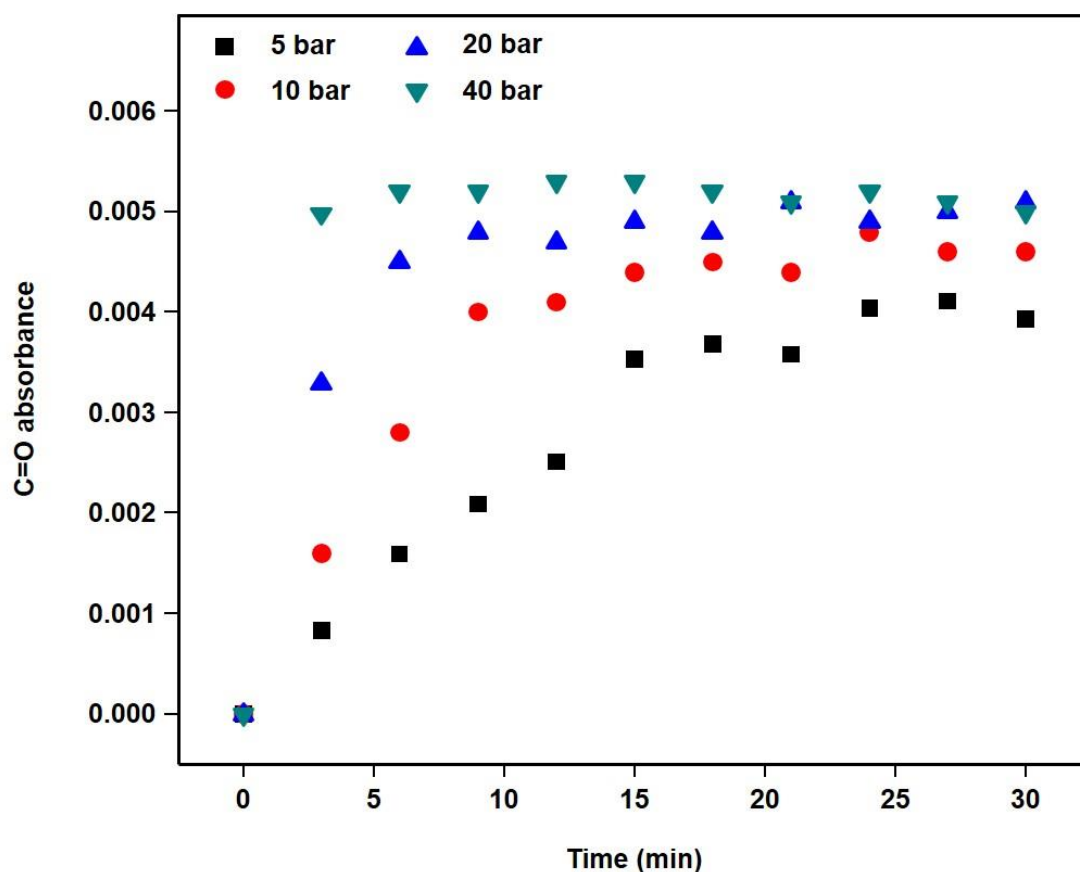
Figure 7: Optimization study *via* online *in-situ* ATR-IR measurement: effect of CO_2 pressure at 30 °C (3 wt.% MCC).

4.3.3 Influence of cellulose concentration

The concentration of cellulose during solubilization influences the viscosity of the solution and thus, its processability. The effect of this parameter on the carbonate formation was investigated by varying the cellulose concentration from 10 to 80 mg/mL. The peak intensity of the carbonate absorbance symmetric stretching band at 1665 cm^{-1} was measured after applying 20 bar of CO_2 at 30 °C for 15 min (**Figure 8**). For the lowest concentrations (10 to 40 mg/mL), increasing the cellulose concentration led to linear increase in carbonate formation as depicted by an increase in the intensity of the C=O absorbance band. However, at higher concentrations (50 to 80 mg/mL), a saturation in carbonate was observed. This plateau might be explained by the increase in viscosity, which invariably reduces the stirring rate of the magnetic bar, hence limiting the introduction of CO_2 into the DMSO liquid phase. To verify the role of stirring in the cellulose solvent system, a control experiment without stirring was performed. As expected, the solubilization of cellulose did not occur and the characteristic carbonate absorbance at 1665 cm^{-1} was not detected by infrared spectroscopy

measurements. However, despite reaching a saturation in carbonate, complete cellulose dissolution was achieved at these higher concentrations.
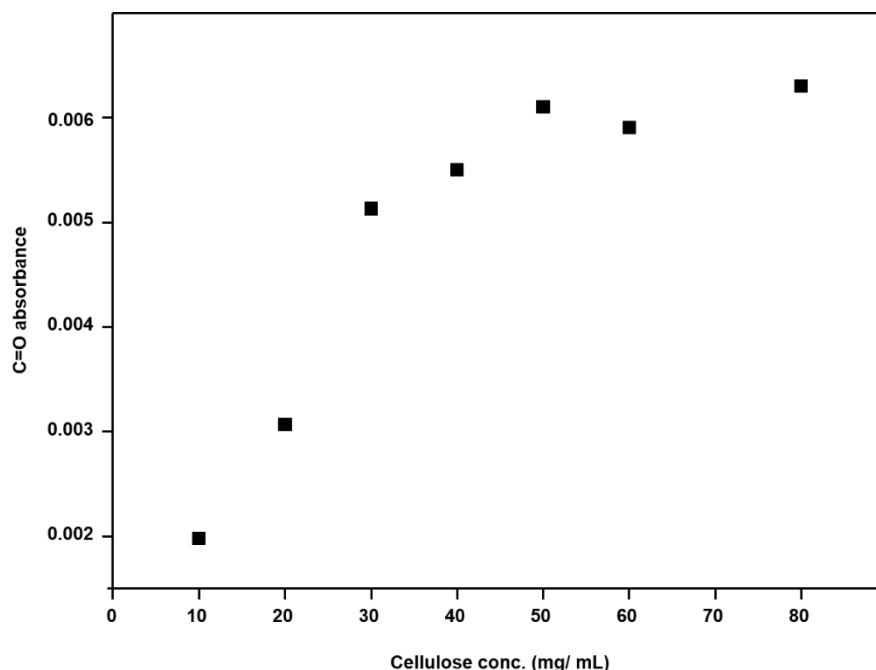

Figure 8: Optimization study *via* online *in-situ* ATR-IR measurement: effect of cellulose concentration (reaction conditions: 30 °C, 20 bar CO_2, 15 min)

Furthermore, the effect of cellulose concentration at higher temperatures (35, 40, 50 and 60 °C) was investigated (see experimental section **Figure 49**). The obtained results describe a linear relationship between cellulose concentration and C=O intensity. Compared to results performed at 30 °C, no saturation in carbonate was observed even at higher concentrations of cellulose. This can be associated to the decrease in viscosity upon increasing temperature which might overcome the limitation at 30 °C. The slight reduction observed at 60 °C is probably due to the increasing effect of temperature on the equilibrium and thereby shifting the latter to the starting reactants as mentioned in the previous paragraphs. To further verify the viscosity-limiting hypothesis, a model reaction employing octanol was carried out. Results showed a linear relationship between octanol concentration (10 to 80 mg/mL) and carbonate formation, with no carbonate saturation at higher concentrations (see experimental section **Figure 50**). Viscosity measurements confirmed that for the same concentration of 30 mg/mL, cellulose had a considerably higher viscosity between 7.05 to 7.15 Pa.s compared to octanol with viscosity value between 0.19 to 0.27 Pa.s (see **Figure 51**). This lower viscosity of octanol might explain why no saturation in

carbonate formation was observed at all investigated concentrations of octanol when compared to cellulose.

4.3.4 Indirect proof of *in-situ* carbonate formation

In order to trap the intermediate carbonate anion generated during the cellulose solubilization, a model reaction using octanol and benzyl bromide as an electrophile was first carried out. Following a previously published procedure[247], where the synthesis of mixed carbonates using simple alcohols was reported, some modifications to the procedure were made in order to adapt to the CO_2 solvent system, leading to the synthesis of various mixed carbonates starting from octanol and cellulose. In the first trial, a test reaction was carried using octanol leading to the successful synthesis of octyl-benzyl-carbonate, thus confirming that the formed carbonate anion acted as nucleophile in an S_N2 reaction. The success of the reaction was visible from ATR-IR measurement by the appearance of the characteristic symmetric C=O stretching vibration band of carbonic ester at 1745 cm^{-1}, as well as the presence of C-O absorbance at 1255 cm^{-1} arising from the newly formed bond between the carbonate carbonyl group and benzylic carbon of the electrophile (see experimental section **Figure 52**). The structure was further confirmed by ^1H NMR and ^{13}C NMR and are included in the experimental section (**Figure 53**). From electrospray ionization mass spectrometry (ESI-MS), the exact mass $((M+Na)^+ = 287.16)$ of the octyl-benzyl-carbonate was confirmed $((M+Na)^+ \, m/z = 287.16)$.

Upon transferring the reaction to cellulose, the corresponding cellulose-benzyl-carbonate was synthesized (see **Scheme 21**).
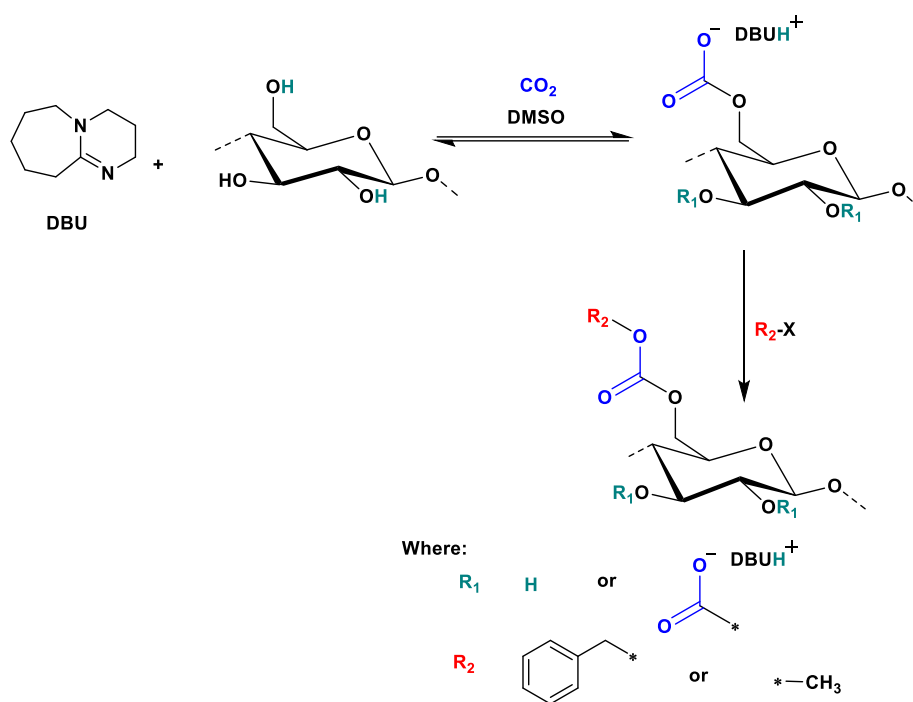
Scheme 21: Synthetic route for an indirect proof of *in-situ* formed carbonate anion by electrophile trapping.

The success of the reaction was evident from infrared spectroscopy by the appearance of the symmetric C=O stretching vibration band of carbonate ester at 1740 cm^{-1}. Furthermore, the new C-O symmetric absorption band at 1256 cm^{-1} was also present in the IR spectrum (**Figure 9**).
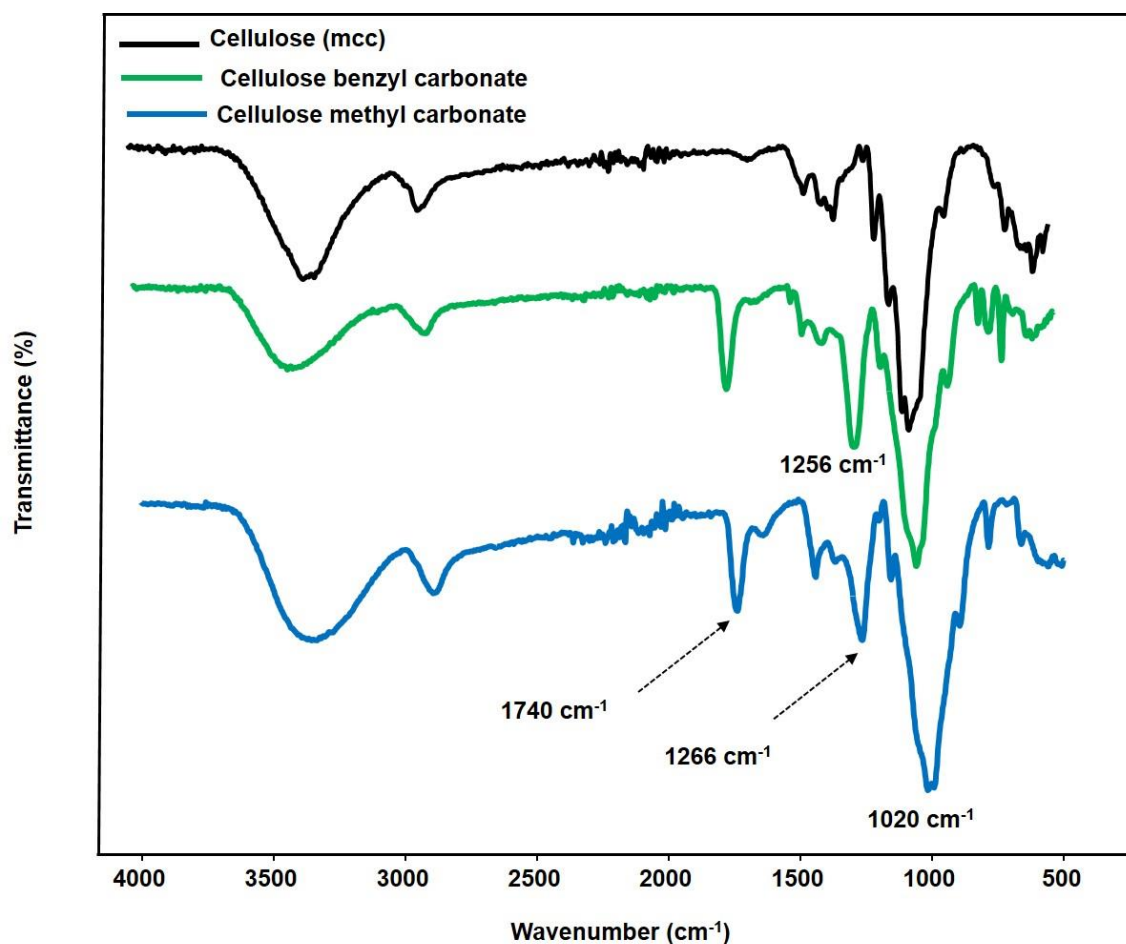
Figure 9: ATR-IR spectra of synthesized cellulose carbonate (methyl and benzyl); spectra are normalized with the intensity of the glycopyranose oxygen absorption at 1020 cm^{-1}.

In addition, the obtained cellulose carbonate was soluble in DMSO, hence allowing ^{1}H NMR and ^{13}C NMR measurements. The proton and carbon spectra of cellulose-benzyl-carbonate is shown in **Figure 10**. The presence of the introduced aromatic group was identified by the broad signal at 7.38 ppm. Compared to the aromatic region of benzyl bromide starting compound, there is a significant difference due to the change in the environment of these aromatic protons after coupling to cellulose. More importantly, the benzylic CH_2 protons in the cellulose carbonate are slightly shifted towards the lower field (5.17 ppm), when compare to the benzylic CH_2 signal in benzyl bromide (4.69 ppm). The broad signals between 3.12 to 5.04 ppm are attributed to the protons in the cellulose backbone. In the ^{13}C NMR, the presence of the carbonate carbonyl peak is indicated by the peak at 154.98 ppm alongside the quaternary carbon of the aromatic ring (135.10 ppm) and the aromatic carbons (128.08, 127.84 and 127.57 ppm). The assigned ^{1}H and ^{13}C NMR peaks of the obtained cellulose-benzyl-carbonate are similar to results reported for cellulose-phenyl-carbonate.[173]
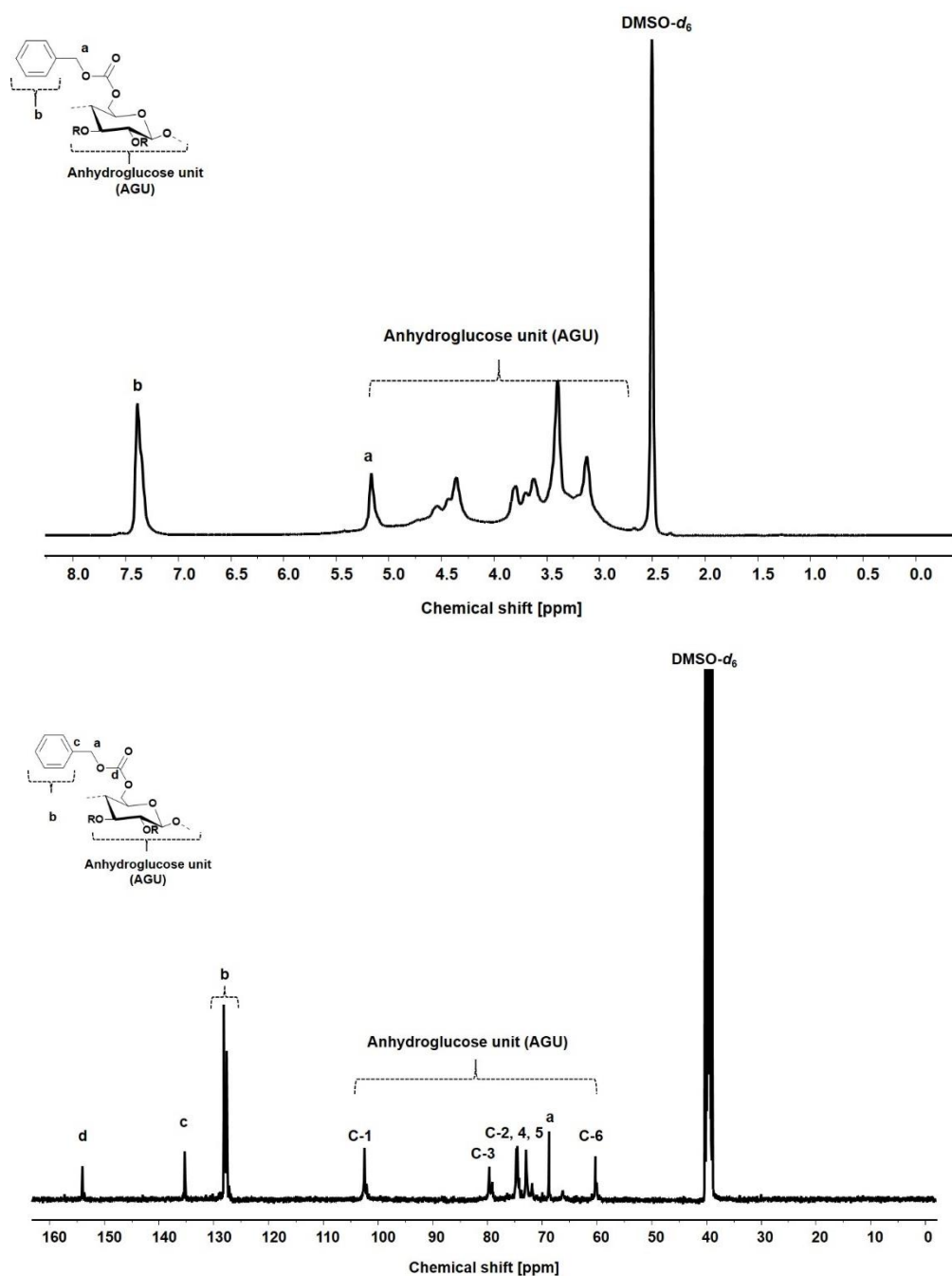
Figure 10: ¹H (top) and ¹³C (bottom) NMR spectra of cellulose-benzyl-carbonate in DMSO (d₆).

The DS of the cellulose-benzyl-carbonate was calculated from ^{31}P NMR following a reported procedure by King and co-workers.[248] The unreacted hydroxyl groups of cellulose were allowed to react with a phosphorylating agent, revealing a broad signal between 137.0 to 145.0 ppm (see **Figure 54**), whose integration relative to an internal standard is employed for DS calculation. A DS value of 1.06 was obtained for the cellulose-benzyl-carbonate.

To show the scope of this reaction, methyl iodide was also employed as an electrophile to trap the carbonate. The obtained cellulose-methyl-carbonate gave similar characteristic FT-IR peaks at 1740 cm^{-1} (see **Figure 9**). The product was soluble in DMSO allowing further structure confirmation *via* ^{1}H and ^{13}C NMR (see experimental section **Figure 55**). The assigned peaks for the synthesized carbonate is similar to a previous report where the same compound was synthesized using dimethylcarbonate in an ionic liquid.[174] Hence, for the first time, a conclusive evidence of the presence of such intermediate carbonate anions during the cellulose solubilization in the investigated switchable solvent system was proven. In the future, the confirmation of this intermediate carbonate offers the possibility to investigate and design novel modification protocols for cellulose. This is evident from the successful cellulose chemical transformation investigations reported in the subsequent sections.

4.3.5 XRD measurements

The solubilization of cellulose followed by regeneration leads to a change in its crystal structure (crystallinity). X-ray diffraction (XRD) is the method of choice in order to evaluate this change. X-ray measurements have been previously employed to characterize regenerated cellulose from ionic liquids.[249] Similarly, Xie *et al.* showed a complete transformation of the native cellulose from cellulose I to II after regeneration in distilled water, employing a non-derivative CO_2 switchable solvent system (solubilized at 60 °C within 2 h).[155] The change in crystallinity upon regeneration reveals the efficiency of the solubilizing solvent. In this regard, the effect of temperature (30 and 60 °C) and time (15 and 60 min) on the crystal structure of the regenerated cellulose was investigated using DBU as super base. After solubilization, cellulose regeneration was performed by precipitation in distilled water, followed by drying under vacuum at 60 °C for 24 h. The dried samples were then analyzed by XRD and displayed in **Figure 11**. The disappearance of characteristic cellulose I diffraction 2θ peaks at 15.4° and 22.6° followed by appearance of characteristics cellulose II 2θ peaks at 12.2°, 20.1° and 21.6° indicates their transformation from cellulose I to II. Furthermore, no obvious difference was observed in the crystal structure when solubilization was carried out at 30 or 60 °C. The same statement applies for solubilization performed for 60 min, when compared to the optimized time of 15 min. These results confirm that the previously discussed optimized mild conditions (30 °C

and 15 min), are sufficient to achieve complete cellulose dissolution, which in turn allows to perform cellulose modifications in homogeneous solution.
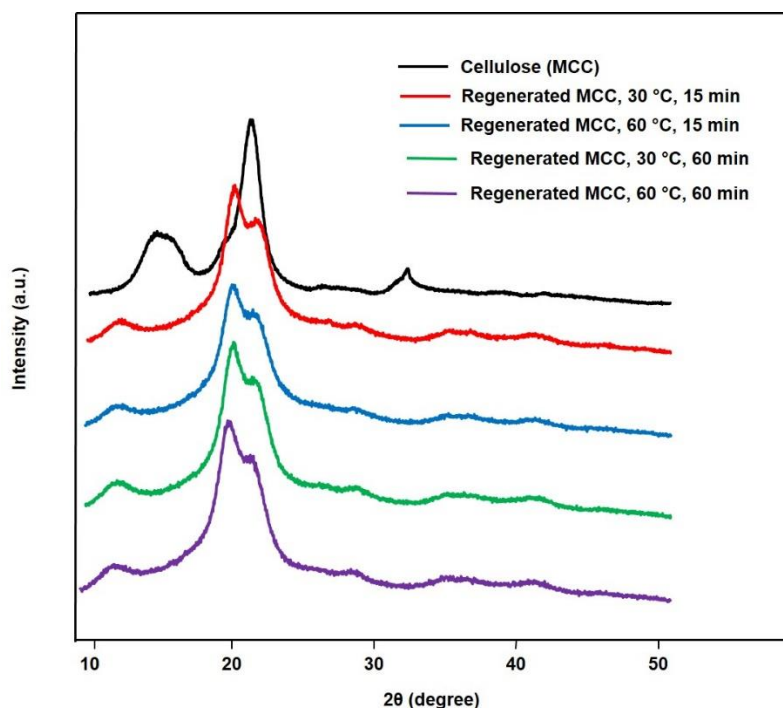

Figure 11: X-ray diffraction patterns of cellulose (MCC) and regenerated cellulose for different solubilization time (15 and 60 min) and temperatures (30 and 60 °C).

4.4 Conclusions

In this chapter, an optimization study on the DBU-CO_2 switchable solvent system for cellulose solubilization was reported. Upon optimization, complete cellulose dissolution was achieved within 10 to 15 min at 30 °C applying CO_2 at moderately low pressures (2 to 5 bar). The efficiency of the reported system was confirmed by XRD after cellulose regeneration. Furthermore, the intermediate *in-situ* generated cellulose carbonate anion was successfully trapped leading to formation of cellulose-carbonate, hence proving for the first time, their existence. As demonstrated in **Chapter 4.3.4**, the optimized solvents system and its understanding allows the design of novel cellulose derivatization strategies in homogeneous solution. In line with the objective of this thesis in ensuring sustainability during cellulose modification, the herein described solvent system is a promising starting point. Therefore, in the subsequent chapters, this solvent system will be employed for the development of cellulose-based materials.

5. Results: Sustainable cellulose regeneration

This chapter and the associated parts in the experimental section are adapted from the following literature

K.N. Onwukamike, L. Lapuyade, L. Maillé, S. Grelier, E. Grau, H. Cramail, M.A.R. Meier, Sustainable approach for Cellulose aerogel preparation from the DBU-CO_2 switchable solvent system, *ACS Sustainable. Chem. Eng.* **2019**, 7(3), 3329.
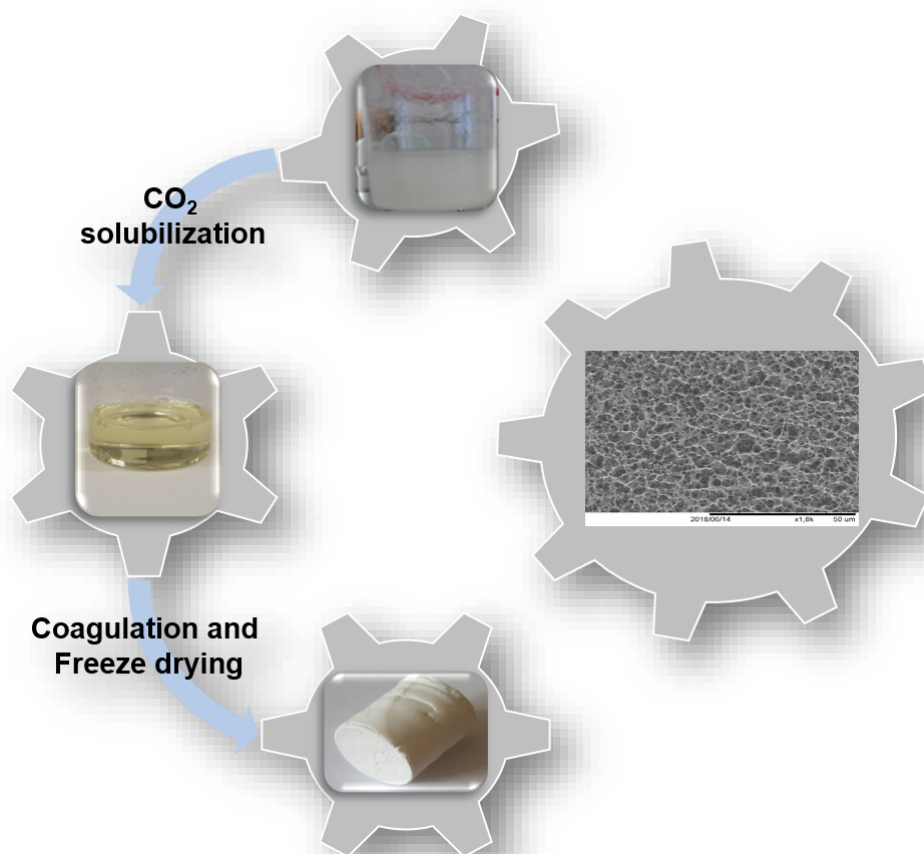
5.1 Abstract

Regeneration of cellulose affords the possibility to shape cellulose into interesting materials without the need for any chemical modification. Therefore, in this chapter, the use of the previously described optimized DBU-CO_2 switchable solvent system (**Chapter 4**), was employed for the preparation of cellulose aerogels. In this study, the general solubilization and coagulation approach, followed by freeze-drying, was adopted. The easy, fast and mild solubilization step (15 min at 30 °C), allows for a rapid preparation procedure. The effect of various processing parameters such as cellulose concentration, coagulating solvent and the super base on important aerogel characteristics including apparent density, porosity, morphology and pore size, were investigated. The obtained density values ranged between 0.05 and 0.12 g/cm^3 with porosity values between 92 and 97 %. The morphology of the obtained cellulose aerogels was studied using scanning electron microscopy (SEM) showing a random and open large macroporous cellulose network with pore sizes between 1.1 and 4.5 μm depending on the processing conditions. In addition, specific surface areas determined by N_2 adsorption applying the BET equation ranged between 19 and 26 m^2/g. The effect of the coagulating solvent and the super base on the crystallinity was investigated using X-ray diffraction (XRD) showing an amorphous crystal structure with a broad 2θ diffraction peak at 20.6°. In addition, no chemical modification was observed in the prepared aerogels from infrared spectroscopy. Finally, the recovery and re-use of the solvent system was demonstrated, thus making the process more sustainable.

5.2. Introduction

The absence of a thermal transition or melting point, makes direct processing of cellulose not possible.[26] However, cellulose can be shaped into various forms through solubilization and subsequent regeneration. Viscose, the most common and industrially relevant material consisting of regenerated cellulose fibers with diameters of ten microns, is made in this way.[26] In this case, cellulose is solubilized by first transforming it to a xanthate in alkaline medium using CS_2, resulting in viscose, which is then regenerated in acidic solution.[26] Other cellulose objects such as highly porous

beads have been reported being made from 8 % NaOH-water mixtures[250] or from NaOH-urea-water mixtures.[251] Of interest for the present study are the so-called cellulose-based aerogels (aero cellulose).

Aerogels are classified as materials with highly porous structures and voids filled with gases such as air; they show very low densities and a high specific surface area.[252,253] They are usually obtained from their wet gels by drying in a way that maintains their pores. Examples of such drying processes include freeze-drying or drying with super critical CO_2. In this way, the strong capillary forces, which will otherwise lead to a collapse of the structure during drying, are overcome. The most common inorganic aerogels are based on silica,[252] whereas resorcinol-formaldehyde aerogels are the most common organic representatives made *via* the sol-gel process.[254,255] Aerogels are a very interesting class of material, finding applications as thermal insulators,[256] as electrodes for electrochemical applications (after pyrolysis),[257] and for bio-medical use (controlled drug release or as scaffolds).[258,259] Interestingly, aerogels can also be prepared from cellulose with the first attempt reported by Kistler in the 1930's.[260,261] Examples on aerogel preparation from cellulose I such as bacterial cellulose or micro- or nanofibrillated cellulose, have been reported.[257,262,263] Silylated cellulose nanofibril sponges have been reported to be able to selectively remove oil from water.[264] On the other hand, the use of regenerated cellulose (cellulose II, for instance from agricultural waste sources) offers a cheaper and more viable source for aerogel preparation. For the production of bacterial cellulose fibres for instance, high amounts of nutrients are required. Most importantly, regenerated cellulose can be prepared from various cellulose types without the need for further preparation procedures (in contrast to nanocellulose). For cellulose II, the aerogels are prepared *via* the solubilization and coagulation approach. The procedure is explained briefly as follows: cellulose is solubilized first, followed by transferring it into a mold where an anti-solvent (so-called coagulating solvent) such as water or ethanol is added in order to exchange the more polar and higher boiling cellulose solvent. After solvent exchange, depending on the drying method being employed, a second solvent exchange might be necessary. For example, for super critical CO_2 drying, compatible solvents such as ethanol are used, whereas for freeze-drying water is used instead.

The first and most challenging step of preparing cellulose aerogels from regenerated cellulose II, requires the complete solubilization of the polymer. This step is

challenging because cellulose is insoluble in common organic solvents as well as in water as previously explained (**Chapter 2.5**). Thus, only solvents capable of disrupting these hydrogen bonds can solubilize cellulose. In this regard, Innerlohinger and co-workers employed *N*-methyl morpholine-*N*-oxide monohydrate (NMMO·H_2O) to solubilize cellulose for cellulose aerogel preparation.[252] Factors such as cellulose concentration and preparation methods were investigated regarding their influence on the density and on the volume shrinkage of the obtained aerogels. Their results showed that increasing cellulose concentrations generally led to an increase in the density. They reported aerogel density values between 0.02 and 0.2 g/cm^3, with an open-pore nanofibrillar aerogel morphology typical for supercritical CO_2 drying. Following a similar cellulose aerogel preparation approach, Wang *et al.* used a 8% LiCl-DMSO solvent mixture for cellulose solubilization and subsequent coagulation in ethanol.[265] To aid the dissolution step, the cellulose was first activated by soaking in ethylenediamine (EDA) for 24 h at room temperature, with dissolution achieved after heating to 75 °C for 24 h. The resulting solubilized cellulose solution was then coagulated using ethanol and dried *via* supercritical CO_2 to afford the desired aerogel. The obtained densities ranged from 0.068 to 0.137 g/cm^3 with mesoporous structures containing pore sizes ranging between 10 to 60 nm. The use of a salt melt based on calcium thiocyanate (Ca(SCN)$_2$.4H_2O) has been reported separately by Hoepfner *et al.*[266] and Jin *et al.*[267] In their reports, cellulose was solubilized at temperatures ranging between 110 and 140 °C within 1 h. As with the previous procedures, coagulation was done using water or ethanol for freeze-drying or super critical CO_2 drying, respectively. The obtained aerogels (or cryogel for freeze dried) showed an increase in density with increased cellulose concentrations, as well as a nanofibrillar structure for the supercritical CO_2 dried samples.[266,267]

A more robust study on the structure development and morphology control of cellulose aerogels was reported by Budtova and Buchtová.[268] In their report, cellulose solubilization was achieved in an ionic liquid-DMSO solvent mixture. Here, the ionic liquid, [C$_2$mim]$^+$[OAc$^-$] was used. Cellulose was dissolved by first heating it to 70 °C in DMSO for 2 h followed by the addition of the ionic liquid with further heating at 70 °C within 2-24 h depending on the cellulose concentration. The cellulose gels were prepared following the general coagulation approach of the solubilized cellulose using ethanol. Various drying methods were investigated such as vacuum, freeze-drying and

super critical CO_2 drying. The authors classified the obtain samples based on the drying method as follows: xerogels (vacuum dried), cryogel (freeze-dried) and aerogel (supercritical CO_2 dried). As expected, xerogels were completely non-porous, as the high capillary forces during drying led to a collapse of the porous structure. The xerogels had very high density values close to those of microcrystalline cellulose (about 1.5 g/cm^3).[269] On the contrary, in the case of freeze-dried or super critical CO_2-dried samples, the porous structure of the gels was kept with porosities between 86 and 96 %. Of importance to note was the difference in the density as well as the volume shrinkage between both drying methods. Aerogels obtained from freeze-drying showed less volume shrinkage (before and after drying) compared to supercritical CO_2 drying. In addition, lower density values (typically below 0.1 g/cm^3) were obtained for freeze-dried gels compared to values between 0.1-0.2 g/cm^3 for supercritical CO_2 dried samples.[268]

The effect of various cellulose solvents on the morphology and properties of cellulose aerogels has been reported by Liebner and co-workers.[270] Solvents investigated included: ionic liquid/DMSO ($[C_2mim]^+[OAc^-]$-DMSO), tetrabutyl-ammonium fluoride/dimethylsulfoxide (TBAF-DMSO), *N*-methyl morpholine-*N*-oxide monohydrate (NMMO·H_2O) and calcium thiocyanate octahydrate-lithium chloride; CTO ($Ca(SCN)_2$·8 H_2O-LiCl). The solubilized cellulose was coagulated using ethanol followed by supercritical CO_2 drying to afford the desired aerogels. Their results showed that these solvents played a significant role in the bulk properties of the aerogels such as morphology and porosity. For instance, while aerogels made from ($[C_2mim]^+[OAc^-]$-DMSO showed a more random short nanofiber network that assembled into a globular super structure, those from TBAF-LiCl showed a more homogeneous interwoven nanofiber network with interconnected nanopores. In contrast to that, aerogels from NMMO·H_2O and CTO showed a more random network of cellulose nanofibers. The authors correlated these differences to the mechanism of gel formation in the different solvents. In the case of ($[C_2mim]^+[OAc^-]$ and TBAF-LiCl, the aerogel formation followed the spontaneous one-step phase separation mechanism, which is entirely controlled by diffusion, whereas, NMMO and CTO-derived aerogels followed a two-step phase separation mechanism. In the latter case, the first phase separation occurs during the cooling of the dissolved cellulose solution, which gives time for an alignment of the cellulose fibres into longer nanofibres. The

second phase separation step occurs during the addition of the anti-solvent (coagulating solvent), which also leads to further alignment of the cellulose fibres in close proximity to the already ordered longer nanofibers networks from the first phase separation step. The consequence is an increased crystallinity (cellulose II) and better mechanical properties (higher compressional stress) of the resulting aerogels.[270]

However, the solvents used in these previous studies, such as LiCl-DMSO, NMMO and ionic liquids are either toxic (acute toxicity LD_{50}, rat LiCl = 526 mg/kg), thermally unstable[95,96] or non-inert,[135,136] respectively. Furthermore, no investigation on the recycling or re-use of any of these solvents has been reported. As renewability is not enough to ensure sustainability,[121] neglecting of other aspect of Green Chemistry[18,108,189] during cellulose transformation simply shifts the carbon footprint to other stages of the life cycle.

Having previously described a cheaper, easy and mild cellulose solvent system based on CO_2 (**Chapter 4**), the question arose if it would be possible to shape cellulose into aerogels from this solvent system following the well-developed solubilization-coagulation approach. Therefore, within this chapter, the preparation of cellulose aerogels from the DBU-CO_2 switchable solvent system will be described. The focus herein will be the fast, mild and easy solubilization step as well as the influence of processing parameters such as the cellulose concentration, coagulating solvent as well as other super bases on important aerogel characteristics including porosity and morphology. Importantly, as one of the objectives of this study is to establish a more sustainable solvent system for cellulose aerogel preparation, the recycling and re-use of the solvent system will be demonstrated.

5.3. Results and discussions

5.3.1 Proposed mechanism of cellulose gel formation

The preparation of aerogels from regenerated cellulose has been proposed to occur through two different mechanisms and depends on the type of the solvent employed.[270] As shown from the reports of Liebner *et al.*,[270] solvents such as ionic liquids and TBAF-LiCl follow the one-step phase separation mechanism whereas NMMO·H_2O and CTO (Ca(SCN)$_2$·8 H_2O-LiCl) follow the two-step phase separation mechanism. Looking at the differences between these solvents (regarding the solubilization temperature), a two-step phase separation mechanism is proposed for the CO_2 switchable solvent system. In this case, the first phase separation step involves the removal of CO_2 after the cellulose solubilization (similar to the cooling-induced first phase separation step described by Liebner *et al.*[270]), whereas the second phase separation occurs during the anti-solvent addition. The general cellulose aerogel preparation approach employed for the current study is shown in **Scheme 22**.
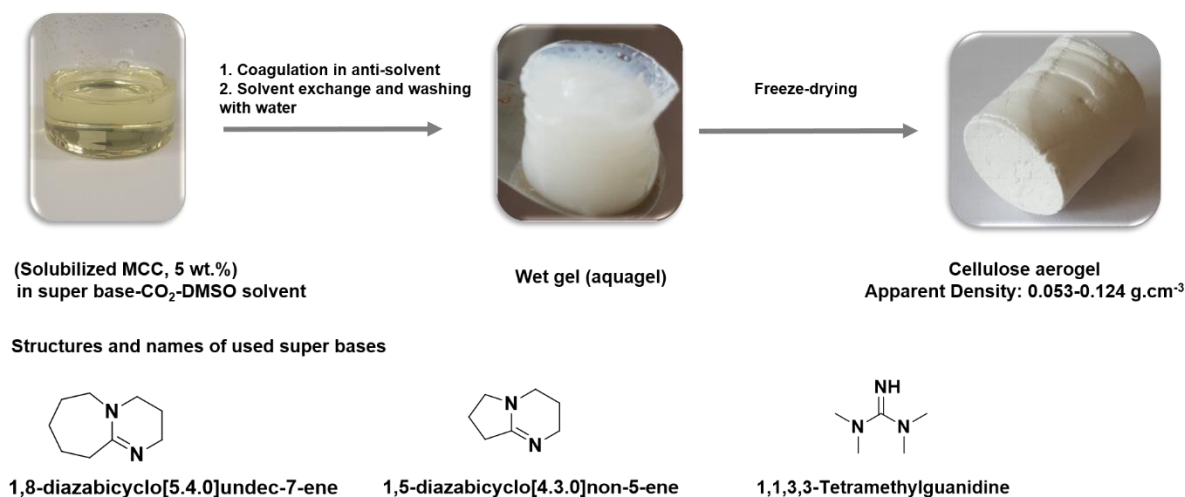
Scheme 22: General procedure for cellulose aerogels preparation from the DBU- CO_2 switchable solvent system.

5.3.2 Apparent density (bulk density)

Density is one of the most important properties of aerogels, with values ranging between 0.002 to 0.3 g/cm^3.[257,268] Such low densities arise from the fact that most of the material's volume is occupied by air. Therefore, the drying process is relevant during the aerogel preparation. In this regard, freeze drying or supercritical CO_2 drying are recommended, as they avoid pore collapse. In the course of this project, freeze-drying was selected, as it has been reported to result in less volume shrinkage compared to supercritical CO_2 drying.[268] In addition, freeze-dried aerogels have been reported to have lower densities compared to their super critical CO_2-dried counterparts,[268] as well as provide a faster approach for aerogel preparation. To avoid any misunderstanding, it is also important to point out the limitation of this approach, such as the influence of ice-crystals formed during water freezing that might "disturb" the already formed cellulose network of the aerogel. One way to at least limit this influence (by reducing the ice crystal size) is to dip the sample into liquid nitrogen before subjecting it to freeze-drying.[266] The apparent density (also referred to as bulk density in some reports)[252] of the aerogels was determined gravimetrically as in previous reports by taking the ratio between the measured weight to its volume.[252] For each formulation, 2-4 measurements were performed and their average value considered.

The effect of various processing parameters such as cellulose concentration, coagulating solvent and the super base on the apparent density were investigated. In the first instance, the effect of concentration was investigated by varying it from 5 to 10 wt.% using the DBU-CO_2-based solvent system and water as the coagulating solvent. Samples with lower concentrations (1, 2, 3, 4 wt.%) were unstable during the coagulation step and were therefore not further analyzed. The results (**Figure 12**), showed a linear-like increase of the apparent density from 0.08 g/cm^3 to 0.12 g/cm^3 as the cellulose concentration was increased from 5 to 10 wt.%. These results are consistent with previous reports.[252,268]
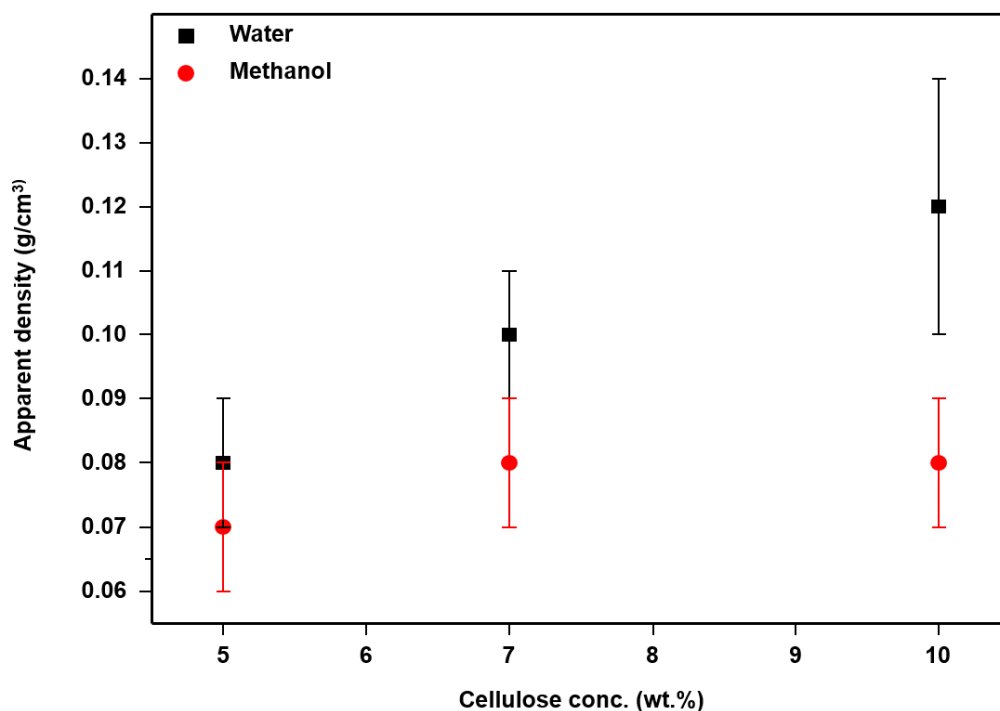
Figure 12: Effect of cellulose concentration on the apparent density of the aerogel.

Upon replacing water with methanol as the coagulating solvent, while keeping all the other processing parameters constant, a gradual increase of the apparent density was observed from 0.07 g/cm^3 to 0.08 g/cm^3 as the cellulose concentration was increased from 5 to 10 wt.%. As seen in **Figure 12**, for the same cellulose concentration, methanol-coagulated aerogels had lower densities compared to their water-coagulated counterparts. As a difference in the apparent density of the aerogels was observed by simply changing the coagulating solvent, other solvents such as ethanol and isopropanol were investigated. In addition, in one approach the coagulation process was carried out in the absence of any added anti-solvent (referred to here as the no-solvent coagulated aerogel). In this case, the coagulation was allowed to proceed in the DBU-DMSO solvent mixture after the release of CO$_2$, without any addition of an anti-solvent. After coagulation was complete, the wet sample was then washed repeatedly using methanol to remove DMSO and DBU followed by a solvent exchange with water to allow for freeze-drying. The comparison of all these solvents on the apparent densities using 5 wt.% MCC is shown in **Figure 56** (see experimental section **Chapter 8.4**). Considering their standard deviation, the obtained results are similar with apparent density values between 0.07 and 0.08 g/cm^3. Methanol was selected for further experiments investigating other bases than DBU in the solvent system, because it showed the least tendency to disrupt the solubilized cellulose

surface during the coagulation step, as well as its ease of recovery. Furthermore, alcohols show an acceptable solvent type according to the GSK solvent sustainability guide.[271] To investigate the effect of the super base on the apparent density, cellulose was solubilized (MCC, 5 wt.%) using other super bases (TMG and DBN) as described in the experimental section **Chapter 8.4** using methanol for coagulation. From the results obtained (experimental section **Figure 57**), similar apparent density values ranging between 0.05 and 0.07 g/cm^3 were obtained.

The porosity of the aerogel was calculated from the density results using the general approach,[268,272,273] from eq.2 as follows:

$$\text{Porosity (\%)} = 100 \times \left(1 - \frac{\rho_{\text{apparent}}}{\rho_{\text{skeletal}}}\right) \dots\dots\dots\dots\dots\dots\dots\dots\dots\dots\dots\dots\dots\text{eq.2}$$

In the eq.2, ρ_{apparent} is the calculated apparent density of the aerogel and ρ_{skeletal} is the true density of microcrystalline cellulose, which is approximately 1.5 g/cm^3.[269]

The obtained porosity results (see **Table 4**), which are in agreement with those of the density, showed higher porosity for lower density samples. The effect of changing the coagulating solvent on the porosity is as follows: water (94 %) < methanol, ethanol, isopropanol, no solvent (95 %). The highest porosity of 97 % was obtained for TMG-based aerogels followed by DBN (96 %).

5.3.3 Morphology and pore size

The morphology of the resulting aerogels was studied using scanning electron microscopy (SEM). As with the other basic properties of the aerogels, the effect of the cellulose concentration, coagulating solvents as well as the super base on the morphology of the aerogels was investigated. For the DBU-based aerogel and using water as the coagulating solvent, the cellulose concentration was increased from 5 to 10 wt.%. The resulting SEM images for 5 wt.% is shown in **Figure 13**, the others are displayed in the experimental section (**Figure 58**-**Figure 60**).
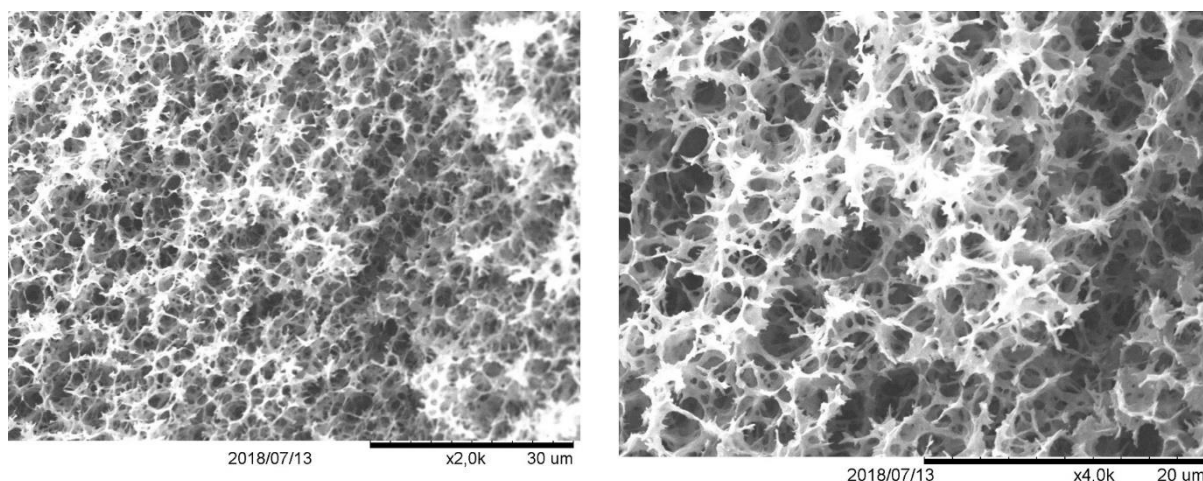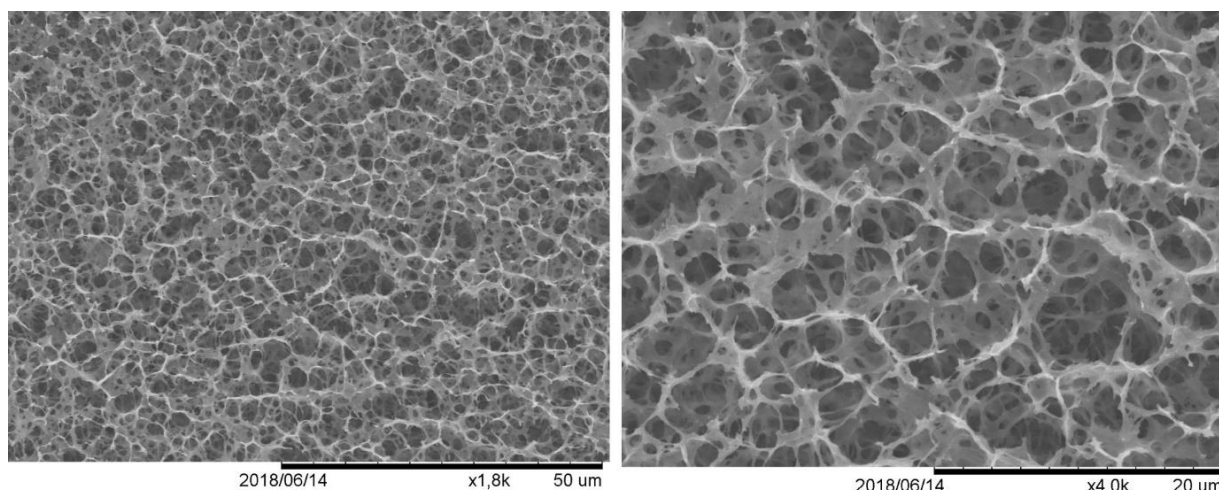
Figure 13:SEM images of cellulose (5 wt.% MCC) aerogels obtained *via* freeze-drying (cellulose solubilized in DBU-CO_2 solvent system and coagulated using water).

As can be seen from these images, highly open and interconnected large macroporous cellulose networks with non-porous pore walls of around 200-500 nm were observed. These nonporous pore walls probably resulted from ice-crystals growth during the freeze-drying step, which causes compactness of the cellulose fibres. This morphology is typical for freeze-dried aerogel samples and similar to those reported by Budtova *et al.*[268] However, unlike in their reports, the pore walls are not "flat-like" and appear much thinner. Also, the much finer nanofiber network that is characteristic of supercritical CO_2-dried aerogels[266,267] is not observed, because it is most likely destroyed during the freeze-drying process due to ice growth of the freezing water. A similar morphology was observed when water was replaced with methanol as the coagulating solvent for all investigated concentrations (see experimental section **Figure 60**-**Figure 62**). Furthermore, using 5 wt.% cellulose (MCC), the effect of other coagulating solvents such as ethanol, isopropanol as well as no solvent on the morphology of the aerogels was investigated. The SEM images of isopropanol and ethanol-coagulated aerogels are displayed in the experimental section (**Figure 63** and **Figure 64**). While similar morphologies as previously described for water and methanol-coagulated samples were obtained for ethanol and isopropanol, the sample coagulated without addition of an anti-solvent showed a more uniform and homogeneous cellulose network as seen in **Figure 14**.
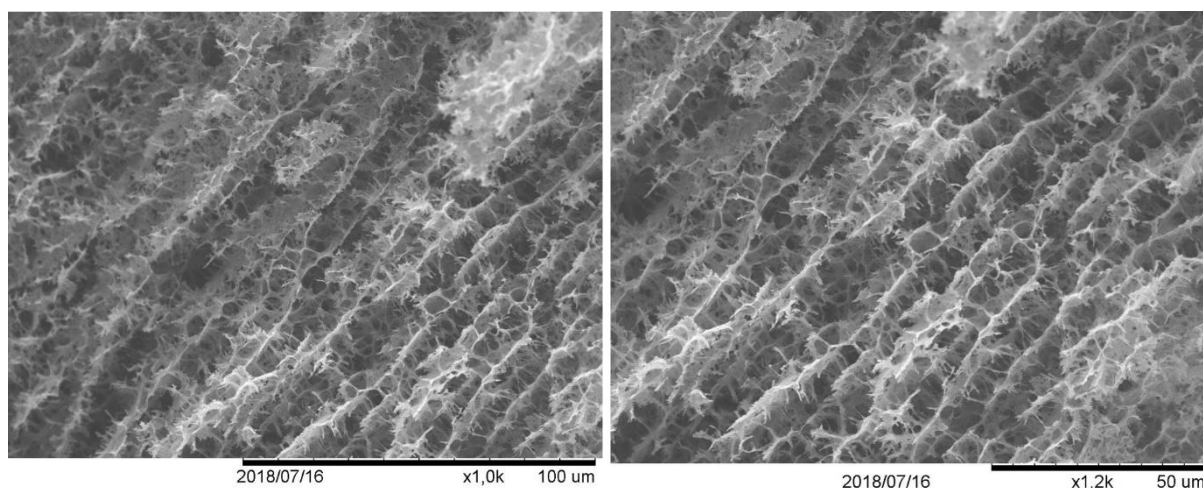
Figure 14: SEM images of cellulose (5 wt.% MCC) aerogels obtained *via* freeze-drying (cellulose solubilized in a DBU-CO_2 solvent system and coagulated without addition of an anti-solvent).

In addition, the effect of the super base on the aerogel morphology was investigated. Using 5 wt.% cellulose and methanol as coagulating solvent, the SEM images for the aerogels using TMG and DBN are shown in the experimental section (**Figure 65** and **Figure 66**). The results show a slightly difference in the morphology compared to the DBU-solvent based aerogel (compare **Figure 13**). In the DBN-solvent based aerogel, the interconnected large macroporous cellulose networks are arranged in a "ridge-like" manner with about 8.21 ± 0.8 µm separation between the "ridges". Between these "ridges" a similar morphology as described for the DBU-solvent samples can be observed. In the TMG-solvent samples, a mixture of "ridge-like" arranged micropores and the typical observed open and random microporous cellulose network is observed. When methanol was replaced with ethanol and using TMG as super base (**Figure 15**), the "ridge-like" morphology similar to that of DBN-methanol aerogel could be seen more clearly.

Figure 15: SEM images of cellulose (5 wt.% MCC) aerogels obtained *via* freeze-drying (cellulose solubilized in a TMG-CO$_2$ solvent system and coagulated using ethanol).

While it will require more detailed studies to fully describe these observed changes, it can be concluded that the solvents as well as their composition (considering the super base as part of the solvent system) can have an influence on the morphologies of the aerogels. This slight variation can therefore be applied for tuning the morphology for a given application. Investigation on cellulose pulp (CP) using water or ethanol for coagulation and DBU as a super base gave similar morphologies (**Figure 67** and **Figure 68**) compared to MCC. However, the CP aerogels showed a higher resistance to breakage when compressed by hand compared to MCC aerogels, probably due to a higher molecular weight of the cellulose pulp.

The pore size was estimated from the SEM data as described in the experimental section **Chapter 8.4**, keeping in mind that this results in a relatively high error margin and can only be used to estimate the range of the pore size, especially for large macropores as observed in the present study. A total of sixty pores was considered for each sample. More accurate methods, such as nitrogen adsorption (Barrett-Joyner-Halenda, BJH approach) do not allow the estimation of a wide range of pore size, while mercury porosimetry faces the limitation of compressing the aerogel pores and not able to enter the pores.[268] Therefore, SEM was used as a fast approach for estimating the pore size range. The effect of the various processing parameters such as cellulose concentration, coagulating solvents, and super base on the pore size was investigated. Using water as a coagulating solvent and DBU as super base in the solvent system, the cellulose concentrations was varied (5, 7 and 10 wt.%). The

obtained results (**Figure 16**) show that the pore size ranged between 1.2 to 2.2 µm and does not show a clear trend with varying cellulose concentrations.
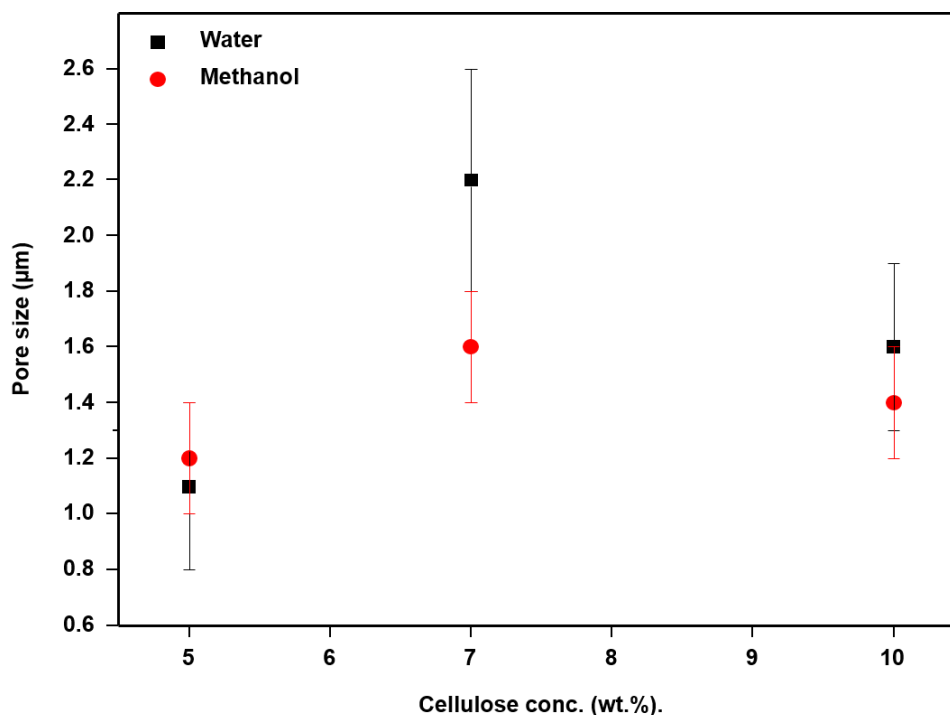

Figure 16: Effect of cellulose concentration on the pore size of cellulose aerogels using DBU as a super base.

However, it is important to point out that from experimental observations, coagulation with water led to a disruption of the solvent surface, thereby affecting the coagulation process. In contrast to water, the lower density of methanol compared to DMSO-DBU led to a more stable process. Therefore, another attempt was made using methanol as the coagulating solvent and the results are included in **Figure 16**. As can be seen, the pore size remained fairly constant (1.2 to 1.6 µm) as the cellulose concentrations was increased from 5 to 10 wt.%. These results are somewhat different to those reported by Budtova *et al.*,[268] where a decrease in pore size was observed with increasing cellulose concentration, while the pore walls remained fairly constant. However, from results obtained during this study, an increased cellulose concentration also led to an increase in the thickness of the pore walls. Such differences are not unusual, considering that the solvents employed play an important role in the aerogel morphology as shown in the works of Liebner *et al.*[270] As described by these authors, ionic liquids, which were employed by Budtova *et al.*,[268] follow a one-step phase separation mechanism for the gel formation, whereas the studied CO_2 switchable

solvent as previously proposed (see proposed mechanism**, Chapter 5.3.1**), rather follows a two-step phase separation mechanism.

In order to get a better picture of the effect of the coagulating solvent on the pore size and using 5 wt.% MCC with DBU as super base, other coagulating solvents such as ethanol, isopropanol and as well as sample without solvent were investigated. The results for these various coagulating solvents on the pore size are included in the experimental section (**Figure 69**). The pore size increased in the order; 1.1 µm (water) < 1.2 µm (methanol, isopropanol) < 1.3 µm (no solvent) < 1.5 µm (ethanol). Considering the standard deviation of these values (see **Table 4**), there appears to be little difference in the pore size when the coagulating solvents were changed. However, a size difference of about 0.4 µm can be observed between water and ethanol as the coagulating solvent. Apart from their difference in polarity and structure, the higher density of water (1.0 g/cm^3) compared to ethanol (0.79 g/cm^3) might be responsible for this observation. The higher density of water implies a faster coagulation, as the solvent exchange between water and DMSO-DBU is faster, leading to smaller pore sizes. The role of the solvent density on the pore size was further investigated by using cellulose pulp instead of microcrystalline cellulose. Using water and ethanol as coagulating solvents, the results obtained showed a lower pore size (0.6 µm) for water-coagulated aerogels compared to 1.1 µm for ethanol-coagulated aerogels (see **Figure 70**). These results, which are consistent with the previous observations, further support the role of the solvent density on the pore size of the aerogels.

In addition, the effect of the super base on the pore size was investigated. In this regard, using 5 wt.% MCC, the super bases DBU, TMG and DBN were applied for solubilizing cellulose. Coagulation was done using methanol, as it is easier to recycle compared to water and also showed the least tendency to disrupt the solubilized cellulose surface during the coagulation step. The results are included in the experimental section (**Figure 71**), show an obvious increase in pore size from 1.2 µm when DBU was used, to 3.5 µm in the case of TMG, and 4.5 µm for DBN. The reason for this obvious difference is not very clear and will require further investigation. However, considering the increasing interest for designing tailored cellulose-based materials (aerogel in this case), these results are promising as they give an idea of how to tune the pore size by simply changing the super base in the solvent system.

In addition, the specific surface area of some aerogels was determined by N_2 adsorption and applying Brunauer-Emmett-Teller (BET) equation. The BET specific surface area results are included in **Table 4** (for samples obtained at various cellulose concentration when DBU and methanol-coagulation was applied). Data obtained showed specific surface areas between 19 and 26 m^2/g, which are within range of previous reports for freeze-dried obtained aerogels.[268]

5.3.4 Crystallinity investigation via X-ray diffraction

The crystallinity of the aerogels was determined *via* X-ray diffraction measurements. Samples made with various coagulating solvents as well as different super bases were compared, as shown in **Figure 17**.
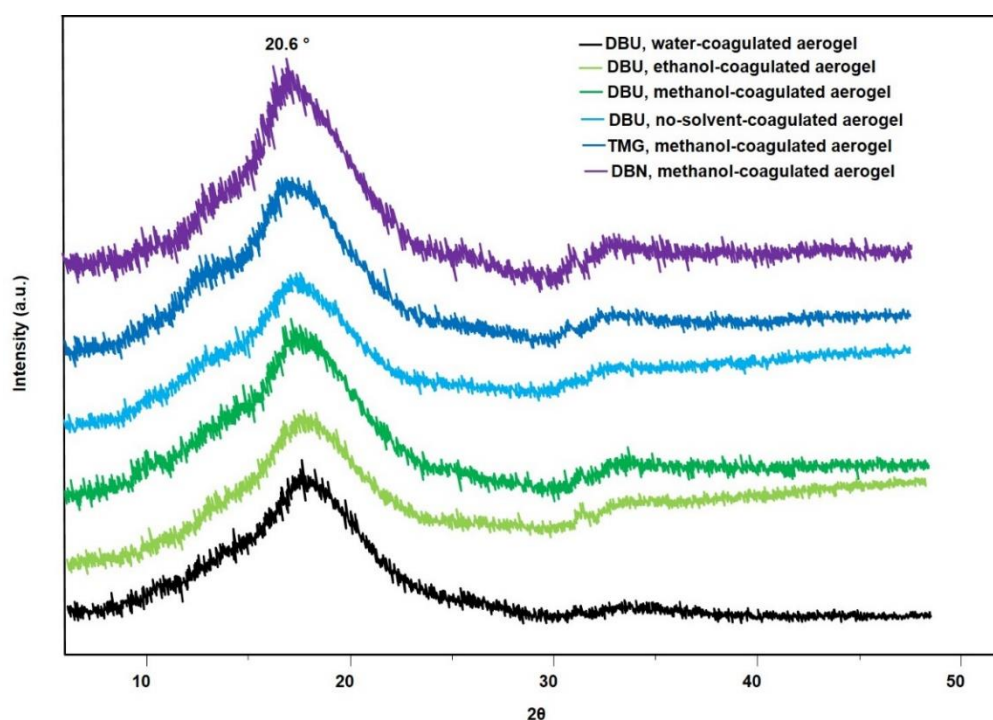
Figure 17: XRD data of cellulose (5 wt.% MCC) aerogels obtained *via* freeze-drying under various processing conditions.

The obtained results showed broad diffraction 2θ peaks at 20.6°, characteristic of a more amorphous cellulose.[120,274] Furthermore, the aerogel coagulated with methanol and using DBU as super base was compared with the native cellulose (MCC) using infrared spectroscopy (see experimental section **Figure 72**). The obtained results showed no newly introduced peaks and also no characteristic peaks from the solvent system were visible (DBU and DMSO), thus showing that no chemical modification occurred during the preparation process. However, an obvious shift and decrease of

the O-H stretching vibration peak from 3301 cm^{-1} in the native MCC to 3395 cm^{-1} in the aerogel was noticed. This can be attributed to the decreased hydrogen bonding in the aerogel sample compared to the native cellulose. Other observed differences between the spectra are associated to their difference in crystalline structure. Thus, the "crystalline band" peak at 1432 cm^{-1} found in the native cellulose is replaced by the "amorphous band" at 898 cm^{-1} in the aerogel sample.[274]

Table 4: Summary of the processing conditions and properties of cellulose aerogels from the CO_2 switchable solvent system.

Sample	Coagulating solvent	Apparent density (g/cm^3)	Porosity (%)	Pore size (µm)	BET specific surface area (m^2/g)
MCC-5%, DBU	water	0.08 ± 0.01	95	1.1 ± 0.3	__
MCC-7%, DBU	water	0.10 ± 0.01	94	2.2 ± 0.4	__
MCC-10%, DBU	water	0.12 ± 0.02	92	1.6 ± 0.3	__
MCC-5%, DBU	methanol	0.07 ± 0.01	95	1.2 ± 0.2	24 ± 1
MCC-7%, DBU	methanol	0.08 ± 0.01	95	1.6 ± 0.2	19 ± 1
MCC-10%, DBU	methanol	0.08 ± 0.01	95	1.4 ± 0.2	26 ± 1
MCC-5%, DBU	ethanol	0.08 ± 0.01	95	1.5 ± 0.2	__
MCC-5%, DBU	isopropanol	0.08 ± 0.01	95	1.2 ± 0.1	__
MCC-5%, DBU	no-solvent	0.08 ± 0.01	95	1.3 ± 0.3	__
MCC-5%, TMG	methanol	0.05 ± 0.01	97	3.3 ± 0.5	__
MCC-5%, DBN	methanol	0.06 ± 0.01	96	4.5 ± 0.7	__
MCC-5%, TMG	ethanol	0.06 ± 0.03	96	4.2 ± 0.6	__
CP-3%, DBU	water	0.10 ± 0.02	94	0.6 ± 0.1	__
CP-3%, DBU	ethanol	0.11 ± 0.02	93	1.1 ± 0.3	__

5.3.5 Investigation of solvent recovery and re-use

Finally, the recovery of the solvent system was demonstrated (details in experimental section **Chapter 8.4**). 60 % of pure DBU could be recovered through cyclohexane extraction from the DMSO-DBU-DBUH$^+$/HCO$_3^-$ mixture. The very low solubility of DBU in cyclohexane means an intensive extraction was required (up to 6 separate extractions to reach 60 % recovery), thus an automated extraction would greatly improve this step. On the other hand, 90 % of the DMSO could be recovered *via* vacuum distillation (25 mbar, 90 °C). A comparison of the pure and recovered solvent was done using infrared spectroscopy (see **Figure 73** and **Figure 74**) and showed no structural differences. In addition, the recovered solvent system (DMSO and DBU) was used for another solubilization of cellulose (5 wt.%) which showed no obvious difference. The demonstration of recovery and re-use of the solvent is a very important consideration for sustainability and makes the process appealing for future sustainable cellulose aerogel preparation.

5.4. Conclusions

In this chapter, an easy and sustainable approach for the preparation of cellulose aerogels from the DBU-CO$_2$ switchable solvent system was studied. Cellulose was first solubilized within 15 min at 30 °C and then the aerogels were prepared *via* the solubilization-coagulation approach followed by freeze-drying to prevent a collapse of the porous structure. Parameters such as cellulose concentration (5, 7 and 10 wt.%), coagulating solvents (water, methanol, ethanol, isopropanol, no-solvent) as well as the super base (DBU, TMG and DBN) on the properties of the aerogels (density, porosity, pore size and morphology) were investigated. Results obtained showed that increasing cellulose concentrations from 5 to 10 wt.% generally led to an increase in the density and an associated decrease in porosity. By varying the various processing parameters, porosity values obtained ranged between 92 and 97 %, with densities between 0.05 and 0.12 g/cm^3. Furthermore, from scanning electron microscopy (SEM), all investigated coagulated solvents showed a random open large macroporous cellulose network morphology with thin non-porous cell walls ranging between 200 and 500 nm and pore size between 1.2 to 2.2 μm. However, the aerogels coagulated without solvent showed a more homogenous open macroporous cellulose

network. Also, changing the super base resulted in a slight difference in the morphology as well as the pore size of the aerogels. A "ridge-like" arranged large macroporous cellulose network was observed for DBN and TMG that was absent in the case of DBU. In addition, the pore size could be tuned from 1.2 µm (DBU) to 3.5 µm (TMG) or 4.5 µm for DBN. The calculated BET specific surface areas ranged between 19 and 26 m^2/g as cellulose concentration was varied between 5 and 10 wt.% for methanol-coagulated aerogel samples.

Furthermore, the recovery (DBU 60 %, DMSO 90 %) and re-use of the solvent system was demonstrated. Finally, the reported detailed study of the effect of the various processing conditions on the properties of the obtained aerogels will allow for a design of cellulose aerogels to suit a given application.

6. Results: Sustainable cellulose derivatization

6.1 Direct transesterification of cellulose using high oleic sunflower

This chapter and the associated parts in the experimental section are adapted from the following literature:

K.N. Onwukamike, S. Grelier, E. Grau, H. Cramail, M.A.R. Meier, Sustainable transesterification of Cellulose with high oleic sunflower oil in a DBU-CO$_2$ Switchable Solvent System, *ACS Sustainable. Chem. Eng.* 2018, 6, 7, 8826.

With kind permission from the American Chemical Society (ACS), copyright © 2018. https://pubs.acs.org/doi/10.1021/acssuschemeng.8b01186

Notice: Further re-use of this material should be directed to the American Chemical Society (ACS).
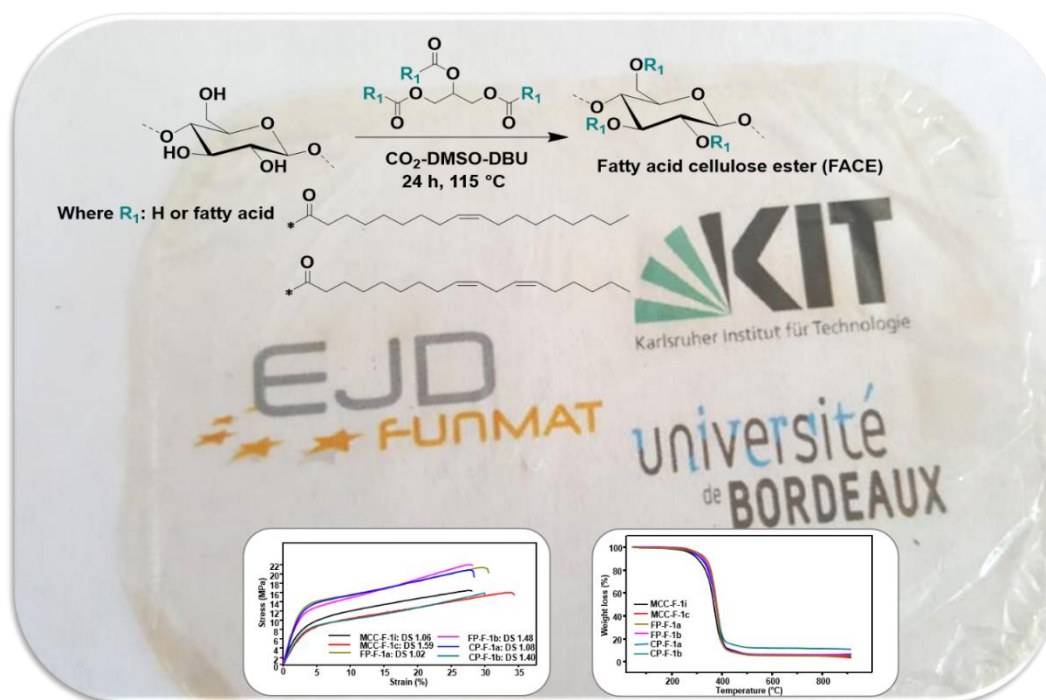
6.1.1 Abstract

Having presented in the previous chapters an optimized CO_2-based sustainable solvent for cellulose (**Chapter 4**) followed by a sustainable regeneration approach to make cellulose aerogels (**Chapter 5**) this chapter focuses on obtaining processable cellulose materials *via* sustainable homogeneous chemical modification. Therefore, transesterification which is a well-known basic reaction was employed. As described in **Chapter 2.5**, ensuring sustainability also depends on the use of non-derivative reactants, therefore plant oil (high oleic sunflower oil) was used directly in the transesterification reaction. With a combination of all these important sustainability considerations, fatty acid cellulose esters (FACEs) were successfully synthesized in the DBU-CO_2 switchable solvent system. Optimization of the reaction parameters (i.e. concentration, temperature, plant oil equivalents, reaction time) was performed using microcrystalline cellulose (MCC) and followed by infrared spectroscopy (ATR-IR). Further confirmation of the FACEs structures was achieved *via* ^{1}H and ^{13}C NMR and ^{31}P NMR revealed DS (degree of substitution) values of up to 1.59. The optimized conditions were successfully applied to filter paper (FP) and cellulose pulp (CP). Characterization of the FACEs showed improved thermal stability after transesterification reactions (up to 30 °C by TGA) and a single broad 2θ peak around 19.8° by XRD, which is characteristic of a more amorphous material. In addition, films were prepared *via* solvent casting and their mechanical properties obtained from tensile strength measurements, revealing an elastic modulus (E) of up to 478 MPa with elongation of about 35 %. The film morphology was studied by scanning electron microscopy (SEM) and showed homogeneous surfaces. In this study therefore, a more sustainable approach towards FACEs that combines cellulose and plant oil (two renewable resources) directly was demonstrated, resulting in fully renewable polymeric materials with appealing properties.

6.1.2 Introduction

Cellulose esters are among the most investigated and produced cellulose derivatives finding applications in the coating industry and as optical media films.[26] A more detailed explanation of their various applications and preparation procedure is described in **Chapter 2.5**. Typically, these substrates are produced industrially *via* heterogeneous modification. Using such processes, the degree of substitution (DS) of the cellulose structure is not easily controlled. In cellulose acetate for example, a DS of 3.0 is usually achieved and de-acetylation is necessary to obtain lower DS values. Furthermore, the stoichiometric use of reagents, the use of strong bases/acids to swell/activate the cellulose backbone as well as the generation of waste during the synthesis affect the sustainability of the process. However, several investigations *via* homogeneous routes have been reported using activated acid derivatives (i.e. acid chlorides or anhydrides) in stoichiometric amounts (see **Chapter 2.5.5**) In the context of Green Chemistry, the use of renewable resources is not enough, rather the entire synthesis process should be considered to ensure sustainability.[121] In a more sustainable approach, acid anhydrides and acyl chlorides should be substituted by esters that are easier to handle, less toxic, non-corrosive, and result in less waste upon esterification (see **Table 3** for E-factor comparison between various cellulose esterification processes). In this regard, the groups of Meier and Barner-Kowollik reported the catalytic transesterification of cellulose using methyl esters and fatty acid methyl ester (FAMEs) in the ionic liquid $[C_4mim]^+[Cl^-]$ with TBD as catalyst.[157] Even though moderate degrees of substitution (DS) of 0.69 were reached, it did pave the way for a more sustainable approach for synthesizing cellulose esters.

Films made from FAMEs have been investigated as sustainable packaging materials.[275,276] In both reports, fatty acid chlorides were used and the cellulose modification was carried out under heterogeneous conditions. Kilpeläinen *et al.*, showed that such FACEs films had good water vapor and air barrier properties with improved mechanical properties.[276] However, the use of acid chlorides as well as the use of pyridine for swelling the cellulose in this report makes the process less sustainable. Therefore, producing cellulose esters by direct utilization of the plant oils would improve the sustainability of this transesterification process by avoiding derivatization steps. This approach was adopted by Söyler and Meier for the catalytic transesterification of starch reaching a DS of 1.3.[177] In this case plant oils (high oleic

sunflower oil and olive oil) were used directly and reaction carried out in DMSO with TBD as catalyst.[177] The obtained fatty acid starch esters were soluble in most organic solvents and showed good mechanical properties. However, utilizing starch raises the debate about "food or fuel" due to its very important role as food. Thus, replacing starch with cellulose will address this concern. Furthermore, the highly linear structure and higher molecular weight of cellulose is a challenge in terms of processing on the one hand, but will result in materials with improved mechanical properties.

So far, the only report on utilizing plant oils directly for cellulose modification is from Dankovich and Hseih.[277] The authors heterogeneously modified cellulose (cotton) surfaces using several plant oils (soybean, rapeseed, olive coconut oil and sunflower oil) in order to increase the hydrophobicity of the fibers. The procedure involved first solubilizing the plant oils in acetone or ethanol then allowing cellulose (cotton) to swell in this solution, after which the solvents were removed and the samples were heated between 110 and 120 °C for 1 h to improve the surface modification.

However, there is no report on homogeneous modification of cellulose using plant oils directly, the advantages of which has been highlighted above. Thus, this chapter focus on the direct transesterification of cellulose with plant oils in the previously described optimized DBU-CO_2 switchable solvent system (**Chapter 4**). It is important to mention that apart from DBU, also TBD would be a suitable catalyst for this type of reaction, which can also directly react with CO_2.[177,278] However, DBU is cheaper, and most importantly a liquid and thus easier to handle and to recover in this switchable solvent process. To show the scope of the developed protocol, three cellulose sources: microcrystalline cellulose (MCC), cellulose filter paper (FP) and cellulose pulp (CP) were investigated using high oleic sunflower oil without any pre-treatment. The reaction conditions were optimized and a thorough characterization of the obtained materials is reported.

6.1.3 Results and Discussions

Description of reaction mechanism

Taking into account the reports of Söyler and Meier on the transesterification of starch with plant oils[177] and the modification of carbohydrate in the DBU-CO_2 switchable solvents,[156,172] the homogeneous transesterification of cellulose was investigated using plant oils (high oleic sunflower oil) without any prior purification/modification. The general scheme of the reaction is shown in **Scheme 23**.
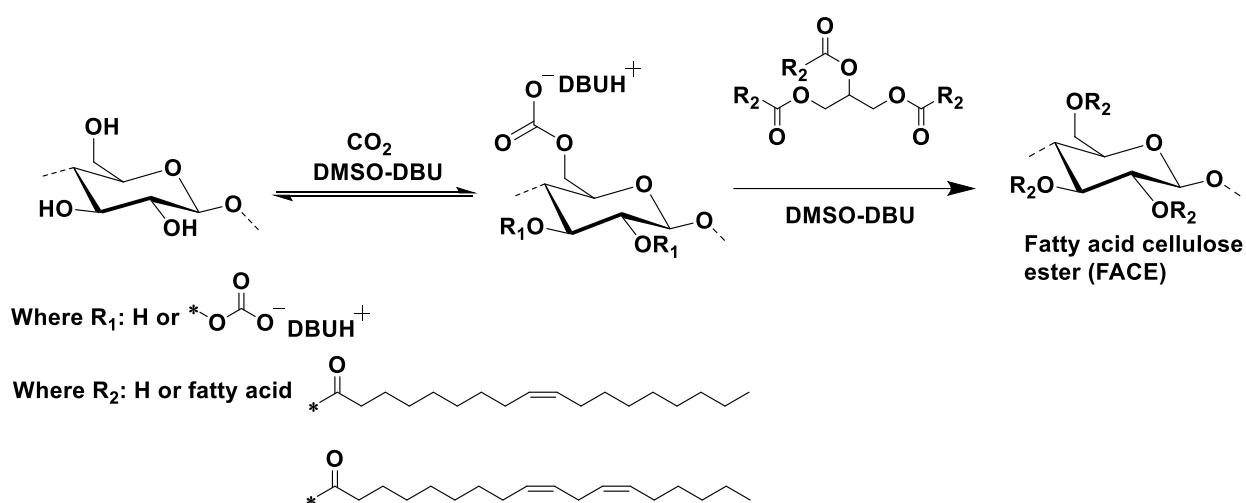
Scheme 23: Cellulose solubilization in DBU-CO_2 switchable solvent system and subsequent transesterification using high oleic sunflower oil.

From previous works on transesterification of carbohydrates (cellulose[157] and starch[177]) using organic base (TBD) as catalyst, 115 °C was observed as the optimal temperature. Thus for the present study, this temperature was chosen. Prior to the transesterification reaction, cellulose was solubilized by applying 5 bar of CO_2 in the presence of DBU (3 eq. per AGU) and DMSO. The completion of the reaction was monitored *via* ATR-IR (**Figure 18**). The FT-IR spectra were normalized to the C-O absorption of the pyranose unit in the cellulose backbone, which is not affected during cellulose modification (about 1025-1050 cm^{-1}) in order to compare the various investigated parameters relative to each other.
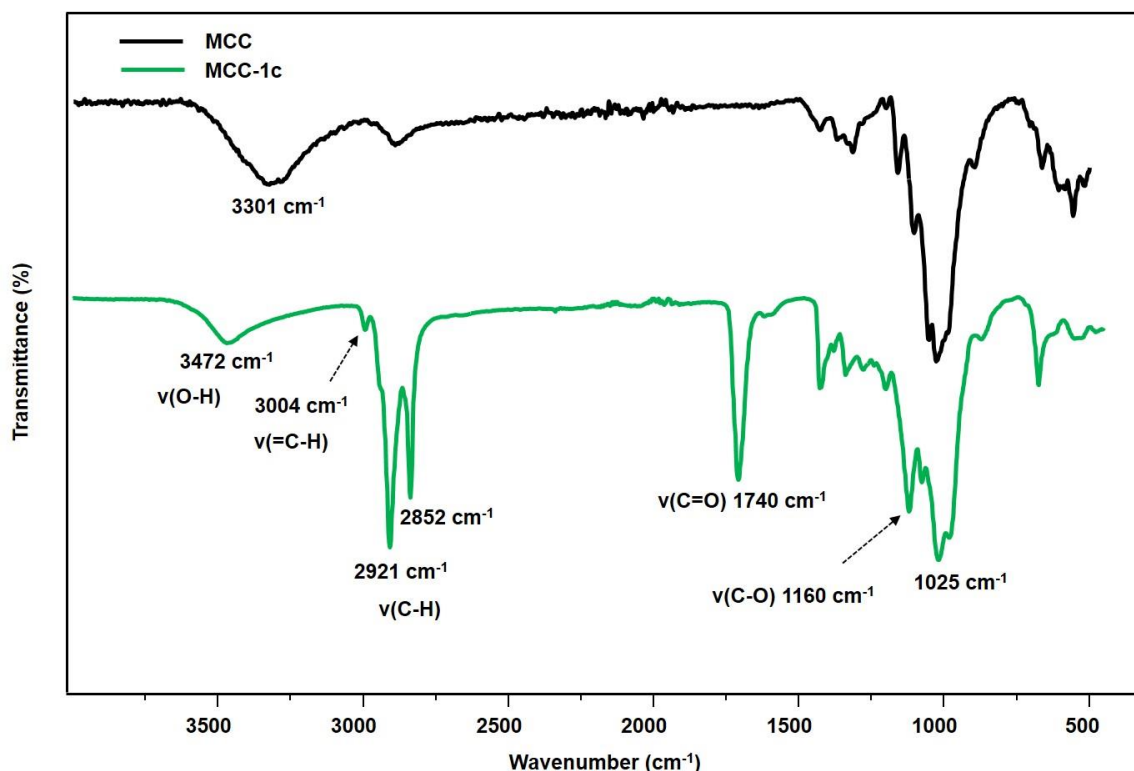
Figure 18: Typical ATR-IR spectra of a fatty acid cellulose ester, MCC-1c (5 wt.% MCC, 3 eq. high oleic sunflower oil/AGU, 115 °C, 24 h) in comparison to native MCC.

After the transesterification, the appearance of the C=O absorbance band characteristic for the newly formed ester group at 1740 cm^{-1} was observed. In addition, the intensity of the O-H stretching bands on the cellulose backbone (about 3300 cm^{-1}) was significantly reduced and shifted towards higher wavenumbers (~3400 cm^{-1}), indicating a decrease in hydrogen bonding in the cellulose backbone. Furthermore, the C-H stretching absorbance bands of CH_2 and CH_3 (2850 to 2925 cm^{-1}) corresponding to the aliphatic chain of the plant oils were observed. The peak at 1160 cm^{-1} is assigned to the C-O stretching band of the newly formed ester bond. In addition, the peak at about 3004 cm^{-1} is attributed to the =C-H stretching band found in oleic acid, which is a major constituent of high oleic sunflower oil (see **Figure 18**).

Typically, transesterification reactions proceed through an equilibrium reaction, thus requiring the removal of one of the products to drive the reaction. The use of catalysts can help to reach this equilibrium faster. In the report of Meier and Barner-Kowollik,[157] on the catalytic transesterification of cellulose using methyl esters, the reaction was driven both by the removal of methanol and presence of TBD as a catalyst.[157] For the DBU-CO_2 solvent system, it was observed that only about 70 % DBU is utilized during the solubilization step of cellulose,[156] thus being available to catalyze the

transesterification reaction. In addition, more DBU catalyst is freed during the reaction as CO_2 is removed in the course of the reaction. It was also observed that the addition of the plant oil to the solubilized cellulose mixture first led to a biphasic mixture, which gradually became homogeneous as the reaction proceeded, as the formed mono- and diglycerides can act as amphiphiles, thus addressing the initial miscibility issue. The presence of such mono- and diglycerides upon transesterification were also observed in the report of Söyler and Meier on transesterification of starch using plant oils.[177]

Effect of cellulose concentration

The optimization of reaction parameters was studied using microcrystalline cellulose (MCC). First, the effect of cellulose concentration was investigated, which was varied from 3 to 5 wt.% and the reaction was performed at 115 °C for 24 h using high oleic sunflower oil (3 eq. per AGU). After normalizing the spectra as mentioned above, the intensity of the C=O absorbance band from the fatty acid cellulose esters (FACEs) (1740 cm^{-1}) were compared to each other as presented in **Figure 19**, revealing that higher cellulose concentrations led to higher degrees of modification as evidenced by the increasing C=O absorbance intensities (**Figure 19**, right side). This is a typical observation; as most organic reaction proceeds more efficiently in concentrated solutions.
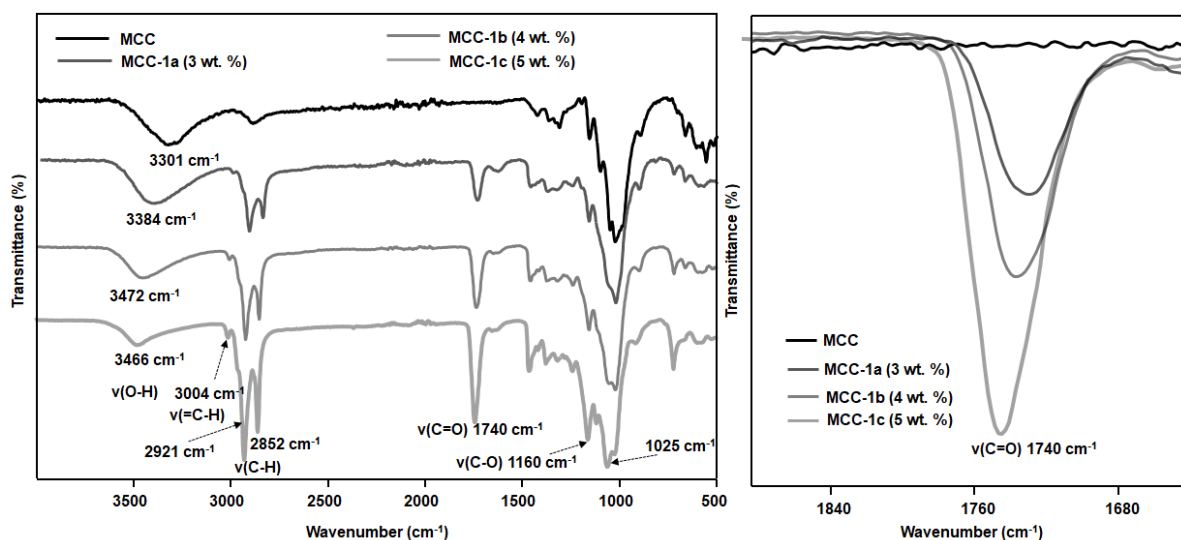
Figure 19: ATR-IR spectra of fatty acid cellulose esters (FACEs) obtained using high oleic sunflower oil at various MCC concentrations:3 wt.% (MCC-1a), 4 wt.% (MCC-1b), 5 wt.% (MCC-1c). Peaks were normalized to the C-O absorbance of the pyranose units at 1025 cm^{-1} (3 eq. high oleic sunflower oil/AGU, 115 °C, 24 h).

In addition, a decrease in the O-H absorbance band (3300 cm^{-1}) was observed. Higher cellulose concentrations were not investigated, since the associated viscosity was too high for our experimental set-up, but might be worthwhile investigating in the future.

Effect of reaction time, temperature and reactant equivalents

Another important parameter to investigate is the reaction time. Using 5 wt.% MCC at 115 °C and 3 eq. of high oleic sunflower oil/AGU, the reaction time was varied between 6 and 48 h and the results are included in the experimental section (**Figure 75**). The obtained results show that up to 24 h (MCC-1c), conversion increased with a slight decrease observed at longer reaction times, indicating degradation and /or hydrolysis of the cellulose backbone and the formed esters, respectively. Furthermore, three different reaction temperatures (90, 100 and 115 °C) were investigated. Using 5 wt.% MCC, the reactions were performed for 24 h. The ATR-IR results are presented in the experimental section (**Figure 76**). The results show that increasing the temperature led to a considerable increase in the conversion, which is due to an increased miscibility and an accelerated reaction. In terms of sustainability, the plant oil equivalents per anhydroglucose unit employed in the reaction is an important parameter. Thus, this was investigated by varying the plant oil equivalents from 1.5 to 6 equivalents triglycerides per AGU of cellulose in the reaction carried out at 115 °C and 24 h (see **Figure 77**). It was observed that increasing the plant oil equivalents from 1.5 to 3 led to a pronounced increase in the intensity of the C=O absorbance band (1740 cm^{-1}). In addition, as seen in **Figure 77**, there was no apparent difference in conversion when 6 eq. of plant oil (triglycerides) were employed. Thus, from a sustainability point of view, using such high excess of the plant oil was not justifiable.

NMR Characterization of FACEs

The structural confirmation of the fatty acid cellulose esters (FACEs) was obtained from ^{1}H and ^{13}C NMR. As a typical example, the NMR results for the experiment performed for 6 h are presented (**Figure 20**). Result show that the vinylic protons of the oleic acid are observed at a chemical shift of 5.34 ppm in ^{1}H NMR, which is slightly moved towards the lower field compared to high oleic sunflower oil (5.19 ppm). The peaks between 5.26-3.07 ppm are attributed to the protons of the cellulose backbone. On the ^{13}C NMR spectrum, the carbonyl carbon of the ester in the plant oil (162.50 ppm) is moved further downfield to 172.24 ppm in the fatty acid cellulose ester

(FACEs) due to the change in its environment. The carbon of the unsaturated aliphatic chain from oleic acid (129.22 ppm) is also visible. The attributed peaks are similar to previous reports on heterogeneously modified cellulose using fatty acids (oleic acid).[276]
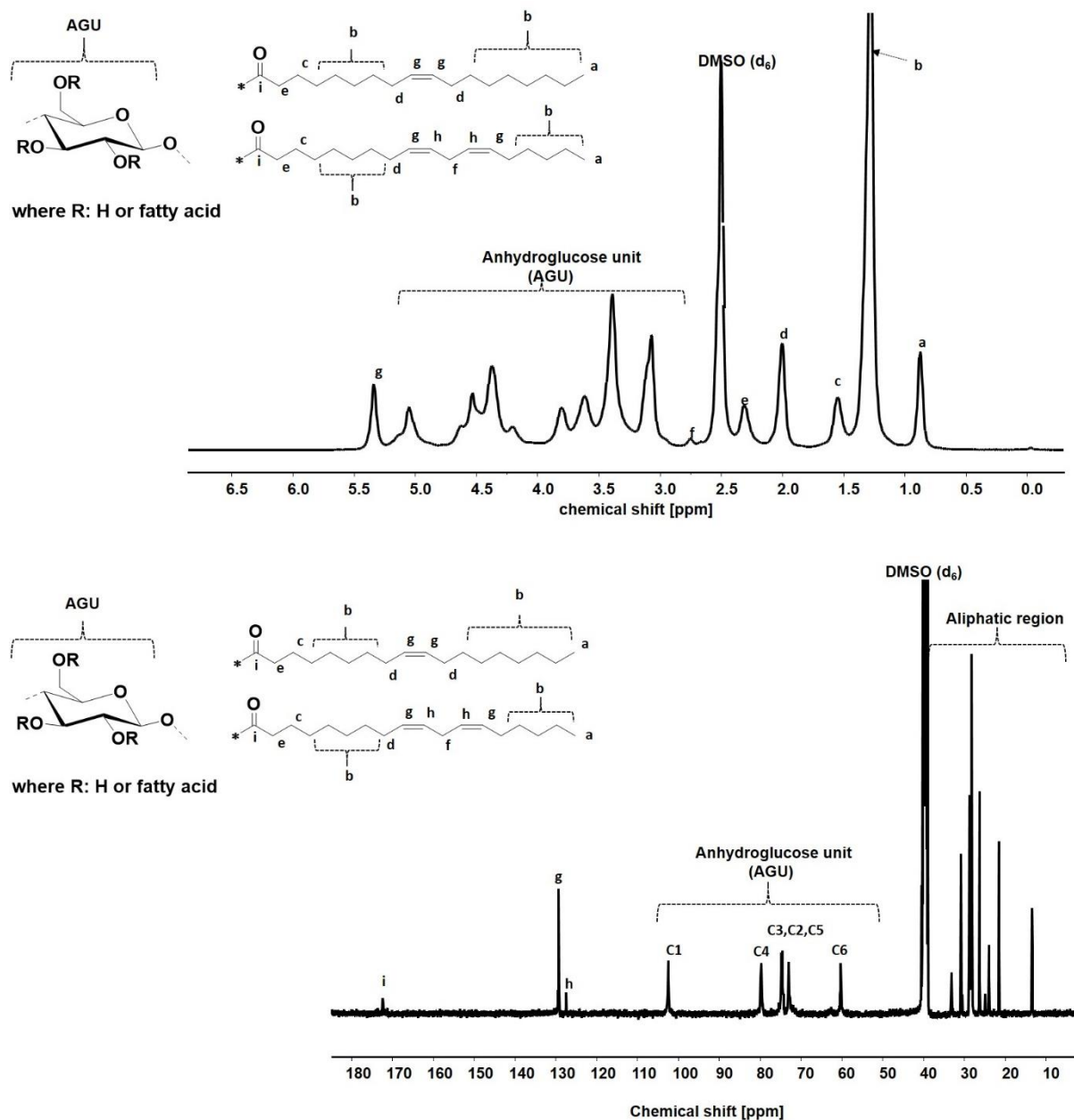

Figure 20: [1]H (top, 1024 scans, 400 MHz) and [13]C (bottom, 6000 scans, 100 MHz) NMR (DMSO,d$_6$) at 90 °C for fatty acid cellulose esters (FACE, MCC-1d, 5 wt.% cellulose, 3 eq. high oleic sunflower oil/AGU, 115 °C, 6 h).

Determination and tuning of degree of substitution (DS) of FACEs

One pertinent advantage of homogeneous cellulose modification over its heterogeneous alternative is the ability to tune the degree of substitution (DS) by varying reaction parameters. The DS of the synthesized fatty acid cellulose esters (FACEs) were determined *via* ^{31}P NMR. This method is based on the reaction between the unreacted hydroxyl groups of the cellulose with a phosphorylating agent revealing a broad peak between 145-137 ppm in the ^{31}P NMR spectrum. The integration of this peak with respect to an internal standard allows the calculation of the DS according to the procedure of Kings *et al.*[248] The ^{31}P NMR data of MCC-based FACEs synthesized by varying the reaction time and plant oil equivalents are displayed in the experimental section **Chapter 8.6** (**Figure 78**-**Figure 82**). The results obtained showed that the DS can be varied from 0.34 to 1.59 as the reaction time was increased from 6 to 24 h. Further increase of the reaction time (48 h) led to a decrease in the DS (1.44). This decrease could be attributed to possible degradation of the cellulose backbone at longer reaction time. The complete results are presented in the **Table 5**. In addition, it was possible to tune the DS from 1.06 to 1.59 by varying the plant oil equivalence from 1.5 eq. to 3 eq. per AGU of cellulose. The reactions carried out at 90 °C and 100 °C led to lower conversions. These samples could not be solubilized for DS calculation. This ability to tune the DS value over a wide range using various reaction parameters is interesting in order to target specific material properties. Overall, the highest value with a DS of 1.59 was reached after 24 h at 115 °C. Longer reaction times or higher temperatures (130 °C) did not increase the DS. This might be due to the increasing steric hindrance introduced by the long aliphatic groups, thus preventing further modification.

Table 5: Control of degree of substitution (DS) of fatty acid cellulose esters with reaction time.

Sample	Reaction time (h)	DS
MCC-1d	6	0.34
MCC-1e	12	0.50
MCC-1c	24	1.59
MCC-1f	48	1.44

 Reaction conditions: 3 eq. high oleic sunflower oil per AGU cellulose (MCC), 5 wt.% MCC, 115 °C (DS calculated from ^{31}P NMR)

Effect of cellulose type and DS on the properties of FACEs

FT-IR and NMR characterization

In order to investigate the effect of the cellulose source as well as the conversion (DS) on the material properties of the obtained fatty acid cellulose esters (FACEs), two different DS samples (DS ~1.0 and above 1.4) from each cellulose sources were synthesized. The cellulose sources investigated include: microcrystalline cellulose (MCC), cellulose pulp (CP) and cellulose Whatman™ filter paper No. 5 (FP). This was achieved by varying the plant oil equivalents (1.5 eq. and 3 eq. triglycerides per AGU of cellulose) at 115 °C for 24 h. The ATR-IR spectra of the obtained fatty acid cellulose esters (FACEs) are presented in the experimental section (see **Figure 77**, **Figure 83** and **Figure 84**). The results obtained showed that the reaction efficiency does not depend on the type of cellulose used. The synthesized FACEs using 3 eq. of plant oils were soluble in THF, thus allowing further confirmation of the structures *via* ^{1}H and ^{13}C NMR These results are included in the experimental section (**Figure 85**-**Figure 87**). The results are similar to those previously shown in **Figure 20**. However, it was observed that the higher conversions in these samples led to much stronger aliphatic peaks from the plant oil. This made the cellulose backbone less visible, despite the high temperature (50 °C) and large number of scans (6000 scans for ^{13}C and 1024 scans for ^{1}H) employed during the NMR measurements. However, from the ^{13}C NMR, the characteristic vinylic protons (130.68 ppm) and carbonyl carbon atoms (173.36 ppm) of the introduced fatty acids are visible. Furthermore, the degree of substitution (DS) of all the six synthesized FACEs were determined (see ^{31}P NMR spectra in the experimental section: **Figure 80**, **Figure 82**, **Figure 88**-**Figure 91**). These results are equally summarized in **Table 6**.

Determination of Molecular weight

The relative molecular weights of the synthesized fatty acid cellulose esters (FACEs) was determined from size exclusion chromatography (SEC) in dimethylacetamide-lithiumbromide (DMAc-LiBr) for samples with DS of around 1.0 and in THF for higher DS samples (see **Table 6**). All measurements were performed relative to poly(methyl methacryate) (PMMA) standards. The SEC traces of the measurements in THF are presented in **Figure 21** and those in DMAc-LiBr (lower DS samples) are included in the experimental section (**Figure 92**) The results are equally included in **Table 6**. As

observed in **Figure 21**, the highest molecular weights (shorter retention time) were obtained for cellulose filter paper (190.0 KDa) followed by cellulose pulp (132.0 KDa) with microcrystalline cellulose having the lowest molecular weight (89.0 KDa). The dispersity (Đ) values ranged from 1.67 to 3.3. Larger dispersity values were obtained for measurements performed in DMAC-LiBr compared to those in THF. This difference is likely due to the difference in the swelling behavior of the polymers in these solvents. Furthermore, as expected from **Table 6**, among the same cellulose source, higher molecular weights were obtained for samples with higher DS values (MCC-1c, FP-1b and CP-1b). This can be attributed to the higher hydrodynamic radius with an increasing amount of long aliphatic side chains that are associated with increasing conversion (DS). However, it is important to point out that since the measurements for the lower DS samples were performed in DMAc-LiBr instead of THF, it is difficult to compare these results with each other.
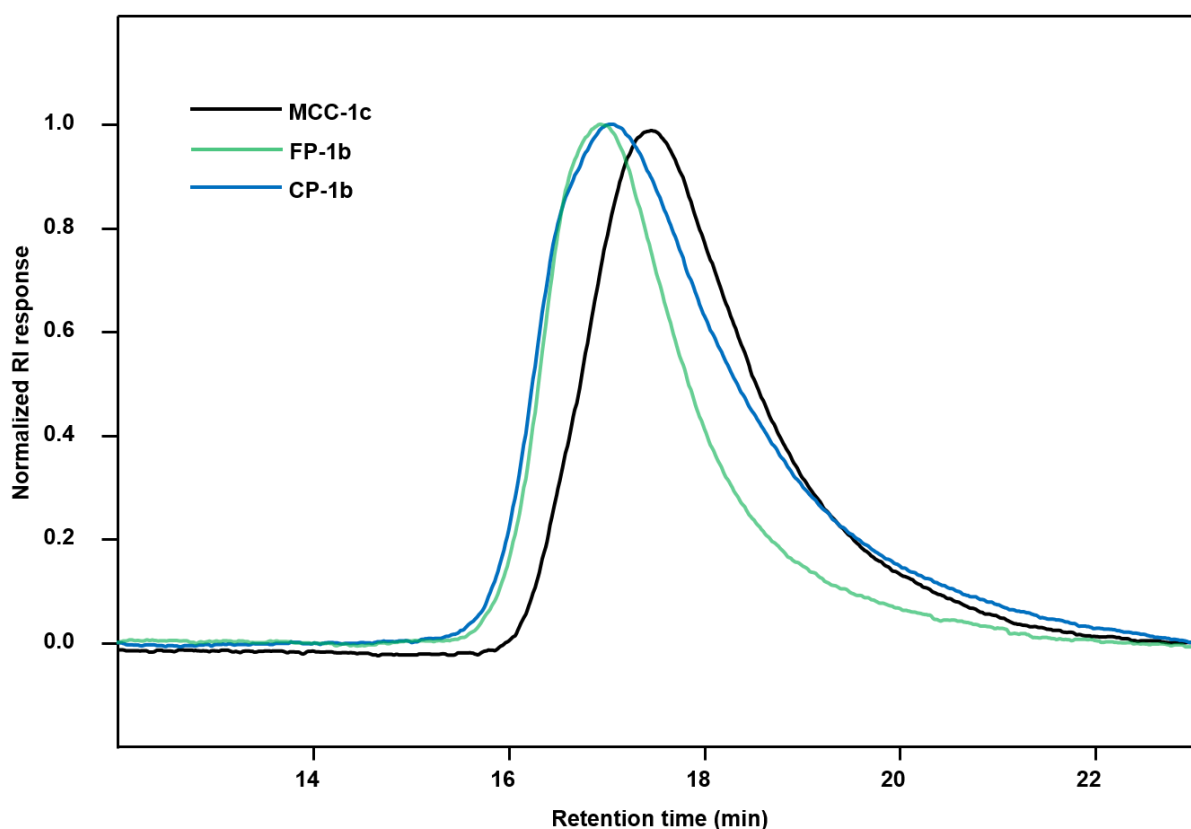
Figure 21: SEC traces (THF) of fatty acid cellulose esters (FACEs) from microcrystalline cellulose (MCC-1c; DS 1.59), cellulose filter paper (FP-1b; DS 1.48) and cellulose pulp (CP-1b; DS 1.40).

Determination of Crystallinity

In addition, the crystal structure (crystallinity) of the various cellulose sources and their resulting fatty acid cellulose esters (FACEs) were determined by X-ray diffraction experiments. The results from microcrystalline cellulose (MCC) and the resulting FACEs (MCC-1c, MCC-1i) are shown in **Figure 22**. For comparison purposes, the result of regenerated cellulose from a CO_2-DBU solvent system is included. From the obtained results, it was observed that after transesterification, the characteristic cellulose I crystal 2θ peaks at 15.4° and 22.6° disappear and are replaced by a broad 2θ peak at around 19.8° that is characteristic for a less crystalline cellulose (more amorphous) as previously reported.[155]
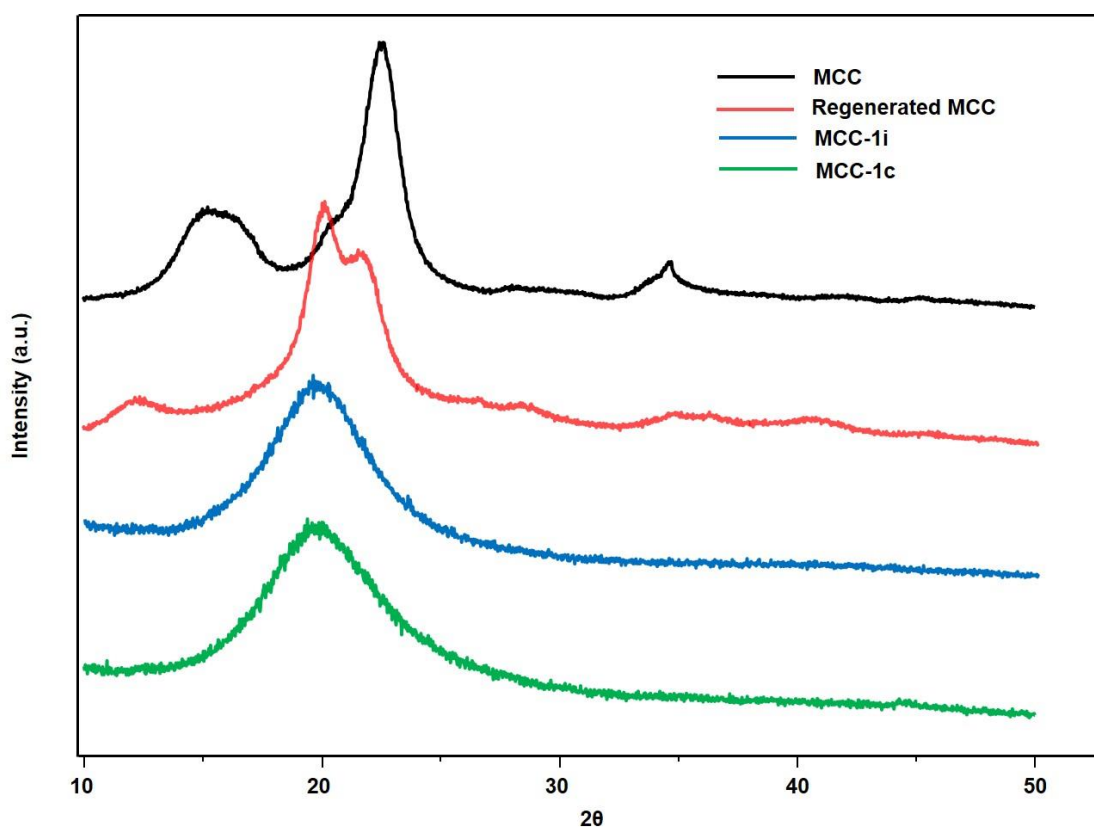
Figure 22: X-ray diffraction pattern of microcrystalline cellulose (MCC), regenerated MCC and fatty acid cellulose esters (FACEs) resulting from microcrystalline cellulose (MCC-1c, MCC-1i).

As can be seen from **Figure 22**, for the regenerated cellulose, the 2θ peaks (12.2°, 20.1° and 21.6°), which are characteristic of the cellulose II crystalline phase, are clearly visible. These observed changes in the cellulose crystal structure can be explained by considering that during the solubilization of cellulose, the breaking of *intra-* and *inter-*molecular hydrogen bonds result in a more amorphous structure. In

the case of regeneration (in anti-solvents like water), the cellulose chains are able to reorganize to the cellulose II crystal structure (thermodynamically more stable).[26] However, as observed from **Figure 22**, the transesterification process obviously prevented the re-organization of the cellulose chains after solubilization, thus mostly retaining the amorphous cellulose structure. Similar amorphous XRD diffraction patterns were obtained for FACEs synthesized from filter paper (FP-1a, FP-1b) and cellulose pulp (CP-1a, CP-1b) (see experimental section **Figure 93** and **Figure 94**). The 2θ peaks of all the FACEs investigated are included in **Table 6**.

Investigation of thermal stability

The thermal stability of the samples was determined by thermogravimetric analysis (TGA). The samples were heated from 25 to 900 °C (10 °C/min) under N_2 atmosphere. The results for FACEs prepared from microcrystalline cellulose (MCC) is presented in **Figure 23** whereas those from cellulose pulp and filter paper (FP) are included in the experimental section (**Figure 95** and **Figure 96**). The results for $T_{d, 5\%}$ and $T_{d, 95\%}$ are shown in **Table 6**. Typically, all the samples showed a single major degradation step resulting in over 95 % weight loss
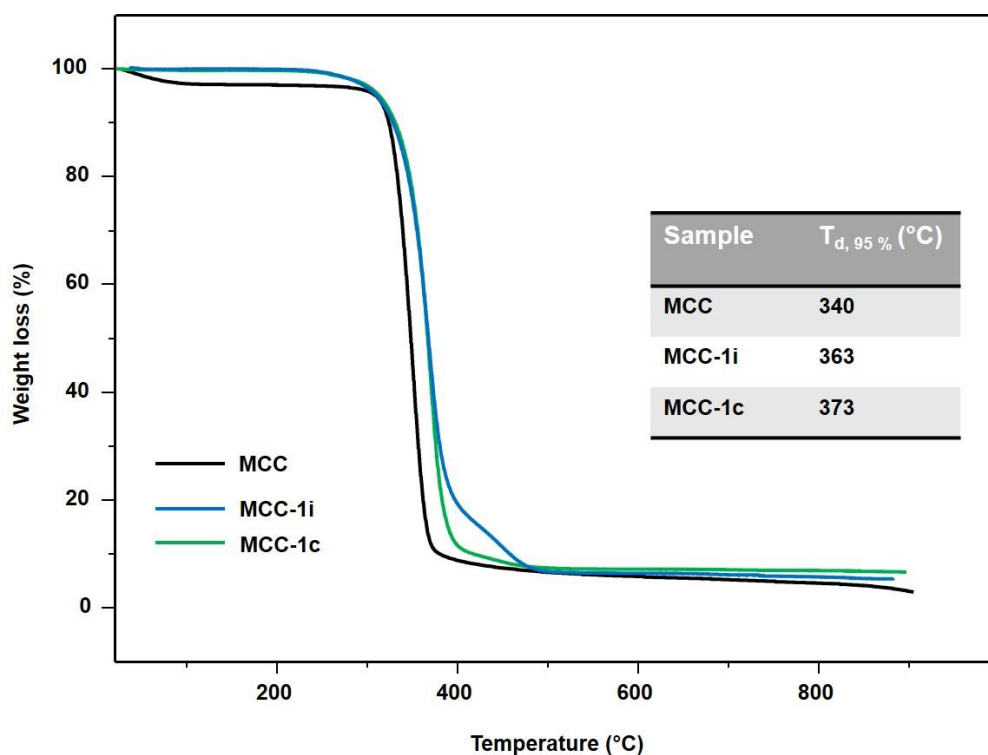
Sample	$T_{d, 95\%}$ (°C)
MCC	340
MCC-1i	363
MCC-1c	373

Figure 23: Thermogravimetric analysis (TGA) of microcrystalline cellulose (MCC) and resulting fatty acid cellulose esters (FACEs) from MCC (MCC-1c, MCC-1i) (5 wt.% cellulose, 24 h, 115 °C.

Generally, the obtained results (see **Table 6**), show an improved thermal stability after transesterification reactions (up to 30 °C). Moreover, for all the investigated cellulose sources, higher DS samples resulted in a relatively higher thermal stability. For instance, for MCC the onset degradation temperature ($T_{d,\,5\%}$) was increased from 280 °C to 302 °C and 320 °C for DS 1.06 and 1.59, respectively. Similar trends were observed in the case of cellulose filter paper and cellulose pulp (see **Table 6**).

In the case of $T_{d,\,95\%}$, the degradation temperature of MCC was increased from 340 °C to 363 °C (DS 1.06) and 373 °C (DS 1.59). The $T_{d,\,95\%}$ of filter paper (350 °C) increased to 366 °C (DS 1.02) and 373 °C (DS 1.48). Equally, the $T_{d,\,95\%}$ of cellulose pulp (355 °C) was increased to 369 °C (DS 1.08) and 379 °C (DS 1.40).

Table 6: SEC data, degree of substitution (DS) values, degradation temperature (T_d) and XRD data of fatty acid cellulose esters (FACEs).

Sample	^{a}DS	^{b}M$_n$ (KDa)	^{b}M$_w$ (KDa)	^{b}Đ	^{c}T$_{d,\,95\%}$ (°C)	^{d}XRD (2θ) (deg)
MCC	---	---	---	---	340	22.6, 15.4
MCC-1i	1.06	63.4	167.3	2.6	363	19.6
MCC-1c	1.59	89.0	170.0	1.89	373	19.7
FP	---	---	---	---	350	22.8, 15.1
FP-1a	1.02	100.6	330.9	3.3	366	19.7
FP-1b	1.48	190.0	318.0	1.67	373	19.7
CP	---	---	---	---	355	22.6, 15,9
CP-1a	1.08	132.1	356.4	2.7	369	19.5
CP-1b	1.40	139.0	263.0	1.90	379	19.3

^{a}Determined from ^{31}P NMR. ^{b}Obtained from SEC measurements in THF or DMAc-LiBr. ^{c}Calculated from Thermogravimetric analysis (TGA), ^{d}Obtained from X-ray diffraction measurements.

Investigation of FACEs films properties

FACEs film processing and morphology investigation

Since one of the aims of modifying cellulose using plant oils is to introduce processability to the material, six FACEs films were prepared *via* a solvent cast method. It is important to mention that solvent casting can certainly not be considered sustainable, as it involves the use of volatile solvents. However, it was the best possible option to establish important material properties. In the future, more

sustainable processing options have to be considered. The FACEs with a DS of about 1.0 were not soluble in THF, thus films were prepared from pyridine solutions (MCC-F-1i, FP-F-1a, CP-F-1a). The films of FACEs with a higher DS were prepared in THF (MCC-F-1c, FP-F-1b. CP-F-1b). As shown in **Figure 24**, the obtained films showed good transparency.
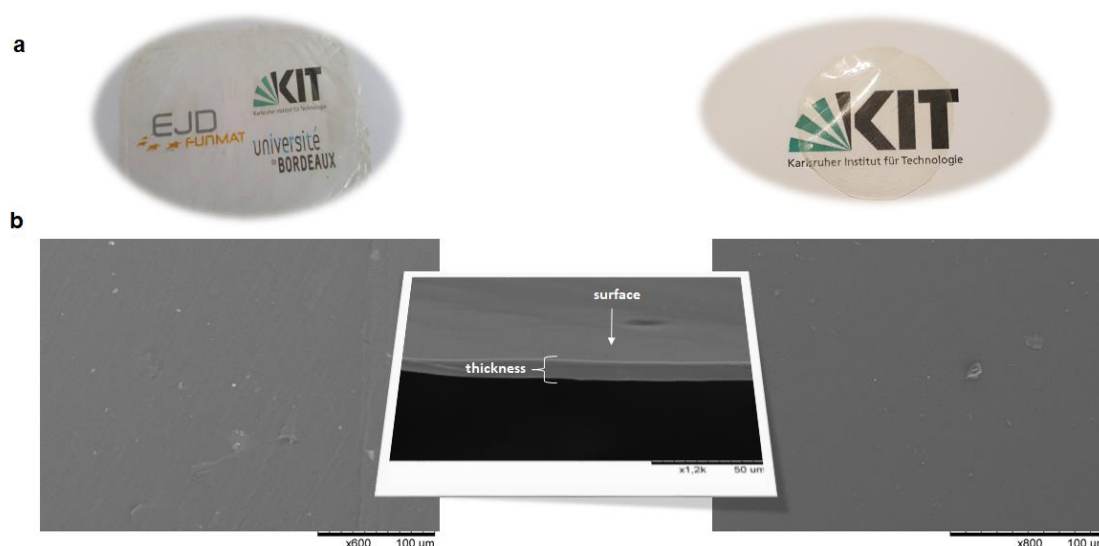
Figure 24: a) Images of thin films of fatty acid cellulose esters from MCC-F-1c (right) and CP-F-1b (left). b) SEM surface images of MCC-F-1c (right), FP-F-1b (TS section with surface in view, middle) and CP-F-1b (left). (Films made *via* solvent cast from solubilized FACEs in THF).

The surface morphology of the films was determined *via* scanning electron microscopy (SEM). Results showed homogeneous surfaces without any holes (**Figure 24b**).The transverse section (TS) is also visible (**Figure 24b** middle), again confirming the homogenous nature of the prepared films. The results obtained for all the other FACEs films analyzed did not show any difference between samples from different cellulose sources or with different DS values.

Thermal stability investigation of FACEs films

Furthermore, the thermal stability of the films was determined using thermogravimetric analysis (TGA), the results are presented in **Figure 25** and are included in **Table 6**. Generally, the films show a single degradation step with similar degradation temperature ($T_{d, 95\%}$) values comparable to their preceding precursors, thus showing that the materials did not lose their thermal stability during the film formation. It was

also observable that, irrespective of the cellulose samples, thermal stability was influenced by the DS.
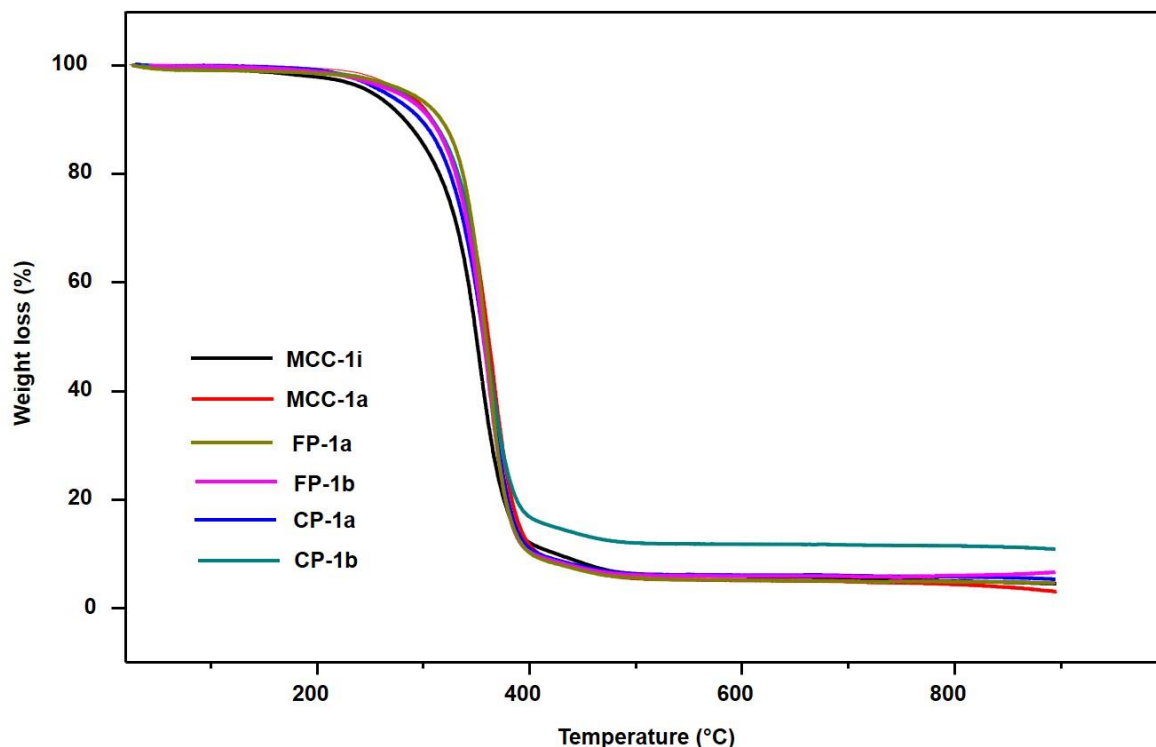
Figure 25: Thermogravimetric analysis (TGA) of fatty acid cellulose esters (FACEs) films (MCC-F-1i, MCC-F-1c, FP-F-1a, FP-F-1b, CP-F-1a, CP-F-1b).

Generally, films from higher DS samples exhibited a slightly higher thermal degradation temperature ($T_{d, 95\%}$). All films analyzed had relatively high $T_{d, 95\%}$ between 359 to 368 °C, thus showing the improved thermal stability of the prepared films when compared to the starting cellulose samples (MCC $T_{d, 95\%}$ = 340 °C, FP $T_{d, 95\%}$ = 350 °C, CP $T_{d, 95\%}$ = 355 °C). This result is consistent with the previous observations on the increased stability introduced by the aliphatic side chain from the plant oil (compare **Figure 25** to **Figure 23**, **Figure 95** and **Figure 96**).

Tensile strength measurements of FACEs films

As a potential packaging material, the mechanical properties of the FACEs films was investigated *via* tensile strength measurements. For each sample, three to five measurements were done, the average values of maximum stress (δ) and strain (%) including their standard deviations were calculated and are shown in **Table 7**. The stress-strain curves of the various FACE films are displayed in **Figure 26**.
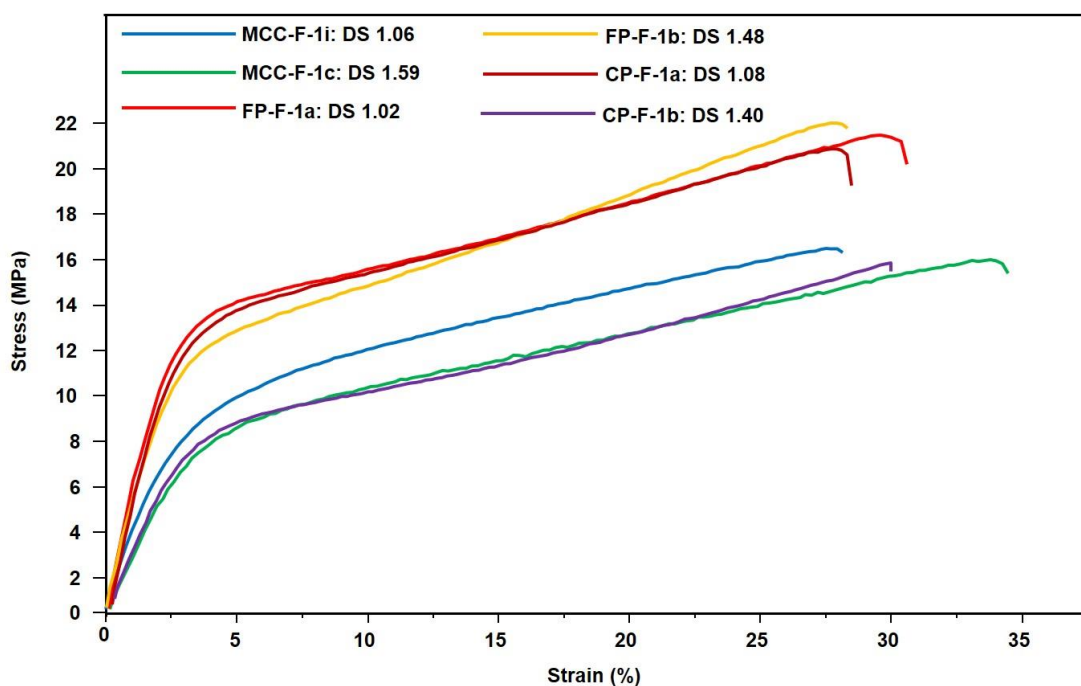
Figure 26: Tensile strength measurements of fatty acid cellulose esters (FACEs) films (initial speed at 5 mm/min).

The elastic or Young´s modulus (E) was determined from the linear region of the stress-strain curves. The average value from three to five measurements was calculated and their standard deviation determined (see **Table 7**).

Table 7: Thermal and mechanical characterization of fatty acid cellulose esters (FACEs) cast films.

Sample	[a]T_d (°C)	[b]Young´s Modulus, ε (MPa)	[b]Maximum stress (MPa)	[b]Elongation at break, strain (%)
MCC-F-1i	367	375.00± 4.0	16.00± 2.0	27.00± 3.0
MCC-F-1c	368	233.00± 20.0	16.19 ± 0.5	33.57 ± 1.8
FP-F-1a	360	458.38 ± 29.0	21.04 ± 1.4	30.54 ± 2.0
FP-F-1b	362	444.58 ± 23.6	21.96 ± 2.4	27.62 ± 1.7
CP-F-1a	359	478.26 ± 30.6	21.69 ± 2.3	27.70 ± 3.2
CP-F-1b	362	262.12 ± 13.5	15.89 ± 1.7	30.07 ± 0.9

[a]Evaluated from Thermogravimetric analysis (TGA), [b]Determined from tensile strength measurements

As seen in **Figure 26** and **Table 7**, a higher Young´s modulus (E) was obtained for films with lower DS. In the MCC films for example, E decreased from 375 MPa to 233 MPa as the DS increased from 1.06 to 1.59. This may be due to the higher remaining amount of free hydroxyl groups, which are able of hydrogen bonding. The same reason could explain the slightly higher elongation values (over 30 %) obtained

for films with higher DS values, as the increasing presence of aliphatic side groups from the fatty acids increases the flexibility. Among the investigated cellulose samples, cellulose pulp showed the highest value of E (478 MPa) followed by cellulose filter paper (458 MPa) and microcrystalline cellulose (376 MPa). The latter lower value is most likely a result of the significantly lower molecular weight of the MCC samples. In addition, cellulose filter paper and cellulose pulp showed similar maximum stress values (around 22 MPa). The herein obtained values of E are significantly higher than those reported for FACE films made *via* heterogeneous modification of cellulose using oleic acid (E = 50.13 MPa).[276] It can therefore be concluded that the direct combination of both plant oil and cellulose under homogeneous conditions led to FACE films with improved plasticity and mechanical strength. These improved mechanical properties are interesting for potential applications in packaging as well as other cellulose-based materials.

6.1.4 Conclusions

In this chapter, a sustainable approach for the homogeneous transesterification of cellulose using plant oils (high oleic sunflower oil) directly in the DBU-CO_2 solvent system was reported. The solubility of cellulose was accomplished within 15 min. at 30 °C. Subsequent transesterification was performed at 115 °C for 24 h reaching a maximum degree of substitution (DS) of 1.59. No further catalyst was employed in the transesterification reaction, as the unreacted DBU from the solubilization step played a catalytic role. Compared to previous works where fatty acid methyl esters were used, the direct utilization of plant oils prevents derivatization steps, thus meeting one of the goals of Green Chemistry. Furthermore, the possibility to tune the DS from 0.34 to 1.59 by changing the reaction parameters was demonstrated. In addition, the versatility of this procedure was shown by successfully applying on various cellulose sources: microcrystalline cellulose (MCC), cellulose Whatman™ filter paper, No. 5 (FP) and cellulose pulp (CP). The obtained fatty acid cellulose esters (FACEs) showed improved thermal stability ($T_{d, 95\%}$ up to 30 °C compare to the starting samples). From XRD measurements, a single broad 2θ peak at around 19.8° characteristic for amorphous cellulose phase was obtained for all synthesized FACEs. Finally, films produced from these FACEs showed good thermal stability ($T_{d, 95\%}$ up to 368 °C) as well as high elastic moduli (up to 478 MPa), maximum stress of about 22 MPa and maximum elongation (strain) of about 35 %. The homogeneity of the films was

confirmed with scanning electron microscopy (SEM). In addition, the developed protocol offers the possibility for a further post modification *via* the double bonds on the introduced fatty acid backbone.

Finally, the combination of using a greener solvent, non-protecting group chemistry (transesterification), non-derivative and bio-derived reactant (high oleic sunflower) makes this approach more sustainable than previous reports. As previously shown in **Chapter 2.5.5**, a comparative low E-factor (3.4) was calculated for this study compared to similar reports (see **Table 3** for comparison). The overall sustainability consideration during this study as well as a demonstration of cellulose processability will therefore lead to cellulose-based materials with lower environmental impact than their petroleum-based alternatives.

6.2 Direct cellulose derivatization by multicomponent reactions

6.2.1 Abstract

In this chapter, the Ugi five component reaction (Ugi 5-CR) was used for direct cellulose modification. This approach provides a non-phosgene route for the synthesis of cellulose carbamate. In the first instance, the reaction was carried out in the optimized DBU-CO_2 switchable solvent system described in **Chapter 4**. Therefore, the *in-situ* generated cellulose carbonate during the solubilization step was used as the acid component. Together with the preformed imine (reaction between aldehyde and amine) and an isocyanide, the Ugi 5-CR was carried out under various reaction conditions. Reaction parameters investigated include: effect of cellulose concentration, temperature, reaction time and use of Lewis acid catalysts. Results obtained from infrared spectroscopy showed little or no modification. Further structure characterizations were not carried out as the obtained modified cellulose products were not soluble in possible solvents. The reaction was not improved by replacing the solvent with the ionic liquid (1-*N*-ethyl-3-methyl imidazolium acetate). Hence, the expected Ugi 5-CR modification for cellulose was not successful.

6.2.2 Introduction

Ugi five component reaction (Ugi 5-CR), a variation of the previous described Ugi 4-CR (**Chapter 2.6.2.2**), was discovered by Ivar Ugi in 1961. In this case, whereas the other components (amine, carbonyl and isocyanide) remained the same, the acid component was replaced by an alcohol (methanol) and CO_2.[279] The reaction results in the formation of α-(alkoxyl carboxylamine)amide (carbamate-protected aminoamide), **8** as shown in **Scheme 24**.
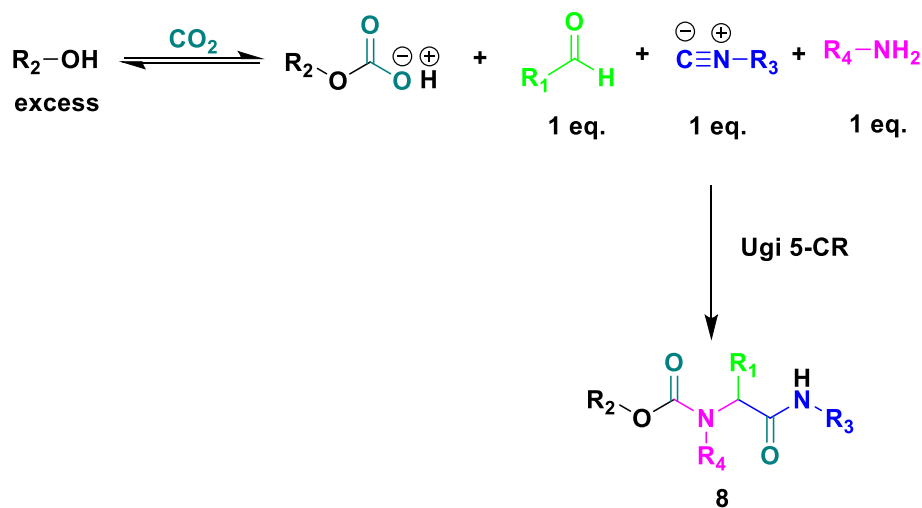
Scheme 24: General reaction scheme of Ugi 5-CR, adapted from Armstrong and Keating.[280]

Armstrong & Keating, expanded the scope of this reaction to include other alcohols apart from methanol, as well as the use of other oxidized carbon sources (CS_2 and COS).[280] The group of Meier employed this strategy in combination with efficient thiol-ene polymerization to synthesize highly functionalized polycarbonates, polyamides, polyurethanes and polyhydantoins.[281]

With the increasing need to valorize cellulose into advanced functional materials, multicomponent reactions can allow for this possibility. Compared to classical reactions for cellulose modification such as esterification, etherification or carbonylation, that introduces one functionality on the modified cellulose, multicomponent reactions on the other hand can introduces multiple functionalities in one step. In addition, multicomponent reactions allow the use of varieties of each component, thereby opening the possibilities for synthesizing and tuning the properties of the modified cellulose by simply changing these components. In addition, the atom efficiency of multicomponent reactions coupled with the direct utilization of CO_2 as a C-1 carbon source makes this approach attractive.

So far, the direct use of cellulose as the hydroxyl source for Ugi 5-CR has not been reported. Therefore, the goal of this project was to apply this reaction for the direct modification of cellulose without any derivatization using the optimized DBU-CO_2 solvent system,[156] described previously. Through this approach, phosgene will be avoided for the synthesis of cellulose carbamate, thereby improving the sustainability aspect of the process. Furthermore, the multi-functionality introduced by this approach

may allow for the possibility to tune the properties of such modified cellulose by simply changing the components. This is interesting as it can assist in designing cellulose-based materials covering a wide range of applications.

6.2.3 Results and Discussions

For direct modification of cellulose *via* MCRs, the Ugi 5-CR is best suited as it allows for the use of alcohol and CO_2 in place of the carboxylic acid component in a classical Ugi 4-CR. Interesting, during the optimization study of the DBU-CO_2 switchable solvent system described in **Chapter 4**, the presence of the *in-situ* generated cellulose carbonate was confirmed unambiguously. Therefore, the first attempt on this reaction was carried out in this solvent system.

Reaction in DBU-CO_2 switchable solvent system

As a fast, mild and sustainable solvent for cellulose, the DBU-CO_2 switchable solvent system offers a lot of potential for various homogenous modification on cellulose. In this regard, the first attempt of the Ugi 5-CR was carried out in this solvent system as depicted in **Scheme 25**. The presented mechanism is similar to that proposed by Armstrong *et al.*[280] The reaction starts with the formation of the cellulose carbonate anion, **9** by the reaction of the hydroxyl groups on cellulose and CO_2. From the detailed study of this solvent system, the presence of this *in-situ* generated carbonate anion was proven unambiguously by trapping using an electrophile. The already proven presence of the carbonate anion was indeed a step in the right direction towards the desired Ugi-5CR product. In this regard, the first attempt for the reaction was carried out by applying CO_2 (5 bar) to a solution of cellulose suspended in DMSO and DBU (3 eq. per AGU of cellulose) at room temperature for a period of 15 min. leading to the complete dissolution of cellulose. Next, the other components (amine, aldehyde and isocyanide) were added. The reaction was then allowed to run over a period of 24 h at room temperature. Unfortunately, the reaction was not successful as a preliminary infrared spectroscopy (ATR-IR) characterization showed little or no introduction of the expected functional groups in the desired product, **10** (see expected structure in **Scheme 25**) In addition, the obtained "modified" cellulose was not soluble preventing further characterization.
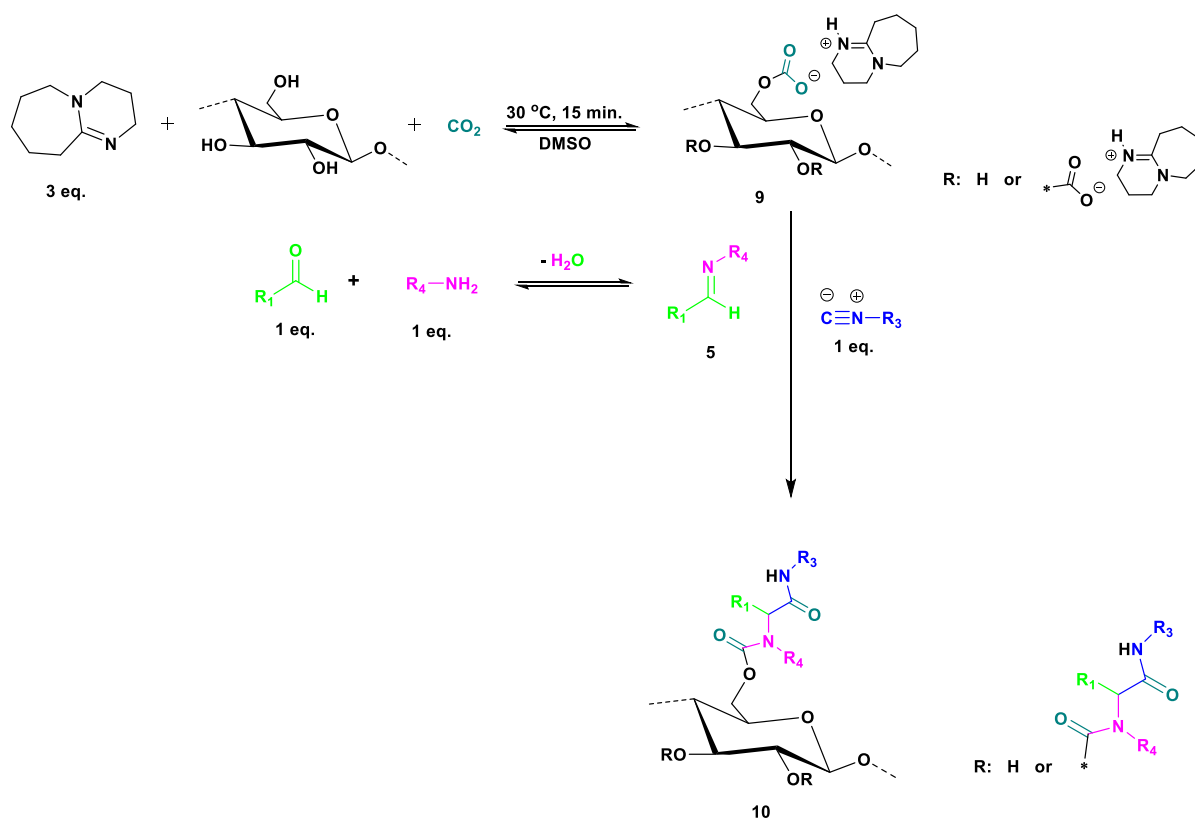
Scheme 25: General reaction scheme for Ugi 5-CR on cellulose in DBU-CO_2 switchable solvent system.

Various reaction conditions were attempted such as: preforming the imine **5** (see **Scheme 25**), cellulose concentrations (1, 2, 3, 4, 5 wt.% in DMSO), reactant equivalents (3, 6, 9 eq. per AGU of cellulose), temperature (30, 40, 50, 60, 90 °C), CO_2 pressure (5, 10, 20, 30 bar), use of catalyst (Schreiner catalyst, bismuth triflate, ytterbium triflate) and reaction time (up to 72 h). Despite these various attempts (up to 50 different experiments), the reaction was still not successful, as evident from the infrared spectra showing little or no presence of expected new functional groups. An example of such spectrum compared to native MCC is shown in **Figure 27**. The observed difference between both spectrum around 3300 cm^{-1} (O-H stretching band) is due to change in crystallinity of the cellulose during the solubilization step.
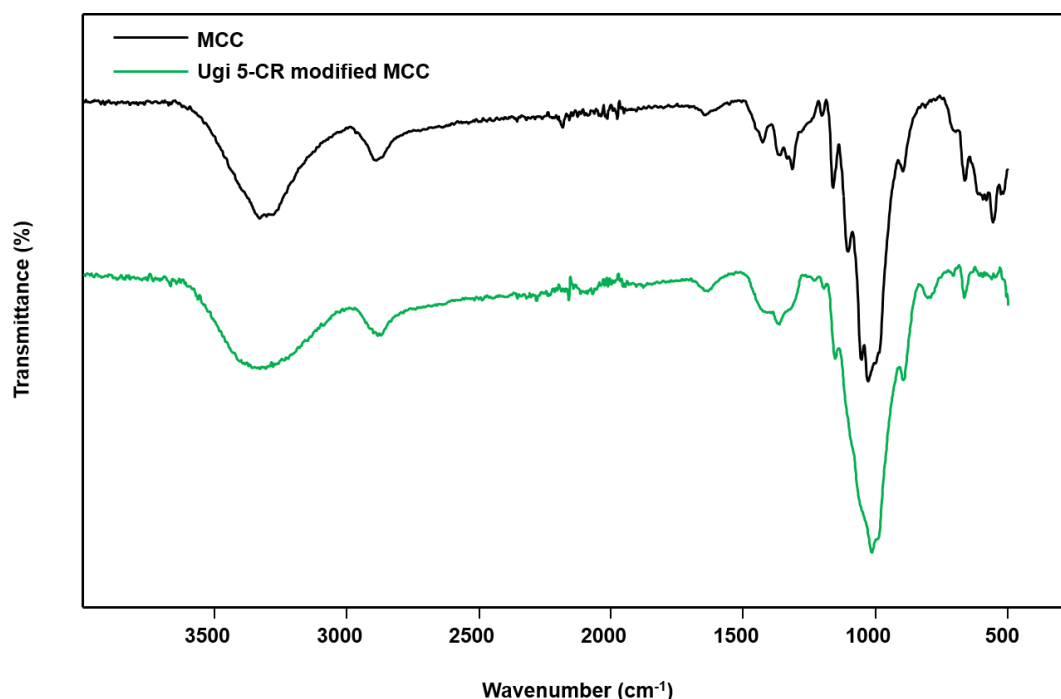
Figure 27: ATR-IR spectra comparison between MCC and Ugi 5-CR modified cellulose.

Looking closely at the mechanism of the Ugi-4CR, which is also similar to the Ugi 5-CR, it was observed that the reaction proceeds best under slightly acidic conditions, which allows the activation of the imine **5**, thus promoting the nucleophilic attack from the isocyanide. Care must be taken as isocyanides are not stable under very acidic conditions. Thus, attempts were made to activate the imine by using various Lewis acids such as Schreiner catalyst, ytterbium triflate [Yb(CF$_3$SO$_3$)$_3$] and bismuth triflate [Bi(CF$_3$SO$_3$)$_3$]. The challenge created by this approach was the difficulty in keeping the cellulose soluble as the acidic catalyst neutralizes the super basicity media required for the cellulose solubilization. While a compromise might be reached between those two conditions, the process becomes more unsustainable. For instance, lanthanides such as ytterbium are rare elements and therefore not sustainable (especially if they cannot be recycled and re-used). In addition, the generation of salts from the reaction between the DBU and the catalyst not only generates waste but also makes it difficult to recycle the DBU. All these un-avoidable challenges therefore defeat the simple and straightforward story envisioned at the start of the project, which was to directly modify cellulose *via* the Ugi-5CR and using CO$_2$ in one step.

Reaction in ionic liquid

As one of the hypotheses for the failure of the reaction was due to the high basicity of the DBU-CO_2 solvent system, an attempt was made using ionic liquids. In this regard, the ionic liquid, 1-*N*-ethyl-3-methyl-imidazolium acetate [C_2mim]$^+$[OAc$^-$], which is used frequently in the literature for homogeneous cellulose modification was employed. First cellulose (3 wt.%) was solubilized in the [C_2mim]$^+$[OAc$^-$]-DMSO (90:10 w/w) solvent. The reaction was carried out alongside *n*-butyl amine, isobutyraldehyde and *tert*-butylisocyanide. After a series of trials, it was discovered that the ionic liquid was indeed non-inert in this reaction. Test reactions between [C_2mim]$^+$[OAc$^-$] and CO_2 showed the formation of a CO_2 protected carbene specie as confirmed from ^{1}H NMR study (see **Figure 28**).
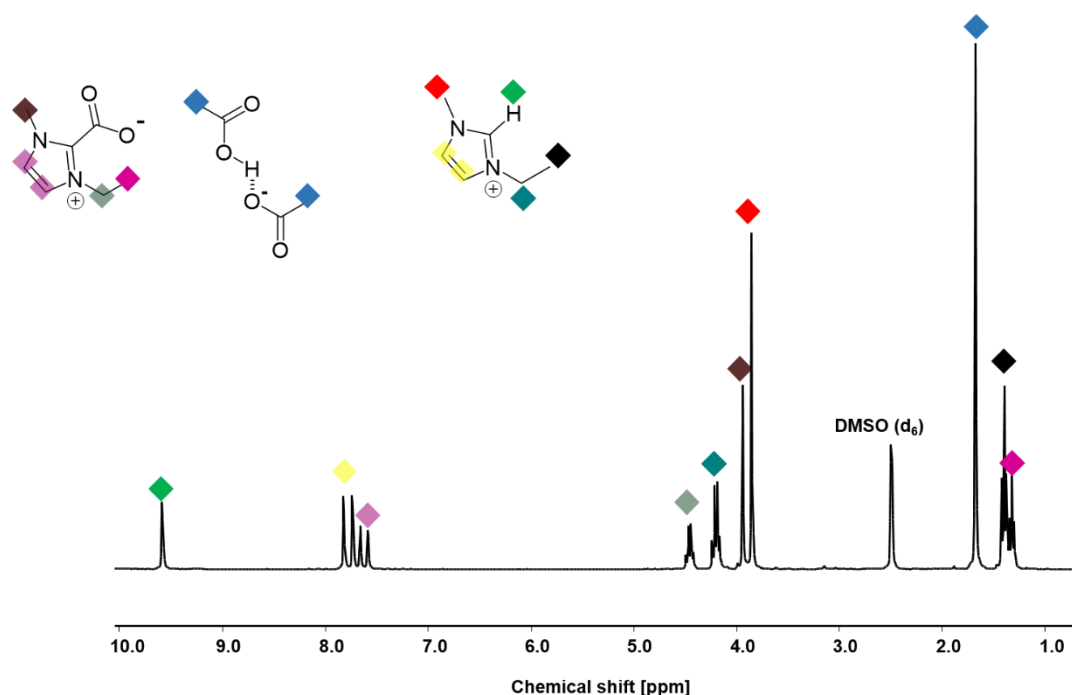
Figure 28: ^{1}H NMR showing the reaction between [C_2mim]$^+$[OAc$^-$] ionic liquid and CO_2.

This result is similar to previous reports from Rogers *et al.*[282,283] The proposed mechanism for this observation starts with a proton abstraction from the C2 position of the imidazole resulting in formation of a carbene specie. The *in-situ* formed carbene then reacts with CO_2 to form a carboxylate anion (CO_2 protection carbene species). This non-inertness of the ionic liquid prevented further investigation of its application in the Ugi 5-CR modification of cellulose experiments.

6.2.4 Conclusions

In this chapter, an attempt was made to modify cellulose directly by use of multicomponent reactions (Ugi 5-CR). The first trials of the reactions were carried out in the DBU-CO_2 switchable solvent system. Various reaction parameters such as cellulose concentration, reaction time, reactant equivalents, temperature, CO_2 pressure and use of catalyst were investigated. The reaction was monitored by use of infrared spectroscopy (ATR-IR) and showed little or no presence of the expected introduced functional groups. As the obtained "modified" cellulose was not soluble in any common solvents, further characterizations were not possible.

A second attempt of this reaction was done in the ionic liquid 1-*N*-ethyl-3-methyl-imidazolium acetate [C_2mim]$^+$[OAc$^-$], which is used frequently in the literature for homogeneous cellulose modification. The reactions were not successful and a side reaction between the ionic liquid and CO_2 was observed, showing their non-inertness in this type of reactions. In conclusion, cellulose could not be modified satisfactorily through this approach.

6.3 Indirect cellulose derivatization by multicomponent reactions

This chapter and the associated parts in the experimental section are adapted from the following literature:

Z. Söyler, K.N. Onwukamike, S. Grelier, E. Grau, H. Cramail, M.A.R. Meier, Sustainable Succinylation of Cellulose in a CO_2-based Switchable Solvent and Subsequent Passerini 3-CR and Ugi 4-CR modification, *Green Chem.* 2018, 20, 214.

https://pubs.rsc.org/en/content/articlelanding/2018/gc/c7gc02577g#!divAbstract

Notice: The discussed results of Ugi four component modification (Ugi 4-CR) of succinylated cellulose in this chapter are the author's own contribution to the above published work.
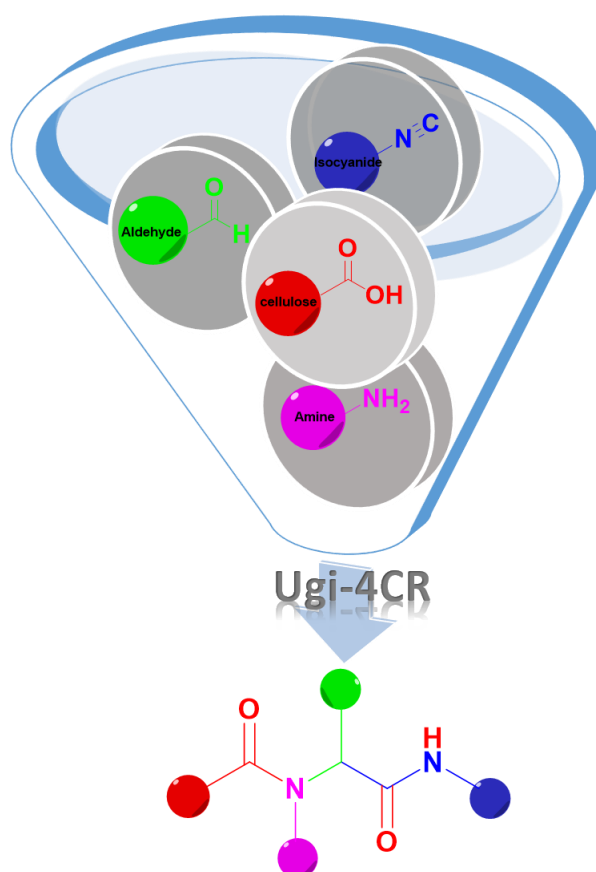
6.3.1 Abstract

As the attempt at direct modification of cellulose was unsuccessful (**Chapter 6.2**) in this current chapter, an indirect approach was adopted. In this case, succinylated cellulose (DS = 2.64), which was kindly provided by Dr. Zafer Söyler was used. The introduced carboxylic acid functionality from the succinylation serves as the acid component for the Ugi-4CR modification. Three modifications were carried out by changing either the aldehyde, amine or isocyanide. The obtained modified cellulose was thoroughly characterized *via* infrared spectroscopy (ATR-IR), ^{1}H and ^{13}C NMR. A conversion of the carboxylic acid into the desired Ugi-4CR product were calculated from ^{31}P NMR and ranged between 88.7 and 99.5 %. Thermal characterization of the modified cellulose was carried out *via* TGA and DSC measurements, showing high thermal stability (up to 290 °C) and T_g between 99 and 116 °C, which could be tuned by simply changing any of the components. Results from size exclusion chromatography gave high molecular weights between 193 and 242 KDa. Thus, with this study not only processability, but also a property control was introduced to cellulose by simply changing the components in the Ugi 4-CR.

6.3.2 Introduction

The general mechanism and some applications of the Ugi 4-CR have been presented in **Chapter 2.6.** MCR reactions such as P-3CR and Ugi 4-CR have been employed previously for cross-linking purposes to make hydrogels using polysaccharides. In this case, the polysaccharide introduces one of the needed components, while at least one of the other components is a bi-functional. Ugi & König employed this technique to develop an alginate-based network for enzyme immobilization.[284] Crescenzi and co-workers have extended this method to prepare hydrogels from other polysaccharides such as hyaluronic acid, carboxyl methyl chitosan, carboxyl methyl cellulose and alginic acid.[285,286] Recently, Stenzel *et al*. reported the surface modification of TEMPO-mediated oxidized cellulose nanofibrils (CNF) *via* P-3CR. The thermoresponsive poly(*N*-isopropylacrylamide) (pNIPAm) side group was coupled *via* the aldehyde component leading to the synthesis of a thermoresponsive cellulose nanofibrils (CNF) after the P-3CR.[287]

So far, the direct use of MCRs for modifying cellulose is not reported. The only report being the collaborative work carried out in the course of this project with Dr. Zafer

Söyler who worked on the P-3CR modification of succinylated cellulose, while this author worked on the Ugi 4-CR. Therefore, the results for the Ugi 4-CR on succinylated cellulose will be discussed in this chapter. A total of three different Ugi-4CR modified cellulose products were synthesized and fully characterized. The main objectives of this study was to introduce processability to cellulose *via* Ugi-4CR, as well as investigate the material properties upon changing the components.

6.3.3 Results and Discussions

The study of Ugi four component modification on succinylated filter paper cellulose (SFP) was carried out in DMSO as a solvent. The first trial of the reaction was done using 2-phenylpropionaldehyde, *n*-butyl amine and *tert*-butylisocyanide. The carboxylic acid component was then provided by the succinylated cellulose (succinylated filter paper, SFP). The SFP with a DS of 2.64 (from ^{31}P NMR) was synthesized by Dr. Zafer Söyler using the DBU-CO$_2$ switchable solvent system. The general reaction scheme for the Ugi 4-CR on succinylated cellulose is shown in **Scheme 26**.
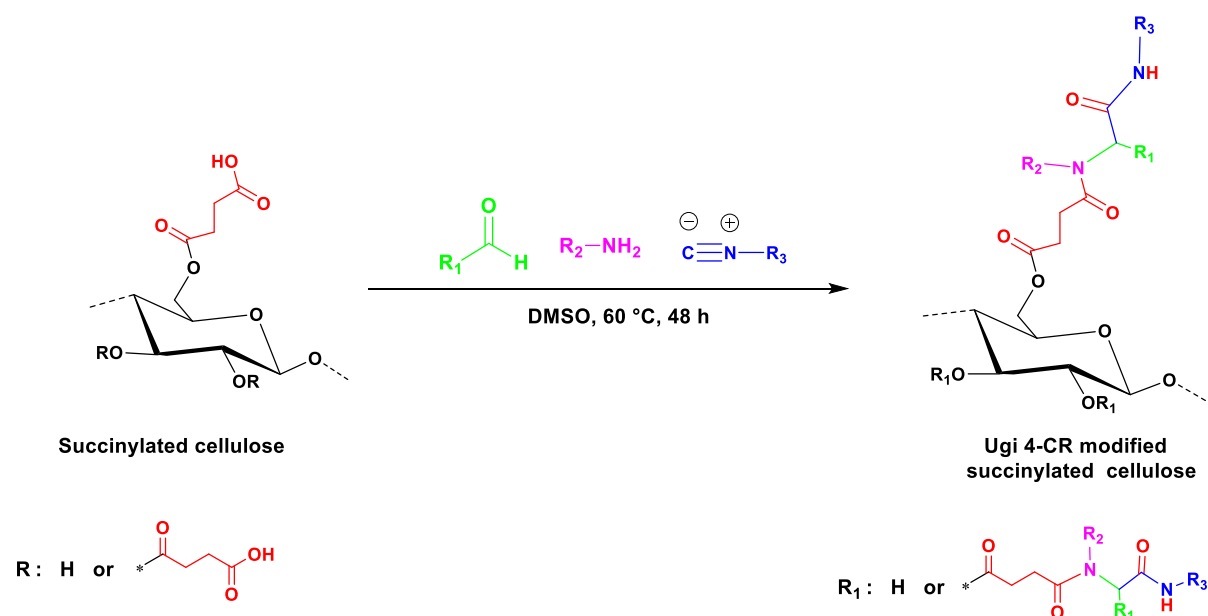
Scheme 26: The general reaction scheme for Ugi 4-CR modification of succinylated cellulose.

As concentration plays an important role in multicomponent reactions, various concentrations were investigated with 50 mg/mL giving the best results, and has thus been employed for the rest of the experiments. For the reaction performed using 2-phenylpropionaldehyde, *n*-butyl amine and *tert*-butylisocyanide (**U1**), an isolated yield of 83 % was achieved and the preliminary success of the reaction was evident from infrared spectroscopy. The spectra comparing cellulose filter paper (FP), succinylated filter paper (SFP) and the Ugi 4-CR modified cellulose (**U1**) are shown in **Figure 29**. After succinylation, the v(O-H) stretching vibration peak at 3300 cm^{-1} in the native cellulose was replaced by a broader peak between 3664-2384 cm^{-1} corresponding to the v(O-H) stretching vibration in the introduced carboxylic acid function. In addition, the v(C=O) stretching vibration of the carbonyl function of the carboxylic acid was visible at 1704 cm^{-1}. After the Ugi 4-CR modification, the broad peak in the succinylated cellulose was replaced by a less broad peak at 3380 cm^{-1} assigned to the v(N-H) stretching vibration of the amide function as well as unreacted v(O-H) stretching vibration in the native cellulose. Furthermore, the v(C=O) stretching vibration peak at 1704 cm^{-1} in the carboxylic acid moiety was replaced with a peak at 1739 cm^{-1} arising from the introduced ester function as well as two new peaks at 1678 cm^{-1} and 1622 cm^{-1} from the two amides present in the formed Ugi 4-CR product.
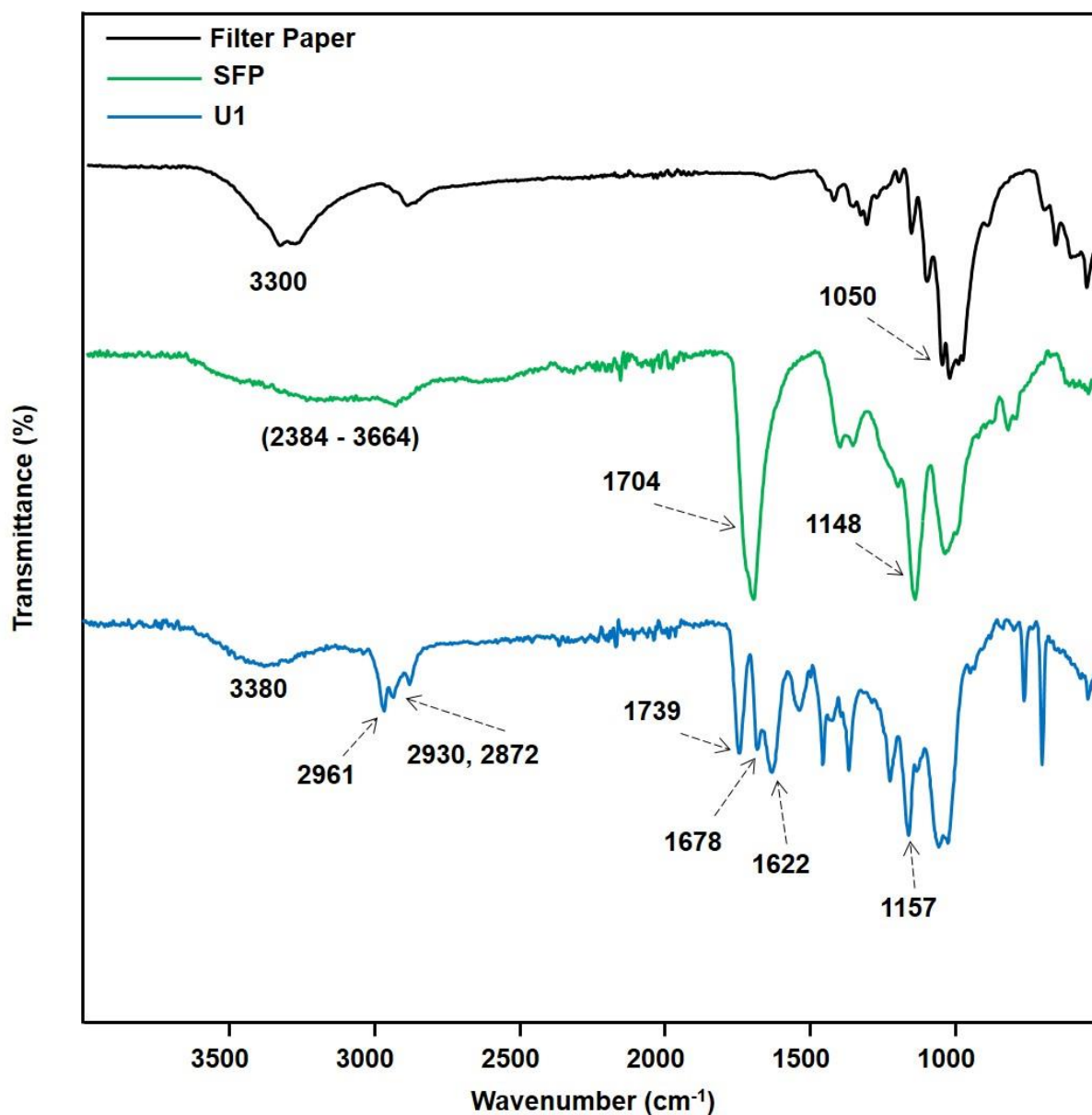
Figure 29: ATR-IR spectra comparison between filter paper cellulose (SF), succinylated cellulose (SFP), and Ugi 4-CR modified succinylated cellulose (**U1**).

As the obtained **U1** product was soluble in THF, further confirmation of the structure was evaluated using ^{1}H and ^{13}C NMR and presented in **Figure 30**.
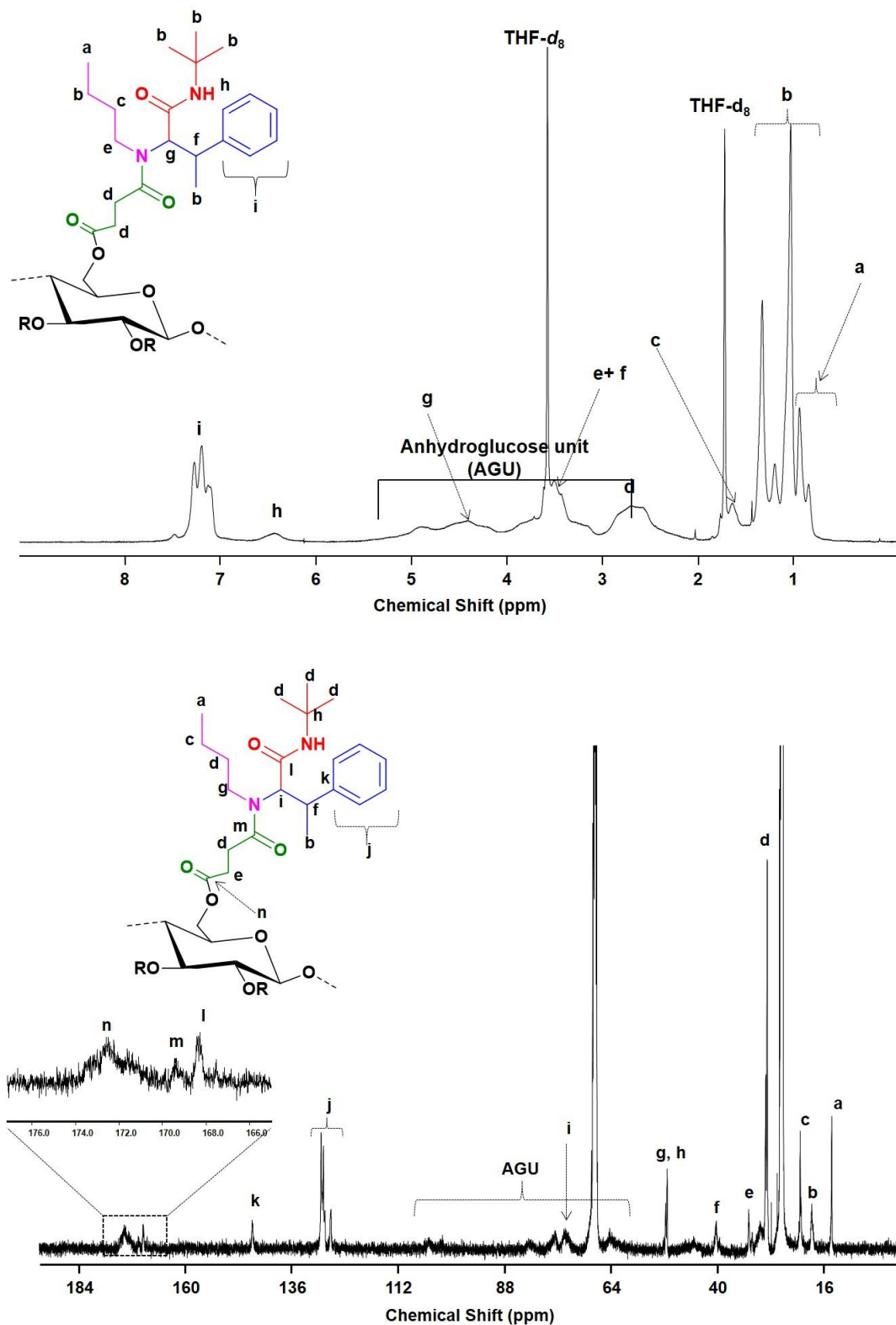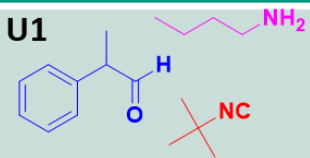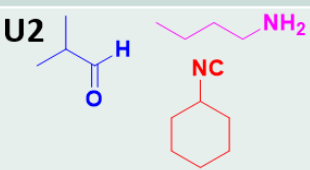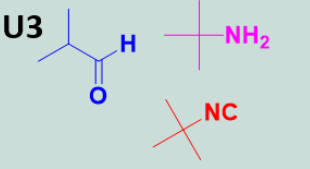
Figure 30: ^{1}H NMR (top) and ^{13}C NMR (bottom) of Ugi 4-CR modified succinylated cellulose (U1) in THF(d_8).

The assignment of the peaks from the ^{1}H and ^{13}C NMR are similar to previous reports of Ugi 4-CR products.[288] From the ^{1}H NMR data, the aromatic protons chemical shift was observed between 7.14-7.15 ppm. In addition, the chemical shift of the amide proton was visible at 6.50 ppm. The protons from the cellulose backbone were less visible appearing between 3.10-5.42 ppm, whereas the introduced aliphatic protons were more visible around 0.88-1.38 ppm. Furthermore, from the ^{13}C NMR, three characteristic peaks of the three carbonyl carbons present in the molecule were observed at 168.28, 169.42 and 172.53 ppm corresponding to the two amides and one ester functions respectively. Also visible were the chemical shifts from the aromatic carbons between 125.96-128.80 ppm.

Upon confirmation of the success of this reaction, variations in either the aldehyde, amine or isocyanide components were made leading to a total of three Ugi 4-CR modified cellulose compounds (see **Table 8**).

Table 8: Reaction conditions, yield and conversion of Ugi 4-CR of succinylated cellulose.

Reactants	Conditions	Yield[a] (%)	Conversion[b] (%)
U1	2 eq, 48 h, 60 °C 50 mg mL^{-1}	83	88.7
U2	2 eq, 48h, 60 °C 50 mg mL^{-1}	92	97.6
U3	2 eq, 48 h, 60 °C 50 mg mL^{-1}	89	99.6

[a]Yields were calculated from DS values. [b]Conversions were calculated *via* ^{31}P NMR.

All products were obtained with isolated yields between 83 and 92 %. As expected, the reaction performed using highly sterically demanding components (**U1**) gave the lowest yield, whereas simple components (**U3**) led to the highest yield.

The structural confirmation of the products was done *via* infrared spectroscopy (see **Figure 97**-**Figure 99**), and ^{1}H and ^{13}C NMR characterizations (**Figure 100** and **Figure 101**). The results obtained for both ATR-IR and NMR characterizations were similar to those reported for **U1**. However, slight variations were visible from ^{1}H and ^{13}C NMR due to the structurally differences between the products (details in experimental section **Chapter 8.6**). Furthermore, the conversion calculations of all products was done *via* ^{31}P NMR. The ^{31}P spectra for **U1** is presented in **Figure 31**, whereas those from **U2** and **U3** are included in the experimental section (**Figure 102** and **Figure 103**).
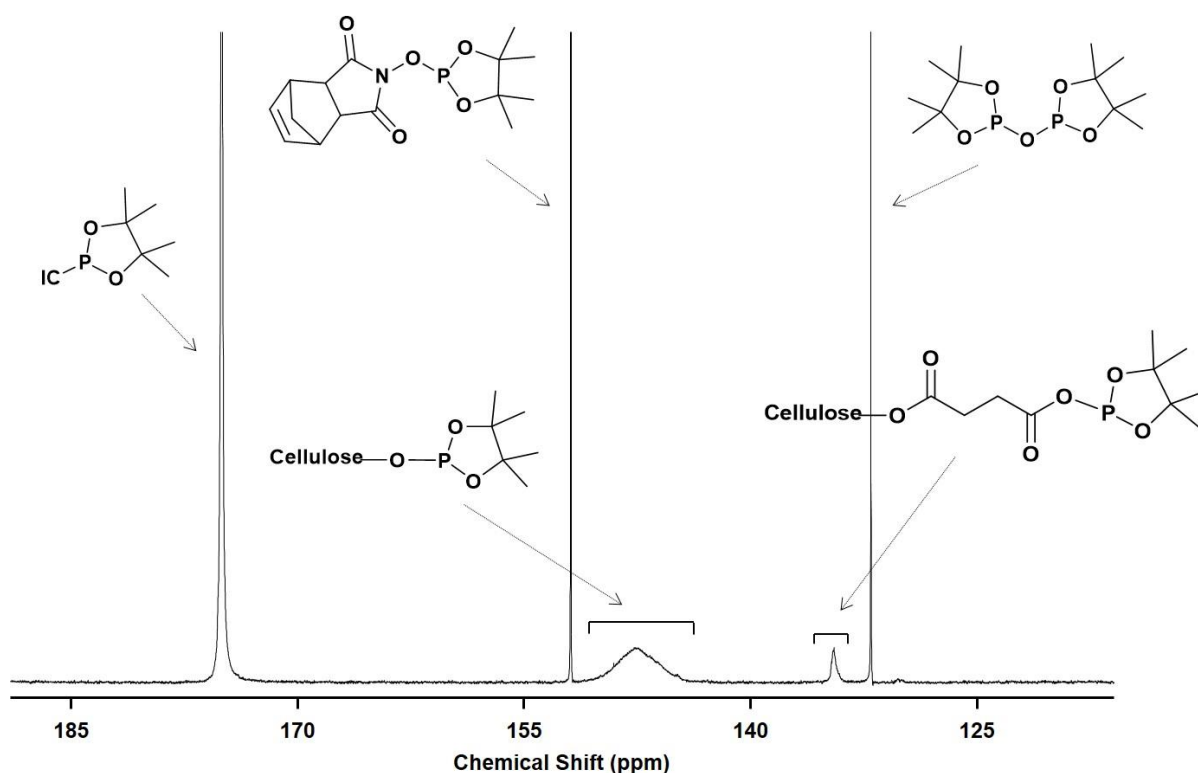
Figure 31: ^{31}P NMR of Ugi 4-CR modified succinylated cellulose (**U1**) in CDCl₃.

^{31}P NMR is a reported reliable approach to not only determine the degree of substitution of modified cellulose (DS), but can also be employed for calculating the conversion. This method works by the addition of a phosphorylating agent alongside an internal standard to a known amount of the cellulose sample. The phosphorylating agent reacts with any unreacted hydroxyl group giving a broad peak at a chemical shift between 145-137 ppm and also with the internal standard giving a sharp peak at 152 ppm. The ratio between these two peaks is then used in calculating the DS according to a previous report.[248] Also visible from the ^{31}P NMR was a small sharp peak around 133 ppm resulting from the reaction between the un-reacted carboxylic

acid in the succinylated cellulose with the phosphorylating agent. This obviously show that a conversion of 100 % was not achieved (with 100 % implying a conversion of all the 2.64 carboxylic acid per AGU of the cellulose since a DS of 2.64 of the SFP was used). The absence of a complete conversion makes it difficult to estimate the conversion of the Ugi 4-CR modification directly, since no reference is available. In order to overcome this limitation, a simple MCR (P-3CR) modification was carried out on the same succinylated cellulose. Results from ^{31}P NMR showed a complete disappearance of carboxylic acid peak at 133 ppm (conversion of 100 %). The P-3CR modified cellulose product was therefore used as a reference to calculate the conversion of all Ugi 4-CR modified cellulose samples. The detailed method for calculating the conversion is shown in the experimental section **Chapter 8.6**. The calculated conversion of all Ugi 4-CR modified cellulose samples ranged between 88.7 and 99.6 % (see **Table 8**). The obtained conversions correlated nicely with the components used, with more sterically demanding components (**U1**) resulting in lower conversion compared to their simple counterparts (**U3**). Furthermore, the purity of all products were confirmed by elemental analysis showing a complete absence of sulphur, which would otherwise have been present if all the used DMSO solvent was not removed (**Table 9**).

Table 9: Elemental analysis of Ugi 4-CR modified succinylated cellulose products.

Product	C %	N %	H %	S %
U1	62.16	6.63	8.91	0
U2	60.80	7.33	9.02	0
U3	63.13	7.30	8.94	0

To ensure that the modification was indeed occurring on the polymer and not low molecular weight cellulose, the molecular weight of all isolated products was determined by size exclusion chromatography (SEC) technique. As the modified cellulose samples were soluble in dimethylacetamide-Lithium bromide, (1% w/w), SEC measurements was possible. A comparison between the succinylated cellulose (SFP) and subsequent Ugi 4-CR modified cellulose is shown in **Figure 32**. In addition, the obtained data for their molecular weights and distribution are presented in **Table 10**. The results show that higher molecular weights were obtained for the succinylated cellulose product (271 KDa) compared to the Ugi 4-CR modified cellulose (193 to

242 KDa). However, since the succinylated cellulose and Ugi 4-CR samples have not only a different functionality but a different swelling behaviour, it will be inappropriate to make a comparison between them. The high molecular weights obtained for the Ugi 4-CR cellulose samples show indeed the success in carrying out such a complex modification on cellulose and still being able to maintain its high molecular weight. Though it will be difficult to rule out any form of polymer degradation, the mildness of this procedure most likely have reduced such to a minimum.
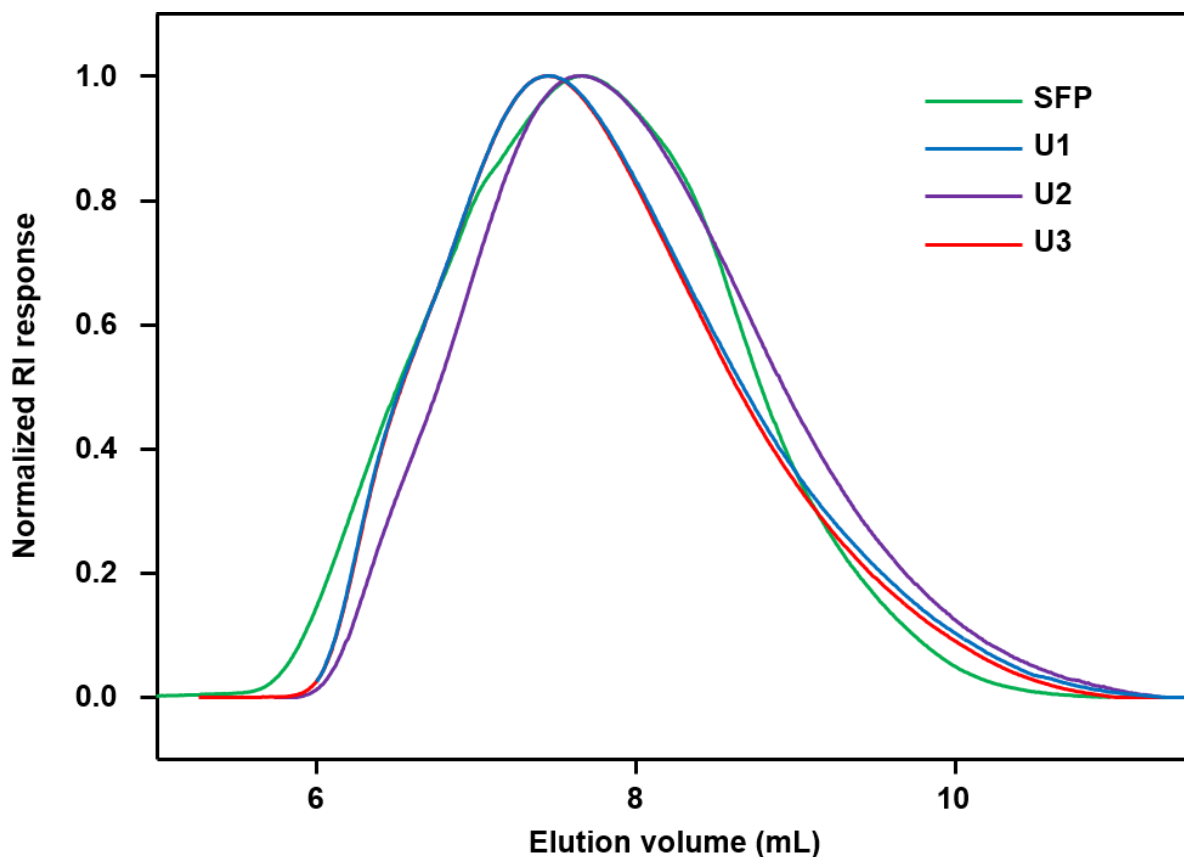
Figure 32: SEC traces of succinylated cellulose (SFP) and Ugi 4-CR modified cellulose (**U1**, **U2**, **U3**) measurement relative to poly(methyl methacrylate) calibration in DMAc-LiBr (1% w/w).

Table 10: Molecular weight and distribution data for succinylated cellulose (SFP) and Ugi-4CR modified succinylated cellulose.

Product	$^{a}M_n$ (KDa)	$^{a}M_w$ (KDa)	Dispersity (Đ)
SFP	271	714	2.6
U1	193	533	2.7
U2	242	656	2.7
U3	225	647	2.8

[a]Data obtained from the GPC performed in DMAc/LiBr relative to PMMA calibration.

In order to develop cellulose-based materials that will compete favourable with their petroleum-based counterpart, their thermal stability is important. In this regard, the thermal stability of the synthesized Ugi 4-CR modified cellulose was investigated by thermal gravimetric calorimetry (TGA) and shown in **Figure 33**.
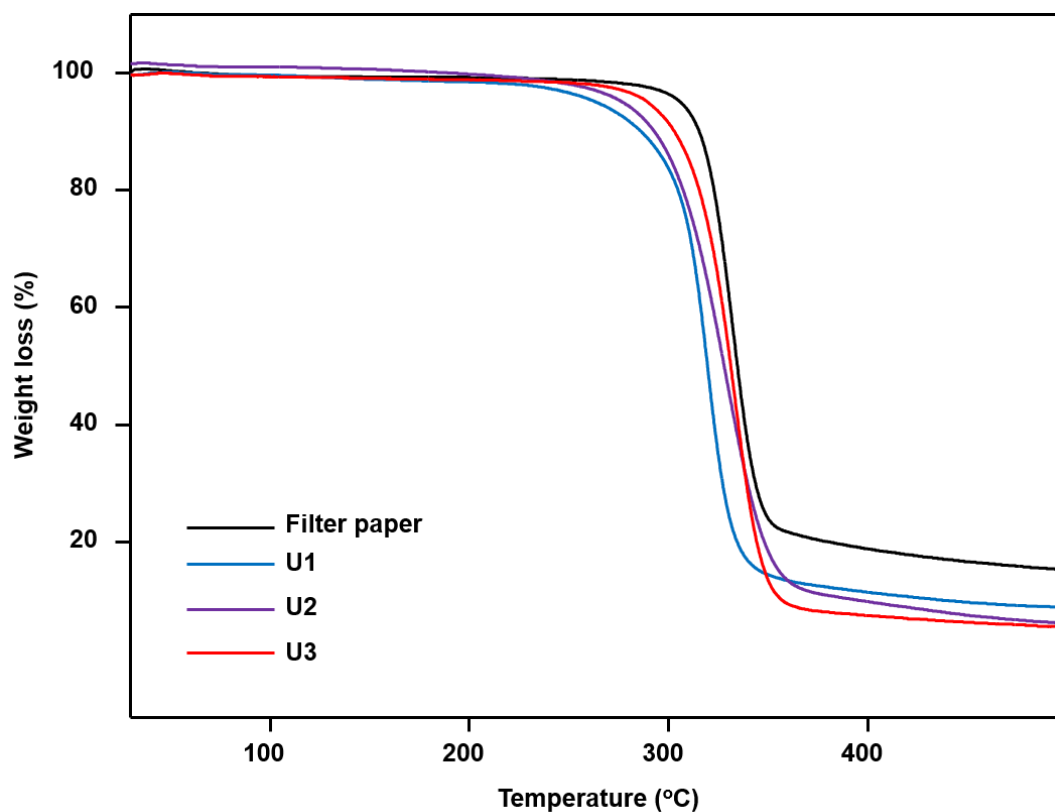
Figure 33: TGA of filter paper cellulose (FP) compared to Ugi 4-CR modified cellulose (**U1**, **U2**, **U3**).

Results obtained showed relatively high thermal degradation temperature for the Ugi 4-CR modified cellulose samples ($T_{d,5\%}$ between 263-290 °C), which is not very far from that of the starting filter paper cellulose ($T_{d,5\%}$ = 305 °C).

As designing a multifunctional and processable cellulose based material was one of the objective in this study, differential scanning calorimetry (DSC) measurements were carried out. The results obtained are shown in **Figure 34**, including data from the un-modified cellulose filter paper as comparison.
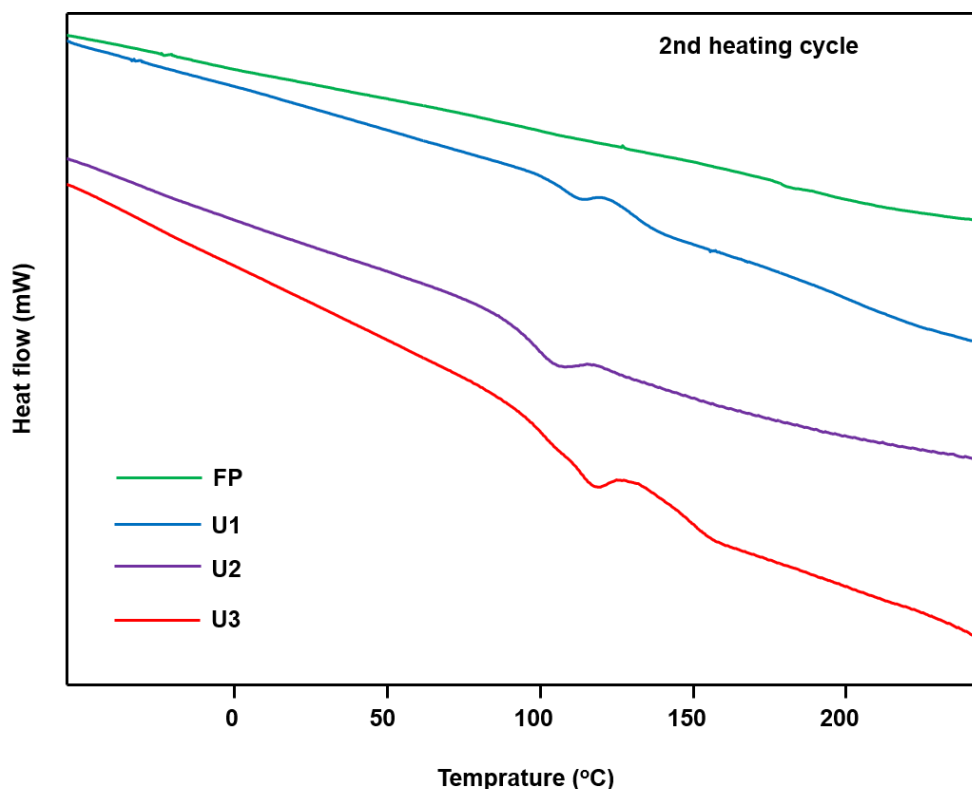
Figure 34: DSC data (2nd heating cycle) of succinylated filter paper cellulose (SFP) compared to Ugi 4-CR modified cellulose (**U1**, **U2**, **U3**).

As seen from **Figure 34**, the starting filter paper cellulose (FP) had no thermal transition. It was therefore exciting to see that all the Ugi 4-CR modified cellulose samples show T_g values between 99 and 116 °C. Also noteworthy was the observed influence on the T_g by a simple change of any components in the MCR. In this way, the thermal property of the modified cellulose could be tuned over this temperature range. Thus, not only a processable cellulose-based material with high molecular weight was achieved, but the ability to tune this property by simply changing one of the components was established.

6.3.4 Conclusions

In this chapter, the goal of achieving a route to possibly processable cellulose-based material through the Ugi four component reaction (Ugi 4-CR) was achieved. In this regard, a sustainable derived succinylated filter paper cellulose with a DS of 2.64 was used (SFP). Alongside an amine, an aldehyde and isocyanide, a total of three (3) Ugi 4-CR modified cellulose products were synthesized (**U1**, **U2**, **U3**). The isolated yields obtained ranged between 88.7 and 99.6 % depending on the components used. Preliminary success of the reaction was obtained *via* infrared spectroscopy (ATR-IR). As the modified cellulose samples were soluble in THF, further confirmation of the structures *via* ^{1}H and ^{13}C NMR could be achieved. Furthermore, high molecular weights between 193 and 242 KDa were obtained from size exclusion chromatography (SEC) measurements, showing the mildness of the developed procedure in achieving successful MCR on high molecular weight cellulose. In addition, high thermal stability was obtained (263 to 290 °C) which is similar to the starting filter paper (305 °C). Finally, from DSC measurements, all modified cellulose samples showed T_g values between 99 and 116° C. This indeed shows the successful introduction of processability into cellulose which has remained a big challenge limiting their wide spread application. The obtained T_g values could be tuned over this range of temperature by simply changing one of the components in MCR modification. It is thus the expectation of this study that this simple structure-function relationship could be employed in the future to design target-based cellulose materials for a given application.

6.4 Perspective of multicomponent reactions

This chapter and the associated parts in the experimental section are adapted from the following literature:

K.N. Onwukamike, S. Grelier, E. Grau, H. Cramail, M.A.R. Meier, On the direct use of CO_2 in multicomponent reactions: Introducing the Passerini four component reaction, *RSC Adv.* 2018, 8, 31490.

https://pubs.rsc.org/en/content/articlelanding/2018/ra/c8ra07150k#!divAbstract

Permission from the Royal Society of Chemistry (RSC), copyright © 2018.
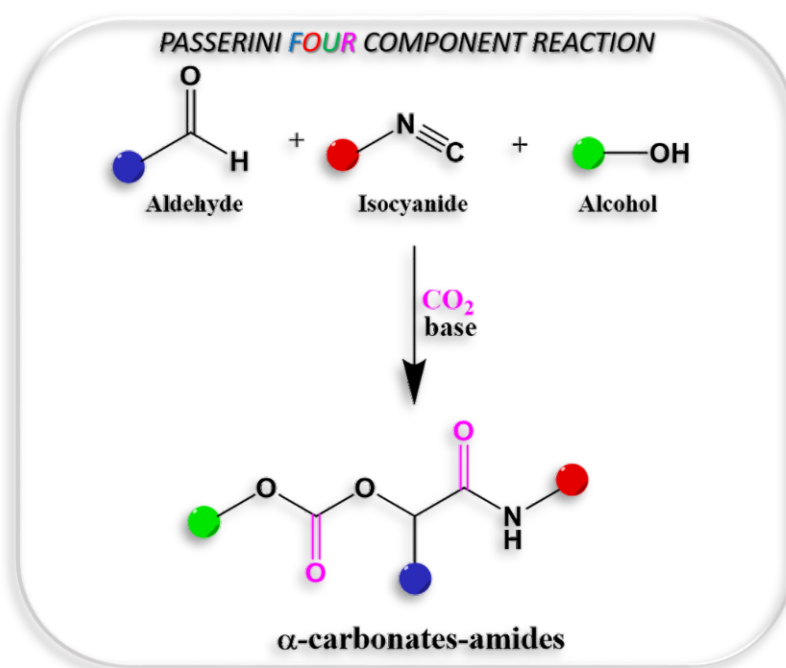
6.4.1 Abstract

In this chapter, a novel isocyanide-based multicomponent reaction, the Passerini four component reaction (P-4CR) is introduced, by replacing the carboxylic acid component of a conventional Passerini three component reaction (P-3CR) with an alcohol and CO_2. Key to this approach is the use of the previously described CO_2 switchable solvent system, allowing the synthesis of a variety of α-carbonate-amides. The reaction was first investigated and optimized using butanol, isobutyraldehyde, *tert*-butyl isocyanide and CO_2. Parameters investigated included the effect of reactant equivalents, reactant concentration, solvent, catalyst, catalyst concentration and CO_2 pressure. Among all investigated parameters, the purity of the aldehyde and its tendency to oxidize was one of the most critical parameters for a successful P-4CR. After optimization, a total of twelve (12) P-4CR compounds were synthesized with conversions ranging between 16 and 82 % and isolated yields between 18 and 43 %. Their structures were confirmed *via* ^{1}H and ^{13}C NMR, infrared spectroscopy (ATR-IR) and high resolution mass spectrometry (ESI-MS). In addition, three (3) hydrolysis products of P-4CR (α-hydroxyl-amides) were successfully isolated with yields between 23 and 63 % and fully characterized (^{1}H, ^{13}C NMR, ATR-IR and ESI-MS) as well. The successful development and proof of this approach could open up new modification routes for carbohydrates having hydroxyl groups such as cellulose in the future.

6.4.2 Introduction

Apart from the classic P-3CR,[192,224] many variations have been reported mostly replacing the aldehyde or acid component with an alcohol and activated phenolic compound respectively.[289,290] Taguchi and co-workers reported on the direct utilization of aliphatic alcohols alongside an isocyanide and an α,β-unsaturated aldehyde in the presence of an Indium(III) catalyst to form α-alkoxy-amide products.[289] El Kaim *et al.* employed the so-called Passerini-Smiles reaction of *o*-nitrophenol as a replacement of the acid component and synthesized a library of α-aryloxy-amide products.[290] Chatani *et al.* reported the reaction of cyclic and acyclic acetals with isocyanides in the presence of $GaCl_3$ as catalyst.[291] Here, the isocyanide inserts into the C-O bond of the acetals, finally resulting in α-alkoxy-imidates. Denmark and Yan reported the asymmetric α-addition of isocyanides to aldehydes. In this case, the reaction was catalyzed by a combination of a weak Lewis acid, $SiCl_4$ activated by a chiral Lewis

base (bisphosphoramide). The desired α-hydroxyl-amides were obtained after basic workup.[292]

Very important for the herein reported results, Jessop and co-workers introduced switchable solvent systems involving CO_2 alongside a super base in 2005.[153] The unique nature of this solvent system was its ability to switch from a non-polar to a polar solvent in the absence or presence of CO_2, respectively, by the reversible formation of a carbonate anion/protonated base complex. The system is very versatile and allows applications such as straight-forward product purification,[293,294] as CO_2 capturing agents,[245] for the selective extraction of hemicellulose from wood,[295] and also as sustainable solvent for cellulose solubilization.[154,155] An optimization study of the DBU-CO_2 switchable solvent system was previously described (see **Chapter 4**), including an unambiguous proof that carbonate anions are indeed formed *in situ*.[156] The formation of this *in situ* carbonate not only led to a mild dissolution of cellulose in DMSO, but also allowed an activation of the cellulose hydroxyl groups, leading to a milder modification such as succinylation.[172] In this regard, a high DS value of 2.64 was reported for the reaction carried out at room temperature in 30 min.[296] Tunge and co-workers reported a related approach of alcohol activation using CO_2 in the absence of any base catalyst.[297] In this case, allyl alcohols were reacted directly with CO_2 leading to the formation of an *in-situ* allyl-carbonate, which forms a π-allyl complex with a Pd-precursor that can then react with nucleophiles (here derived from nitroalkanes, nitriles and aldehydes) in a Tsuji-Trost like fashion.[297]

In this chapter, the idea is to utilize this *in-situ* generated carbonate anion as an acid component (i.e. nucleophile) in a typical P-3CR and is thus the starting point of the herein reported results. In this case, the CO_2 is able to activate the alcohols and is incorporated as a carbon source; introducing one carbon atom into the desired compound. This study therefore is the first report of the Passerini four component reaction (P-4CR) as a variation of the P-3CR, achieved by replacing the acid component in the P-3CR by an alcohol and CO_2. The utilization of CO_2 as a carbon source is both interesting from an environmental and sustainable perspective, as well as to extend the scope and achievable structural variety of MCRs. Finally, it is the expectation of this chapter that this approach can be further applied for the modification of carbohydrates containing hydroxyl groups and even cellulose in the future.

6.4.3. Results and Discussions

As a starting point and to prove the hypothesis of a possible P-4CR, a first investigation was carried out using butanol, isobutyraldehyde, *tert*-butylisocyanide and CO_2 in dichloromethane (DCM) as a solvent. In addition to the formation of the expected P-4CR product, the formation of a P-3CR by-product and the hydrolysis of the P-4CR product, resulting in the formation of α-hydroxyl-amide, was observed (see **Scheme 27**).
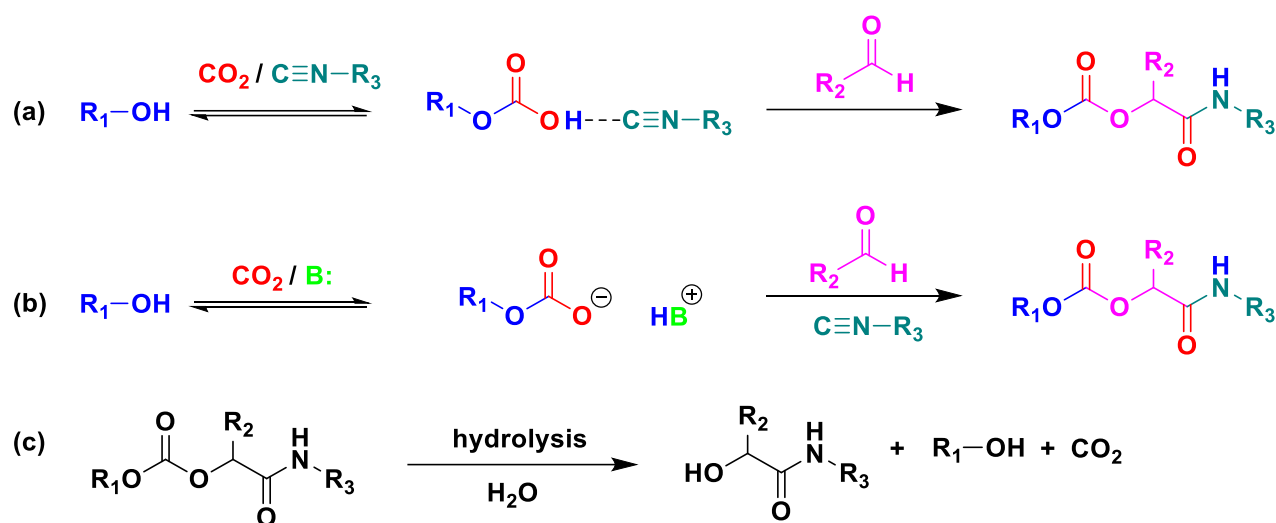
Scheme 27: Formation of P-4CR products in the absence (**a**) and presence (**b**) of a base catalyst. **c**) Hydrolysis of the P-4CR product. (see **Figure 38** for synthesized structures).

Further investigations revealed that the observed P-3CR side product resulted from the presence of the respective carboxylic acids originating from the oxidation of the used aldehyde component. The isobutyraldehyde used for the optimizations had a lower purity (92 % from ^{1}H NMR) than reported by the manufacturer (99.5 %). Further investigations showed that freshly distilled aldehydes gave the best results for a P-4CR and the P-3CR could be supressed to less than 5 %, although it could not be completely suppressed. Nevertheless, this first proof-of-principle reaction clearly showed that the anticipated reactivity of the carbonate anion allows for a P-4CR. For optimizing the P-4CR, several parameters, such as the effect of solvent, reactant concentration, reactant equivalents, catalyst concentration and CO_2 pressure, were investigated. Dichloromethane (DCM, 1.84 M) was employed as solvent for the first test experiments as it has been reported to be a suitable solvent for the P-3CR.[207] One equivalent of butanol, isobutyraldehyde and *tert*-butylisocyanide was employed, while

the reaction was performed at 10 bar CO_2 for 48 h at room temperature. The conversion of butanol was followed *via* gas chromatography (GC) *versus* an internal standard (tetradecane). For the first trial, a conversion of 38 % was reached after 48 h (see **Figure 35**. The presence of the desired P-4CR product (*m/z* 273.19) was indicated by gas chromatography-mass spectrometry (GC-MS). In addition, the presence of the hydrolysis product of the P-4CR (*m/z* 174.10) as well as the P-3CR product (*m/z* 243.16) were confirmed by GC-MS.
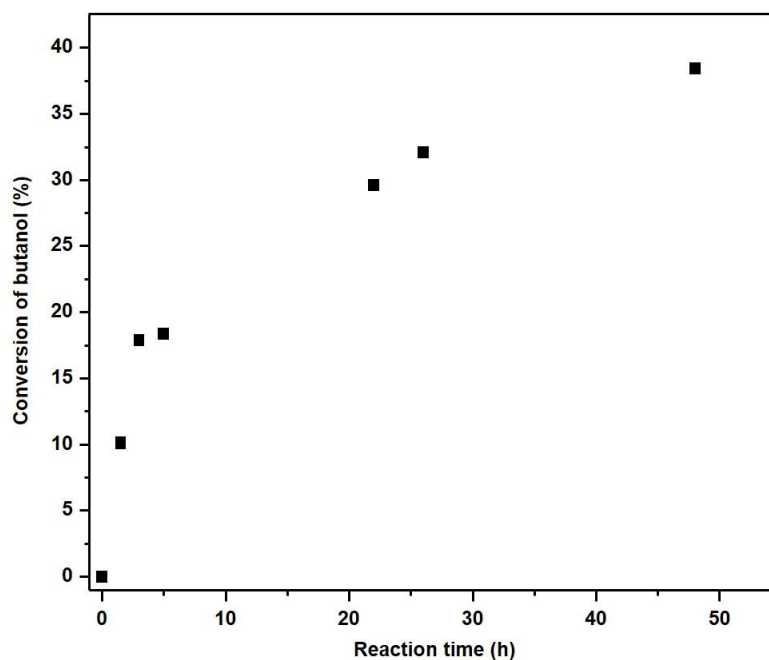
Figure 35: Conversion of butanol over time observed via GC-MS (1.84 M, 1 eq. isobutyraldehyde, 1 eq. *tert*-butylisocyanide, 10 bar CO_2, 48 h at room temperature).

The formation of the three products was followed over time *via* GC and the results are illustrated in **Figure 36**.
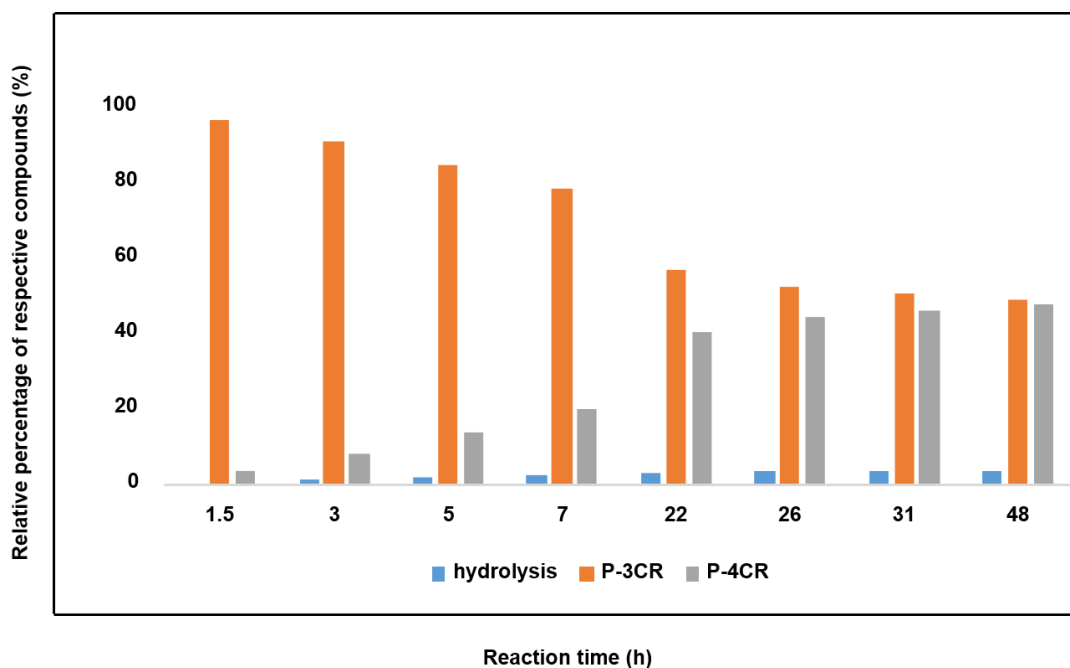
Figure 36: Relative percentage of the formed compounds (P-4CR, P-3CR and hydrolysis of P-4CR products, compare **Scheme 27**) over time (results obtained from GC). Reaction conditions: one equivalent each of butanol, isobutyraldehyde and *tert*-butylisocyanide at 10 bar CO_2 in DCM (1.84 M) at room temperature.

As seen from **Figure 36**, within the first five hours, the P-3CR accounted for most of the observed products. However, an increased formation of the P-4CR was observed as the reaction proceeded. In addition, some hydrolysis of the P-4CR product was observed with time. Considering the P-3CR side reaction, a two-fold excess of aldehyde and isocyanide components was employed in the next reaction, resulting in an improved butanol conversion of 56 %.

As solvents play a key role in multicomponent reactions, different solvents (dimethyl sulfoxide, methyl-THF and chloroform) were investigated next. While similar conversions were obtained for all the solvents investigated, different hydrolysis tendencies were noticed. By comparing the relative percentage between the P-4CR and its hydrolysis product, an increased formation of hydrolysis product in the order chloroform > DMSO > methyl-THF > DCM was observed. This trend might be explained considering the acidity of the solvents, e.g. chloroform is the most acidic solvent tested herein. For DMSO, the high hydrolysis rate observed is probably due to the presence of unavoidable water impurity in the solvent. Methyl-THF showed a

relatively low tendency towards hydrolysis, but led to a higher degree of oxidation of the aldehyde and thus an increase of the P-3CR side product (see experimental section **Figure 104**), probably due to possible peroxide impurities.[298] DCM showed the lowest tendency towards hydrolysis and equally resulted in the highest selectivity towards the targeted P-4CR product. It should however be noted here that the observed hydrolysis products (α-hydroxyl amides) are valuable compounds finding possible application for synthesis of biological active compounds.[299] Furthermore, as multicomponent reactions usually provide higher conversions and yields at higher concentrations, this parameter was investigated by doubling the previously applied concentration. As expected, the conversion of butanol increased from 56 % (1.84 M with respect to butanol) to 73 % (3.68 M with respect to butanol) in DCM.

Presumably, the mechanism of the P-4CR proceeds *via* the *in-situ* formation of a carbonate anion initiated by a base catalyst,[153–156] (see **Scheme 27b**). The carbonate then reacts as the acid component with the isocyanide and aldehyde component in the typical fashion of the conventional P-3CR.[192] However, in the so far discussed set of experiments, no base catalyst was employed. It was therefore interesting to note, that the P-4CR occurred nevertheless. This initially unexpected reactivity could be due to an activation of the alcohol by the isocyanide (**Scheme 27a**). Isocyanides were used as a weak Lewis base in previous reports in literature.[300–302] Equally, alcohol activation by other Lewis bases has been reported.[303] To verify the alcohol activation hypothesis, an *in situ* ^{1}H NMR study was performed (utilizing butanol in CDCl$_3$). In this context, the spectra of butanol, butanol in the presence of stoichiometric amounts of *tert*-butylisocyanide and butanol in the presence of stoichiometric amounts of triethylamine were compared. The respective study is displayed in the **Figure 37**.
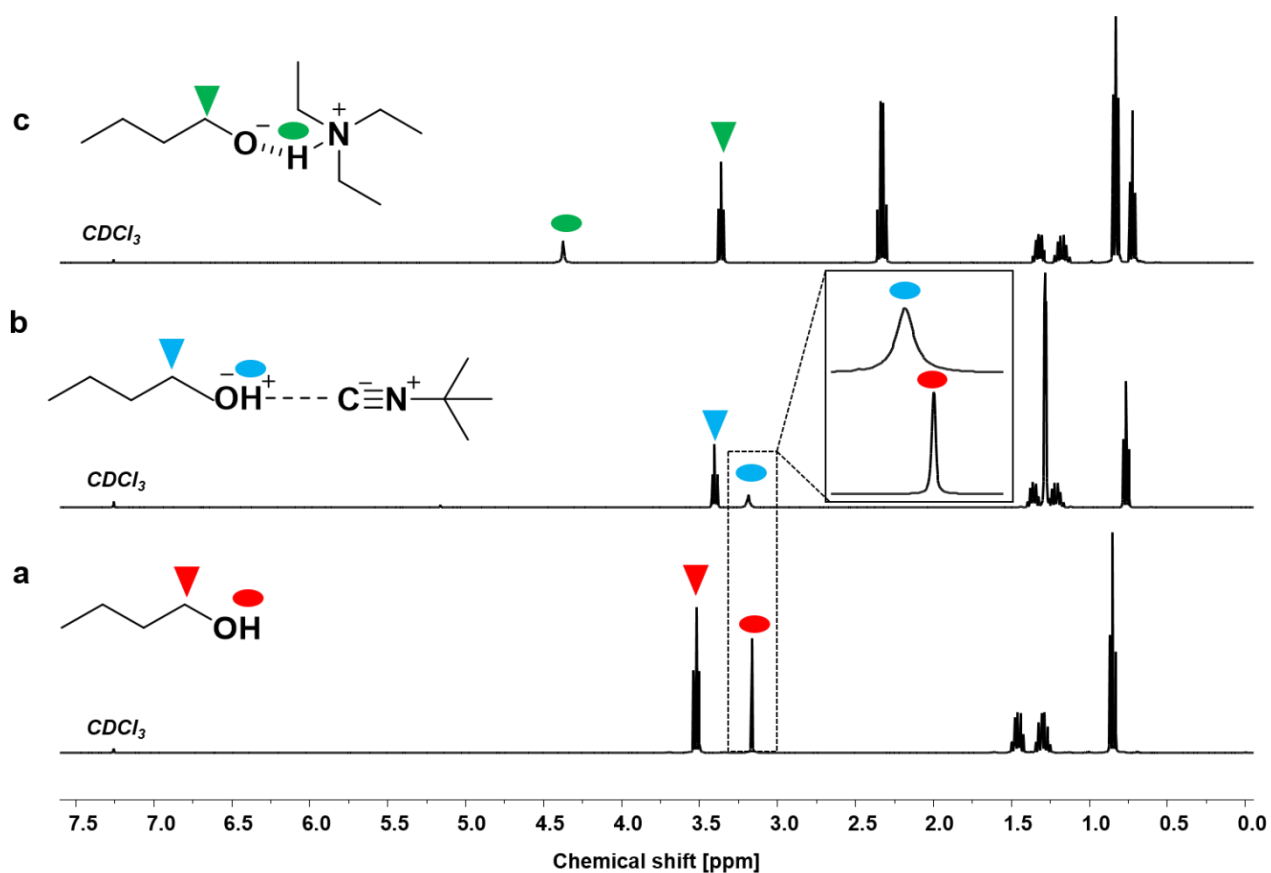
Figure 37: ¹H NMR verification of the Lewis behaviour of isocyanide, ¹H (CDCl₃) NMR comparison between butanol (**a**), butanol and *tert*-butylisocyanide (**b**), butanol and triethylamine (**c**).

From this ^{1}H NMR study, a slight downfield chemical shift of the OH proton (from 3.16 ppm to 3.20 ppm) and significant signal broadening, characteristic of *H*-bonding, was observed for butanol in the presence of *tert*-butylisocyanide (see **Figure 37b**) compared to the spectrum of butanol without isocyanide in CDCl₃. Similar proton signal broadening of the OH proton, most probably caused by *H*-bonding, has also been reported for Schiff bases.[304,305] Comparing the spectrum of butanol with the spectrum of butanol in the presence of Et₃N, a downfield chemical shift of the OH proton (from 3.16 ppm to 4.38 ppm) was observed, while displaying similar signal broadening (**Figure 37c**). These results indicate H-bonding of the OH proton and hence, activation of the alcohol by the isocyanide acting as a Lewis base.

The effect of a catalyst was thus evaluated next. As mentioned above, a basic catalyst is able to activate the hydroxyl group, thereby increasing the carbonate anion formation. Thus, triethylamine, Et₃N (10 mol.%) was tested first. The obtained results were compared with the reaction without addition of the catalyst and are included in the experimental section (**Figure 105**). As expected, the presence of the catalyst

further accelerated the reaction. A conversion of almost 70 % was reached within 24 h (compared to 48 h required to achieve similar conversion in the absence of the catalyst). In addition, the overall selectivity towards P-4CR increased (see **Figure 105 b** and **c**). However, a slight increase in the amount of formed hydrolysis product was also observed in the presence of the base catalyst, as one could expect (compare **Figure 105 b** and **c**). In another set of experiments, the two catalysts Et_3N and DBU were compared. The obtained results showed similar conversion of butanol (about 70 %) after 24 h. However, an increased hydrolysis of the P-4CR product was observed for the reaction with DBU compared to Et_3N (see experimental section **Figure 106**), probably due to the higher basicity of DBU compared to Et_3N. In addition, the formation of the P-3CR side product was less pronounced for Et_3N. Hence, Et_3N was used for the following experiments, screening for catalyst concentration employing 5, 10 and 15 mol.%. This study revealed that the conversion of butanol remained at about 70 % for both 5 and 10 mol.%. However, the *quasi* conversion decreased to 52 % when 15 mol.% of catalyst were used. This decrease can be explained by the observed increased hydrolysis of the P-4CR product, which reforms butanol and thus counterfeits a lower butanol conversion (see **Scheme 27** and **Figure 107**). As 10 mol.% catalyst loading gave slightly better results, this catalyst loading was employed for investigating the effect of CO_2 pressure. Three CO_2 pressures were investigated (5, 10 and 15 bar) and the results are presented in experimental section (**Figure 108**), revealing a slight increase in butanol conversion from 58 % to 69 % as the CO_2 pressure was increased from 5 to 10 bar. However, a slight decrease was observed at 15 bar (62 % conversion). Furthermore, the highest relative percentage of P-4CR was obtained at 10 bar of CO_2. Therefore, 10 bar of CO_2 was selected for further experiments.

Using the described optimized conditions (3.84 M with respect to butanol, DCM as solvent, 1 eq. of alcohol, 2 eq. of aldehyde and isocyanide with respect to butanol, 10 bar CO_2 at room temperature (22-25 °C)), the scope of the P-4CR was investigated by varying the used components (see synthesized structures including their conversion and isolated yield in **Figure 38**).
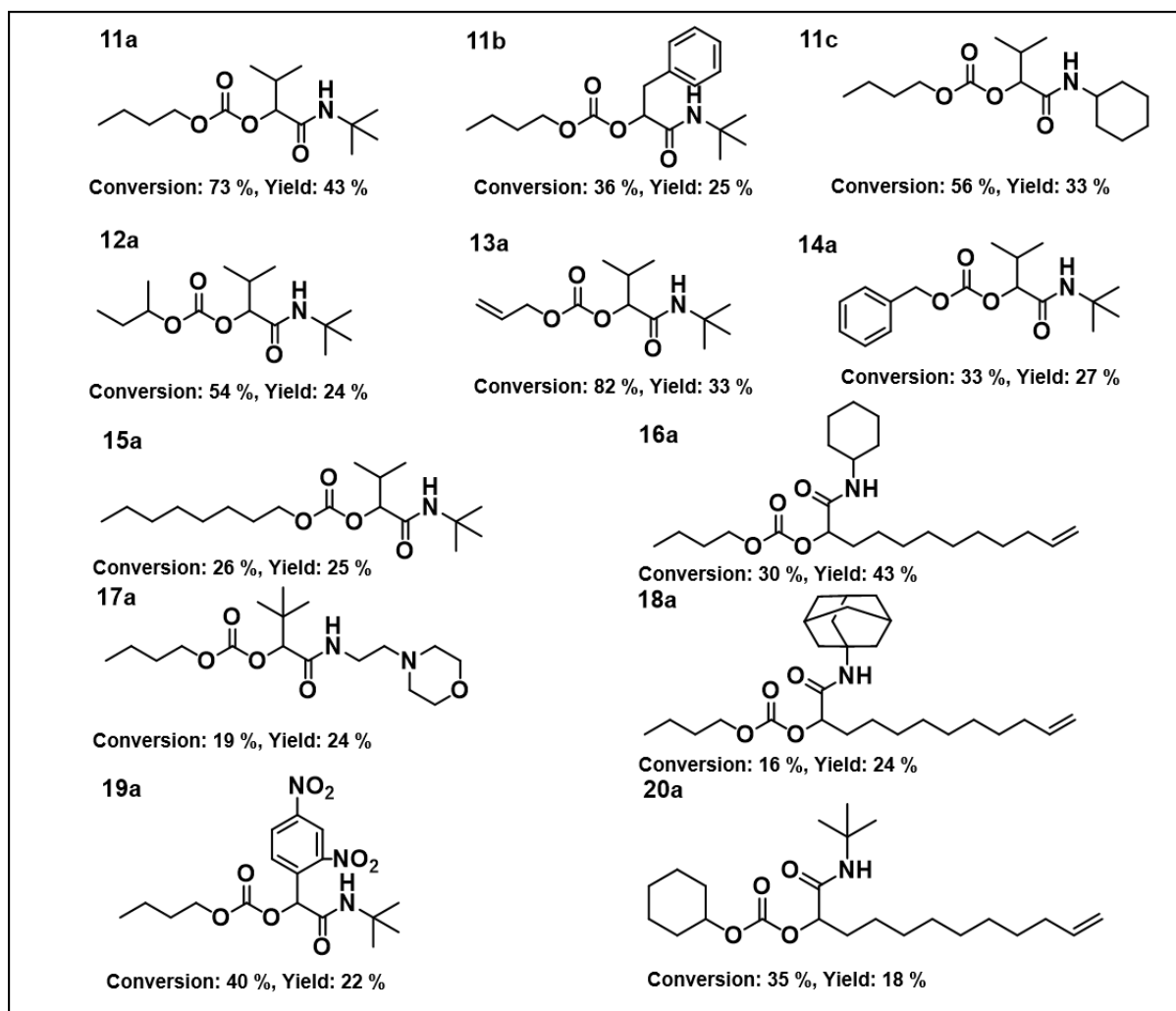
Figure 38: Structures of the synthesized P-4CR products including their conversion and isolated yields.

For the synthesis of **11a**, butanol, isobutyraldehyde and *tert*-butylisocyanide were used. A conversion of about 70 % was reached within 24 h, longer reaction times (up to 45 h) led to an increase of selectivity of the targeted P-4CR compound **11a**. Compound **11a** was isolated in 43 % yield after column chromatography. This value is within the range of previously reported Ugi 5-CR products.[280] Armstrong & Keating reported similar results when other alcohols apart from methanol were used in this Ugi-5CR.[280] It is also important to point out that in the case of methanol, an excess (over 10 times) was utilized in order to achieve high conversion and yields.

The preliminary structural confirmation of **11a** was done using infrared spectroscopy (ATR-IR) showing the characteristic C=O stretching absorbance band of the carbonate (1743 cm^{-1}) and the amide (1654 cm^{-1}) as seen in **Figure 39**.
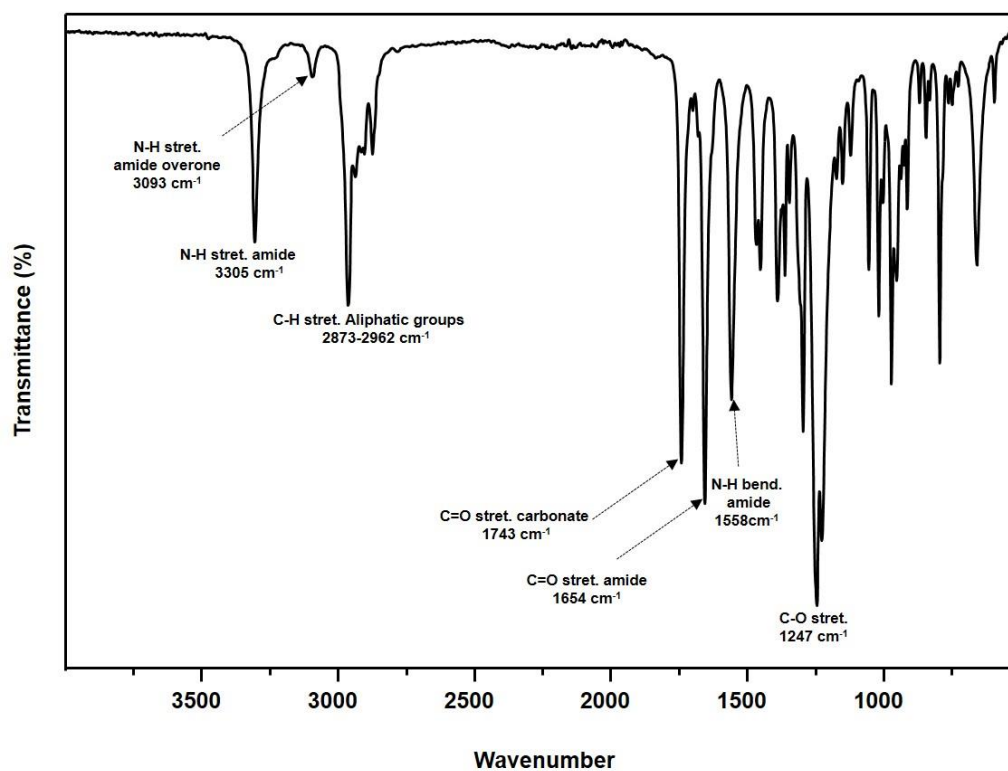
Figure 39: ATR-IR spectrum of P-4CR product **11a**.

Further structural confirmation of **11a** was done *via* ^{1}H and ^{13}C NMR performed in CDCl$_3$. The spectra are shown in **Figure 40**.
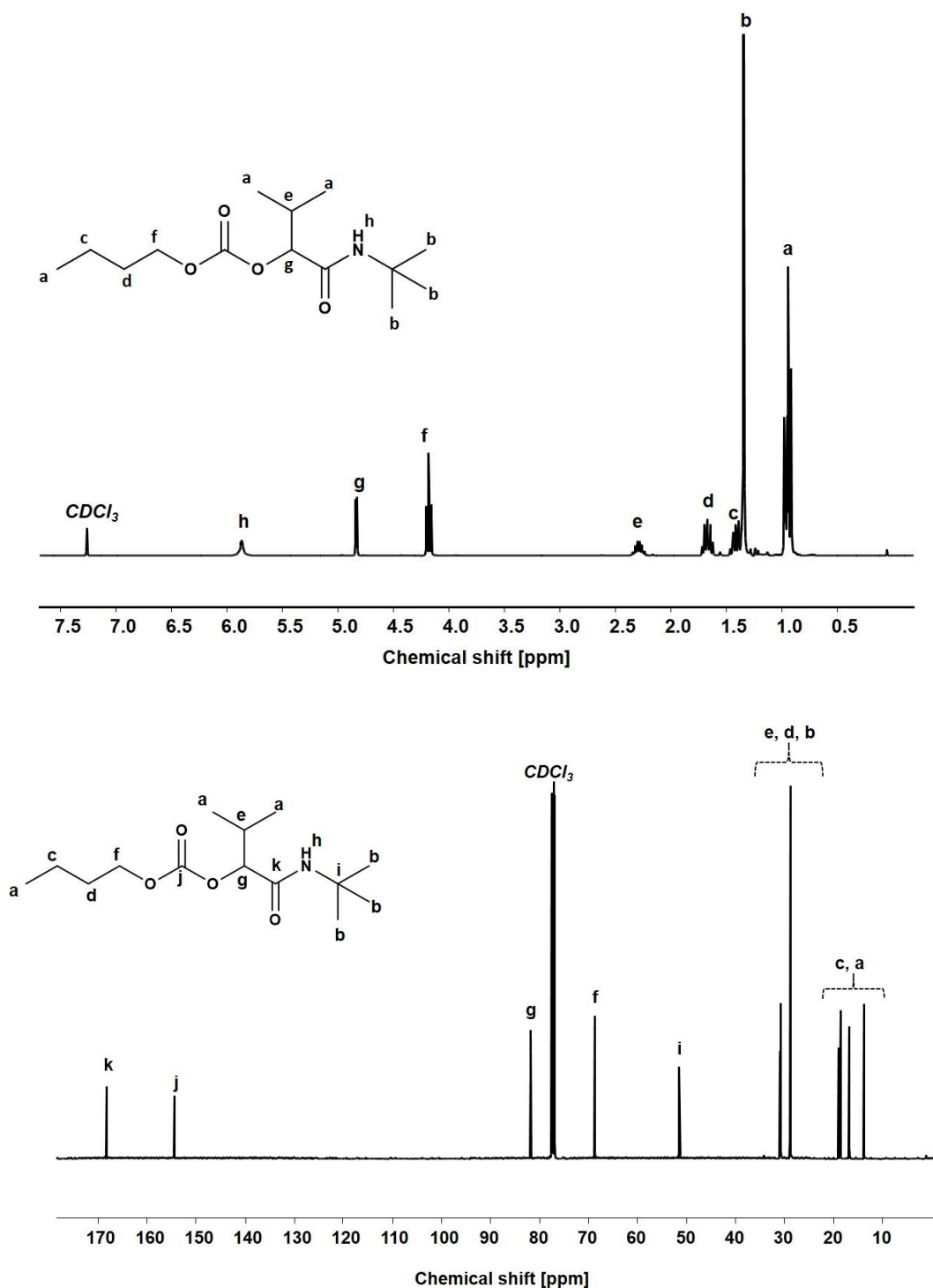
Figure 40: ^{1}H NMR (top) and ^{13}C NMR (bottom) of P-4CR **11a**, measured in CDCl$_3$.

The attribution of the proton and carbon peaks are similar to previous reports of P-3CR,[207] as well as Ugi-5CR.[281] In the ^{1}H NMR spectrum, the amide proton is visible at 5.87 ppm. The proton signal at the tertiary carbon at 4.83 ppm and the 9H from the *tert*-butyl side chain at 1.35 ppm confirm the proposed structure. From the ^{13}C NMR, two characteristic carbonyl carbon chemical shifts are observed at 168.78 ppm

(amide) and 154.93 ppm (carbonate). Furthermore, the tertiary carbon in the isocyanide side chain is observed at 51.70 ppm. Finally, the mass of the molecule was confirmed by high resolution ESI-MS ($[C_{14}H_{27}NO_4Na]^+$ calculated *m/z* = 296.19, obtained *m/z* = 296.18278).

Employing similar conditions, a total of twelve molecules were synthesized and equally characterized (see structures in **Figure 38**). On the example of butanol, five variations of the aldehyde and four isocyanide variations were demonstrated. In addition, a secondary alcohol (2-butanol), an unsaturated alcohol (allyl-alcohol), benzyl-alcohol, octanol and cyclohexanol were utilized. The respective P-4CR products were obtained with conversions ranging from 16 to 82 % and isolated yields between 18 and 43 %. Lower conversions were obtained for reactions involving sterically demanding side chains such as 1-adamantyl **17a** (19 %) and 2-morpholinoethyl **18a** (16 %). In the course of these investigations, it was observed that the P3-CR side-reaction can be supressed to less than 5% by immediate utilization of a freshly distilled aldehyde component.

The obtained P-4CR compounds were fully characterized *via* ^{1}H and ^{13}C NMR, infrared spectroscopy (ATR-IR) and high-resolution mass spectrometry (HR-ESI-MS) (see NMR spectra in the experimental section **Figure 109**-**Figure 120**). In the case of **11b**, employing phenyl acetaldehyde, the P-3CR side reaction was not observed. However, in this case (phenyl acetaldehyde), the presence of a proton in *α*-position to the aromatic ring led to an Aldol condensation side-product. The Aldol side reaction was favoured when the base catalyst was used, as expected. Hence, for this reaction, no catalyst was utilized and a butanol conversion of 36 % was reached after 24 h (without much improvement with longer reaction time). Noteworthy, the P-4CR products from benzyl-alcohol **14a** and octanol **15a** were less prone to hydrolysis. Their higher hydrophobicity compared to butanol could explain this tendency. The reaction performed with allyl alcohol **13a** required longer reaction times to achieve suitable conversions (30 h, conversion 50 %) and showed the highest tendency towards hydrolysis, which also increased over time. Running the reaction even longer (48 h) resulted in 82 % conversion. The P-4CR product was isolated in a yield of 33 %, while 23 % of the hydrolysis product was isolated (see following paragraph for details). Attempt to introduce an aromatic side chain *via* the aldehyde component (benzaldehyde) was unsuccessful, as only the P-3CR and hydrolysis products were

formed. In addition, benzaldehyde is very easily oxidized to the corresponding acid (despite distillation before usage). Thus, 2,4-dinitrobenzaldehyde was used instead to obtain **19a**. A conversion of 40 % was achieved after 48 h with 22 % isolated yield. In a similar manner, the formation of the P-4CR product was not observed when *tert*-butanol was used. Again, only P-3CR and the hydrolysis product of P-4CR were observed *via* GC-MS. Nevertheless, this demonstrates that also tertiary alcohols can be used in this reaction, whereby only one of the two possible products (*i.e.* the hydrolysis product) is accessible so far.

Characterization of the Hydrolysis products of P-4CR

The observed hydrolysis of the P-4CR lead to formation of *α*-hydroxyl-amide products that are equally useful. Therefore, three of these products with various structural architectures were isolated (see **Figure 41**).
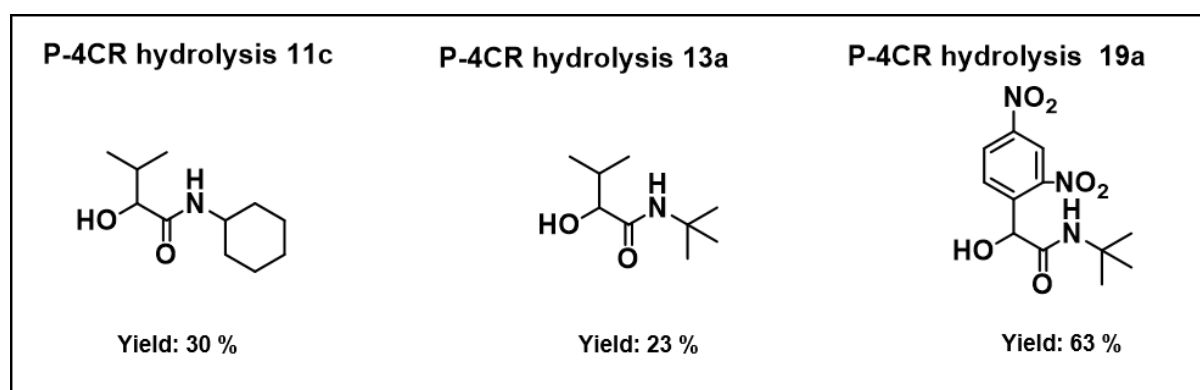
Figure 41: Structures and isolated yields of the P-4CR hydrolysis products.

The hydrolysis product of P-4CR **11c**, **13a** and **19a** were isolated in a yield of 30 %, 23 % and 63 %, respectively and their structures confirmed by ^{1}H and ^{13}C NMR (see experimental section **Figure 121**-**Figure 123**). From the ^{1}H NMR spectra of the hydrolysis products of **11c**, **13a,** and **19a**, the amide proton chemical shifts were visible at 6.19, 6.31 and 6.72 ppm, respectively. Also noticeable is the presence of the alcoholic proton chemical shift at 2.45, 3.05 and 4.63 ppm, respectively. The obvious shift towards the lower field in the case of hydrolysis product **19a** is due to the proximity of the alcoholic proton to the aromatic ring, leading to a deshielding effect. In addition, the characteristic aromatic protons in this molecule are visible between 7.90-8.77 ppm. The presence of the amide bond was further confirmed from their ^{13}C NMR results. The carbonyl carbon of the amide gives a signal around 172.00 ppm for hydrolysis

products **11c** and **13a**, whereas that of **19a** was 168.19 ppm. Furthermore, the characteristic aromatic carbon atoms in the latter molecule appeared between 148.72-142.23 ppm for the carbon atoms connected to the nitroxide side group, and 127-130 ppm for the other aromatic carbon atoms. In addition, from infrared spectroscopy (ATR-IR) all three hydrolysis compounds, showed a sharp absorbance band around 3330 cm^{-1} which is attributed to the N-H stretching band of the amide. This sharp peak overlaps with a broad signal at 3219, 3258 and 3295 cm^{-1} for the hydrolysis products of **11c**, **13a**, and **19a** respectively and attributed to the –OH absorbance band. The =CH stretching band in the aromatic containing hydrolysis product **19a** was visible at 3124 cm^{-1}. Furthermore, the same amide functional group showed a C=O stretching absorbance band around 1640 cm^{-1} (for hydrolysis products **11c** and **13a**) and 1655 cm^{-1} for the hydrolysis product **19a**. Furthermore, the C-O of their hydroxyl groups gave a stretching absorbance band between 1060 and 1025 cm^{-1} for all the hydrolysis products. Finally, their masses confirmed from high resolution mass spectroscopy (HR-ESI-MS).

6.4.4. Conclusions

In this chapter, a novel variant of the Passerini reaction, the Passerini four component reaction (P-4CR) was reported. This was achieved by replacing the carboxylic acid component in a conventional P-3CR with an alcohol and CO_2. Upon optimization of the reaction parameters (reaction time, reactant equivalents, reactant concentration, solvent, catalyst concentration and CO_2 pressure), twelve P-4CR products were successfully synthesized with conversions ranging from 16 to 82 % and isolated yields between 18 and 43 %. In addition, hydrolysis of the P-4CR products leading to the formation of *α*-hydroxyl-amides was observed. Three of these hydrolysis products were isolated with yields between 23 and 63 %. Furthermore, the formation of P-3CR products was observed, which occurred due to the oxidation of the employed aldehyde components. The success of this study does not only expand the structural diversity of multicomponent reactions, but the direct utilization and activation of CO_2 as a carbon building block is equally noteworthy. The application of this procedure for carbohydrates with hydroxyl functional groups is also envisioned in future.

7. Conclusions and Outlook

Cellulose remains a very viable and potential alternative to the un-sustainable petroleum-derived polymers. To achieve a truly sustainable cellulose-based material, its renewability combined with sustainability is necessary. Such sustainability considerations based on the Principles of Green Chemistry, should take into account the solvent used, reactants, derivatization method and finally the end product as well as the waste produced. During all these steps, a need to evaluate and compare between alternatives is important to choose the best available option. At the end, the goal is to ensure that the processes do not simply shift the "environmental burden" to other stages of the process cycle. Therefore, from the onset of developing a new cellulose modification protocol, the entire process should be carefully evaluated for sustainability.

The solubilization of cellulose opens up many potential routes for valorizing this interesting polymer. As cellulose is not soluble in most solvents including water, the first goal of this thesis was to investigate on a sustainable cellulose solvent. In this regard, the DBU-CO_2 switchable solvent system was studied and optimized. The optimization allowed dissolution of cellulose (up to 8 wt.%) within 15 min at 30 °C. This fast, mild and easy-recyclable solvent system became the starting point for the other studies carried out on cellulose in this thesis.

In the first investigation on processing cellulose, aerogels were prepared through the solubilization and coagulation method. This process was easier to achieve due to the optimized CO_2 solvent system. The morphology of the obtained aerogels under various processing conditions was studied by scanning electron microscopy (SEM). In addition, the solvent recovery was demonstrated, an important aspect of sustainability. Furthermore, and to avoid any pre-derivatization, homogeneous cellulose modification was carried out using high oleic sunflower directly. The obtained fatty acid cellulose esters (FACEs) could be processed into films, which showed very good mechanical properties (elastic modulus up to 478 MPa) and improved thermal stability (increase by 30 °C compared to starting cellulose samples). In another study, the use multicomponent reaction was employed to synthesize processable and multi-functional cellulose materials. In this case, a pre-derivative cellulose (succinylated)

sample was used. The resulting Ugi 4-CR modified cellulose showed T_g between 99 and 116 °C, that could be tuned by simply changing one of the components.

As a future perspective route for carbohydrates valorization, a novel multicomponent reaction, the Passerini four component reaction (P-4CR), was introduced. This reaction allowed the direct use and incorporation of CO_2 as a carbon source into the P-4CR compounds. The use of CO_2, a major contribution to global warming, is a step in the right direction. As many carbohydrates including cellulose contain hydroxyl groups, this reaction could be used for their derivatization in the future.

As an outlook, it is the expectation of this thesis that researchers working on this very interesting polymer are encourage to always incorporate sustainability considerations in their investigations. The increasing awareness on the need for sustainability in the past decades has also led to an increase interest in cellulose. Therefore, it is important that the issue of sustainability is not allowed to lag behind the various valorization researches on cellulose. Rather, cellulose and sustainability considerations should be investigated side-by-side. In the future, a cellulose-based material should be truly sustainable to be able to replace their petroleum alternative.

8. Experimental Section

8.1 Materials

The following chemicals were used without further purification: Allyl-alcohol (99 %), benzyl alcohol (99 %), butanol (99.5 %), 1-octanol (99 %), phenyl acetaldehyde (98 %, stabilized) and trimethylamine (99.7 %) were purchased from Acros Organics. 1-Adamantyl isocyanide (95 %), benzyl bromide (98 %), 2-chloro-4,4,5,5-tetramethyl-1,3,2-dioxaphospholane (TMDP, 95 %), cyclohexanol (99 %), cyclohexyl isocyanide (98 %), 2-butanol (99.5 %, anhydrous), *Endo-N*-hydroxy-5-norbornene-2,3-dicarboximide (97 %), 2,4-dinitrobenzaldehyde (97 %), isobutyraldehyde (≥ 99.5 %), 7-methyl-1,5,7-triazabicyclo[4.4.0]-dec-5-ene (MTBD, 98 %), 2-morpholinoethyl isocyanide (≥ 98 %), *tert*-butanol (≥ 99.5 %, anhydrous), *tert*-butyl isocyanide (98 %), tetradecane (≥ 99.5 %) and undecylenic aldehyde (95 %) were obtained from Sigma Aldrich. Dimethyl sulfoxide (DMSO, anhydrous, ≥ 99.9 %), 1,5-diazabicyclo[4.3.0]non-5-ene, DBN (98 %), 1-pentyl isocyanide (97 %), butylamine (99.5 %), 2-phenylpropionaldehyde (98 %), isobutyraldehyde (≥ 99 %) were purchased from TCI Europe N.V. Others include: 1,8-diazabicyclo[5.4.0]undec-7-ene (DBU > 98 %, TCI Europe N.V, *Chapter 4*, 6.1, 6.4; 99 %, Alfa Aesar, *Chapter 5*; 98 %, Sigma Aldrich, *Chapter 6.3*), dimethyl sulfoxide (DMSO, VWR, 99%), trimethyl acetaldehyde (ABCR, 97%), methyl iodide (> 99.9 %, VWR) and 1,1,3,3-tetramethylguanidine (TMG, 99 %, abcr, *chapter 4*, 98 %, Alfa Aesar, *chapter 5*). Deuterated chloroform (CDCl$_3$-*d,* Merck), deuterated tetrahydrofuran (THF, d$_8$) and deuterated dimethyl sulfoxide (DMSO−*d$_6$*) were purchased from Merck. Carbon dioxide (CO$_2$) with purity over 99.9 % was obtained from Air Liquide. Cyclohexane, ethyl acetate and dichloromethane were distilled before usage, while tetrahydrofuran (THF), ethanol (96 %), methanol and isopropanol was of technical grade and used without further purification. Microcrystalline cellulose (MCC powder) was purchased from Sigma-Aldrich and cellulose filter paper, No. 5 from Whatman™. Cellulose pulp (CP) was purchased from Rayonier Advanced Materials Company (Tartas Biorefinery, France) and was produced by ammonium sulphite cooking and bleached with an elementary chlorine free (ECF) process (purity in alpha-cellulose is 94 %).

All cellulose samples were dried at 100 °C for 24 h under vacuum to remove free water before use. High oleic sunflower oil was purchased from T + T Oleochemie GmbH, 63755 Alzenau, Germany.

8.2 Instruments

In-situ Fourier transform infrared (FT-IR) spectroscopy

The optimization study on the DBU-CO_2 solvent system (**Chapter 4**) was monitored *in-situ* with Attenuated total reflectance-infrared spectroscopy (ATR-IR). Single beam spectra were recorded within the frequency range (400 to 4000 cm^{-1}) with a 4 cm^{-1} resolution. 30 scans were collected for each measurement.

Infrared spectra of all other samples were recorded on a Bruker alpha-p instrument using ATR technology within the range 4000 to 400 cm^{-1} with 24 scans.

Nuclear Magnetic Resonance Spectroscopy (NMR)

^{1}H NMR spectra were recorded using Bruker Prodigy operating at 400 MHz and 80 °C (for cellulose-benzyl-carbonate and cellulose-methyl-carbonate) and with 1000 scans and a time delay d1 of 1 second. Data were reported in ppm relative to DMSO−d_6 at 2.50 ppm. ^{13}C NMR spectra were recorded using a Bruker Prodigy operating at 100 MHz and 80 °C with 6000 scans and a time delay d1 of 2 seconds. Data are reported in ppm relative to DMSO−d_6 at 39.52 ppm. For octyl-benzyl-carbonate, ^{1}H NMR spectra were recorded using Bruker Avance DPX operating at 300 MHz with 64 scans and a time delay d1 of 1 second and data were reported in ppm relative to DMSO−d_6 at 2.5 ppm. The respective ^{13}C NMR spectra were recorded using a Bruker Avance DPX operating at 75 MHz with 1024 scans and a time delay d1 of 2 seconds and data reported relative DMSO−d_6 at 39.52 ppm. All products were dissolved in DMSO−d_6 with concentrations between 10 and 20 mg/mL.

For the fatty acid cellulose esters (FACEs) samples (**Chapter 6.1**) the ^{1}H NMR spectra were recorded using a Bruker Prodigy spectrometer operating at 400 MHz and measurements done at 90 °C (DMSO−d_6) and at 50 °C (THF-d_8) with 1024 scans and a time delay d1 of 1 second. Data were reported in ppm relative to DMSO−d_6 (2.5 ppm) and THF-d_8 (1.73 and 3.58 ppm). ^{13}C NMR spectra were recorded using a Bruker

Prodigy spectrometer operating at 100 MHz at 90 °C (DMSO) and 50 °C (THF-d$_8$) with 6000 scans and a time delay d1 of 2 seconds. Data are reported in ppm relative to DMSO−d_6 (39.52 ppm) and THF-d$_8$ (25.49 and 67.57 ppm). All products were dissolved with concentrations between 10 and 20 mg/mL.

For Ugi-4CR modified succinylated cellulose samples (**Chapter 6.3**) the ^{1}H NMR spectra were recorded on a 500 MHz DRX Bruker Avance spectrometer operating at a frequency of 499.97 MHz for ^{1}H and a frequency of 125 MHz for ^{13}C measurements. 1024 scans were recorded for the ^{1}H NMR measurements with a time delay d1 of 5 seconds at 50 °C. The data are reported in ppm relative to THF−d_8 at 1.73 and 3.58 ppm. For the ^{13}C NMR measurements, 6000 scans were recorded with a time delay d1 of 5 seconds at 50 °C. The data are reported in ppm relative to THF−d_8 at 25.37 and 67.57 ppm. All products were dissolved in THF−d_8 with the concentrations between 30 and 50 mg/mL.

For the P-4CR products (**Chapter 6.4**) the ^{1}H NMR spectra were recorded on a 500 MHz WB Bruker Avance I spectrometer operating at a frequency of 499.97 MHz for ^{1}H- and a frequency of 125.72 MHz for ^{13}C-measurement on a 8 mm TXI probe head with actively shielded z-gradients (at θ =0°) and on a 4 mm triple HCX MAS probe head (at ca. θ = 65°) at 298 K, regulated with a Bruker VTU-3000. Measurements were done at ambient temperature in CDCl$_3$ and data are reported in ppm relative to 7.26 ppm and 77.16 ppm for ^{1}H and ^{13}C, respectively.

^{31}P NMR Method for DS determination

Degree of substitutions (DS) were determined by ^{31}P NMR using a Bruker Ascend™ 400 MHz spectrometer with 1024 scans, a delay time d1 of 5 seconds and a spectral width of 90 ppm (190−100 ppm). Samples were prepared according to the following procedure: an exact amount of 25 mg of a sample was weighted and dissolved in 1 mL of pyridine. Next 1-1.5 mL of CDCl$_3$ were added alongside 2-chloro-4,4,5,5-tetramethyl-1,3,2-dioxaphospholane (2-Cl-TMDP, 100 µl, 0.63 mmol). The solution was allowed to homogenize after which the internal standard, *endo-N*-hydroxy-5-norbornene-2,3-dicarboximide (150 µL, 123.21 mM in Pyridine : CDCl$_3$ / 3:2, 0.0154 mmol) was added and the solution was stirred for further 30 minutes.

Then, 600 µl of the solution were transferred to the NMR tube. DS values were calculated according to the reported equation.[248]

Viscosity measurements

The viscosities of cellulose and octanol were measured using MALVERN Rotational Rheometer KINEXUS lab+. Prior to the viscosity measurement, solubilized cellulose (MCC) in the DMSO-DBU-CO_2 solvent system was prepared with a concentration of 30 mg/mL. The shear rate was increased from 1 to 100 s^{-1} while measuring the change in shear viscosity (Pa.s). The viscosity of the sample was collected within the stable region of shear viscosity upon increasing the shear rate. Similar measurements were done for octanol with the same concentration.

X-ray Diffraction (XRD) measurements

X-ray diffraction (XRD) patterns were collected on a PANalitycal X'pert MPD-PRO Bragg-Brentano θ-θ geometry diffractometer equipped with a secondary monochromator and an X'celerator detector over an angular range of 2θ = 8-80°. Each acquisition lasted for 1 hour and 27 min. The Cu-Kα radiation was generated at 45 KV and 40 mA (lambda = 0.15418 nm). The samples were prepared on silicon wafer sample holders (PANalytical zero background sample holders) and flattened with a piece of glass.

Freeze-drying

The samples were dried using an Alpha 1-2 LD$_{plus}$ model freeze dryer from CHRIST. Prior to the freeze drying, the samples was frozen by dipping in liquid N_2 for up to 5 minutes.

Scanning Electron Microscopy (SEM)

The surface morphologies of the Cellulose aerogels (**Chapter 5**) and Fatty acid cellulose esters (FACEs) films (**Chapter 6**), were measured using a HITACHI TM-1000 tabletop microscope. Prior to the measurements, the samples were made conducting by metallization using Au (30 seconds, 35 mA).

Size exclusion chromatography (SEC)

For FACEs samples with a DS of about 1.0, measurements were performed using a SEC system with DMAc-LiBr (0.008 mg/mL LiBr) as eluent whereas THF was used for samples with higher DS. Sample concentration of 2 mg/mL was used and measurements performed on a Polymer Laboratories PL-GPC 50 Plus Integrated System containing an autosampler, a PLgel 5 µm bead-size guard column (50 × 7.5 mm), followed by three PLgel 5 µm Mixed-C columns (300 × 7.5 mm), and a refractive index detector at 50 °C with a flow rate of 1 mL/min. The system was calibrated against poly(methyl methacrylate) standards with molecular weights ranging from 700 to 2×10^6 Da. The dissolved samples were filtered through polytetrafluorethylene (PTFE) membranes with a pore size of 0.2 µm prior to injection.

Thermogravimetric Analysis (TGA)

For FACEs samples (**Chapter 6.1**) TGA measurements were performed using a TGA Q-500 from TA Instruments. The samples (about 10 mg) were heated from 25 to 900 °C under N_2 at a heating rate of 10 °C/min. After the measurements, weight loss was calculated in order to determine the degradation temperature ($T_{d, 95\%}$) of the samples. $T_{d, 95\%}$ is defined as temperature at which over 95 % of the weight loss of sample occurred.

For Ugi-4CR modified succinylated cellulose (**Chapter 6.3**), TGA measurements were conducted with a Netzsch STA 409C instrument applying α-Al_2O_3 as a crucible material and reference sample. The samples (~ 20 mg) were heated from 25 °C to 500 °C under nitrogen flow with a heating rate of 5 K/min. Weight loss of the sample was evaluated for the determination of the thermal degradation.

Tensile strength measurement

The FACEs films were prepared into bone shape (25 x 4 mm), and tensile strength measured using a GABO EXPLEXOR instrument with a 25N sensor. Initial speed was set at 5 mm/min. Three to five measurements were performed for each sample and the standard deviation calculated.

Differential scanning calorimetry (DSC)

DSC experiments were carried out with a DSC821e (Mettler Toledo) calorimeter using 100 µL aluminum crucibles. An amount of 30 mg for each sample was measured in two heating cycles of -75 to 250 °C with heating and cooling rate of 15 K/min. The second heating curves were considered for the accurate examination. Samples were measured at least three times for the verification of the results.

Gas chromatography (GC-FID)

For GC measurements, a GC-2010 Plus instrument from Shimadzu with a polar column (Rxi-642Sil MS, length: 30 m, diameter: 0.25 mm, film thickness: 0.25 µm) and a flame-ionization detector (FID) was used. The sample (1 µL) was injected and vaporized at 250 °C. The column was heated from 50 to 280 °C at a rate of 10 K/min.

Gas chromatography-Mass spectrometry (GC-MS).

Electron impact (EI) analyses were conducted using a Varian 431-GC instrument with a capillary column Factor Four^{TM} VF-5ms (30 m × 0.25 mm × 0.25 µm) and a Varian 210-MS ion trap mass detector. Scans were performed from 40 to 650 m/z at rate of 1 scan per second. The oven temperature program applied during the analysis was: initial temperature 95 °C, hold for 1 min, ramp at 15 °C·min^{-1} to 200 °C, hold for 2 min., ramp at 15 °C/min to 300 °C, hold for 5 min. The injector transfer line temperature was set to 250 °C. Measurements were performed in the split-split mode (split ratio 50:1) using helium as carrier gas (flow rate 1.0 mL/min).

Electron Spray Ionization-Mass Spectrometer (ESI-MS)

Spectra were recorded on a Q Exactive (Orbitrap) mass spectrometer (Thermo Fisher Scientific, San Jose, CA, USA) equipped with a HESI II probe to record high resolution electrospray ionization–MS (HR-ESI-MS). Calibration was carried out in the *m/z* range 74–1.822 using premixed calibration solutions (Thermo Fisher Scientific). A constant spray voltage of 4.7 kV and a dimensionless sheath gas of 5 were employed. The S-lens RF level was set to 62.0, while the capillary temperature was set to 250 °C. All samples were dissolved at a concentration range of 0.05 to 0.01 mg/mL in a mixture of THF and MeOH (3:2) doped with 100 µmol sodium trifluoroacetate and injected with a flow of 5 µL/min.

Specific surface area determination

The specific surface area of the aerogel samples (**Chapter 5**), was determined by measuring N_2-adsorption isotherm at 77k with an ASAP 2010 from Micrometrics, and applying the Brunauer-Emmett-Teller (BET) equation. The samples were measured after degassing at ambient temperature between 17 and 25 h.

8.3 Experimental procedures for Chapter 4

ATR set-up description

The ATR set-up used was similar to the previous report of Tassaing *et al.*,[306] Briefly explained, the ATR set-up consists of a home-made Ge ATR accessory with capacity to measure under high temperatures (up to 150 °C) and under high pressures (up to 50 bar of CO_2), coupled with a ThermoOptek interferometer (type 6700) equipped with a globar source; a KBr/Ge beamsplitter and a DTGS (Deuterated TriGlycine Sulphate) detector. The sample holder consists of a stainless steel cell (3 mL volume) screwed above the Ge crystal. Homogeneity inside the cell was achieved by addition of a magnetic stirrer. Cartridge heaters located around the ATR cell and a thermocouple regulated the temperature with an accuracy of 2 °C. The CO_2 inlet located above the cell was connected directly to a CO_2 tank, allowing introduction and control of the pressure.

Sample preparation

3 wt.% of cellulose (MCC) and DBU (3 eq. per Anhydroglucose unit of cellulose) were agitated in 1 mL of DMSO at room temperature for a few minutes and transferred to the ATR cell. Onto evaluating the effect of temperature, the CO_2 pressure was kept constant while the temperature was varied (30, 35, 40, 50 and 60 °C). Equally, for the investigation of the effect of CO_2 pressure, the temperature was kept constant while the CO_2 pressure was altered (5, 10, 20 and 40 bar). After setting the required parameters, the characteristic symmetric stretching vibration bands of C=O (1665 cm^{-1}) of the *in-situ* formed carbonate, C=N (1614 cm^{-1}) of DBU and C=N-H$^+$ (1639 cm^{-1}) of its protonated form were monitored during the optimization study.

Measurement of octanol carbonate stability with temperature
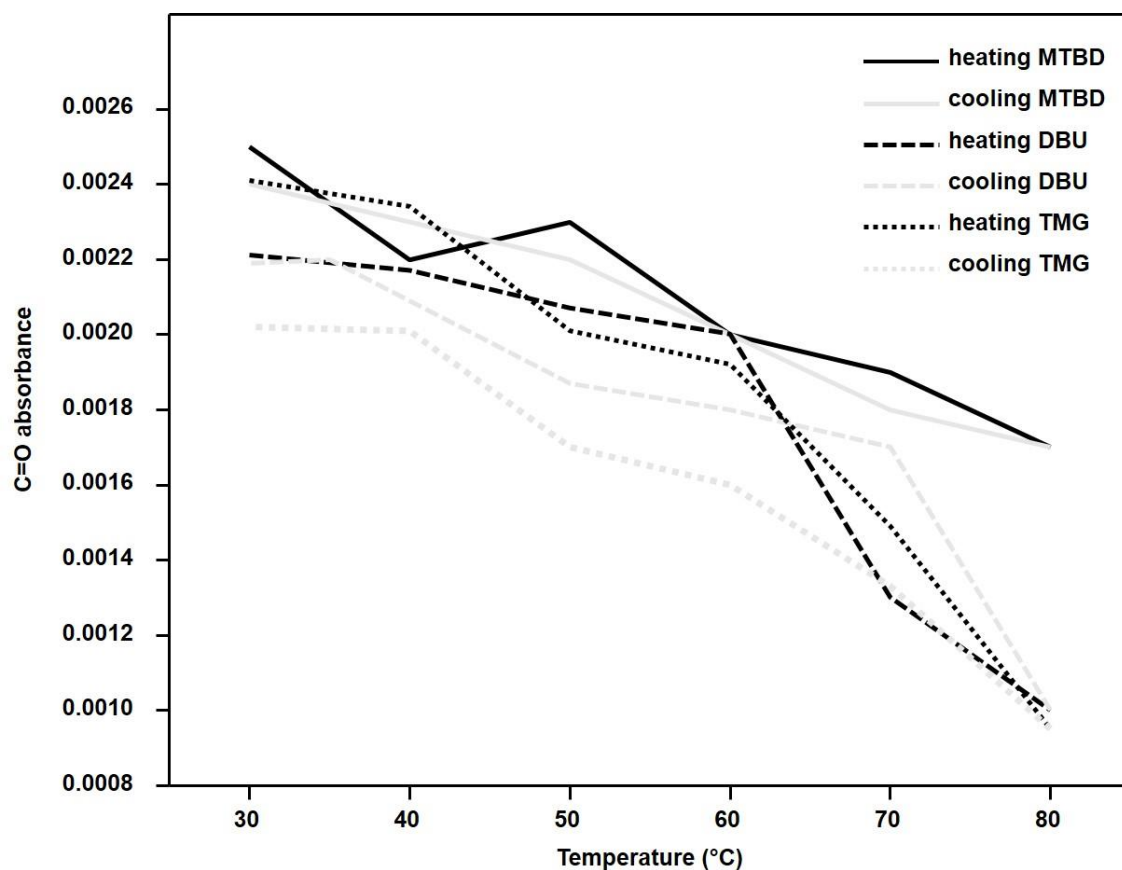
Figure 42: ATR-IR C=O absorbance at 1665cm^{-1} during stability study of *in-situ* carbonate of octanol with temperature using DBU, MTBD and TMG as super bases (conditions: 20 bar of CO_2, 30 °C)

Optimization of temperature and pressure during cellulose solubilization in DBU-CO₂ solvent system

Figure 43: ATR-IR C=O absorbance at 1665 cm^{-1} during cellulose (3 wt.%) solubilization with DBU as super base and 10 bar CO_2 at different temperatures observed over time

Figure 44: ATR-IR C=O absorbance at 1665 cm^{-1} during cellulose (3 wt.%) solubilization with DBU as super base and 20 bar CO_2 at different temperatures observed over time

Figure 45: ATR-IR C=O absorbance at 1665 cm^{-1} during cellulose (3 wt.%) solubilization with DBU as super base and 40 bar CO_2 at different temperatures observed over time.

Figure 46: ATR-IR C=O absorbance at 1665 cm^{-1} during cellulose (3 wt.%) solubilization with DBU as super base at 40 °C and different CO_2 pressures (in bar) observed over time.

Figure 47: ATR-IR C=O absorbance at 1665 cm^{-1} during cellulose (3 wt.%) solubilization with DBU as super base at 50 °C and different CO_2 pressures (in bar) observed over time.

Figure 48: ATR-IR C=O absorbance at 1665 cm^{-1} during cellulose (3 wt.%) solubilization with DBU as super base at 60 °C and different CO_2 pressures (in bar) observed over time.

Influence of the cellulose concentration on carbonate formation
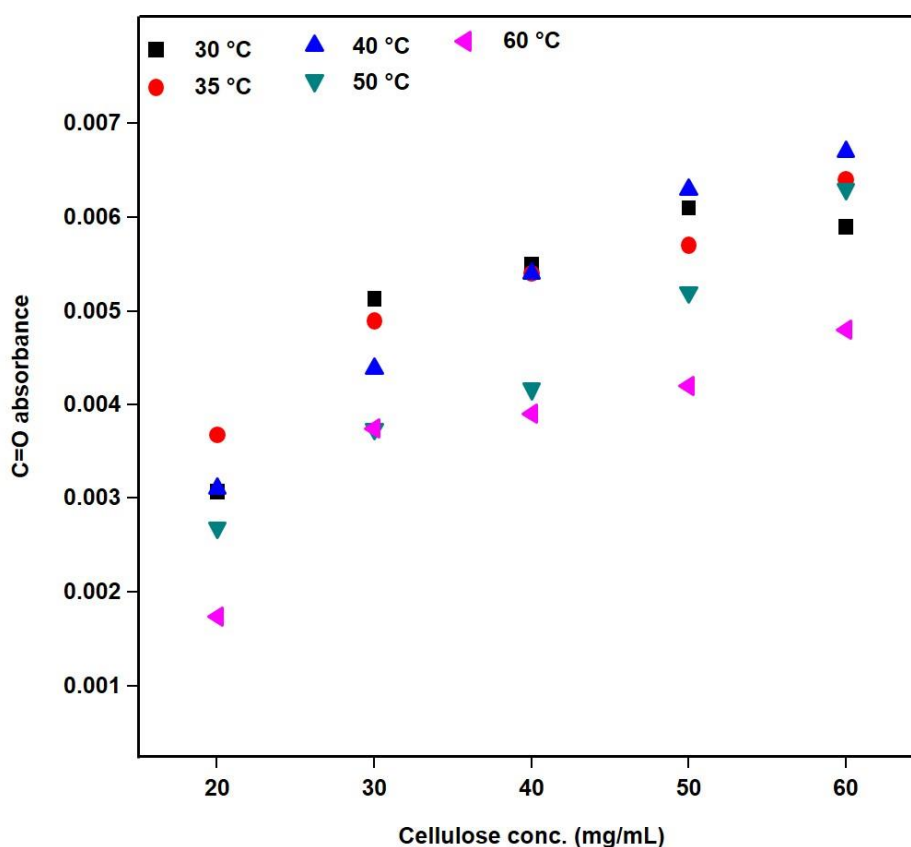
Figure 49: ATR-IR C=O absorbance at 1665 cm^{-1} during variation in cellulose concentration using DBU as super base after 20 bar of CO_2 applied for 15 minutes at various temperatures (30, 35, 40, 50, 60 °C).

Influence of octanol concentration on carbonate formation
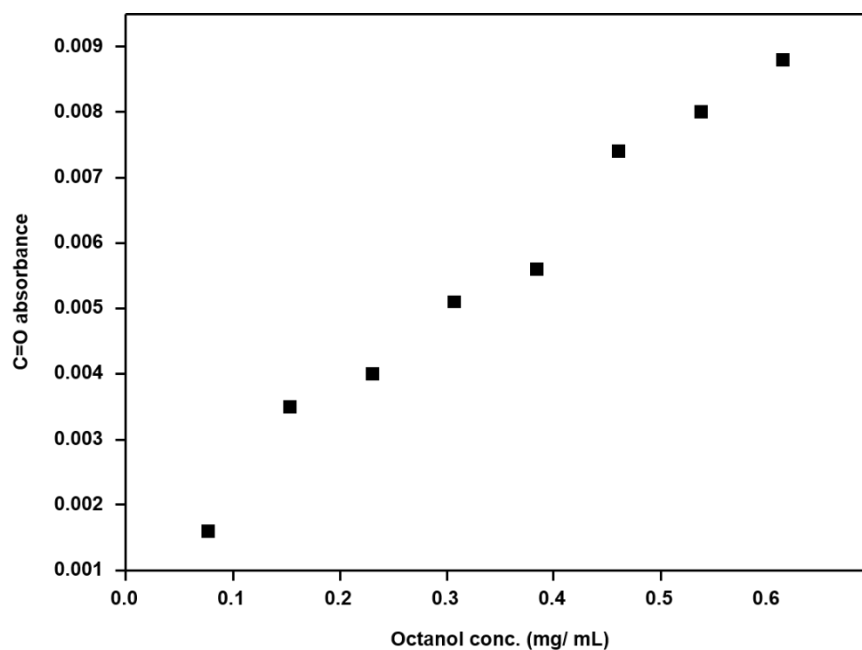
Figure 50: ATR-IR C=O absorbance at 1665 cm^{-1} during variation in octanol concentration using DBU as super base after 20 bar of CO_2 applied for 15 minutes at 30 °C.

Viscosity comparison between octanol and cellulose derived carbonate solvents
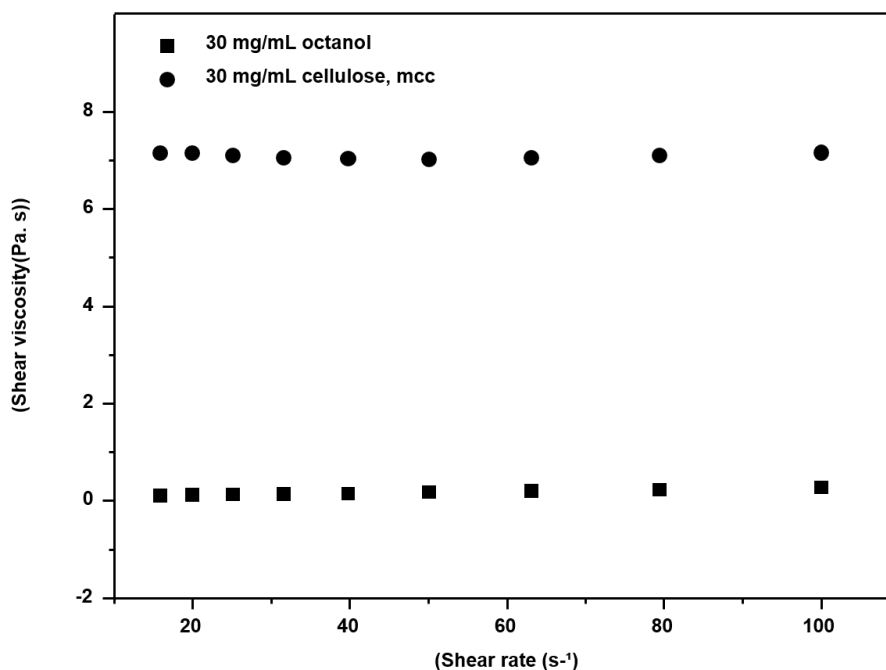
Figure 51: Viscosity measurement comparison between octanol and cellulose in DBU-DMSO-CO_2 solvent at concentration of 30 mg/mL.

Indirect proof of in-situ carbonate formation

Synthesis of octyl-benzyl-carbonate

Octanol (0.50 g, 3.8 mmol, 1.0 eq.) and DBU (0.58 g, 3.8 mmol, 1.0 eq.) were dissolved in DMSO (4.0 mL). The reaction mixture was transferred to a CO_2 pressure reactor and CO_2 (5 bar) was applied for 15 min at 30 °C. Next, benzyl bromide (7.7 mmol, 1.3 g, 2.0 eq.) was added and the reaction was performed under 5 bar CO_2 for 1 h at the same temperature. The crude product was washed with distilled water (20 mL) and extracted with ethyl acetate (40 mL). The organic phase was washed with distilled water (4 × 30 ml), separated and dried over sodium sulfate. After the solvent was removed under reduced pressure, the product was purified *via* column chromatography (cyclohexane:ethylacetate/15:1). Yield: 30 %. ATR-IR (cm^{-1}) 3032 v_s(arom. =C-H), 2967 v_s(C-H), 2929 v_s(C-H), 2859 v_s(C-H), 1744 v(C=O), 1255 v_s(C−O), 1071 v(C−O). ^{1}H NMR (300 MHz, DMSO−d_6) δ (ppm): 7.37 (m, 5H), 5.12 (m, 2H), 4.08 (t, 2H), 1.57 (m, 2H), 1.23 (m, 10H), 0.83 (t, 3H). ^{13}C NMR (75 MHz, DMSO−d_6) δ (ppm): 154.84, 135.53, 128.40, 128.11, 128.05, 68.69, 67.75, 31.17, 28.34, 25.03, 21.69, 13.78. Exact mass $(M+Na)^+$ *m/z* 287.16. Obtained (ESI-MS) *m/z* 287.16.
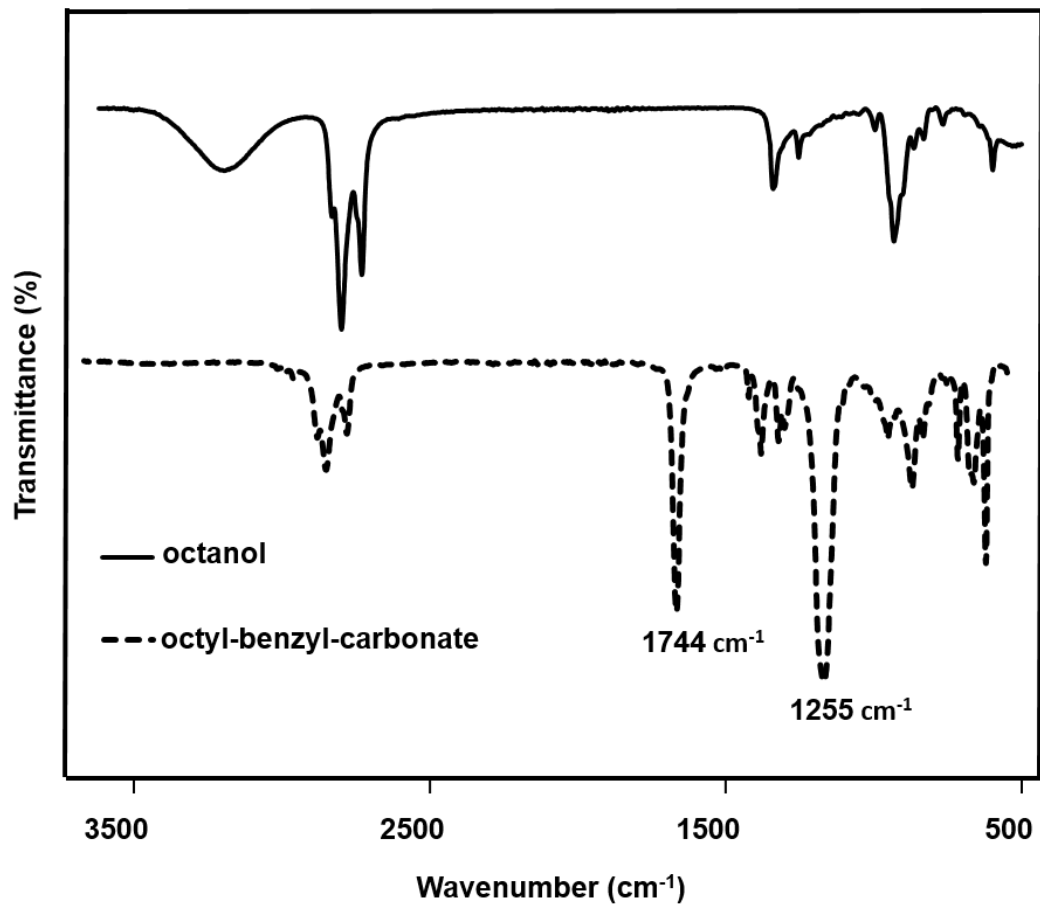
Figure 52: ATR-IR of octyl-benzyl-carbonate
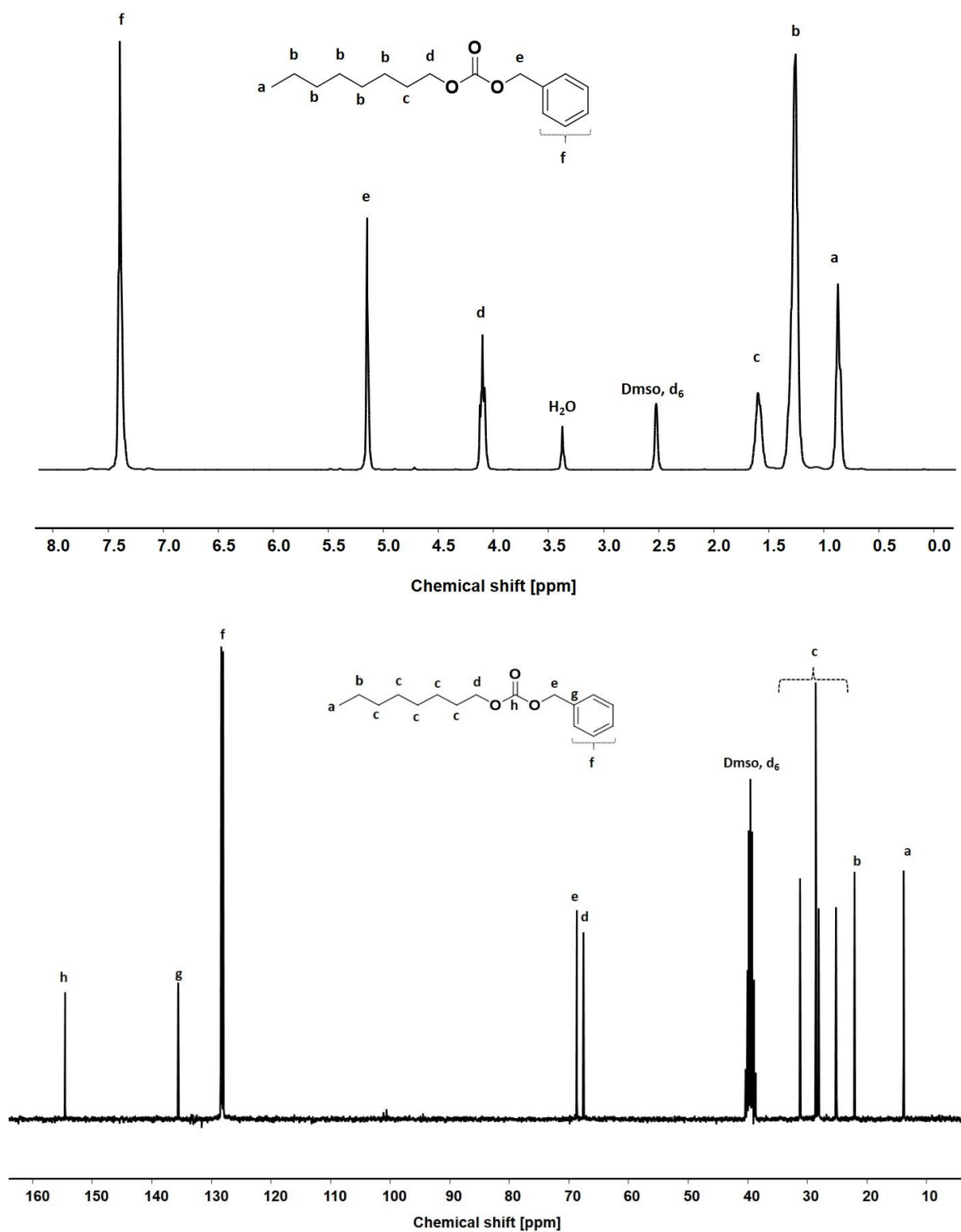
Figure 53: ¹H (top) and ¹³C (bottom) NMR of octyl-benzyl-carbonate.

Synthesis of cellulose benzyl carbonate

3 wt.% of microcrystalline cellulose (0.15 g, 0.93 mmol, 1.0 eq.) was agitated in DMSO (5 mL), followed by addition of DBU (2.8 mmol, 0.42 g, 3.0 eq. per anhydroglucose unit, AGU). The reaction mixture was transferred to a CO_2 pressure reactor where CO_2 was applied at 5 bar for 15 min at 30 °C leading to complete solubilization of cellulose. Thereafter, benzyl bromide (4.6 mmol, 0.79 g, 5.0 eq. per AGU) was added and the reaction allowed to run under 5 bar CO_2 for 1 h at 30 °C. After the reaction, the homogeneous reaction mixture was precipitated in distilled water (100 mL). The precipitate was filtered, washed with distilled water (2 × 50 mL) and methanol (2 × 50 mL). The obtained precipitate was then dried at 60 °C under vacuum for 24 h to obtain the desired product as a white powder. Yield: 0.16 g. ATR-IR: (cm^{-1}) 3395 v(O−H), 3026 v(arom. =C-H), 2884 v_s(C-H), 1740 v(C=O) of carbonate, 1256 v(C−O), 1023 v(C−O) glycopyranose of cellulose. ^{1}H NMR (400 MHz, DMSO−d_6, 80 °C) δ(ppm): 7.38 (br, 5H), 5.17 (br, 2H), 5.04-3.12 (br, AGU, 7H). ^{13}C NMR (100 MHz, DMSO−d_6, 80 °C) δ (ppm): 153.98, 135.10, 128.08, 127.84, 127.57, 102.40, 79.66, 79.15, 74.71, 74.48, 74.19, 72.88, 71.87, 68.74, 60.24.

Synthesis of cellulose methyl carbonate

3 wt.% of microcrystalline cellulose (0.15 g, 0.93 mmol, 1.0 eq.) was agitated in DMSO (5 mL), followed by addition of DBU (2.8 mmol, 0.42 g, 3.0 eq. per AGU). The reaction mixture was transferred to a CO_2 pressure reactor where CO_2 was applied at 5 bar for 15 minutes at 30 °C leading to complete solubilization of cellulose. Methyl iodide (4.6 mmol, 0.66 g, 5.0 eq. per anhydroglucose unit, AGU) was then added and the reaction allowed to run under 5 bar CO_2 for 1 h at 30 °C. After reaction, the homogeneous reaction mixture was precipitated in distilled water (100 mL). The precipitate was filtered, washed with distilled water (2 × 50 mL) and methanol (2 × 50 mL). Afterwards, the precipitate was dried at 60 °C under vacuum for 24 h to obtain the desired product as a white powder. Yield: 0.14 g. ATR-IR (cm^{-1}) 3392 v(O−H), 2895 v_s(C-H), 1740 v(C=O) of carbonate, 1266 v(C−O), 1020 v(C−O) glycopyranose of cellulose.

^{1}H NMR (400 MHz, DMSO−d_6, 80 °C) δ (ppm): 5.15-3.19 (br, AGU, 7H), 3.73 (br, 3 CH_3). ^{13}C NMR (100 MHz, DMSO−d_6, 80 °C) δ (ppm): 154.59, 154.24, 102.40, 79.65, 79.22, 74.71, 74.48, 72.87, 71.83, 60.23, 54.32, 54.02, 48.22.

Characterization of synthesized cellulose carbonate
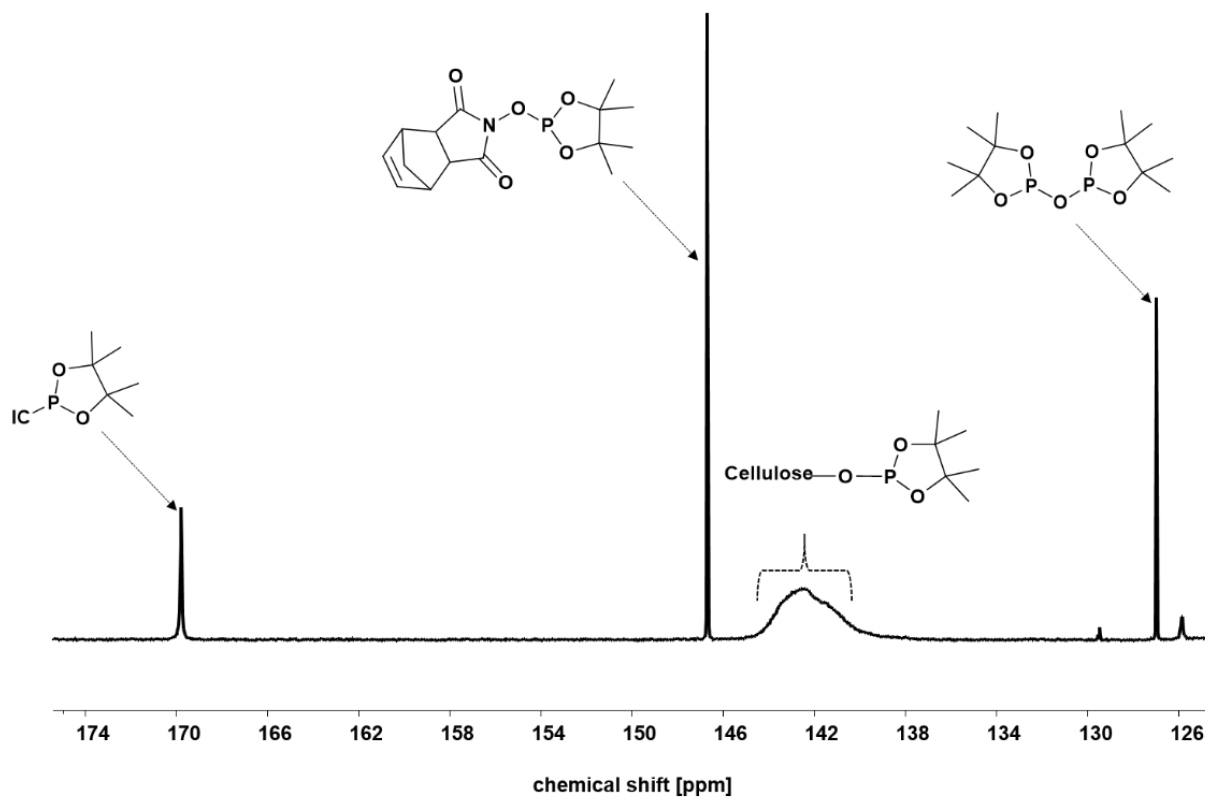
Figure 54: ^{31}P NMR of cellulose- benzyl-carbonate for DS determination.
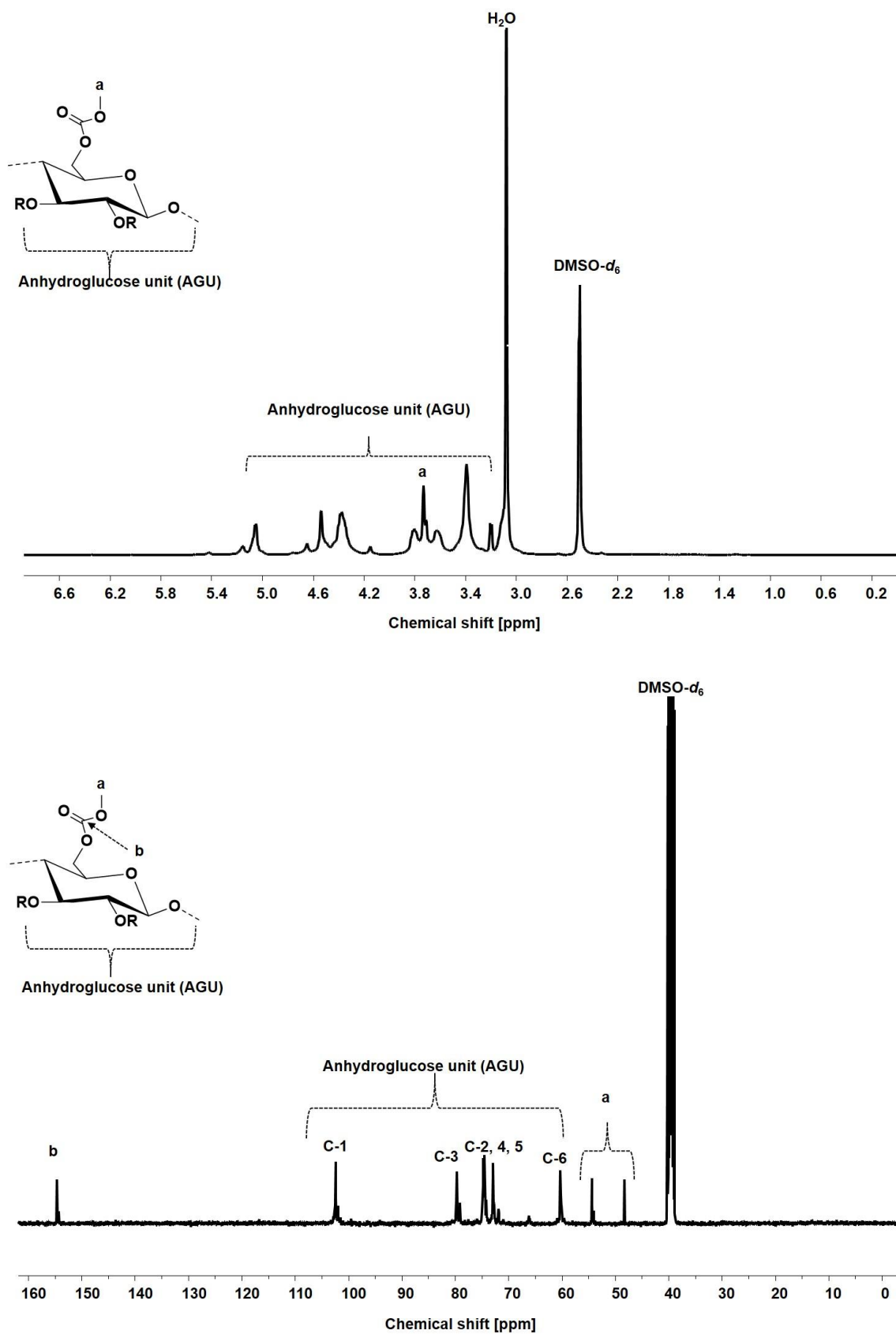
Figure 55: ^1H (top) and ^{13}C (bottom) NMR of cellulose- methyl-carbonate measured in DMSO (d6) at 80 °C.

8.4 Experimental procedures for Chapter 5

General procedure for cellulose aerogel preparation from the CO_2 switchable solvent system.

Cellulose (0.25 g, 1.5 mmol of anhydroglucose unit, 5 wt. %) was stirred in DMSO (5 mL) followed by addition of the super base (DBU = 0.7 g, TMG = 0.53 g DBN = 0.57 g; 4.5 mmol, 3 eq. per anhydroglucose unit). The cloudy suspension was transferred to a steel pressure reactor, where 5 bar of CO_2 was applied at 30 °C (40 °C for DBN and TMG) for 15 min. The obtained clear cellulose solution was transferred to a cylindrical-shaped glass mold (diameter 2.2 cm). 30 mL of the corresponding anti-solvent (water, methanol, ethanol, or isopropanol) was added slowly from the top and allowed to coagulate over a period of 24 h. Next, the anti-solvent was decanted and changed repeatedly until it contained no sign of DMSO or super base (from IR spectroscopy). The wet-precursors now filled with the anti-solvent (if different from water) was exchanged to water to allow for freeze-drying. The samples were frozen using liquid N_2 before being placed under a freeze-dryer for 24 h. The aerogel obtained was then stored inside a vacuum desiccator containing P_4O_{10} as a water absorbent prior to further characterization.

Density measurement

The density (apparent or bulk) of the samples was estimated gravimetrically by taking the ratio of the weight of the samples to their measured volume. An average of 2-4 samples for the same formulation was considered.

Pore size estimation of aerogels

The pore size of the aerogels was estimated from SEM data using ImageJ software by taking the average of sixty randomly selected pore sizes.

Solvent recovery

The study of solvent recovery was performed using methanol as the anti-solvent for coagulation after cellulose solubilization in the DBU-DMSO-CO_2 solvent system. After coagulation was complete, the wet sample was repeatedly washed using methanol, and the methanol was recovered quantitatively *via* rotary evaporation. The remaining fraction in the flask containing DMSO, DBU and DBUH$^+$ was extracted with

cyclohexane. The obtained cyclohexane and DMSO-rich phases were separated. The cyclohexane phase was subjected to the rotary evaporator (45 °C, 200 mbar) leading to a quantitative recovery of cyclohexane, whereas pure DBU remained in the flask. DMSO was recovered from the DMSO-rich phase through vacuum distillation (90 °C, 25 mbar). This way, a separation from the remaining $DBUH^+$ (alongside HCO_3^- from possible reaction between water present in DMSO and CO_2) that could not be extracted using cyclohexane was achieved. The recovered DMSO (recovery yield 90 %) and DBU (recovery yield 60 %) could be used for new cellulose solubilization without any observed difference in cellulose dissolution compared to new reactants.

Effect of coagulating solvent and super base on apparent density of cellulose aerogel
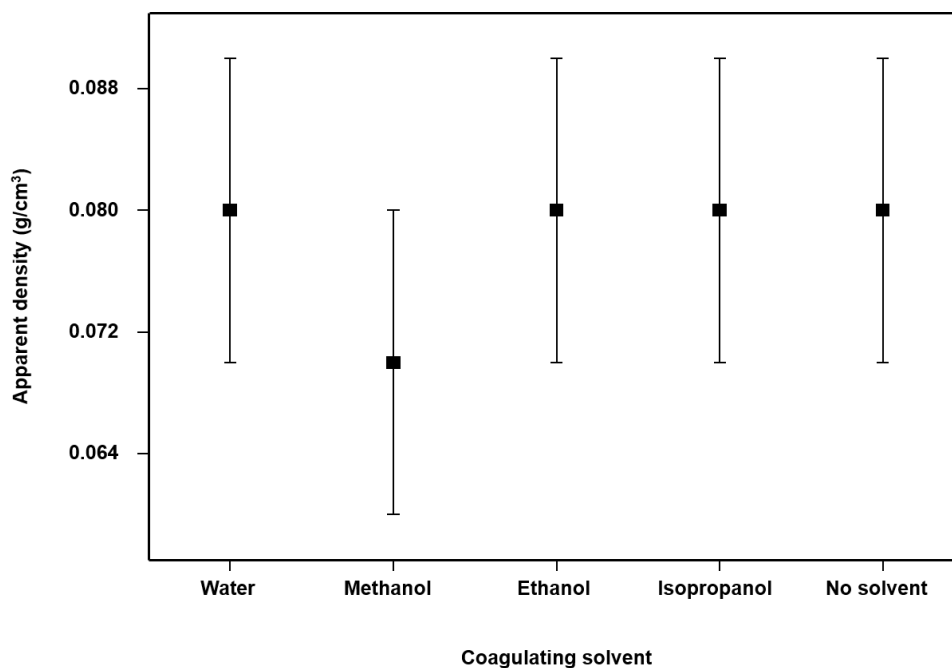
Figure 56: Effect of coagulating solvent on the apparent density of cellulose aerogel using 5 wt.% MC and DBU as a super base.
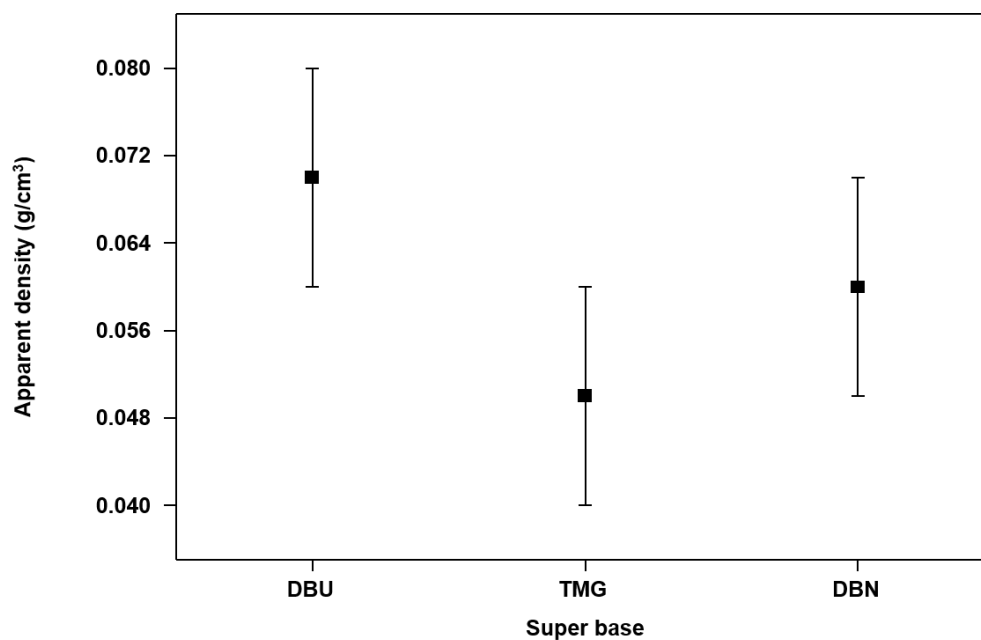
Figure 57: Effect of the super base on the apparent density of cellulose aerogel using 5 wt.% MCC and methanol coagulation.

Morphology studies via SEM of cellulose aerogels under various processing conditions.

Figure 58: SEM image of cellulose aerogel from freeze-drying (using 7 wt.% MCC, DBU as a super base and water coagulation.
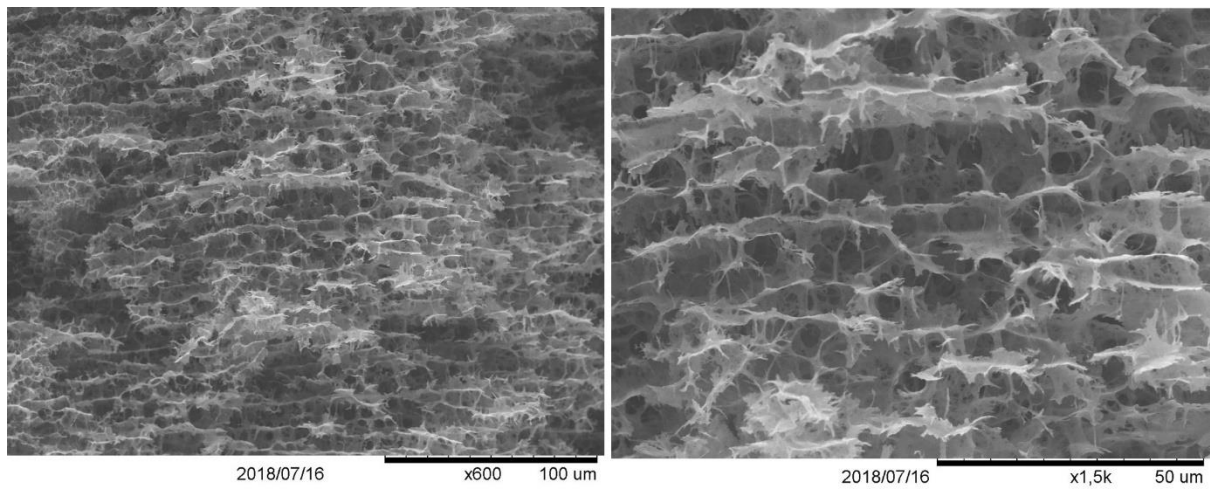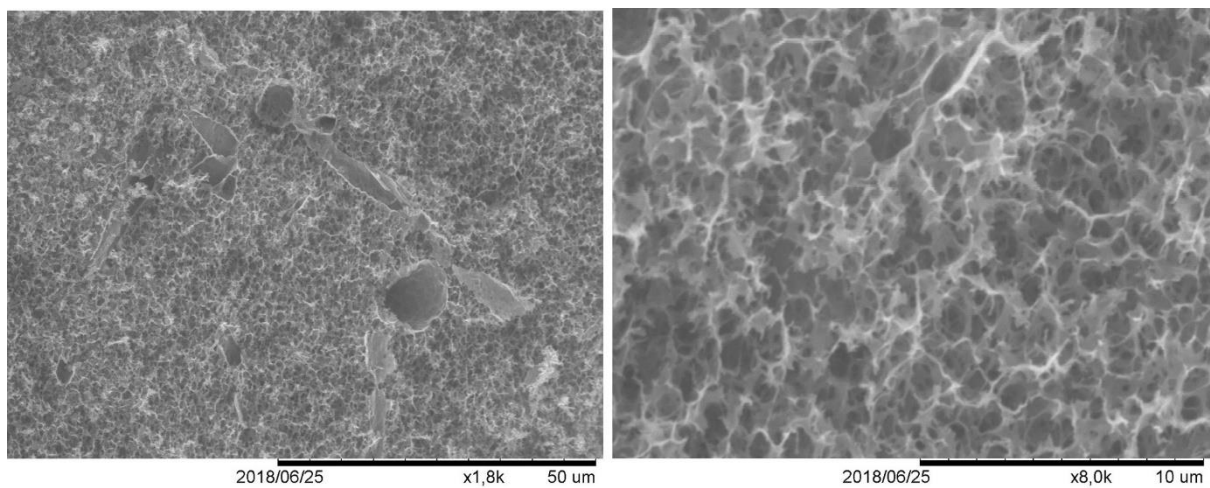

Figure 59: SEM image of cellulose aerogel from freeze-drying (using 10 wt.% MCC, DBU as super base and water coagulation.
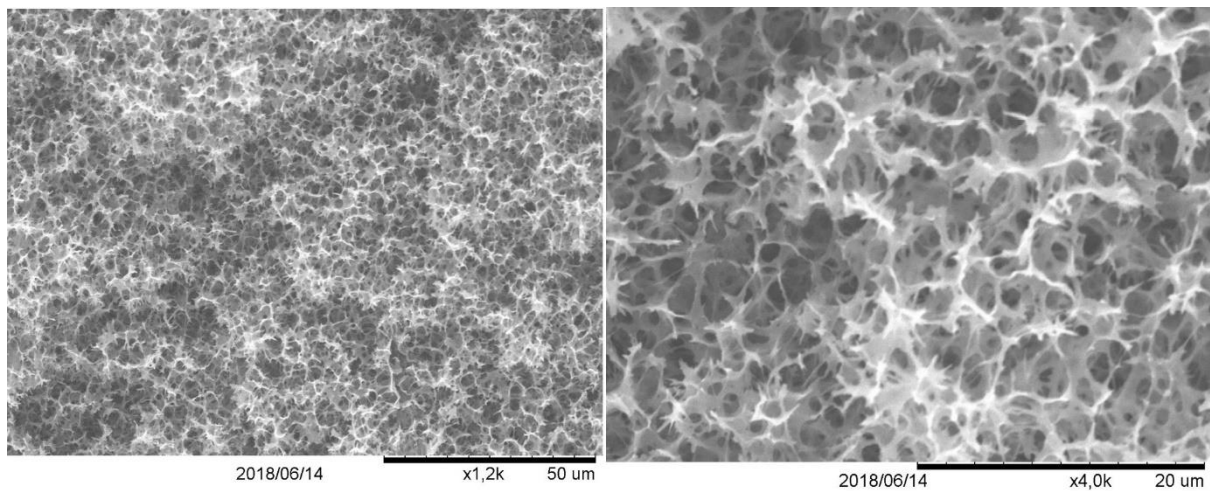
Figure 60: SEM image of cellulose aerogel from freeze-drying (using 5 wt.% MCC, DBU as super base and methanol coagulation.

Figure 61: SEM image of cellulose aerogel from freeze-drying (using 7 wt.% MCC, DBU as super base and methanol coagulation.

Figure 62: SEM image of cellulose aerogel from freeze-drying (using 10 wt.% MCC, DBU as super base and methanol coagulation.

Figure 63: SEM image of cellulose aerogel from freeze-drying (using 5 wt.% MCC, DBU as super base and ethanol coagulation.

Figure 64: SEM image of cellulose aerogel from freeze-drying (using 5 wt.% MCC, DBU as super base and isopropanol coagulation.

Figure 65: SEM image of cellulose aerogel from freeze-drying (using 5 wt.% MCC, TMG as super base and methanol coagulation.

Figure 66: SEM image of cellulose aerogel from freeze-drying (using 5 wt.% MCC, DBN as super base and methanol coagulation.

Figure 67: SEM image of cellulose aerogel from freeze-drying (using 3 wt.% CP, DBU as super base and water coagulation.

Figure 68: SEM image of cellulose aerogel from freeze-drying (using 3 wt.% CP, DBU as super base and ethanol coagulation.

Effect of coagulating solvent and super base on pore size of cellulose aerogel
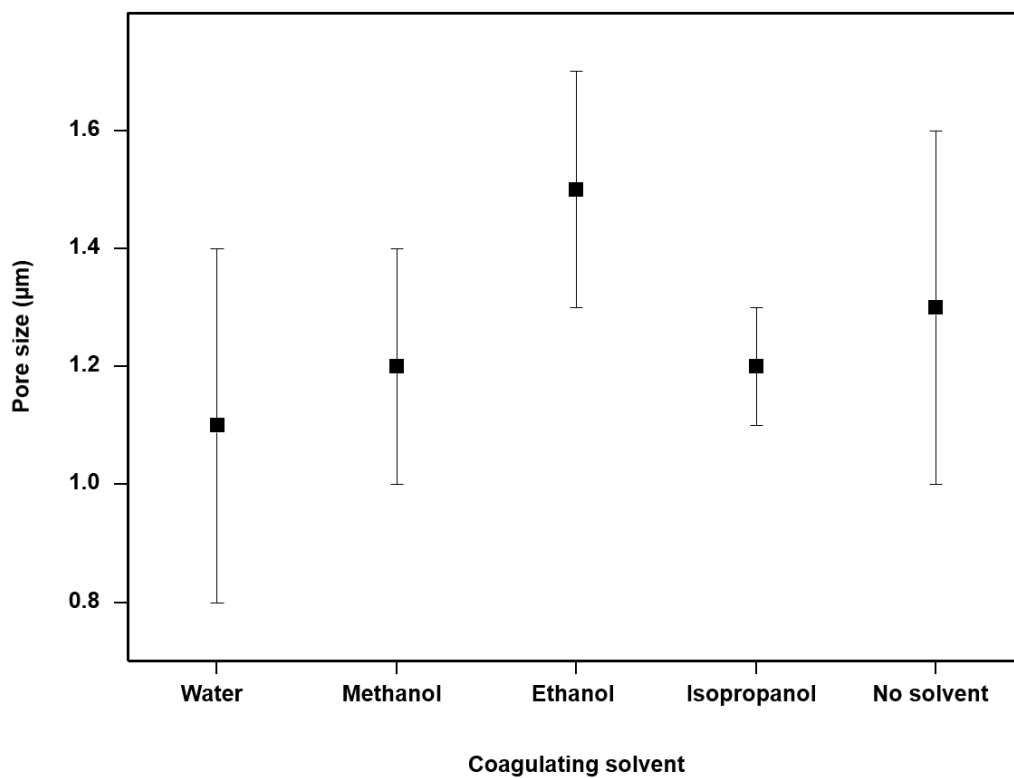
Figure 69: Effect of coagulating solvent on the pore size of cellulose aerogel using 5 wt.% MCC and DBU as a super base.
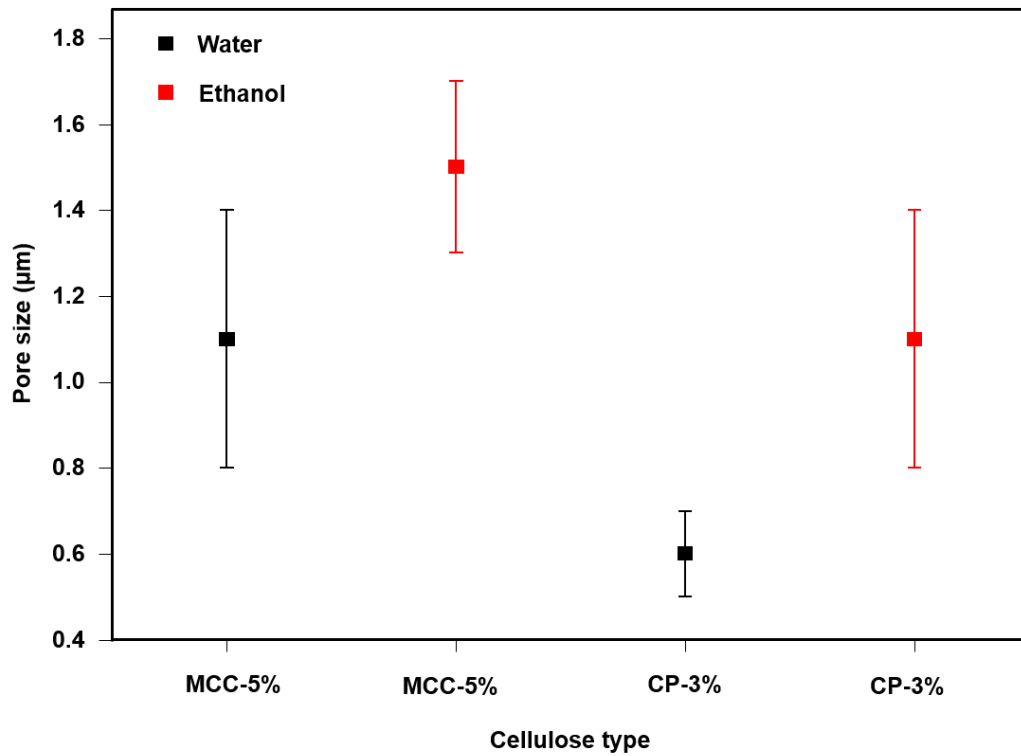
Figure 70: Effect of cellulose type and coagulating solvent on the pore size of cellulose aerogel using DBU as a super base.
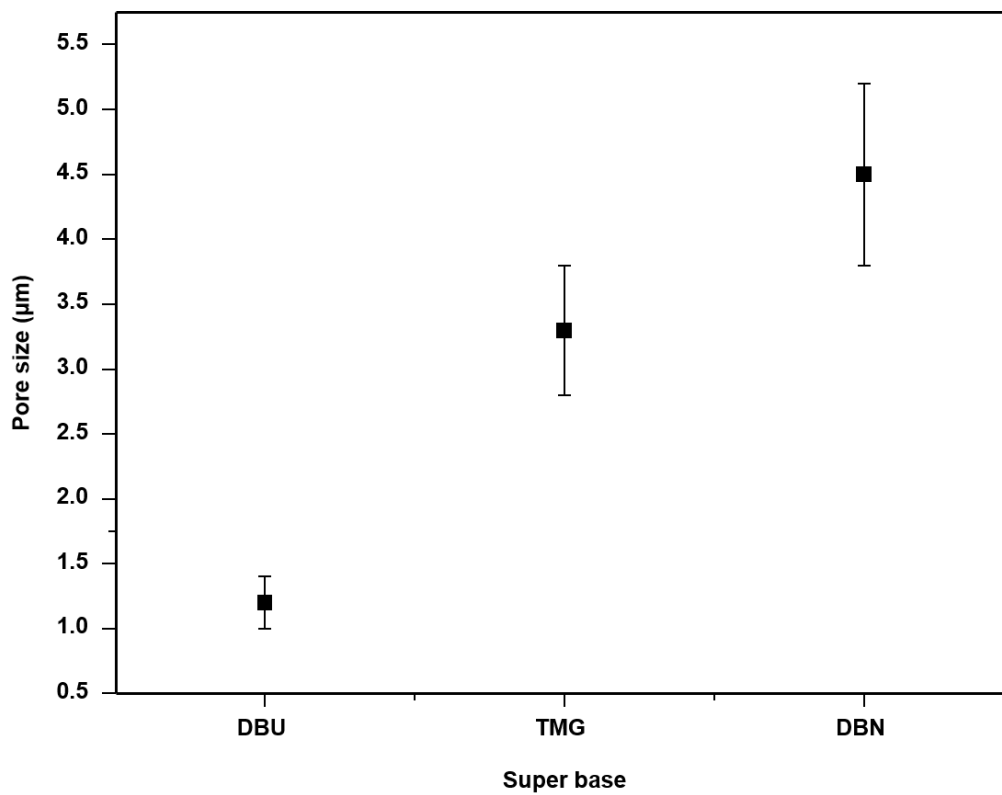

Figure 71: Effect of the super base on the pore size of cellulose aerogel using 5 wt.% MCC and methanol coagulation.

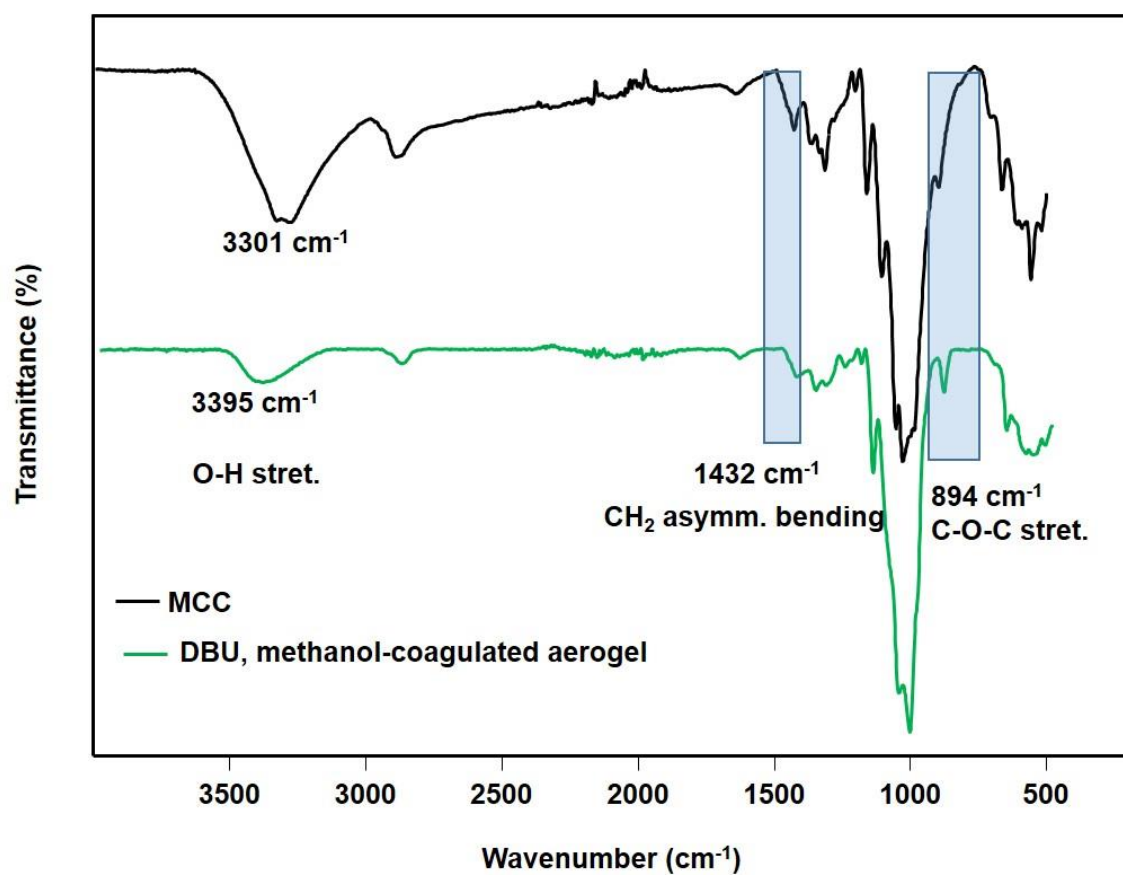**ATR-IR spectra comparison between native MCC and cellulose aerogel**

Figure 72: ATR-IR spectra comparison between MCC and cellulose aerogel from freeze-drying (using 5 wt.% MCC, DBU as super base and methanol coagulation.
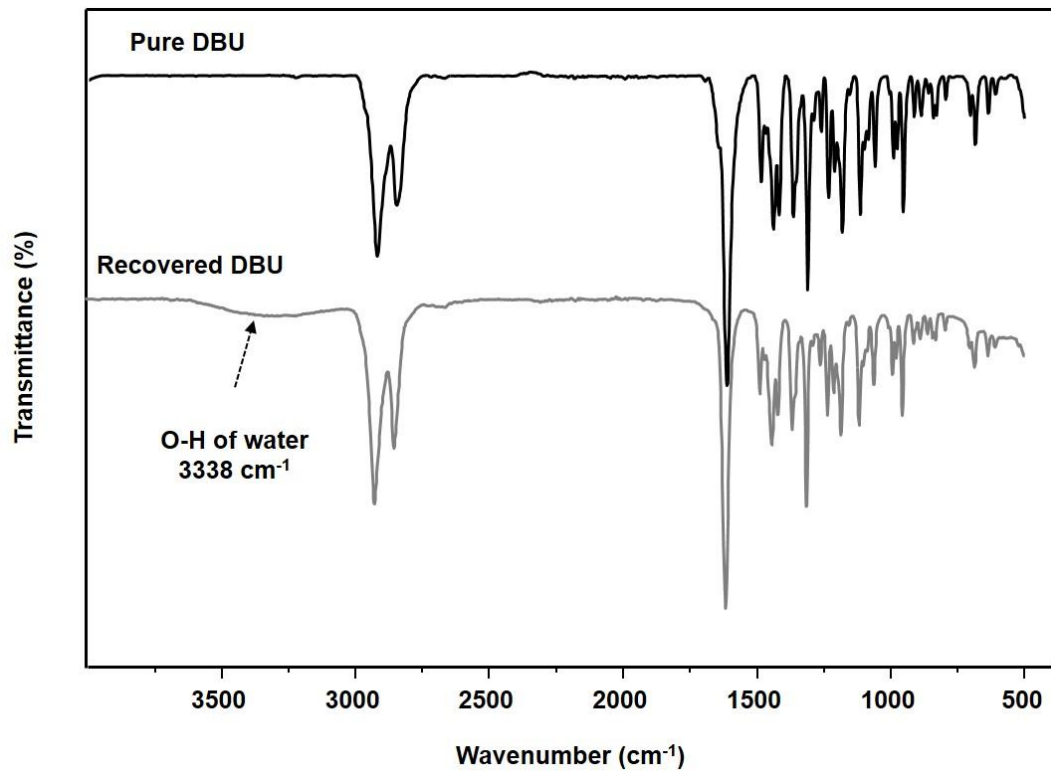
FT-IR spectra comparison between pure and recovered DBU and DMSO

Figure 73: ATR-IR spectra comparison between pure and recovered DBU (using 5 wt.% MCC, DBU as super base and methanol coagulation).
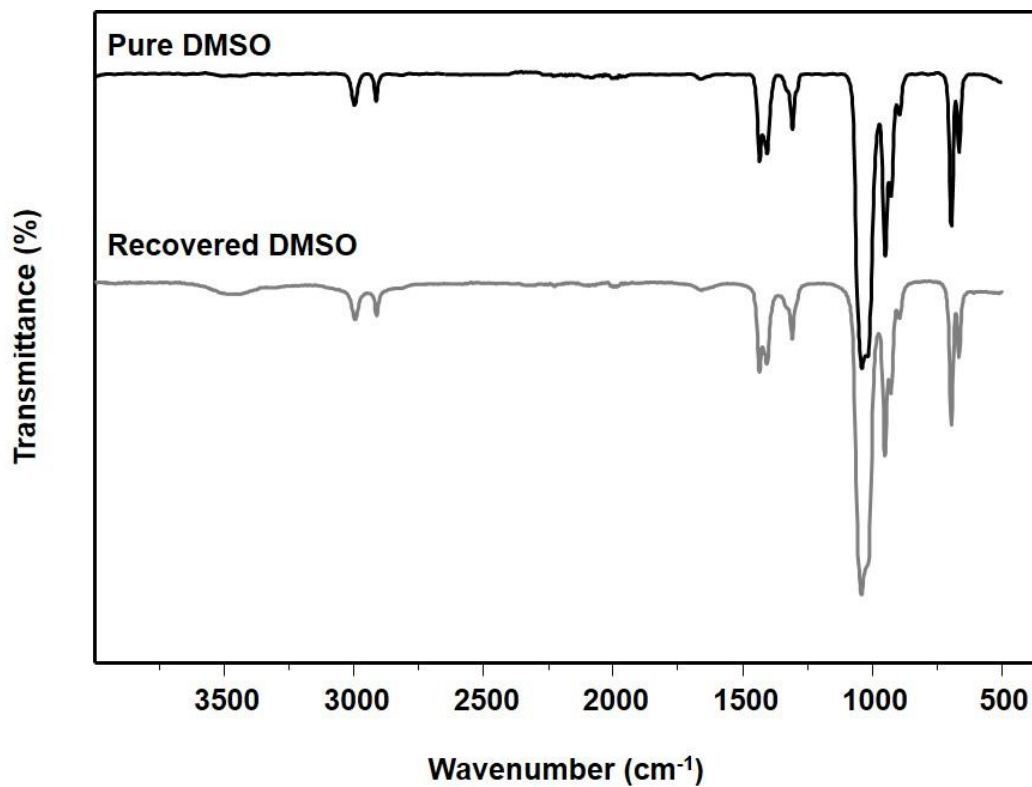

Figure 74: ATR-IR spectra comparison between pure and recovered DMSO (using 5 wt.% MCC, DBU as super base and methanol coagulation).

8.5 Experimental procedure for Chapter 6.1

General procedure for the synthesis of fatty acid cellulose esters (FACEs)

Cellulose (0.25 g, 1.5 mmol, 5 wt.%) was stirred in DMSO (5 mL) followed by addition of DBU (0.7 g, 4.6 mmol, 3 eq. per anhydroglucose unit). The cloudy suspension was transferred to a steel pressure reactor, where 5 bar of CO_2 was applied at 30 °C for 15 min., after which the obtained clear cellulose solution was transferred to a round bottom flask. High oleic sunflower oil (3 eq. triglycerides per AGU, 4.0 g, 5 mmol) was added, stirred vigorously and the reaction was performed at 115 °C from 6 h to 24 h depending on the experiment. Afterwards, the obtained hot homogeneous mixture was added dropwise into 200 mL of isopropanol. The obtained precipitate was filtered and washed twice with isopropanol (2 × 100 mL). After filtration, the precipitate was solubilized in THF (10 mL) and re-precipitated in distilled water (250 mL) to remove any remaining DBU and DMSO. The final precipitate obtained after filtration was dried under vacuum at 60 °C for 24 h leading to a white fibrous material as final product. The same procedure was employed for the other cellulose sources (filter paper and cellulose pulp). Yields obtained ranged from 65 to 80 %.

ATR-IR: $v(cm^{-1})$ = 3466-3395 v(O−H), 3004 v(=C-H), 2921-2884 v_s(C-H), 1740 v(C=O) of esters, 1160 v(C−O), 1025-1050 v(C−O) glycopyranose of cellulose. ^{1}H NMR (400 MHz, DMSO−d_6, 90 °C, 1024 scans) δ (ppm) = 5.34 (br, 2H), 5.24-3.01 (m, AGU, 7H), 2.75 (m, 2H), 2.31 (m, 2H), 2.0 (m, 4H), 1.55 (m, 2H), 1.28 (m, 28H), 0.87 (m, 3H). ^{13}C NMR (100 MHz, DMSO−d_6, 90 °C, 6000 scans) δ (ppm) = 172.18, 129.22, 127.60, 102.41, 79.81, 74.50, 72.87, 60.22, 32.82, 30.80, 30.46, 28.69, 28.58, 28.37, 28.16, 26.22, 24.86, 23.99, 21.55, 13.33.

Procedure for FACEs film preparation

Fatty acid cellulose esters (FACEs) films were prepared by dissolving the products in pyridine or THF (3-4 wt.%) and casting the solution into Teflon plates (100 x 20 mm). The films were formed after the solvent evaporated at room temperature for at least 48 h to ensure complete removal of the solvent, followed by drying under vacuum at 30 °C for 5 h. Film thickness (0.04 to 0.06 mm) was measured using a digital Vernier caliper.

ATR-IR Optimization study of transesterification reaction on MCC using high oleic sunflower oil.
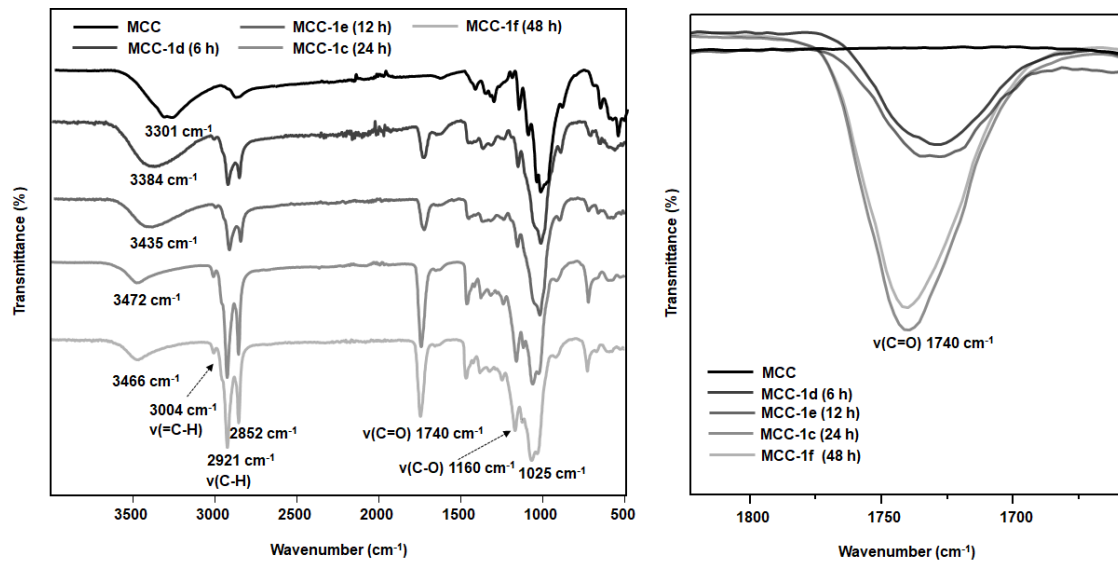

Figure 75: ATR-IR spectra of fatty acid cellulose esters (FACEs) at various reaction time: MCC-1d (6 h), MCC-1e (12 h), MCC-1c (24 h), MCC-1f (48 h). (5 wt.% MCC, 3 eq. high oleic sunflower oil/AGU cellulose, 115 °C).
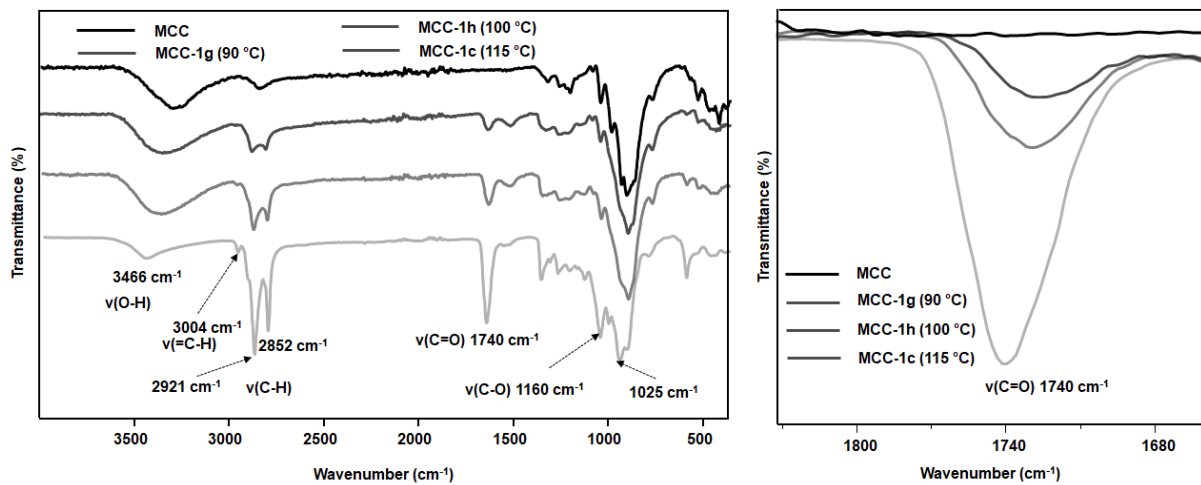

Figure 76: ATR-IR spectra of fatty acid cellulose esters (FACEs) at various reaction temperature: MCC- 1g (90 °C), MCC-1h (100 °C), MCC-1c (115 °C). (5 wt.% MCC, 3eq. high oleic sunflower oil/AGU cellulose, 24 h).
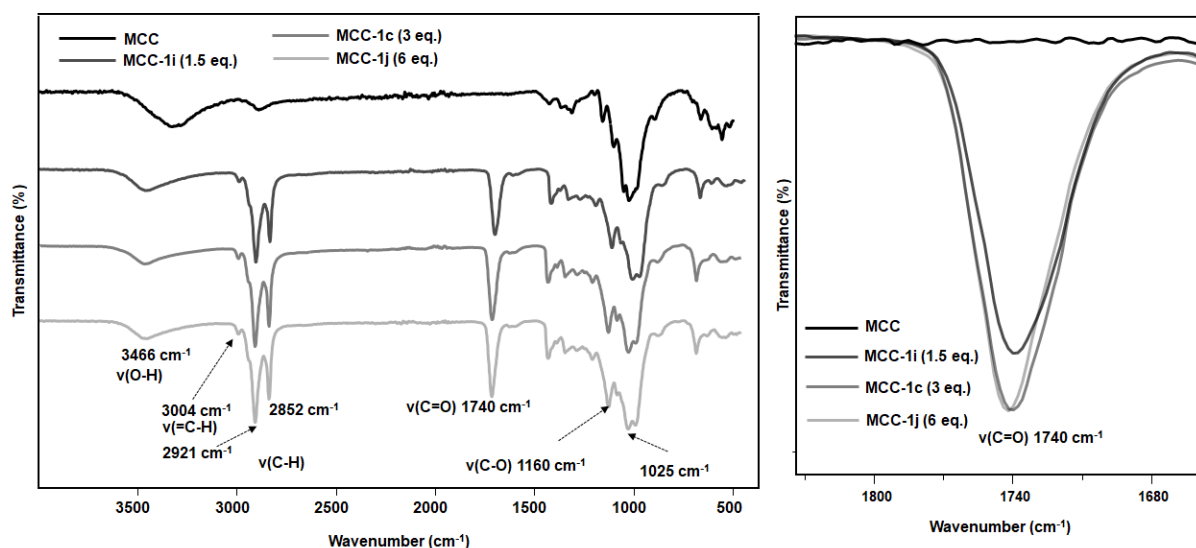
Figure 77: ATR-IR spectra of fatty acid cellulose esters (FACEs) at various high oleic sunflower oil equivalents: MCC-1i (1.5 eq./AGU), MCC-1c (3 eq./AGU), MCC-1j (6 eq./AGU). (5 wt.% MCC, 115 °C, 24 h).

^{31}P NMR spectra for DS determination of MCC-based FACEs upon variation of the reaction time and plant oil equivalents.
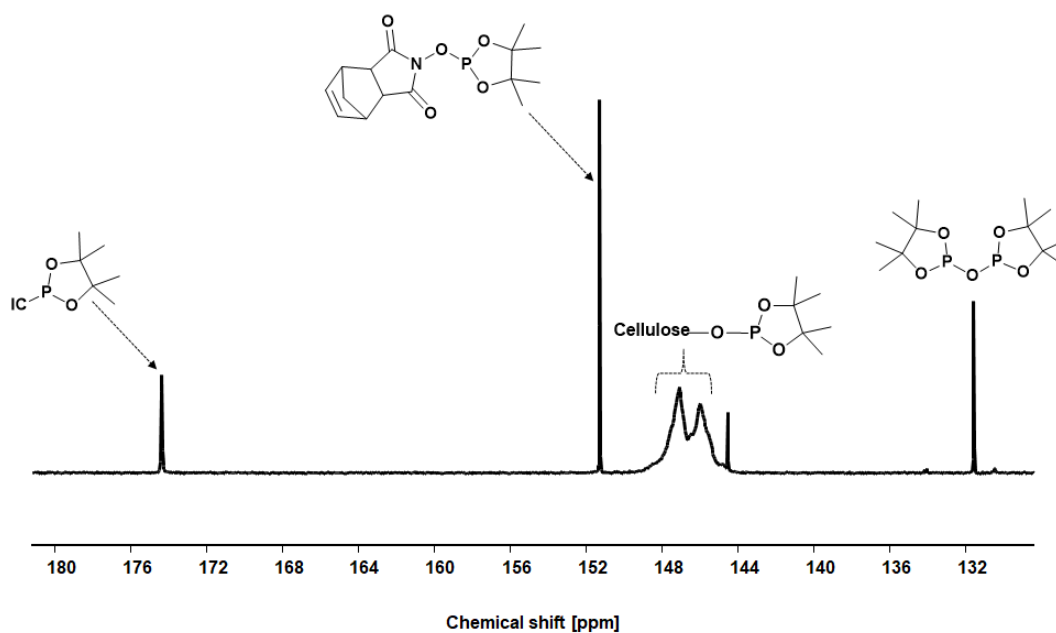

Figure 78: ^{31}P NMR (CDCl$_3$), 400 MHz, 1024 scans: determination of degree of substitution (DS) of fatty acid cellulose ester (MCC-1d). (5 wt.% MCC, 3 eq. high oleic sunflower oil/AGU, 115 °C, 6 h).

Figure 79: ^{31}P NMR (CDCl$_3$), 400 MHz, 1024 scans: determination of degree of substitution (DS) of fatty acid cellulose ester (MCC-1e). (5 wt.% MCC, 3 eq. high oleic sunflower oil/AGU, 115 °C, 12 h).

Figure 80: ^{31}P NMR (CDCl$_3$), 400 MHz, 1024 scans: determination of degree of substitution (DS) of fatty acid cellulose ester (MCC-1c). (5 wt.% MCC, 3 eq. high oleic sunflower oil/AGU, 115 °C, 24 h).

Figure 81: ^{31}P NMR (CDCl$_3$), 400 MHz, 1024 scans: determination of degree of substitution (DS) of fatty acid cellulose ester (MCC-1f). (5 wt.% MCC, 3 eq. high oleic sunflower oil/AGU, 115 °C, 48 h).
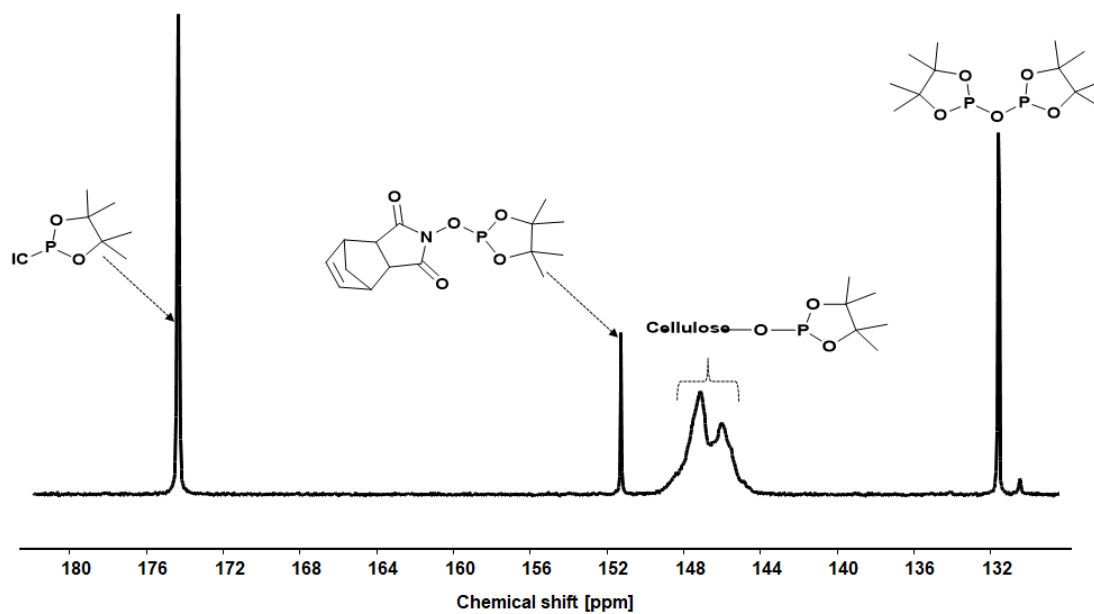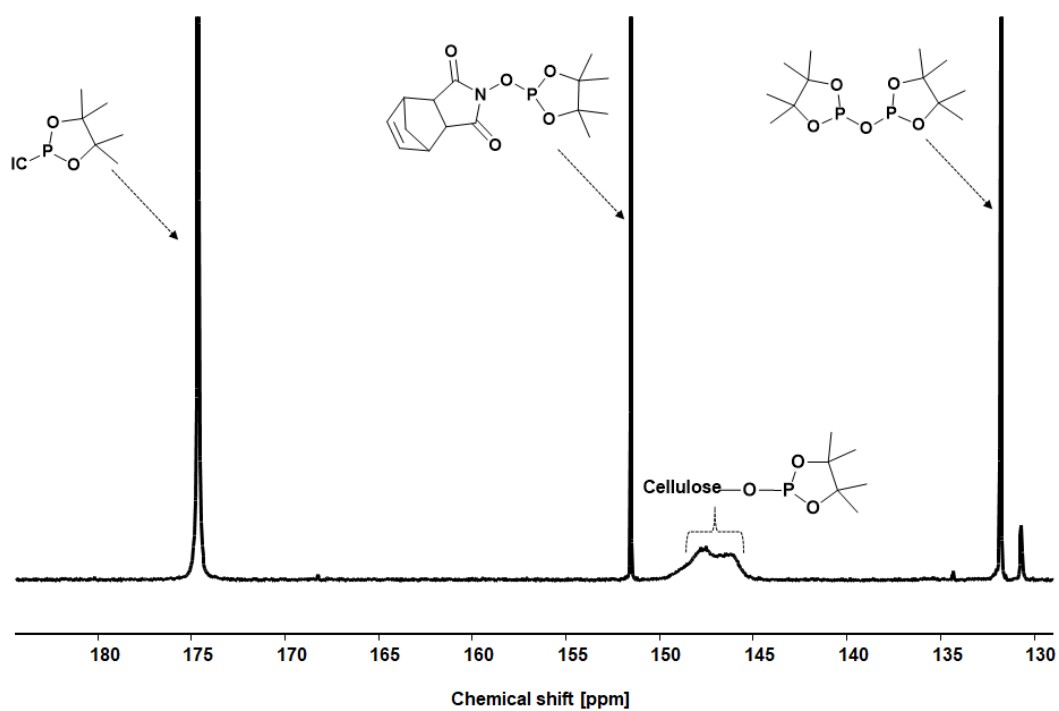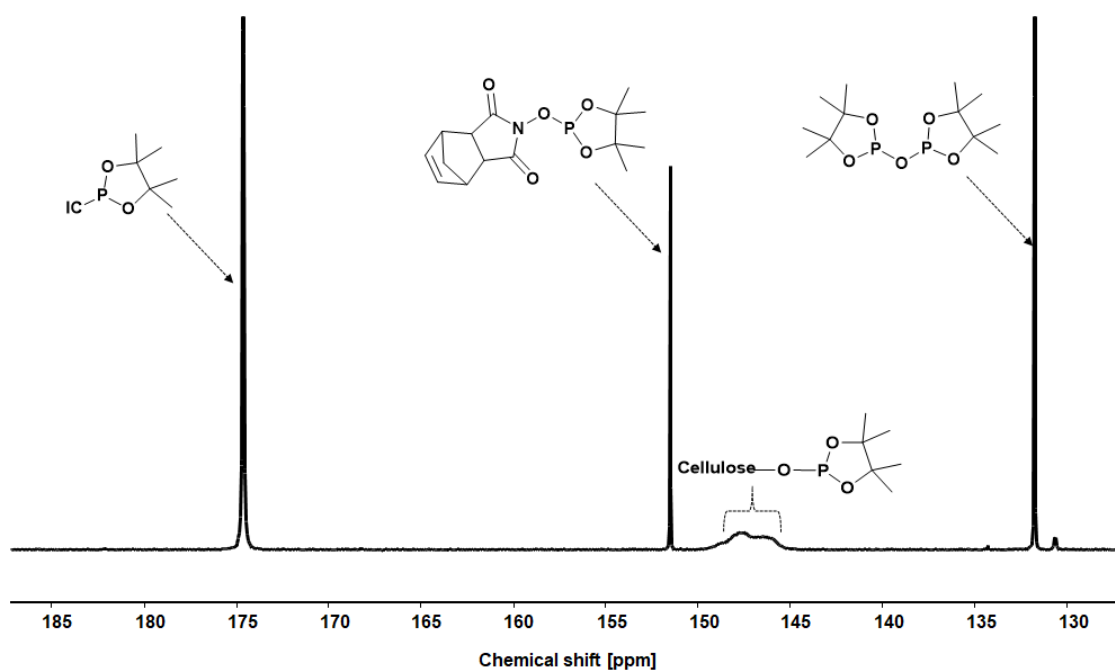

Figure 82: ^{31}P NMR (CDCl$_3$), 400 MHz, 1024 scans: determination of DS of fatty acid cellulose ester (MCC-1i). (5 wt. (%) MCC, 1.5 eq. high oleic sunflower oil/AGU, 115 °C, 24 h.

ATR-IR spectra of FACEs from FP and CP.
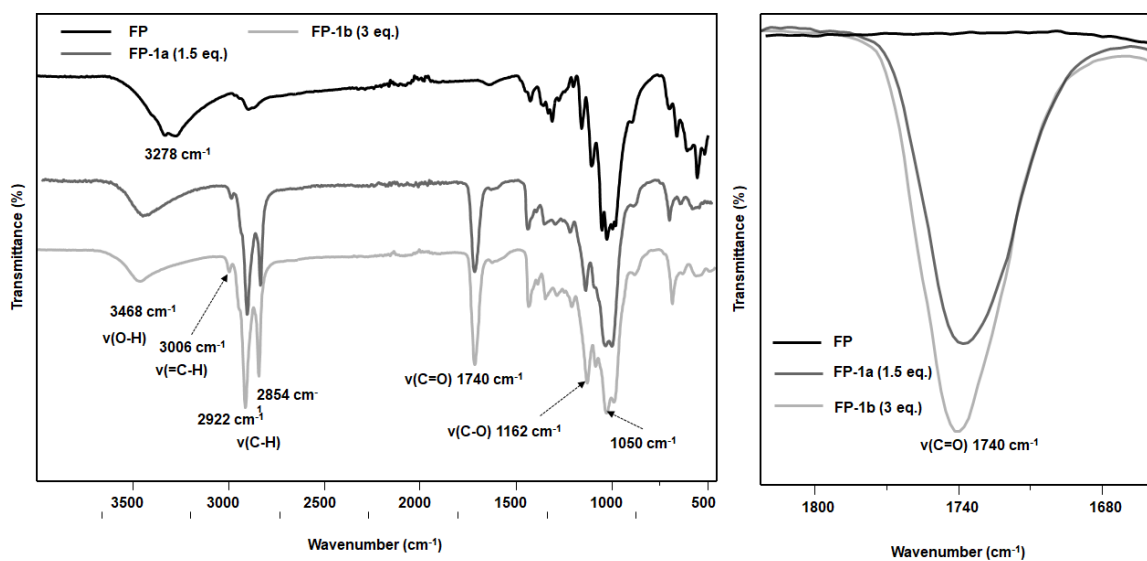
Figure 83: ATR-IR spectra of fatty acid cellulose esters (FACEs) at various high oleic sunflower oil equivalents: FP-1a (1.5 eq./AGU), FP-1b (3 eq./AGU, 5 wt.% FP, 115 °C, 24 h).
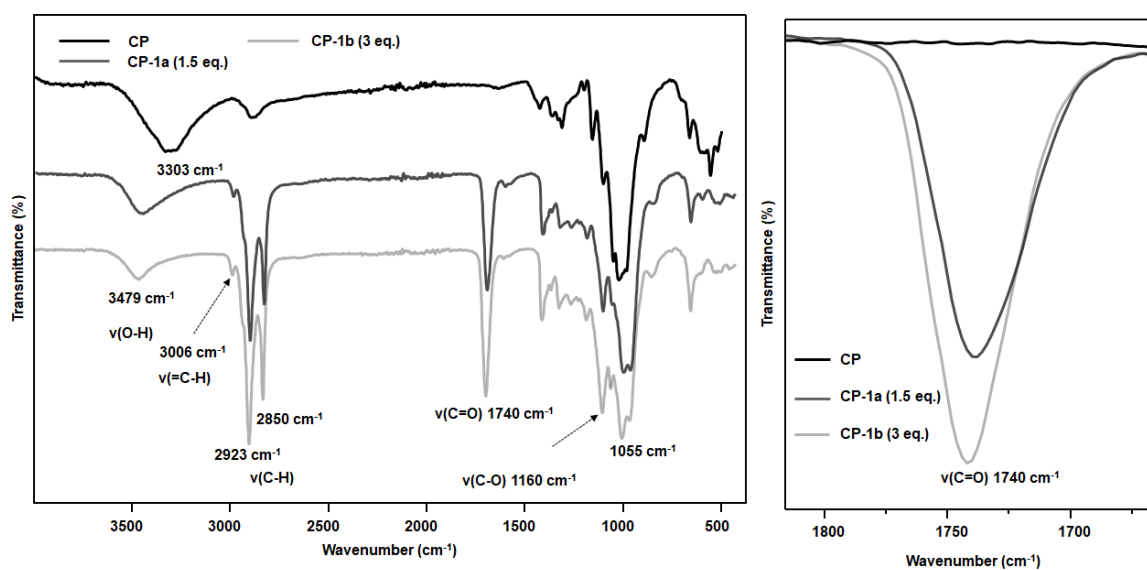
Figure 84: ATR-IR spectra of fatty acid cellulose esters (FACEs) at various high oleic sunflower oil equivalents: CP-1a (1.5 eq./AGU), CP-1b (3 eq./AGU, 5 wt.% CP, 115 °C, 24 h).

¹H and ¹³C NMR characterization of FACEs.

Figure 85: ¹H NMR (top, 400 MHz, 1024 scans at 50 °C) and ¹³C NMR (bottom, 100 MHz, 6000 scans at 50 °C) for fatty acid cellulose esters (FACE): MCC-1c. (5 wt.%, MCC, 3 eq. high oleic sunflower oil/AGU, 115 °C, 24 h, measured in THF, d_8.

Figure 86: ¹H NMR (top, 400 MHz, 1024 scans at 50 °C) and ¹³C NMR (bottom, 100 MHz, 6000 scans at 50 °C) for fatty acid cellulose esters (FACE): FP-1b. (5 wt.% FP, 3 eq. high oleic sunflower oil/AGU, 115 °C, 24 h, measured in THF, d₈.

Figure 87: ^{1}H NMR (top, 400 MHz, 1024 scans at 50 °C) and ^{13}C NMR (bottom, 100 MHz, 6000 scans at 50 °C) for fatty acid cellulose esters (FACE): CP-1b. (5 wt.% CP, 3 eq. high oleic sunflower oil/AGU, 115 °C, 24 h, measured in THF, d$_8$.

³¹P NMR spectra for DS determination of FP and CP-based FACEs

Figure 88: ³¹P NMR (CDCl₃), 400 MHz, 1024 scans :determination of degree of substitution (DS) of fatty acid cellulose esters (FACE): FP-1a. (5 wt.% FP, 1.5 eq. high oleic sunflower oil/AGU, 115 °C, 24 h).

Figure 89: ³¹P NMR (CDCl₃), 400 MHz, 1024 scans: determination of degree of substitution (DS) of fatty acid cellulose esters (FACE): FP-1b. (5 wt.% FP, 3 eq. high oleic sunflower oil/AGU, 115 °C, 24 h).
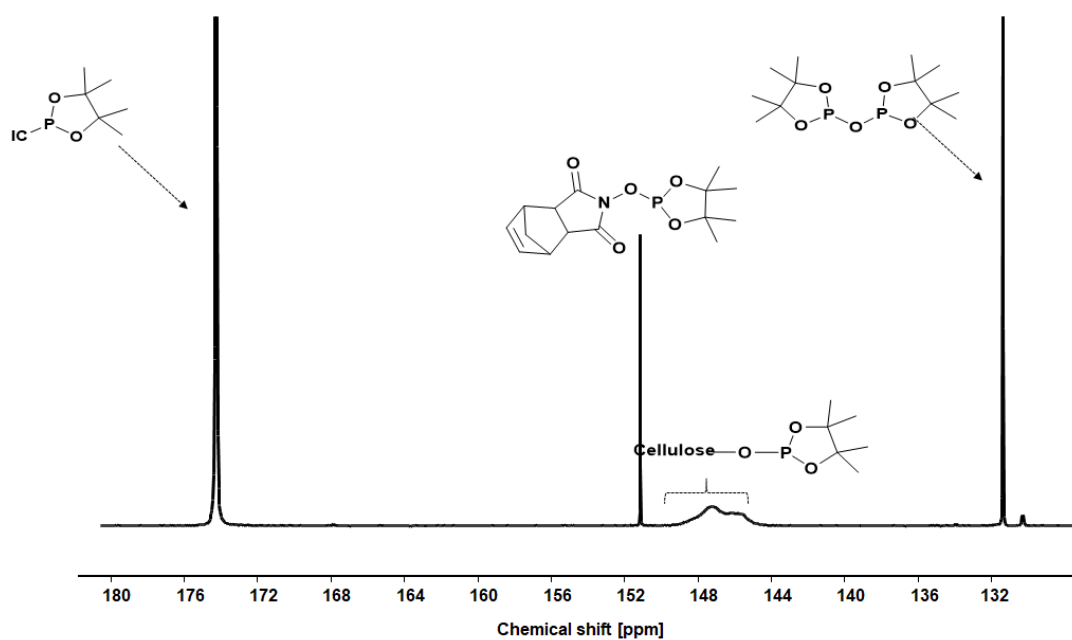
Figure 90: ^{31}P NMR (CDCl₃), 400 MHz, 1024 scans: determination of degree of substitution (DS) of fatty acid cellulose esters (FACE): CP-1a. (5 wt.% CP, 1.5 eq. high oleic sunflower oil/AGU, 115 °C, 24 h).

Figure 91: ^{31}P NMR (CDCl₃), 400 MHz, 1024 scans :determination of degree of substitution (DS) of fatty acid cellulose esters (FACE): CP-1b. (5 wt.% CP, 3 eq. high oleic sunflower oil/AGU, 115 °C, 24 h).

SEC traces (DMAc-LiBr) of lower DS (around 1.0) FACEs.
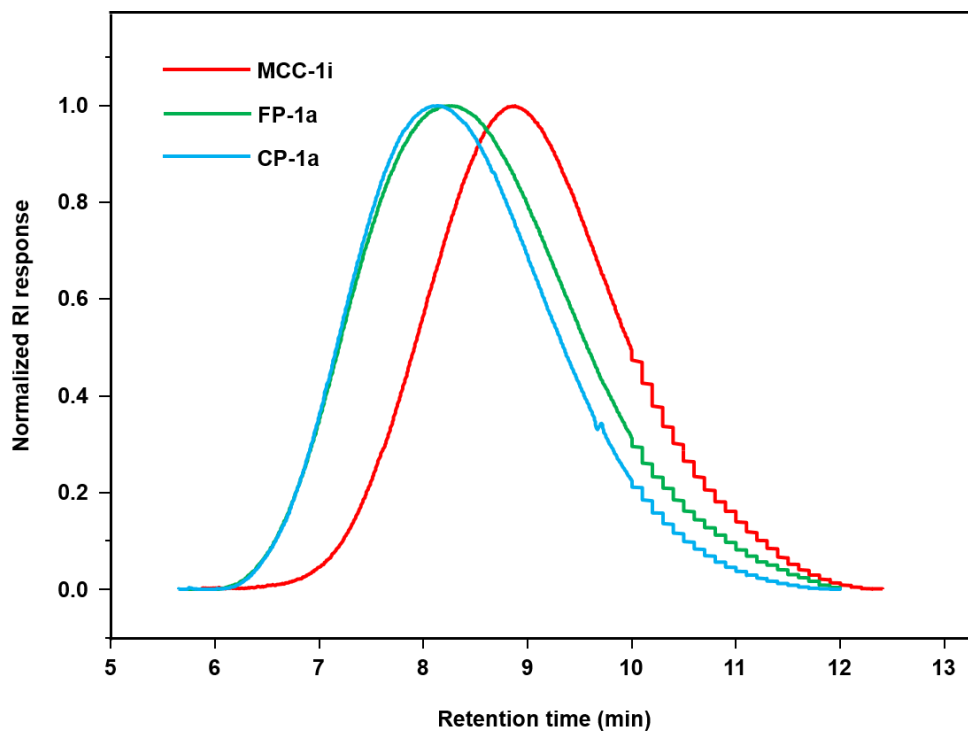
Figure 92: SEC traces (DMAc-LiBr) comparison of fatty acid cellulose esters (FACEs) from microcrystalline cellulose (MCC-1i; DS 1.06), cellulose filter paper (FP-1a; DS 1.02) and cellulose pulp (CP-1a; DS 1.08).

XRD patterns of FACEs of FP and CP.
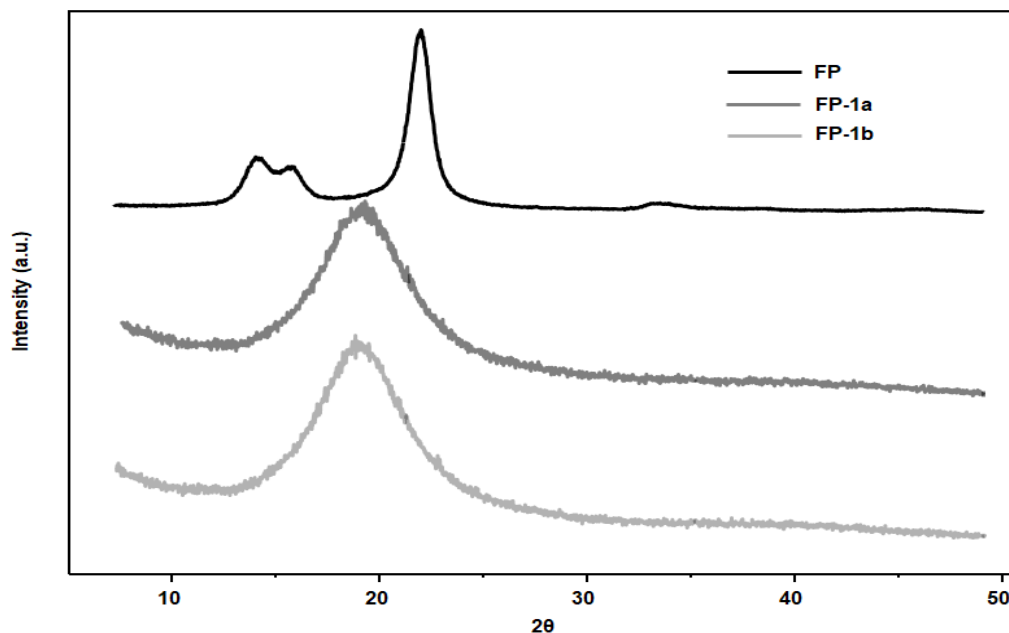
Figure 93: X-ray diffraction pattern of FP and resulting fatty acid cellulose esters (FACEs) (FP-1a, FP -1b) (5 wt.% FP, 24 h,115 °C).
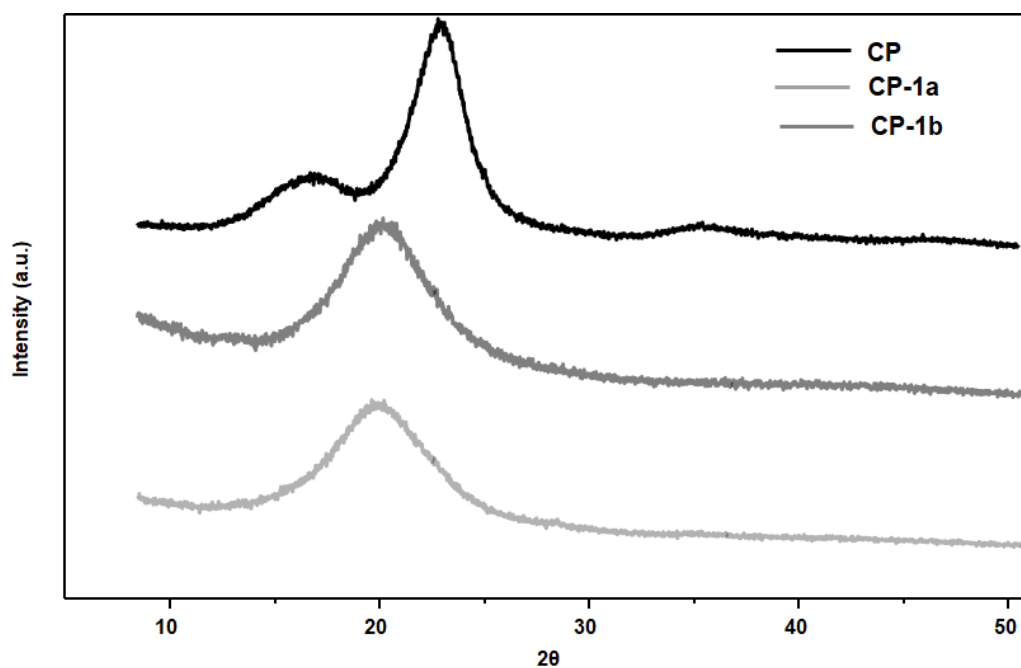
Figure 94: X-ray diffraction pattern of CP and resulting fatty acid cellulose esters (FACEs) (CP-1a, CP-1b) (5 wt.% CP, 24 h, 115 °C).

TGA analysis of FACEs of FP and CP.
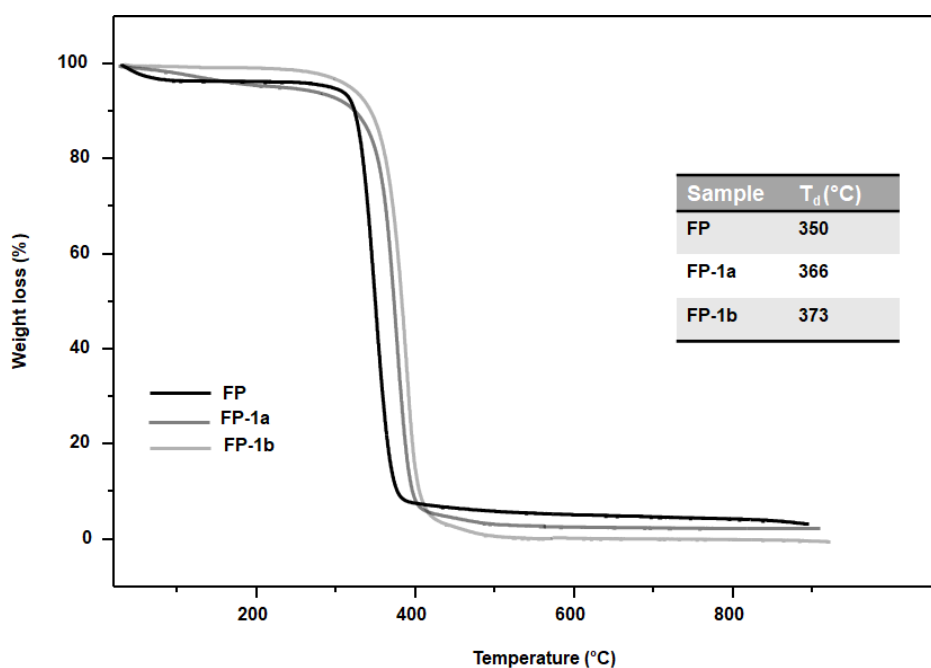
Sample	T_d (°C)
FP	350
FP-1a	366
FP-1b	373

Figure 95: Thermogravimetric analysis (TGA) of FP and resulting fatty acid cellulose esters (FACEs) (FP-1a, FP-1b) (5 wt.% FP, 24 h, 115 °C).
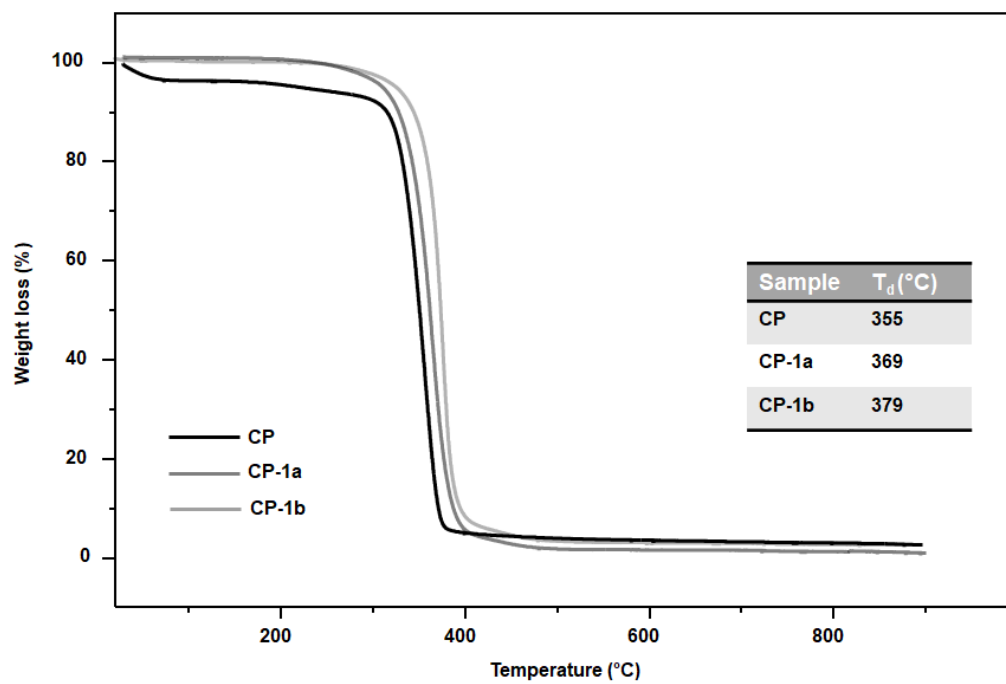
Figure 96: Thermogravimetric analysis (TGA) of CP and resulting fatty acid cellulose esters (FACEs) (CP-1a, CP-1b) (5 wt.% CP, 24 h, 115 °C).

8.6 Experimental procedures for Chapter 6.3

General procedure for the Ugi (4-CR) on succinylated filter paper

Succinylated filter paper (0.1 g, 0.24 mmol, DS: 2.64) was suspended in 2 mL of DMSO and allowed to stir at 50 °C to obtain a clear solution. Afterwards, the (2 eq. with respect to −COOH group, DS: 2.64) corresponding aldehyde (1.26 mmol), amine (1.26 mmol) and isocyanide (1.26 mmol) were added dropwise to the reaction mixture and allowed to stir for 48 h at 60 °C. Upon completion of reaction, the mixture was precipitated in vigorously stirring distilled water (100 mL), the obtained precipitate was washed further with distilled water (100 mL) followed by dissolving in THF (3 mL) and re-precipitated in *n*-hexane (100 mL). This was repeated at least twice to completely remove un-reacted starting materials. The obtained white precipitate was filtered and dried under vacuum at 60 °C, 24 h for further analysis. Yields were calculated from theoretical yields of the respective Ugi products

U1: Yield: 83 % ATR−IR (cm^{-1}): 3642−3132 mixtures of v(N−H) and v(O−H), 2961−2872 v_{as}(CH$_2$), v_s(CH$_2$), 1739 ester v(C=O), 1678, 1622 amide v(C=O), 1157 v(C−O) $^1$H NMR (500 MHz, THF−$d_8$) δ_H ppm: 7.14-7.35 (m, 5H), 6.50 (br, 1H), 4.43 (br, 1H), 3.48-3.55 (m, 3H), 3.10-5.42 (m, AGU, 7H), 2.62 (br, 4H), 1.69 (br, 2H), 1.08-1.38 (m, 14H), 0.88-0.99 (br, 3H). ^{13}C NMR (125 MHz, THF−d_8) δ_C ppm: 172.53, 169.42, 168.28, 143.80, 125.96-128.80, 73.30, 50.53, 50.16, 39.07, 31.85, 27.69-28.02, 20.19, 17.62, 13.08.

U2: Yield: 92 % ATR−IR (cm^{-1}): 3692−3146 mixtures of v(N−H) and v(O−H), 2958−2856 v_{as}(CH$_2$), v_s(CH$_2$), 1743 ester v(C=O), 1672, 1640 amide v(C=O) 1159 v(C−O) ^{1}H NMR (500 MHz, THF−d_8) δ_H ppm: 6.97 (br, 1H), 4.35 (br, 1H), 3.65 (br, 1H), 3.38 (br, 2H), 3.02−5.40 (m, AGU, 7H), 2.67 (br, 1H), 2.45 (br, 4H), 1.22-1.31 (m, 6H), 0.92-1.08 (br, 8H), 0.79-0.92 (m, 9H). ^{13}C NMR (125 MHz, THF−d_8) δ_C ppm: 173.03, 169.87, 168.87, 73.78, 48.77, 45.81, 33.52, 33.34, 32.54, 28.96, 27.84, 26.51, 21.01, 20.15, 19.43, 13.93.

U3: Yield: 89 % ATR−IR (cm^{-1}): 3612−3150 mixtures of v(N−H) and v(O−H), 2963−2872 v_{as}(CH$_2$), v_s(CH$_2$), 1745 ester v(C=O), 1670, 1642 amide v(C=O), 1162 v(C−O). ^{1}H NMR (500 MHz, THF−d_8) δ_H ppm: 7.31 (br, 1H), 4.39 (br, 1H), 3.29 (br, 2H), 3.00−5.40 (m, AGU, 7H), 2.63-2.10 (br, 5H), 1.53 (br, 2H), 1.28 (br,

11H), 0.92(br, 6H), 0.82 (br, 3H). ^{13}C NMR (125 MHz, THF−d_8) δ$_C$ ppm: 173.77, 173.02, 170.69, 73.71, 51.76, 50.99, 30.38, 29.89, 28.89, 28.94, 28.13, 27.83, 20.76, 20.27, 19.83.

ATR-IR spectra of Ugi 4-CR modified succinylated cellulose
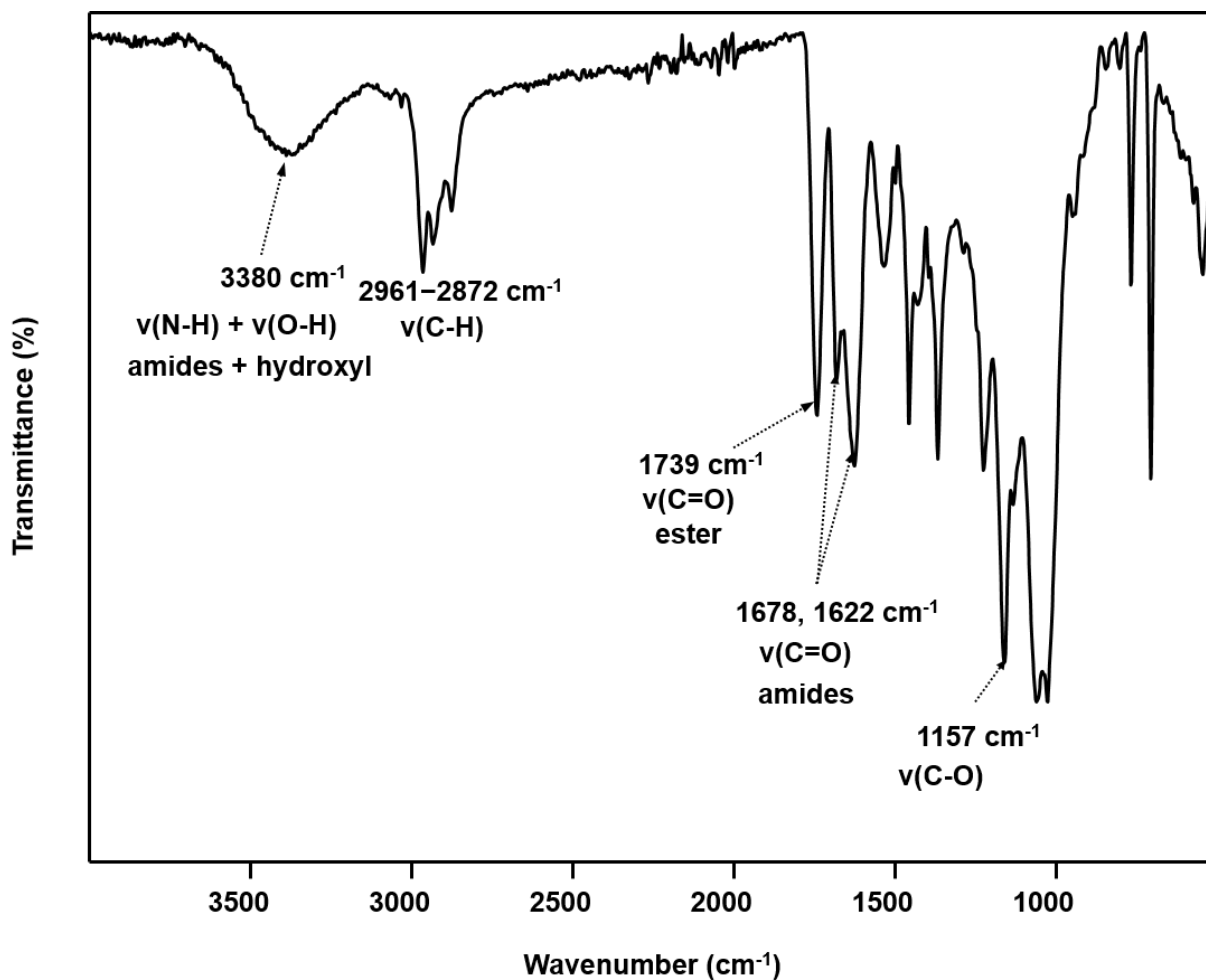
Figure 97: ATR-IR spectra Ugi 4-CR modified succinylated cellulose (**U1**).
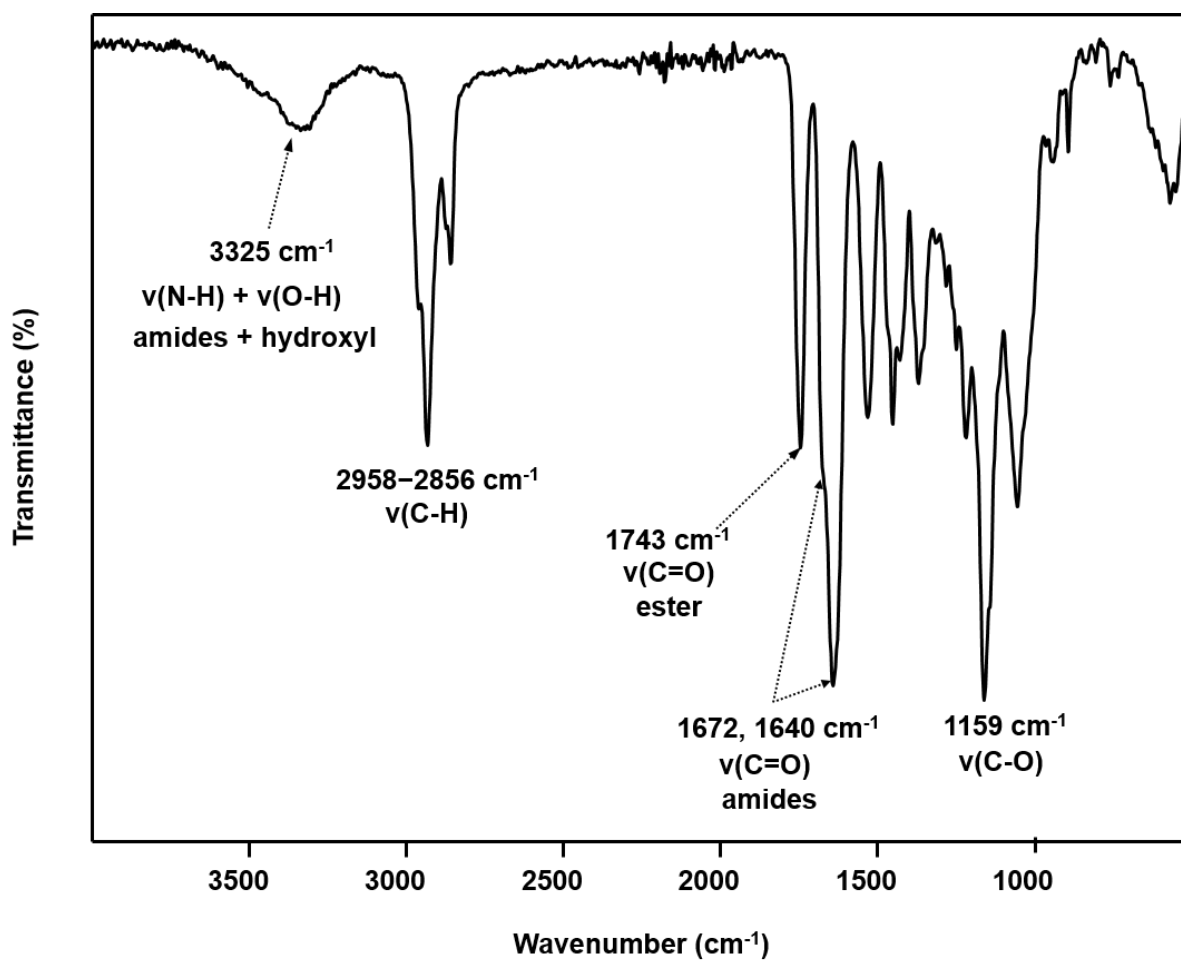
Figure 98: ATR-IR spectra Ugi 4-CR modified succinylated cellulose (**U2**).
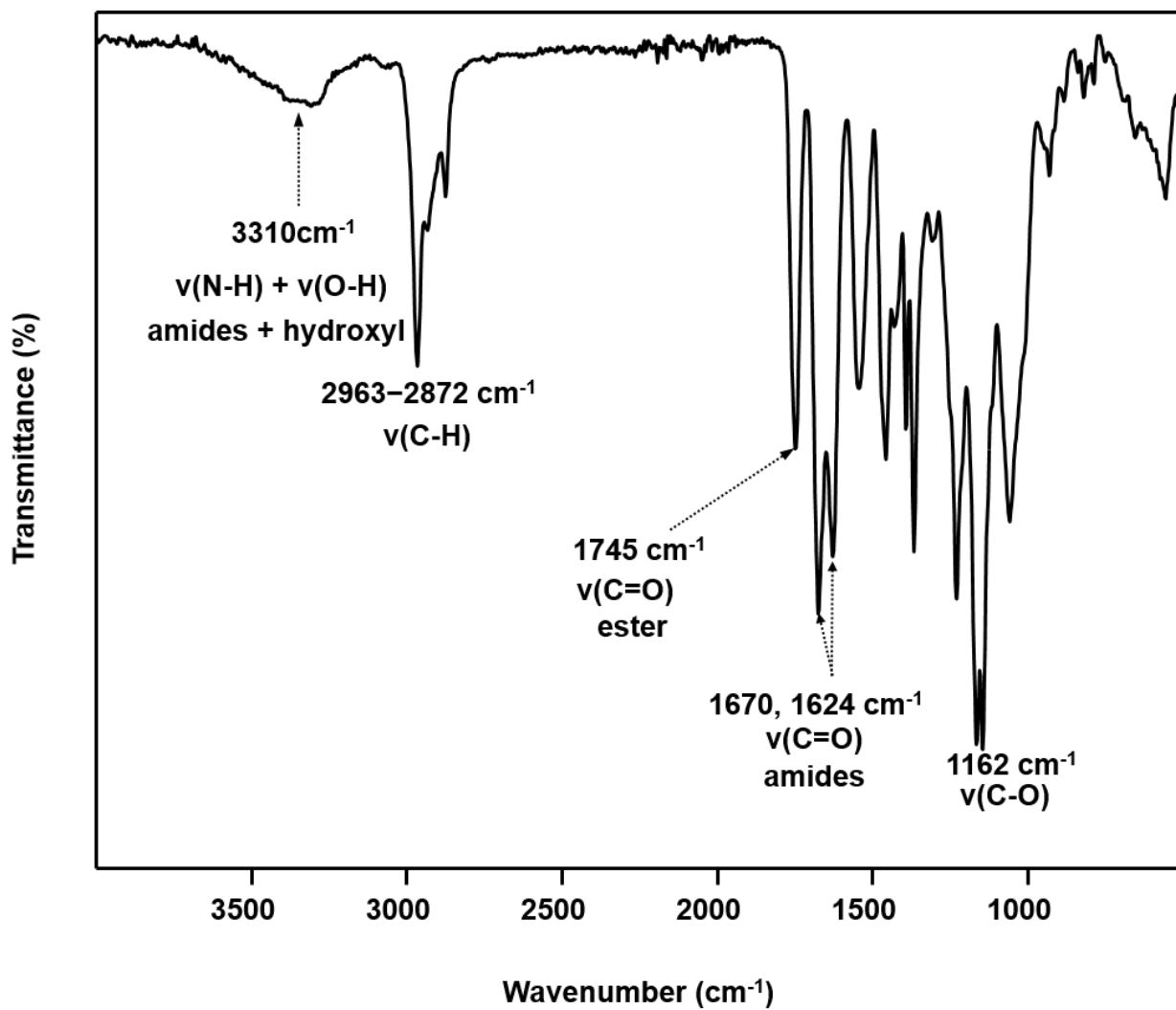
Figure 99: ATR-IR spectra Ugi 4-CR modified succinylated cellulose (**U3**).

NMR spectra of Ugi 4-CR modified succinylated cellulose
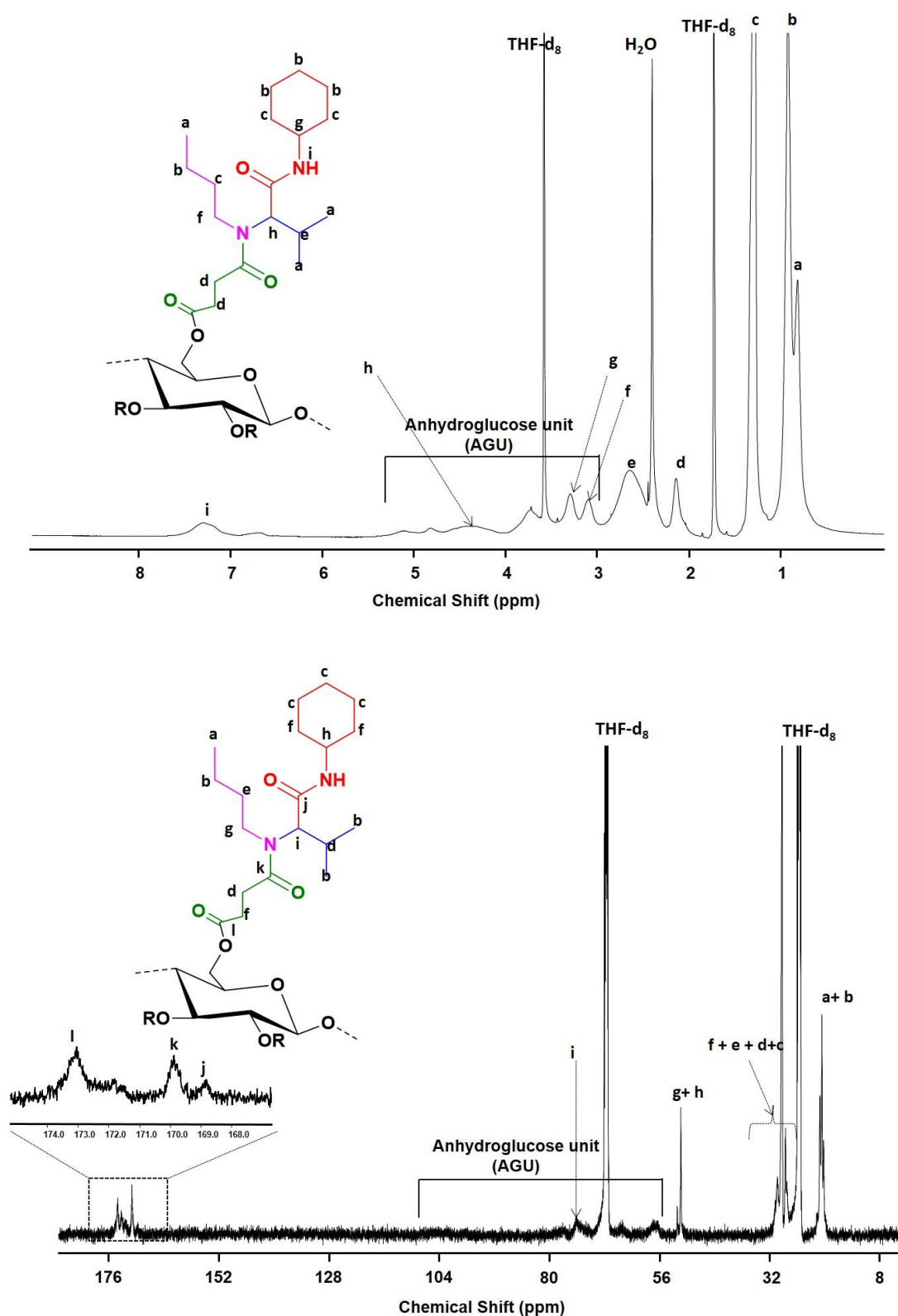
Figure 100: ^{1}H NMR (top) and [13]CN NMR (bottom) of Ugi 4-CR modified succinylated cellulose (**U2**) in THF(d8).
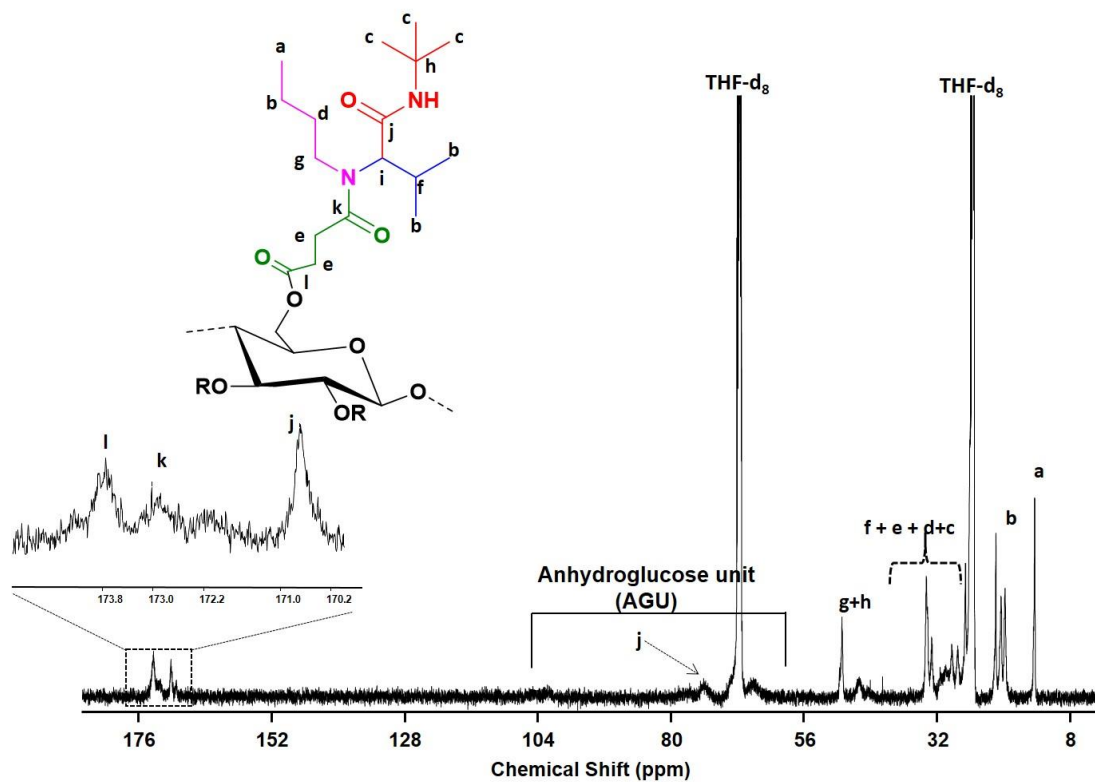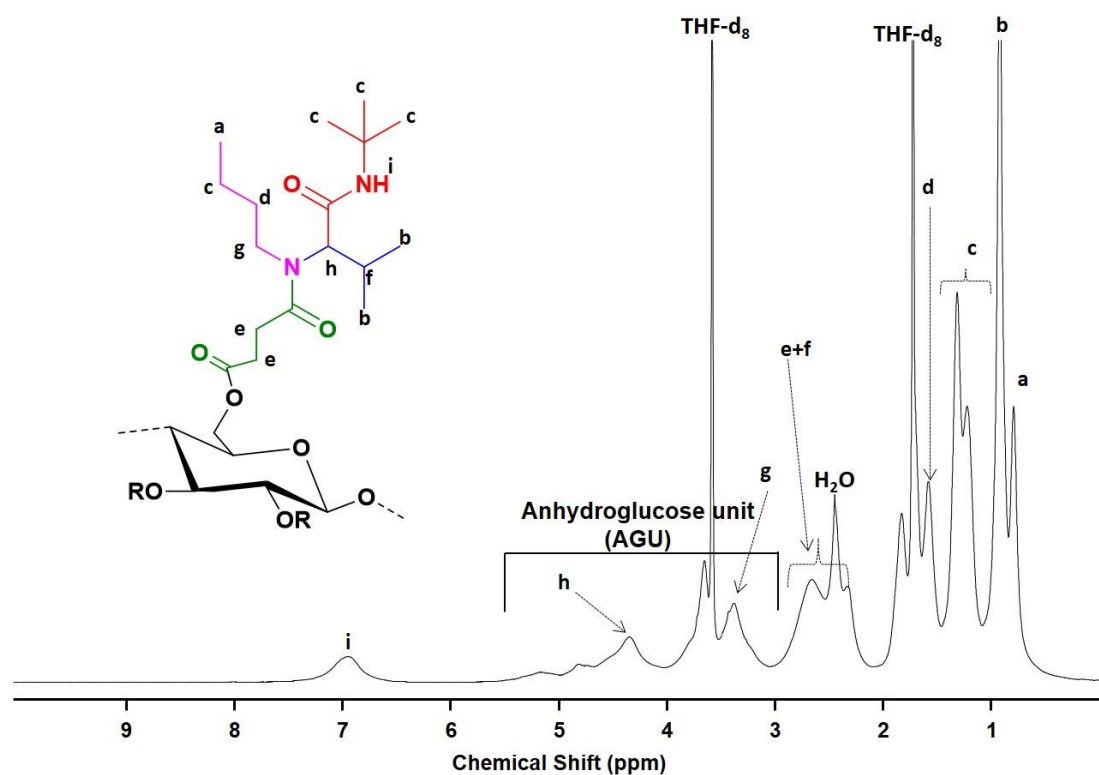
Figure 101: ^{1}H NMR (top) and ^{13}C NMR (bottom) of Ugi 4-CR modified succinylated cellulose (**U3**) in THF(d[8]).

^{31}P NMR spectra for calculating DS and conversion of Ugi 4-CR modified succinylated cellulose
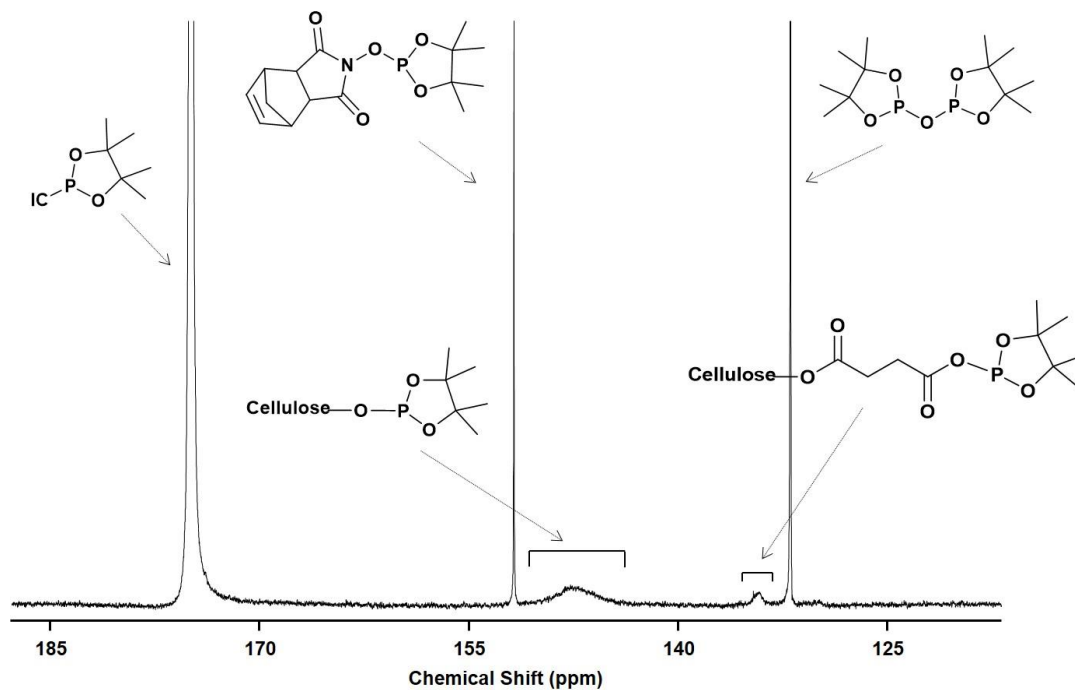
Figure 102: ^{31}P NMR of Ugi 4-CR modified succinylated cellulose (**U2**) in CDCl$_3$.
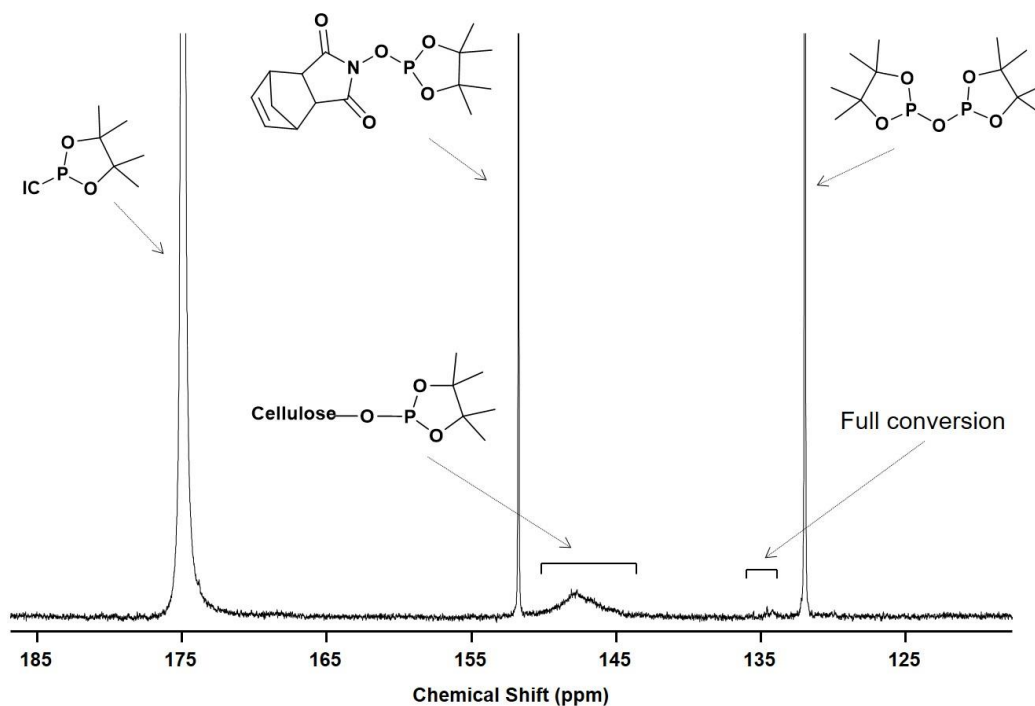
Figure 103: ^{31}P NMR of Ugi 4-CR modified succinylated cellulose (**U3**) in CDCl$_3$.

Method for calculating DS and conversion

The first step for calculating the conversion of the Ugi 4-CR modified succinylated cellulose involve identifying a reference since full conversions were not obtained from these reactions. In this regard, the Passerini three component reaction (P-3CR) was used as it gave full conversion. (i.e. no carboxylic acid peak was detected by ^{31}P NMR). The DS could be calculated following the procedure of Kings *et al.*,[248] by combination of eq. 3 and 4.

$$DS_{31P} = DS_{max} = \frac{\frac{1}{OH_S} - \frac{1}{OH_C}}{MW_S + \frac{1}{OH_S} - 1}$$ eq.3

$$OH_S = \frac{IS_{mol} \times IS_{vol} \times I_R}{1\,000\,000 \times W_S}$$ eq.4

Where:

MW_S: molecular weight (g/mol) of the substituent without including the oxygen atom between cellulose and the substituent (succinylation + Passerini components).

IS_{vol}: amount of internal standard used in volume (mL).

IS_{mol}: amount of internal standard used in millimole (mmol).

I_R: integration ratio of remaining phosphorylated cellulose hydroxyl groups against internal standard.

W_S: sample weight in mg.

DS_{max}: maximum DS obtainable value of 3.0 for unsubstituted cellulose.

OH_C: free hydroxyl groups per weight unit of cellulose = DS_{max}/MW_{AGU} = 3/162.16 = 0.01852 mol/g.

OH_S: free hydroxyl groups per weight unit of substrate (mol/g).

Method for calculating the conversion of Ugi products of succinylated cellulose

The DS value calculated for the P-3CR product, corresponds to the DS of succinylation (since full conversion was achieved), and was taken as reference in calculating the conversion of the Ugi 4-CR products. To minimize error, the same batch of succinylated cellulose was used in all cases. For the calculation of conversions of carboxylic acid moieties in Ugi products, the following equations were applied.

$$\text{Conversion}_{31P} = DS_{\text{Passerini}} = \frac{\frac{1}{COOH_S} - \frac{1}{COOH_c}}{MW_S + \frac{1}{COOH_S} - 1} \text{... eq.5}$$

$$COOH_S = \frac{IS_{mol} \times IS_{vol} \times I_R}{1\,000\,000 \times W_S} \text{.. eq.6}$$

$$COOH_c = \frac{DS_{\text{Passerini}}}{W_{SFP}} \text{.. eq.7}$$

$$\text{Conversion for Ugi-4CR product (\%)} = \frac{\text{Conversion}_{31P}}{DS_{\text{Passerini}}} \times 100\,\% \text{.................. eq.8}$$

Where:

MW_S: molecular weight (g/mol) of the substituent; i.e. molecular weight of the Ugi components without including linking oxygen atom of the carboxylic acid from succinylation.

IS_{vol}: amount of internal standard used in volume (mL).

IS_{mol}: amount of internal standard used in millimole (mmol).

I_R: integration ratio of remaining phosphorylated carboxyl moieties against internal standard.

W_S: sample weight in mg.

$DS_{\text{Passerini}}$: calculated value of 2.64 for P-3CR reference product.

MW_{SFP}: calculated molecular weight of the succinylated cellulose from the DS value of 2.64 = 426 g/mol.

$COOH_S$: free carboxylic acid groups per weight unit of substrate (mol/g).

$COOH_c$: free carboxylic acid groups per weight unit of cellulose = 2.64/426 = 0.0062 mol/g.

8.7 Experimental procedures for Chapter 6.4

General procedure for optimization study of P-4CR

0.41 g of Butanol (1 eq., 5.50 mmol) and 5 mol% tetradecane as internal GC standard (70 µL) were stirred in 1.5 mL of the solvent at room temperature for 1 to 2 min., after which a sample was collected for GC analysis. The mixture was then saturated with CO_2 (5 bar) for 15 min. In the same manner, isobutyraldehyde was pre-saturated with CO_2 (5 bar) for 10 min., after which both solutions were mixed and further saturated with 5 bar of CO_2 for 10 to 15 min. Subsequently, *tert*-butylisocyanide was added and the reaction was performed under 10 bar of CO_2 for 24 h at room temperature (22-24 °C). Samples were then collected over the course of the reaction and analyzed by Gas chromatography (GC) in order to calculate the conversion and the relative percentage between the observed products (P-4CR, P-3CR and hydrolysis product of P-4CR). Parameters investigated during the optimization study include: effect of reaction equivalents (1, 2 eq.), reaction concentration (1.84 and 3.68 M with respect to butanol), catalyst (Et_3N and DBU), catalyst concentration (5, 10 and 15 mol%), CO_2 pressure (5, 10 and 15 bar) and solvent (DMSO, chloroform, methyl-THF, DCM).

Effect of solvent on the relative ratio between observed products

Figure 104: Effect of solvent on the relative percentage between P-4CR, P-3CR and hydrolysis products (1.84 M, 2 eq. isobutyraldehyde, 2 eq. *tert*-butylisocyanide, 10 bar CO_2, 24 h at room temperature). Values obtained through GC measurement using tetradecane as internal standard.

Figure 105: Results obtained by GC of: **a**). Influence of catalyst (10 mol.% Et₃N) on the conversion of butanol over time compared to the reaction without any catalyst (conditions: 3.68 M in DCM, 2 eq. isobutyraldehyde, 2 eq. *tert*-butylisocyanide, 10 bar CO₂, 45-48 h at room temperature). **b**). Relative percentage of respective products (P-4CR, P-3CR and hydrolysis of P-4CR) for the reaction performed without catalyst. **c**). Relative percentage of respective products (P-4CR, P-3CR and hydrolysis of P-4CR) for the reaction performed with 10 mol.% Et₃N as catalyst. (b and c; values are obtained after normalization using tetradecane).

Catalyst comparison on the relative percentage between observed products
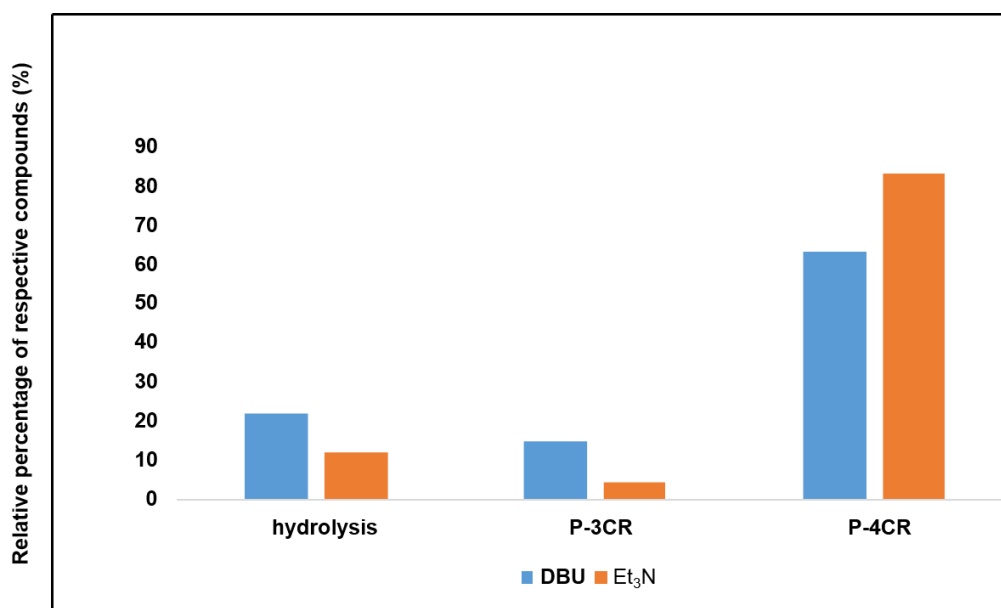
Figure 106: Comparison between Et$_3$N and DBU as catalyst on the relative percentage between P-4CR, P-3CR and hydrolysis products (1.84 M, 2 eq. isobutyraldehyde, 2 eq. *tert*-butylisocyanide, 10 bar CO$_2$, 24 h at room temperature). Values obtained through GC measurement with tetradecane as internal standard.

Effect of Et$_3$N catalyst concentration on the relative ratio between observed products
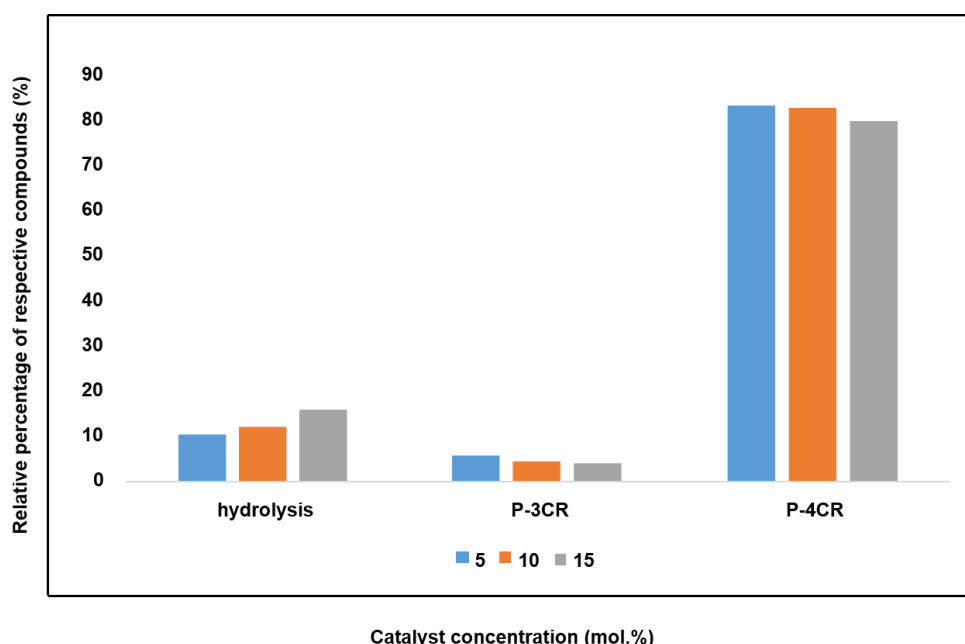
Figure 107: Effect of catalyst concentration using Et$_3$N on the relative percentage between P-4CR, P-3CR and hydrolysis products (1.84 M, 2 eq. isobutyraldehyde, 2 eq. *tert*-butylisocyanide,10 bar CO$_2$, 24 h at room temperature). Values obtained through GC measurement with tetradecane as internal standard.

Effect of CO$_2$ pressure on the relative ratio between observed products
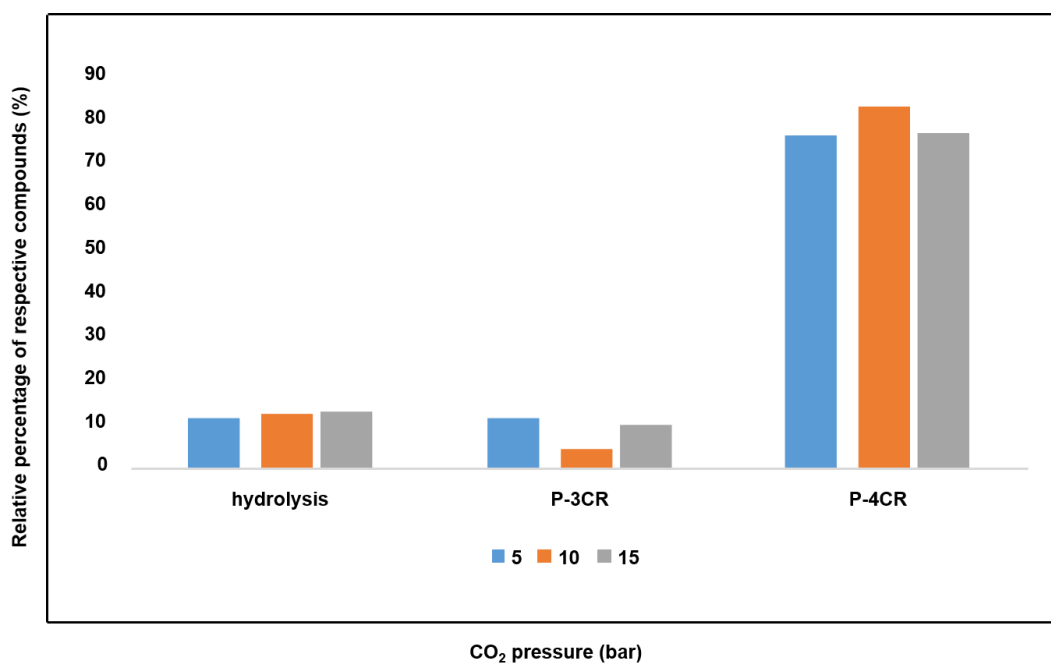
Figure 108: Effect of CO$_2$ pressure on the relative percentage between P-4CR, P-3CR and hydrolysis products (10 mol.% triethylamine, 1.84 M, 2 eq. isobutyraldehyde, 2 eq. *tert*-butylisocyanide, 10 bar CO$_2$, 24 h at room temperature). Values obtained through GC measurement with tetradecane as internal standard.

Synthesis and characterization of P-4CR products

11a. Butyl (1-(*tert*-butylamino)-3-methyl-1-oxobutan-2-yl) carbonate
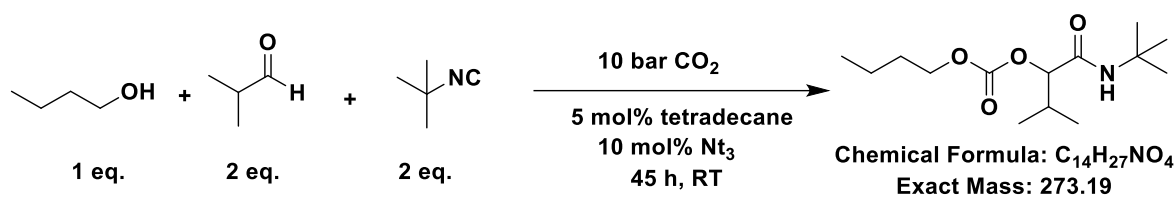
Chemical Formula: $C_{14}H_{27}NO_4$
Exact Mass: 273.19

0.41 g of butanol (1 eq., 5.50 mmol) and 5 mol% tetradecane standard (70 µL) were stirred in 1.5 mL of dichloromethane (DCM) at room temperature for 1 to 2 min, after which a sample was collected for GC analysis (T_0). 10 mol.% triethylamine catalyst (80 µL) was added and the mixture was saturated with CO_2 (5 bar) for 15 min. In the same manner, 0.79 g of isobutyraldehyde (2 eq., 11 mmol, 1.0 mL) was pre-saturated with CO_2 (5 bar) for 10 minutes, after which both solutions were mixed and further saturated with 5 bar of CO_2 between 10-15 min. Furthermore, 0.91 g of *tert*-butyl isocyanide (2 eq., 11 mmol, 1.24 mL) was added and the reaction performed under 10 bar of CO_2 for 45 h at room temperature (22-24 °C). After 45 h, a sample was collected for GC analysis (T_f) in order to calculate the conversion and relative ratio values between observed products. The crude mixture was concentrated *via* rotary evaporation and purified via column chromatography (gradient CH:EE starting from 15:1 to 5:1). The product was obtained as white powder. Conversion: 73 %, isolated yield: 43 %.

^{1}H NMR (500 MHz, CDCl$_3$) δ (ppm) = 5.87 (s, NH, 1H), 4.83 (d, CH, 1H), 4.18 (t, CH$_2$, 2H), 2.29 (m, CH, 1H), 1.67 (dt, CH$_2$, 2H), 1.41 (dt, CH$_2$, 2H), 1.35 (s, 3 CH$_3$, 9H), 0.94 (dt, 3 CH$_3$, 9H).

^{13}C NMR (125 MHz, CDCl$_3$) δ (ppm) = 168.76 (k), 154.93 (j), 82.01 (g), 69.03 (f), 51.70 (i), 31.11 (e), 30.97 (d), 29.06 (b), 19.26 (c), 18.93, 16.97, 14.03 (a).

ATR-IR: ν (cm^{-1}) = 3305.1, 3093.4, 2962.3, 2873.8, 1743.6, 1654.3, 1558.1, 1451.0, 1388.3, 1246.8, 970.3, 799.8, 660.3, 509.0.

Exact mass: $[C_{14}H_{27}NO_4Na]^+$ *m/z* = 296.19, obtained (ESI-MS) = 296.18278
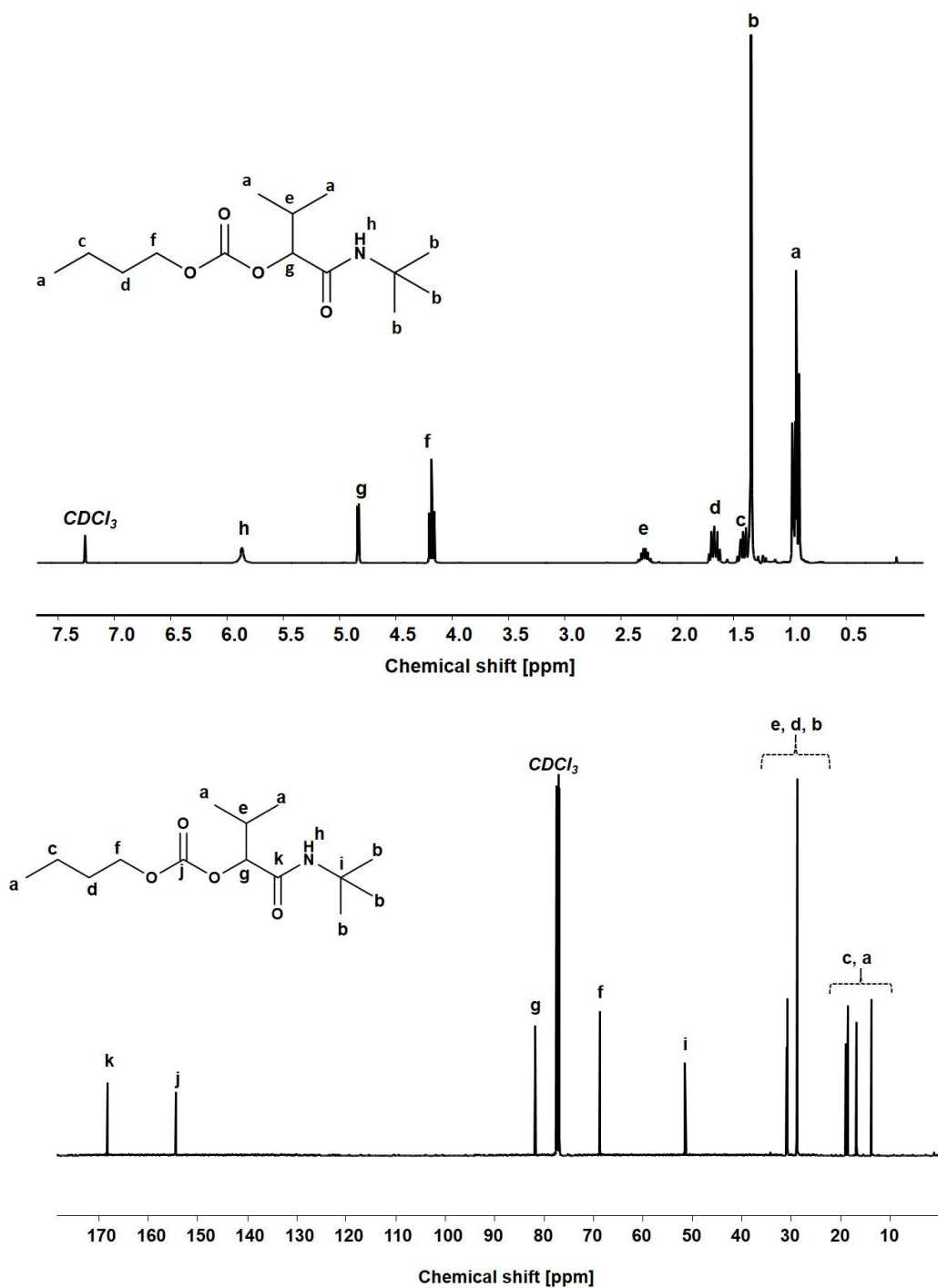
Figure 109: ^{1}H (top) and ^{13}C NMR (bottom) of P-4CR **11a**, measured in CDCl$_3$.

11b. Butyl (1-(*tert*-butylamino)-1-oxo-3-phenylpropan-2-yl) carbonate
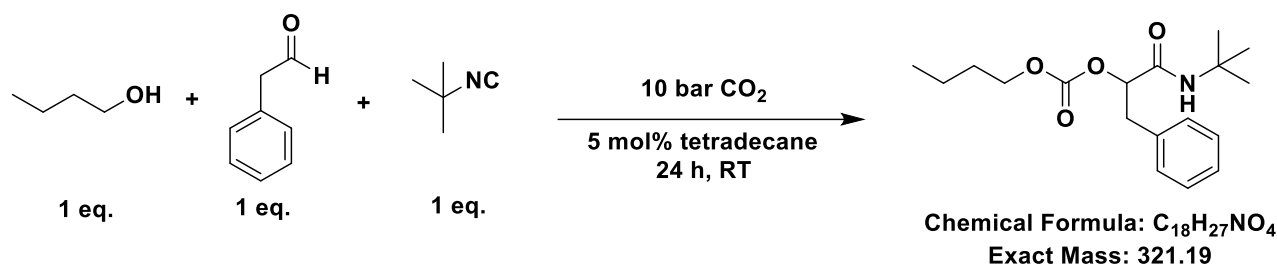
Chemical Formula: $C_{18}H_{27}NO_4$
Exact Mass: 321.19

0.41 g of Butanol (1 eq., 5.50 mmol) and 5 mol% tetradecane standard (70 µL) were stirred in 1.5 mL of dichloromethane (DCM) at room temperature for 1-2 min, after which a sample was collected for GC analysis (T_0). Next, the mixture was saturated with CO_2 (5 bar) for 15 min. In a similar fashion, 0.66 g of phenyl acetaldehyde (1 eq., 5.5 mmol, 0.62 mL) was pre-saturated with CO_2 (5 bar) for 10 min, after which both solutions were mixed and further saturated with 5 bar of CO_2 between 10-15 min. Furthermore, 0.46 g of *tert*-butyl isocyanide (1 eq., 5.5 mmol, 0.62 mL) was added and the reaction was performed under 10 bar of CO_2 for 24 h at room temperature (22-24 °C). After 24 h, a sample was collected for GC analysis (T_f) in order to calculate the conversion and relative ratio values between the observed products. The crude mixture was concentrated *via* rotary evaporation and purified *via* column chromatography (gradient CH:EE starting from 20:1 to 5:1). The product was obtained as white powder. Conversion: 36 %, isolated yield: 25 %.

^{1}H NMR (500 MHz, CDCl$_3$) δ (ppm) = 7.26-7.18 (td, Ar-H, 5H), 5.66 (s, NH, 1H), 5.08 (dd, CH, 1H), 4.05 (m, CH$_2$, 2H), 3.09 (m, CH$_2$, 2H), 1.55 (m, CH$_2$, 2H), 1.30 (dq, CH$_2$, 2H), 1.19 (s, 3 CH$_3$, 9H), 0.87 (t, 3 CH$_3$, 9H).

^{13}C NMR (125 MHz, CDCl$_3$) δ (ppm) = 167.85 (m), 154.05 (l), 135.72 (k), 130.12 128.26, 127.03 (i), 77.68 (g), 68.77 (f), 51.45 (i), 37.94 (e) 30.66 (d), 28.89 (b), 19.11 (c), 13.76 (a).

ATR-IR: ν (cm^{-1}) = 3297.7, 3085.6, 3032.7, 2963.6, 2933.0, 2872.5, 1755.2, 1659.9, 1554.9, 1246.3, 1125.6, 699.2, 511.3.

Exact mass: [C$_{18}$H$_{27}$NO$_4$Na]$^+$ *m/z* = 344.19, obtained (ESI-MS) = 344.18277
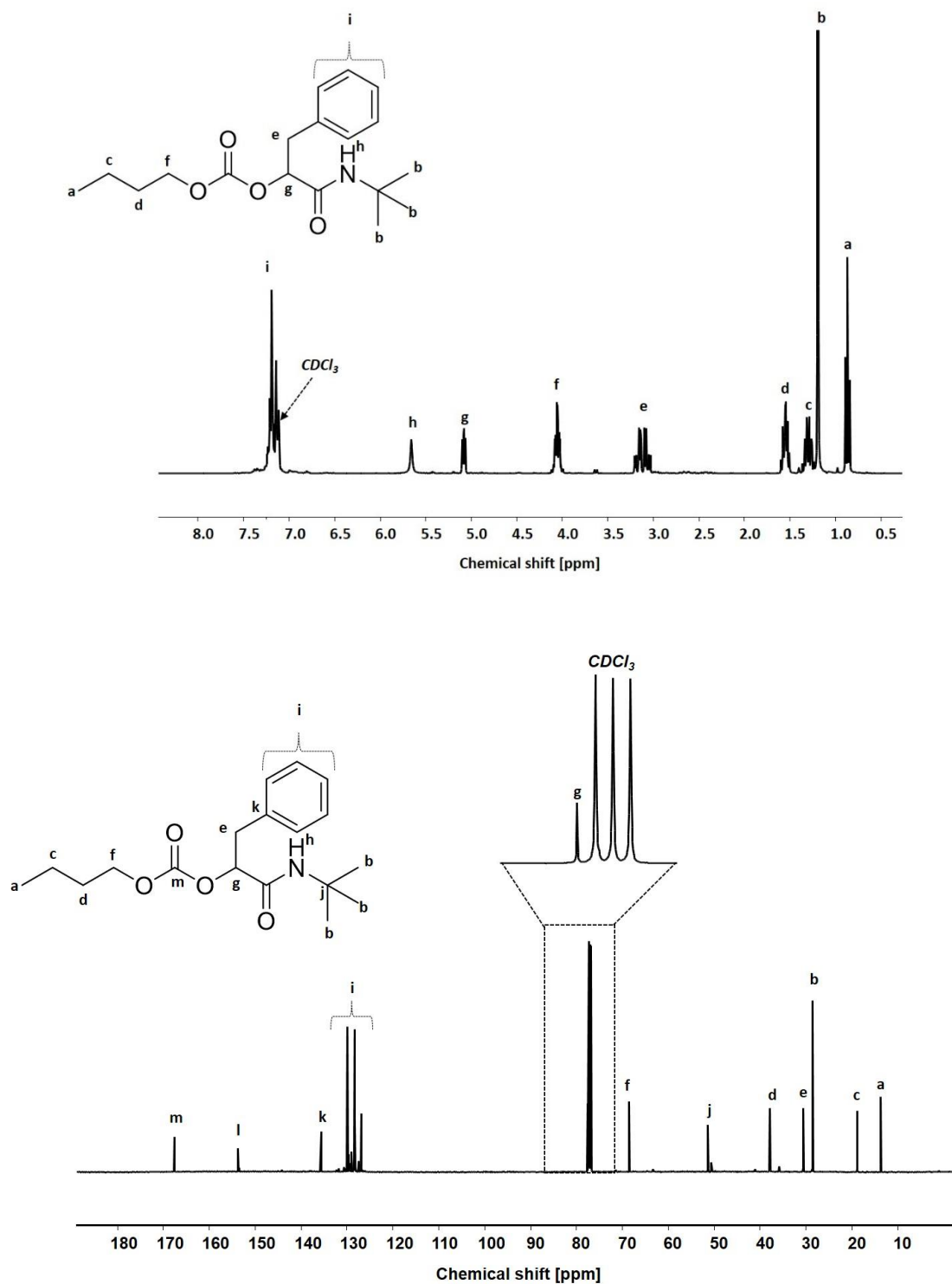
Figure 110: ¹H (top) and ¹³C NMR (bottom) of P-4CR **11b**, measured in CDCl₃.

11c. Butyl(1-(cyclohexylamino)-3-methyl-1-oxobutan-2-yl) carbonate
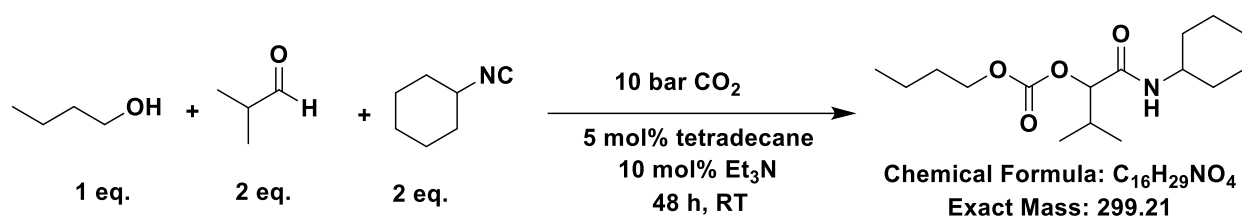
Chemical Formula: $C_{16}H_{29}NO_4$
Exact Mass: 299.21

0.41 g of butanol (1 eq., 5.50 mmol) and 5 mol% tetradecane standard (70 µL) were stirred in 1.5 mL of dichloromethane (DCM) at room temperature for 1-2 min, after which a sample was collected for GC analysis (T_0). 10 mol.% triethylamine catalyst (80 µL) was added and the mixture was saturated with CO_2 (5 bar) for 15 minutes. In a similar fashion, 0.79 g of isobutyraldehyde (2 eq., 11 mmol, 1.0 mL) was pre-saturated with CO_2 (5 bar) for 10 min after which both solutions were mixed and further saturated with 5 bar of CO_2 between 10-15 min. Furthermore, 1.20 g of cyclohexyl isocyanide (2 eq., 11 mmol, 1.38 mL) was added and the reaction was performed under 10 bar of CO_2 for 48 h at room temperature (22-24 °C). After 48 h, a sample was collected for GC analysis (T_f) in order to calculate the conversion and the relative ratio values between the observed products. The crude mixture was concentrated *via* rotary evaporation and purified via column chromatography (gradient CH:EE starting from 15:1 to 5:1). The product was obtained as white powder. Conversion: 56 %, isolated yield: 33 %. The hydrolysis product was isolated in a yield of 30 %.

^{1}H NMR (500 MHz, CDCl3) δ (ppm) = 5.95 (d, NH, 1H), 4.94 (d, CH, 1H), 4.18 (t, CH2, 2H), 3.79 (m, CH, 1H), 2.31 (m, CH, 1H), 1.89 (m, CH2, 2H), 1.72-1.27 (m, 5 CH2, 10H), 1.12 (m, 2 CH2, 4H), 0.95 (dd, 3CH3, 9H).

^{13}C NMR (125 MHz, CDCl3) δ (ppm) = 168.15 (j), 154.62 (i), 81.73 (g), 68.82 (f), 48.01 (e), 33.26, 33.02, 30.88, 30.69 (d + c), 25.57, 24.89 (b), 19.00, 18.68, 16.50, 13.76 (a).

ATR-IR: v(cm[-1]) = 3292.6, 3082.6, 2968.5, 2926.1, 2876.1, 2854.5, 1746.5, 1655.6, 1555.5, 1243.4, 1143.7, 784.5, 656.0.

Exact mass: $[C_{16}H_{29}NO_4Na]^+$ *m/z* = 322.21, obtained (ESI-MS) = 322.19852
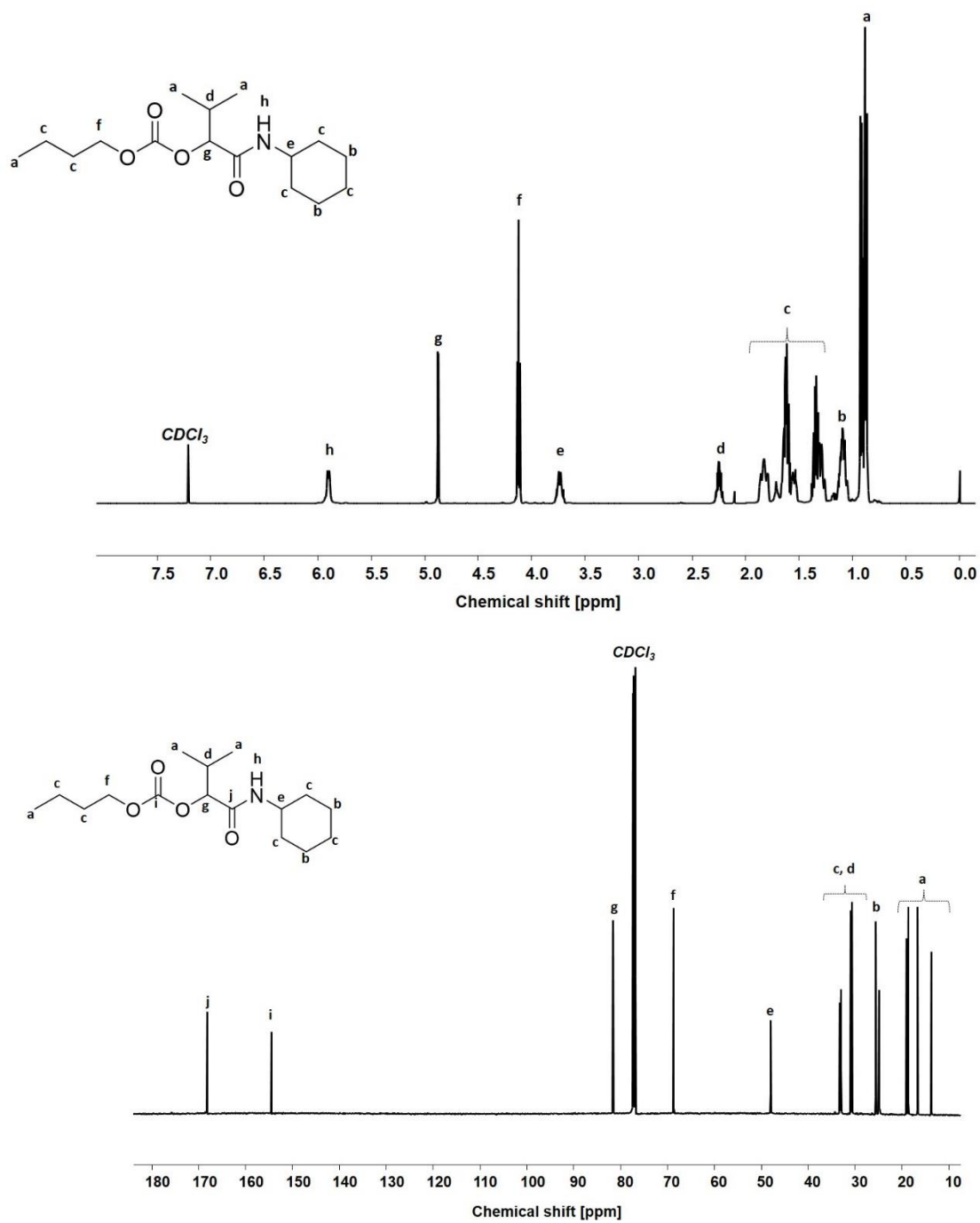
Figure 111: ¹H (top) and ¹³C NMR (bottom) of P-4CR **11c**, measured in CDCl₃.

12a. *sec*-Butyl (1-(tert-butylamino)-3-methyl-1-oxobutan-2-yl) carbonate

Chemical Formula: $C_{14}H_{27}NO_4$
Exact Mass: 273.19
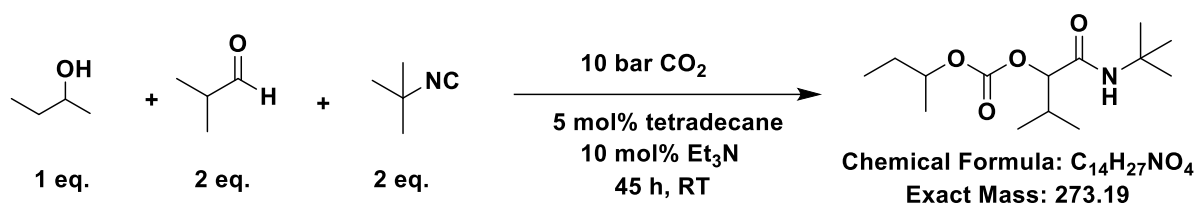
0.41 g of 2-butanol (1 eq., 5.50 mmol) and 5 mol% tetradecane standard (70 μL) were stirred in 1.5 mL of dichloromethane (DCM) at room temperature for 1-2 min, after which a sample was collected for GC analysis (T_0). 10 mol.% triethylamine catalyst (80 μL) was added and the mixture was saturated with CO_2 (5 bar) for 15 min. In a similar fashion, 0.79 g of isobutyraldehyde (2 eq., 11 mmol, 1.0 mL) was pre-saturated with CO_2 (5 bar) for 10 min after which both solutions were mixed and further saturated with 5 bar of CO_2 between 10 and 15 min. Furthermore, 0.91 g of *tert*-butyl isocyanide (2 eq., 11 mmol, 1.24 mL) was added and the reaction was performed under 10 bar of CO_2 for 45 h at room temperature (22-24 °C). After 45 h, a sample was collected for GC analysis (T_f) in order to calculate the conversion and the relative ratio values between the observed products. The crude mixture was concentrated *via* rotary evaporation and purified via column chromatography (gradient CH:EE starting from 15:1 to 5:1). The product was obtained as white powder. Conversion: 54 %, isolated yield: 24 %.

^{1}H NMR (500 MHz, CDCl$_3$) δ (ppm) = 5.87 (s, NH, 1H), 4.82 (d, CH, 1H), 4.72 (m, CH, 1H), 2.28 (m, CH, 1H), 1.63 (m, CH$_2$, 2H), 1.34 (dt, 3 CH$_3$, 9H), 1.28 (t, CH$_3$, 3H), 0.94 (dt, 3 CH$_3$, 9H).

^{13}C NMR (125 MHz, CDCl$_3$) δ (ppm) = 168.46 (k), 154.31 (j), 81.60 (g), 77.53 (f), 51.40 (i), 30.75 (e), 29.02 (d + c), 19.54, 19.49, 18.70, 16.81 (b + a), 9.89 (a).

ATR-IR: $v(cm^{-1})$ = 3307.2, 3092.8, 2966.6, 2933.1, 2875.2, 1741.6, 1663.4, 1560.9, 1360.2, 1247.0, 1108.4, 971.4, 888.3, 648.2, 402.2

Exact mass: $[C_{14}H_{27}NO_4H]^+$ *m/z* = 274.19, obtained (ESI-MS) = 274.20083

Figure 112: ^{1}H (top) and ^{13}C NMR (bottom) of P-4CR **12a**, measured in CDCl$_3$.

13a. Allyl (1-(tert-butylamino)-3-methyl-1-oxobutan-2-yl) carbonate

Chemical Formula: $C_{13}H_{23}NO_4$
Exact Mass: 257.16
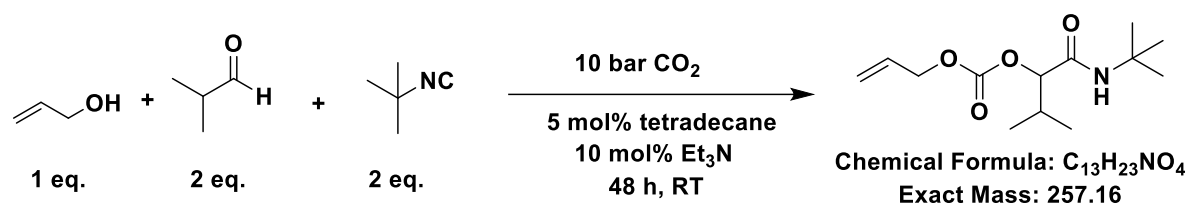
0.32 g of allyl-alcohol (1 eq., 5.50 mmol) and 5 mol% tetradecane standard (70 µL) were stirred in 1.5 mL of dichloromethane (DCM) at room temperature for 1-2 min, after which a sample was collected for GC analysis (T_0). 10 mol.% triethylamine catalyst (80 µL) was added and the mixture was saturated with CO_2 (5 bar) for 15 min. In a similar fashion, 0.79 g of isobutyraldehyde (2 eq., 11 mmol, 1.0 mL) was pre-saturated with CO_2 (5 bar) for 10 min after which both solutions were mixed and further saturated with 5 bar of CO_2 between 10 and 15 min. Furthermore, 0.91 g of *tert*-butyl isocyanide (2 eq., 11 mmol, 1.24 mL) was added and the reaction was performed under 10 bar of CO_2 for 48 h at room temperature (22-24 °C). After 48 h, a sample was collected for GC analysis (T_f) in order to calculate the conversion and the relative ratio values between the observed products. The crude mixture was concentrated *via* rotary evaporation and purified *via* column chromatography (gradient CH:EE starting from 15:1 to 5:1). A second column (1:1, cyclohexane:diethyl ether) was necessary to separate the P-3CR side product from the expected P-4-CR product. The product was obtained as white powder. Conversion: 82 %, isolated yield: 33 %. The hydrolysis product was isolated with a yield of 23 %.

^{1}H NMR (500 MHz, CDCl$_3$) δ (ppm) = 6.01-5.79 (m, NH + =CH, 2H), 5.36 (m, =CH$_2$, 2H), 4.85 (d, CH, 1H), 4.67 (dt, CH$_2$, 2H), 2.28 (m, CH, 1H), 1.35 (s, 3 CH$_3$, 9H), 0.92 (m, 2 CH$_3$, 6H).

^{13}C NMR (125 MHz, CDCl$_3$) δ (ppm) = 168.17 (k), 154.35 (j), 131.35 (g), 119.77 (f), 82.00 (e), 69.10 (d), 51.52 (i), 31.08 (c), 28.82 (b), 18.77, 16.94 (a).

ATR-IR: v(cm^{-1}) = 3306.6, 3092.7, 2967.2, 2935.8, 2880.3, 1748.4, 1661.8, 1561.6, 1367.3, 1297.1, 1239.6, 979.4, 789.6, 657.1, 403.5.

Exact mass: [C$_{13}$H$_{23}$NO$_4$Na]$^+$ *m/z* = 280.16, obtained (ESI-MS) = 280.15144
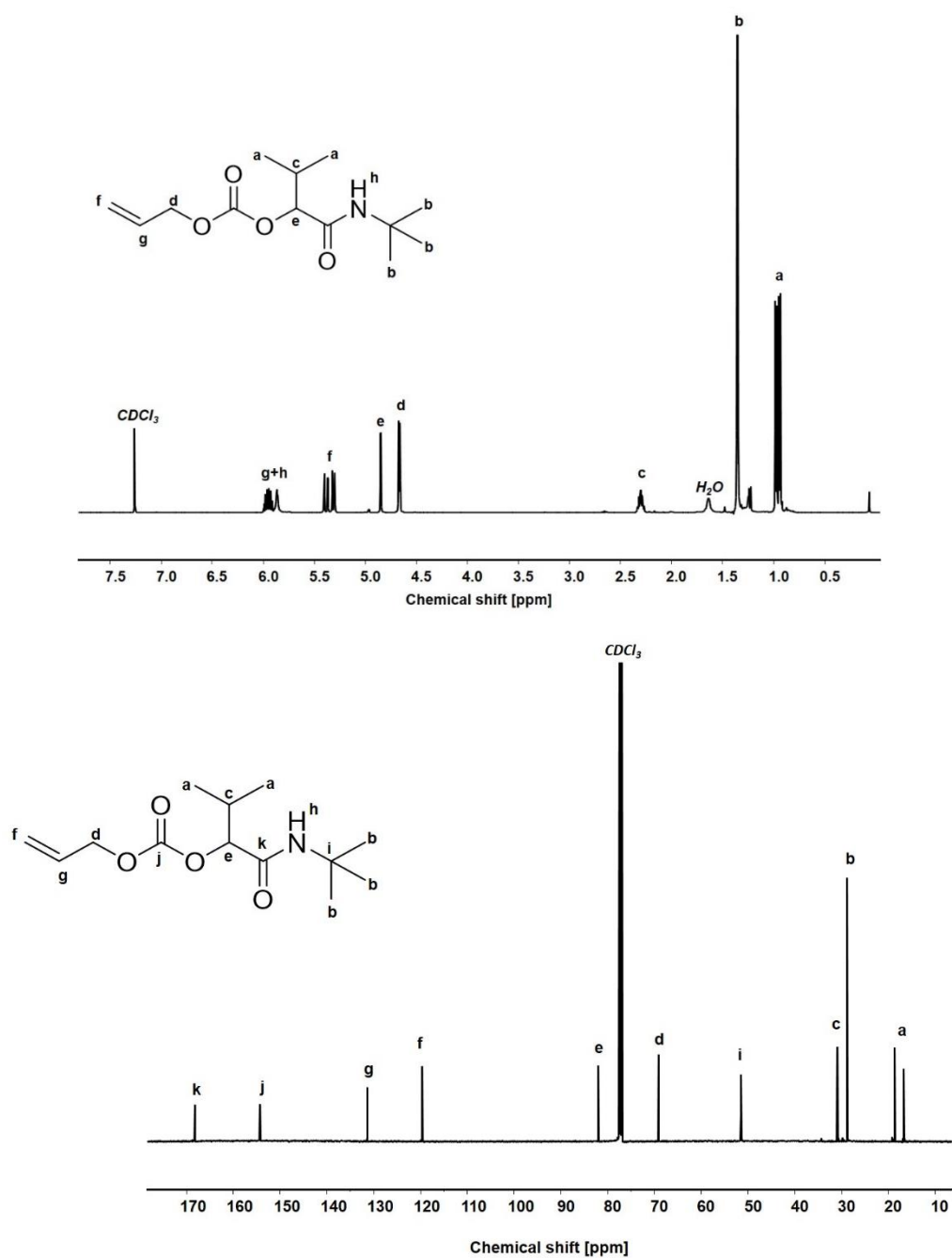
Figure 113: ¹H (top) and ¹³C NMR (bottom) of P-4CR **13a**, measured in CDCl₃.

14a. Benzyl (1-(tert-butylamino)-3-methyl-1-oxobutan-2-yl) carbonate

Chemical Formula: $C_{17}H_{25}NO_4$
Exact Mass: 307.18
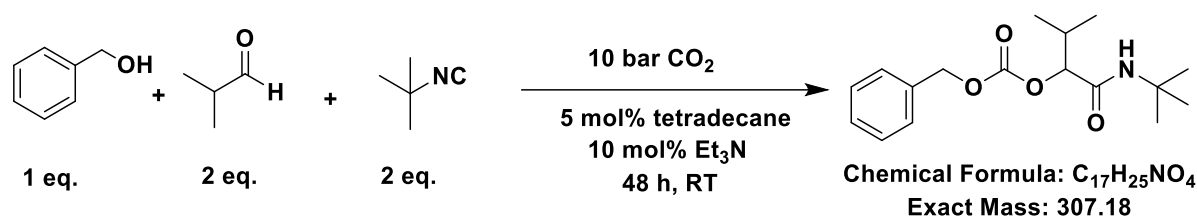
0.60 g of benzyl alcohol (1 eq., 5.50 mmol) and 5 mol% tetradecane standard (70 µL) were stirred in 1.5 mL of dichloromethane (DCM) at room temperature for 1-2 min, after which a sample was collected for GC analysis (T_0). 10 mol.% triethylamine catalyst (80 µL) was added and the mixture was saturated with CO_2 (5 bar) for 15 min. In a similar fashion, 0.79 g of isobutyraldehyde (2 eq., 11 mmol, 1.0 mL) was pre-saturated with CO_2 (5 bar) for 10 min after which both solutions were mixed and further saturated with 5 bar of CO_2 between 10 to 15 min. Furthermore, 0.91 g of *tert*-butyl isocyanide (2 eq., 11 mmol, 1.24 mL) was added and reaction performed under 10 bar of CO_2 for 48 h at room temperature (22-24 °C). After 48 h, a sample was collected for GC analysis (T_f) in order to calculate the conversion and the relative ratio values between the observed products. The crude mixture was concentrated via rotary evaporation and purified via column chromatography (gradient CH:EE starting from 15:1 to 5:1). The product was obtained as white powder. Conversion: 33 %, isolated yield: 27 %.

^{1}H NMR (500 MHz, CDCl$_3$) δ (ppm) = 7.38 (m, Ar-H, 5H), 5.82 (s, NH, 1H), 5.20 (d, CH$_2$, 2H), 4.82 (d, CH, 1H), 2.28 (m, CH, 1H), 1.31 (s, 3 CH$_3$, 9H), 0.94 (dt, 2 CH$_3$, 6H).

^{13}C NMR (125 MHz, CDCl$_3$) δ (ppm) = 168.14 (k), 154.38 (j), 135.00 (i), 128.94, 128.85, 128.61 (g), 82.12 (d), 70.32 (e), 51.46 (h), 30.85 (c), 28.76 (b), 18.65, 16.72 (a).

ATR-IR: ν(cm^{-1}) = 3310.6, 3090.9, 3035.6, 2966.8, 2934.3, 2880.9, 1752.3, 1656.2, 1556.7, 1299.1, 1255.0, 1224.5, 986.3, 733.2, 654.0, 482.9.

Exact mass: [$C_{17}H_{25}NO_4Na$]$^+$ *m/z* = 330.18, obtained (ESI-MS) = 330.16689
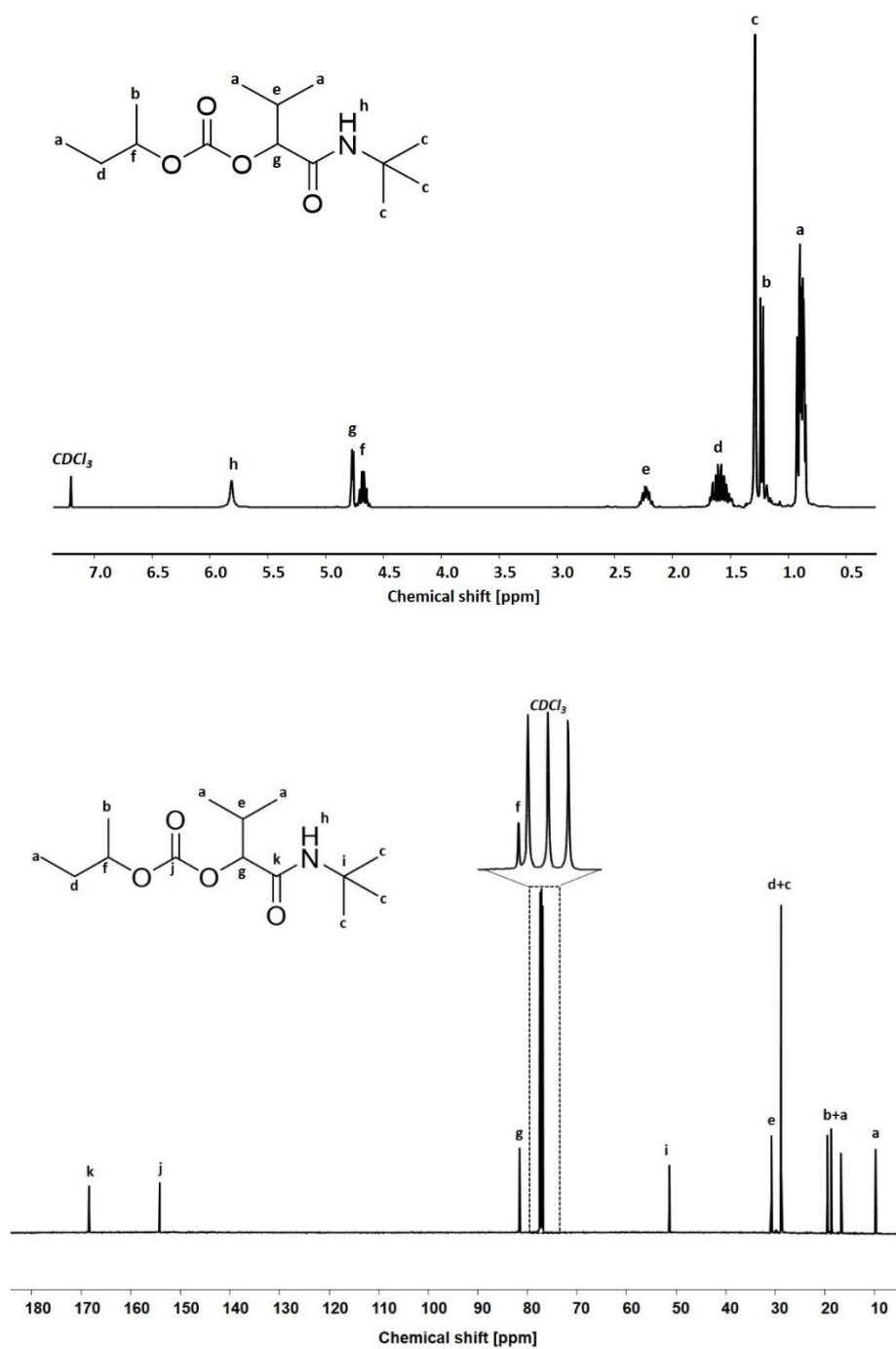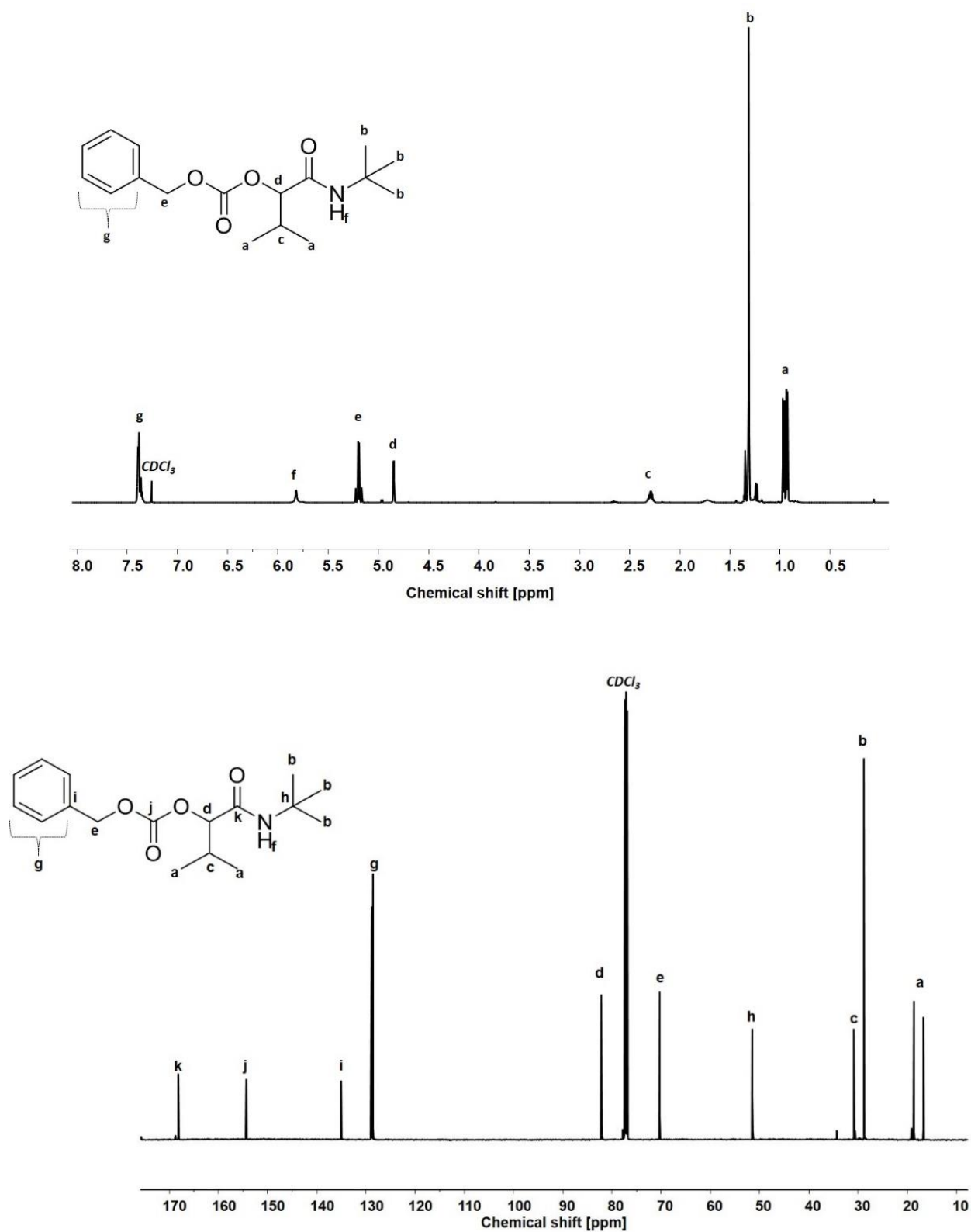
Figure 114: ^{1}H (top) and ^{13}C NMR (bottom) of P-4CR **14a**, measured in CDCl₃.

15a. Octyl (1-(tert-butylamino)-3-methyl-1-oxobutan-2-yl) carbonate

Chemical Formula: $C_{18}H_{35}NO_4$
Exact Mass: 329.26
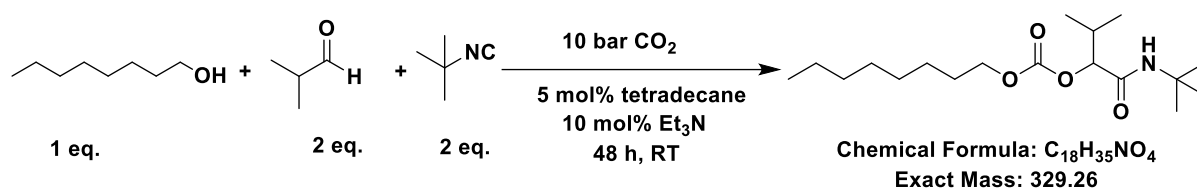
0.72 g of 1-octanol (1 eq., 5.50 mmol) and 5 mol% tetradecane standard (70 μL) were stirred in 1.5 mL of dichloromethane (DCM) at room temperature for 1-2 min, after which a sample was collected for GC analysis (T_0). 10 mol.% triethylamine catalyst (80 μL) was added and the mixture was saturated with CO_2 (5 bar) for 15 min. In a similar fashion, 0.79 g of isobutyraldehyde (2 eq., 11 mmol, 1.0 mL) was pre-saturated with CO_2 (5 bar) for 10 min after which both solutions were mixed and further saturated with 5 bar of CO_2 between 10-15 min. Furthermore, 0.91 g of *tert*-butyl isocyanide (2 eq., 11 mmol, 1.24 mL) was added and the reaction was performed under 10 bar of CO_2 for 48 h at room temperature (22-24 °C). After 48 h, a sample was collected for GC analysis (T_f) in order to calculate the conversion and the relative ratio values between the observed products. The crude mixture was concentrated *via* rotary evaporation and purified via column chromatography (gradient CH:EE starting from 15:1 to 5:1). The product was obtained as a viscous liquid. Conversion: 26 %, isolated yield: 25 %.

^{1}H NMR (500 MHz, CDCl$_3$) δ (ppm) = 5.87 (s, NH, 1H), 4.84 (d, CH, 1H), 4.17 (t, CH$_2$, 2H), 2.29 (m, CH, 1H), 1.71 (m, CH$_2$, 2H), 1.29 (m, 5 CH$_2$ + 3 CH$_3$ 19H), 0.92 (m, 3 CH$_3$, 9H).

^{13}C NMR (125 MHz, CDCl$_3$) δ (ppm) = 168.34 (j), 154.54 (i), 81.76 (f), 68.95 (e), 51.47 (h), 31.87, 30.87, 29.28, 28.82, 25.76, 22.75, 18.68, 16.73, 14.21 (d + c + b + a).

ATR-IR: v(cm^{-1}) =3329.5, 2962.5, 2926.5, 2873.4, 2855.7, 1749.3, 1665.9, 1521.8, 1453.5, 1247.2, 977.4, 787.0.

Exact mass: [C$_{18}$H$_{35}$NO$_4$Na]$^+$ *m/z* = 352.26, obtained (ESI-MS) = 352.24523
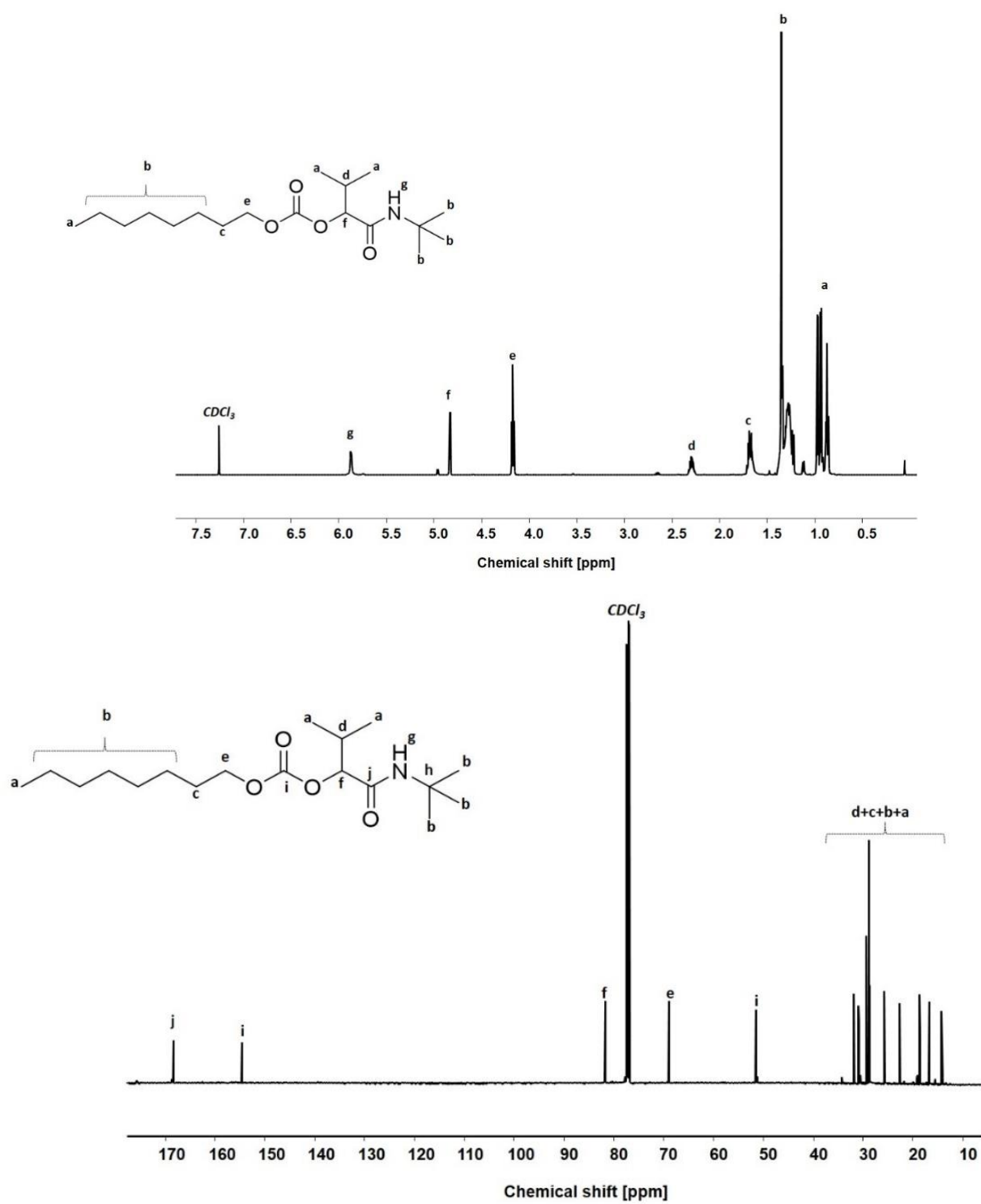
Figure 115: ^1H (top) and ^{13}C NMR (bottom) of P-4CR **15a**, measured in $CDCl_3$.

16a. Butyl (1-(cyclohexylamino)-1-oxododec-11-en-2-yl) carbonate
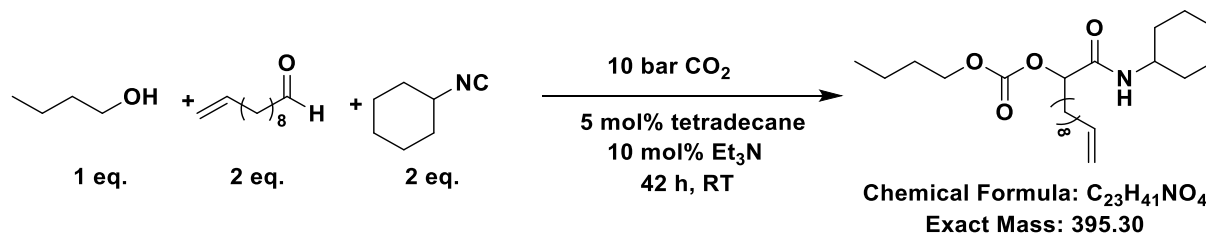
Chemical Formula: $C_{23}H_{41}NO_4$
Exact Mass: 395.30

0.41 g of butanol (1 eq., 5.50 mmol) and 5 mol% tetradecane standard (70 µL) were stirred in 1.5 mL of dichloromethane (DCM) at room temperature for 1-2 min, after which a sample was collected for GC analysis (T_0). 10 mol.% triethylamine catalyst (80 µL) was added and the mixture was saturated with CO_2 (5 bar) for 15 min. Next, 1.86 g of undecylenic aldehyde (2 eq., 11 mmol, 2.28 mL) added after which both solutions were mixed and further saturated with 5 bar of CO_2 between 10-15 min. Furthermore, 1.21 g of cyclohexyl isocyanide (2 eq., 11 mmol, 1.38 mL) was added and the reaction performed under 10 bar of CO_2 for 42 h at room temperature (22-24 °C). After 42 h, a sample was collected for GC analysis (T_f) in order to calculate the conversion. The crude mixture was concentrated via rotary evaporation and purified via column chromatography (gradient CH:EE starting from 15:1 to 5:1). The product was obtained as white powder. Conversion: 30 %, isolated yield: 43 %.

^{1}H NMR (500 MHz, CDCl$_3$) δ (ppm) = 6.00 (d, NH, 1H), 5.80 (m, CH, 1H), 5.01-4.93 (m, HC=CH$_2$,3H), 4.18 (t, CH$_2$, 2H), 3.77 (m, CH, 1H), 2.02 (q, CH$_2$, 2H), 1.87-1.14 (m, 14 CH$_2$, 28H), 0.94 (t, 3 CH$_3$, 9H).

^{13}C NMR (125 MHz, CDCl$_3$) δ (ppm) = 168.62 (j), 154.12 (i), 139.29 (f2), 114.19 (f1), 77.60 (g), 68.60 (e), 48.00 (d), 33.91, 33.01, 32.10, 30.65, 29.38, 29.26, 29.11, 28.95, 25.51, 24.85, 24.49, 18.96 (c + d), 13.71 (a).

ATR-IR: ν(cm^{-1}) = 3287.6, 3077.5, 2915.8, 2848.0, 1745.7, 1654.8, 1556.9, 1246.1, 910.4, 696.3.

Exact mass: [C$_{23}$H$_{41}$NO$_4$Na]$^+$ *m/z* = 418.30, obtained (ESI-MS) = 418.29147
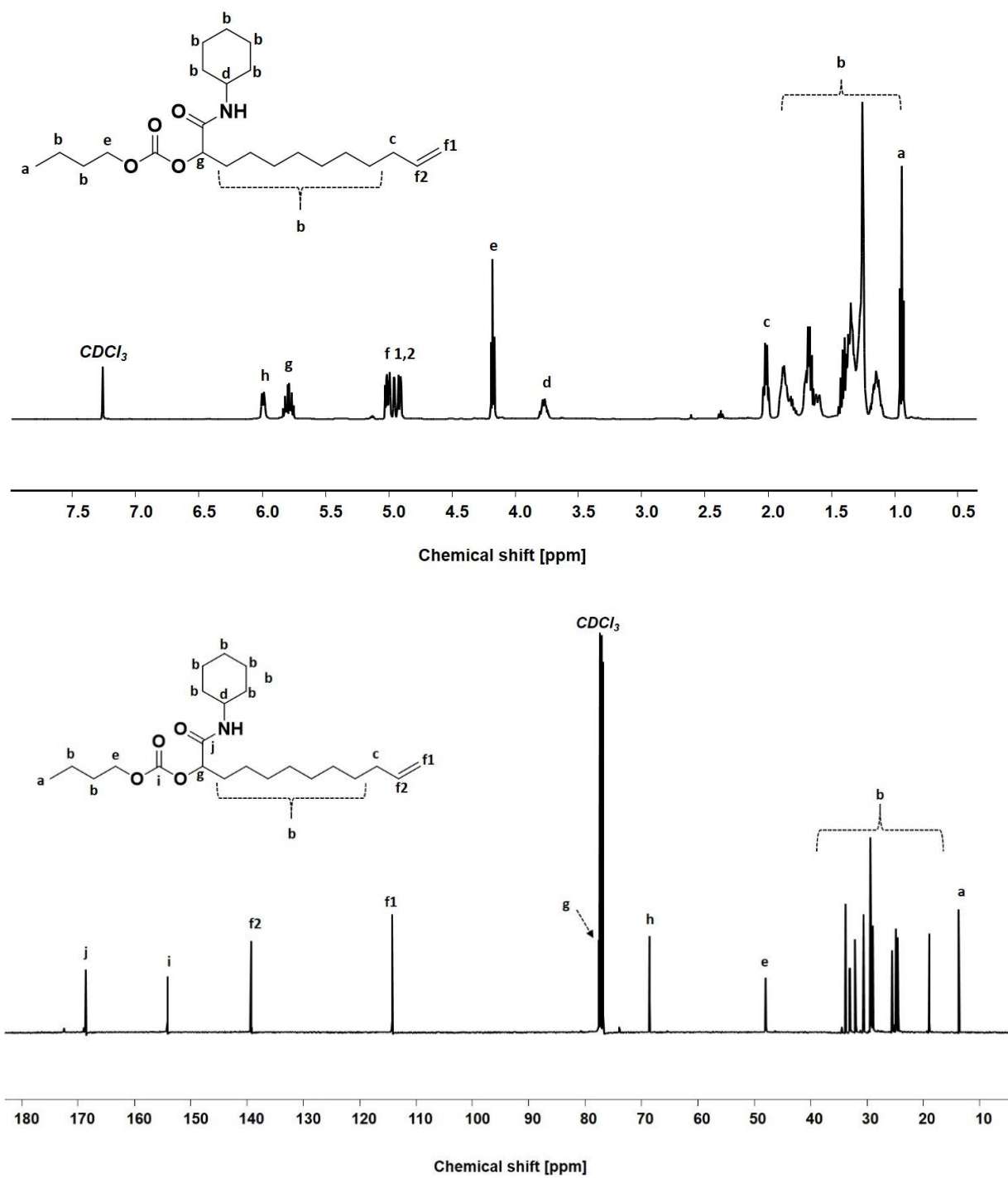
Figure 116: ¹H (top) and ¹³C NMR (bottom) of P-4CR **16a**, measured in CDCl₃.

17a. Butyl (3,3-dimethyl-1-((2-morpholinoethyl)amino)-1-oxobutan-2-yl) carbonate
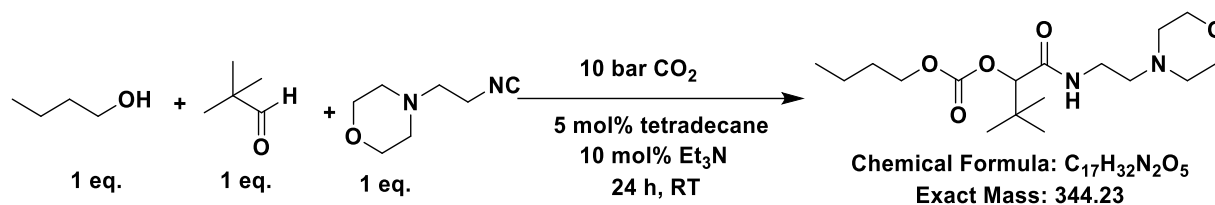
Chemical Formula: $C_{17}H_{32}N_2O_5$
Exact Mass: 344.23

0.41 g of butanol (1 eq., 5.50 mmol) and 5 mol.% tetradecane standard (70 µL) were stirred in 1.5 mL of dichloromethane (DCM) at room temperature for 1-2 min, after which a sample was collected for GC analysis (T_0). 10 mol.% triethylamine catalyst (80 µL) was added and followed by applying of CO_2 (5 bar) for 15 min. Next, 0.48 g of trimethyl acetaldehyde (1 eq., 5.50 mmol, 0.61 mL) was pre-saturated with CO_2 (5 bar) for 15 min, mixed with the CO_2-saturated butanol solution and further allowed under 5 bar of CO_2 for 15 min. Finally, 0.78 g of 2-morpholinoethyl isocyanide (1 eq., 5.50 mmol, 0.76 mL) was added and the reaction performed under 10 bar of CO_2 for 24 h at room temperature (22-24 °C). After 24 h, a sample was collected for GC analysis (T_f) in order to calculate the conversion. The crude mixture was concentrated *via* rotary evaporation and purified via column chromatography (gradient CH:EE starting from 15:1 to 5:1). The product was obtained as a viscous liquid. Conversion: 19 %, isolated yield: 24 %.

^{1}H NMR (500 MHz, CDCl$_3$) δ (ppm) = 6.53 (br, NH, 1H), 4.70 (s, CH, 1H), 4.16 (t, CH$_2$, 2H), 3.43 (m, CH$_2$OCH$_2$, , 4H), 3.32 (m, CH$_2$NCO, 2H), 2.50 (m, 3 CH$_2$N, 6H), 1.67 (m, CH$_2$, 2H), 1.40 (m, CH$_2$, 2H), 1.04 (s, 3 CH$_3$, 9H), 0.94 (t, 3 CH$_3$, 9H).

^{13}C NMR (125 MHz, CDCl$_3$) δ (ppm) = 168.41 (m), 154.56 (l), 84.50 (i), 68.56 (h), 67.00 (g), 56.89, 53.32 (e), 35.31 (f), 34.38 (k), 30.69 (d), 26.17 (b), 18.97 (c), 13.73(a).

ATR-IR: v(cm^{-1}) = 3328.3, 2960.3, 2860.6, 2805.4, 1746.1, 1666.9, 1525.3, 1454.0, 1393.1, 1366.9, 1247.0, 1117.2, 959.4, 794.1.

Exact mass: [C$_{17}$H$_{32}$N$_2$O$_5$H]$^+$ *m/z* = 345.23, obtained (ESI-MS) = 345.23720
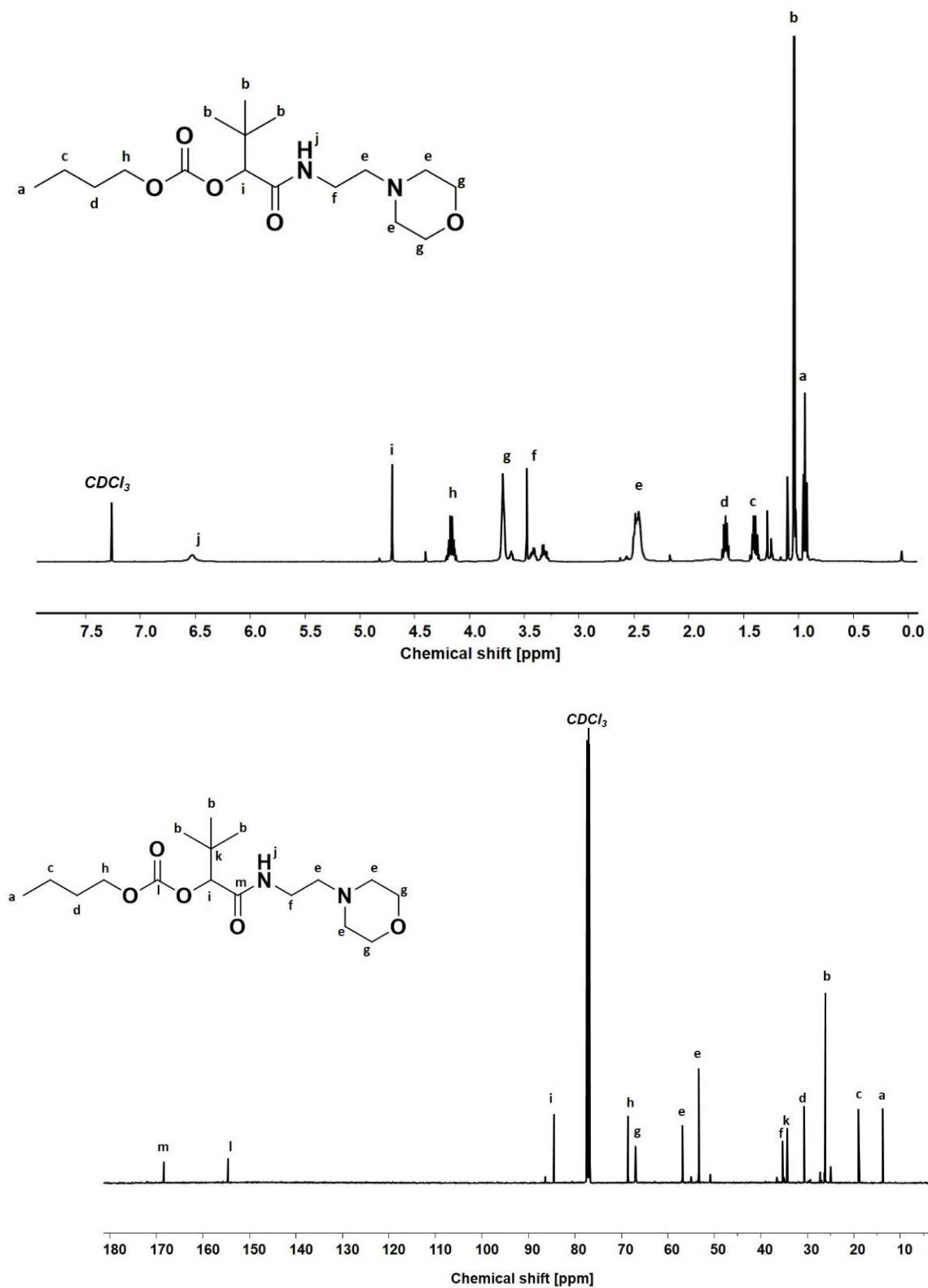
Figure 117: ¹H (top) and ¹³C NMR (bottom) of P-4CR **17a**, measured in CDCl₃.

18a. 1-(adamantan-1-ylamino)-1-oxododec-11-en-2-yl butyl carbonate
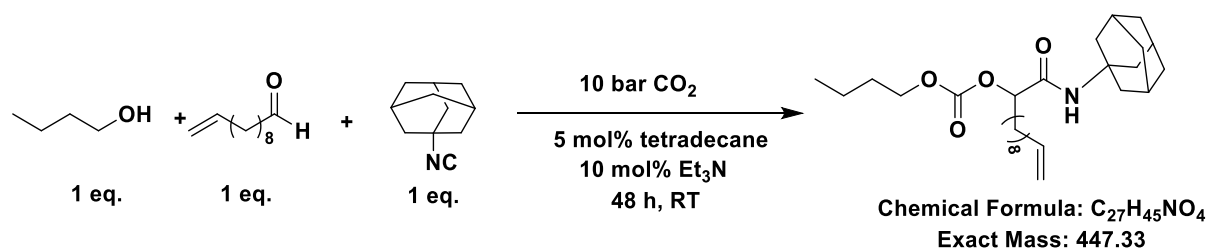
Chemical Formula: $C_{27}H_{45}NO_4$
Exact Mass: 447.33

0.41 g of butanol (1 eq., 5.50 mmol) and 5 mol% tetradecane standard (70 μL) were stirred in 1.5 mL of dichloromethane (DCM) at room temperature for 1-2 min, after which a sample was collected for GC analysis (T_0). 10 mol.% triethylamine catalyst (80 μL) was added and the mixture was saturated with CO_2 (5 bar) for 15 min. Next, 0.93 g of undecylenic aldehyde (1 eq., 5.50 mmol, 1.14 mL) added after which both solutions were mixed and further saturated with 5 bar of CO_2 between 10-15 min. Furthermore, 0.89 g of 1-adamantyl isocyanide (1 eq., 5.5 mmol) was added and the reaction performed under 10 bar of CO_2 for 48 h at room temperature (22-24 °C). After 48 h, a sample was collected for GC analysis (T_f) in order to calculate the conversion. The crude mixture was concentrated via rotary evaporation and purified *via* column chromatography (gradient CH:EE starting from 15:1 to 5:1). The product was obtained as white powder. Conversion: 16 %, isolated yield: 24 %.

^{1}H NMR (500 MHz, CDCl$_3$) δ (ppm) = 5.84-5.78 (m, NH + CH, 2H), 4.97-4.92 (e1 + e2, CH=CH$_2$, 3H), 4.18 (t, CH$_2$, 2H), 2.08-1.67 (m, 8 CH$_2$ + 3 CH, 19H), 1.36-1.26 (m, 8 CH$_2$, 16H), 0.95 (t, 3 CH$_3$, 9H).

^{13}C NMR (125 MHz, CDCl$_3$) δ (ppm) = 168.51 (j), 154.35 (i), 139.43 (e2), 114.34 (e1), 77.74 (f), 68.54 (d), 52.03 (h), 41.56, 36.35, 33.87, 32.04, 30.68, 29.47, 29.40, 29.30, 28.98, 24.48, 18.99 (c + b), 13.75 (a).

ATR-IR: v(cm^{-1}) = 3309.9, 3081.3, 2907.0, 2845.1, 1747.7, 1657.4, 1552.0, 1228.9, 898.6, 630.4.

Exact mass: [C$_{27}$H$_{45}$NO$_4$Na]$^+$ *m/z* = 470.33, obtained (ESI-MS) = 470.32294
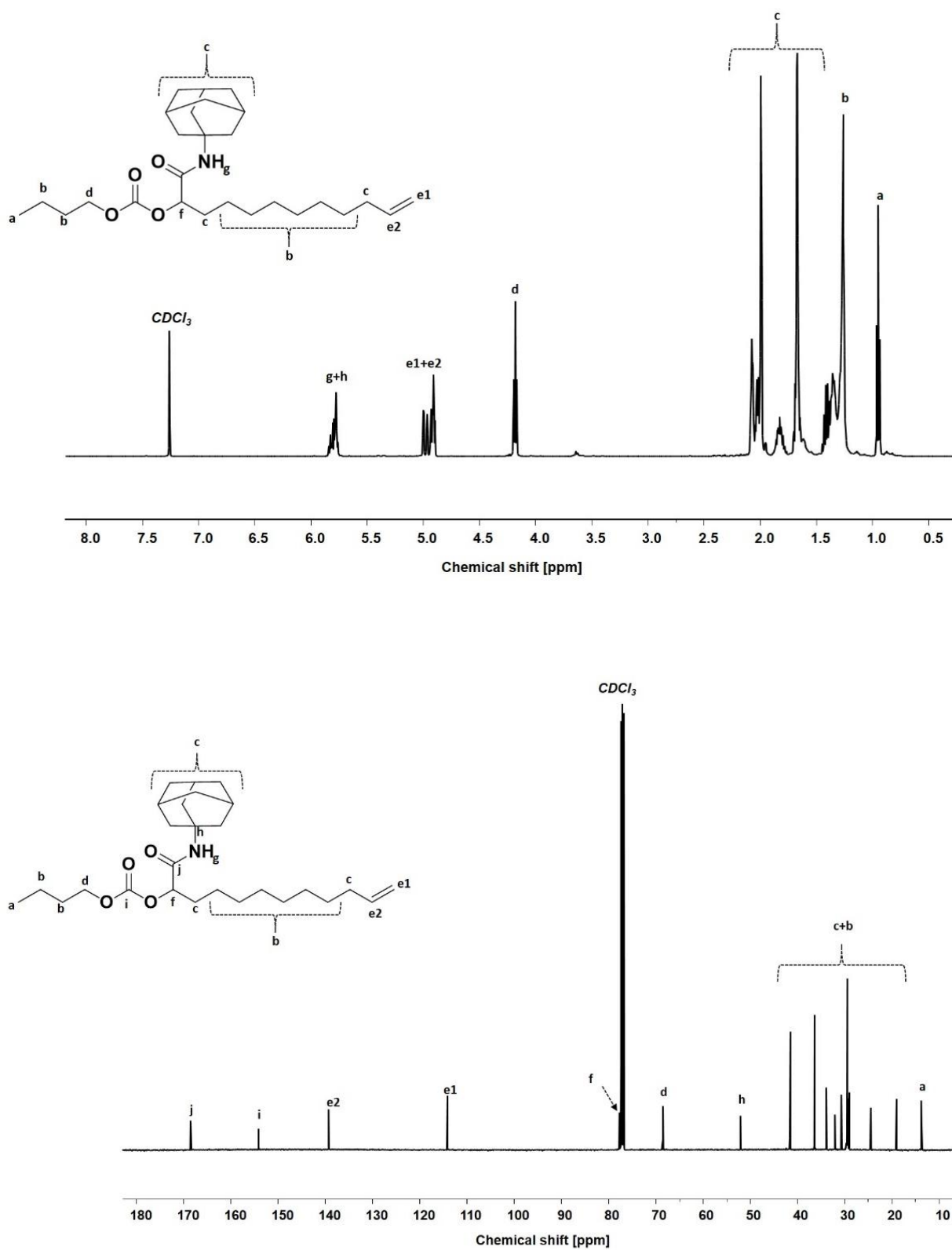
Figure 118: ^{1}H (top) and ^{13}C NMR (bottom) of P-4CR **18a**, measured in CDCl₃.

19a. Butyl (2-(tert-butylamino)-1-(2,4-dinitrophenyl)-2-oxoethyl) carbonate
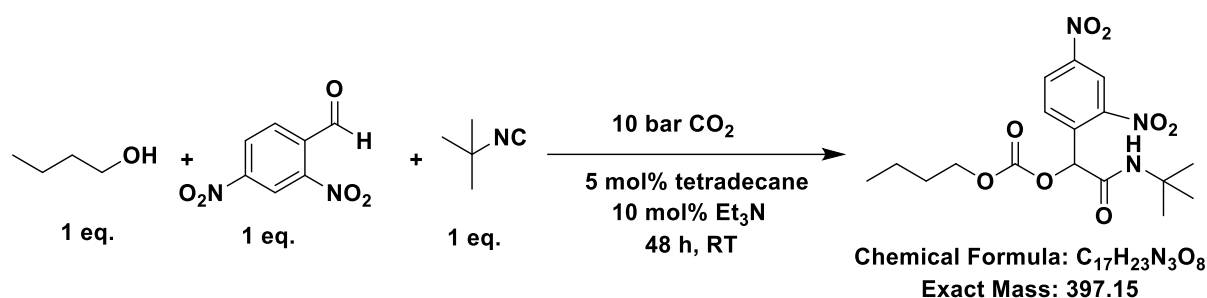
Chemical Formula: $C_{17}H_{23}N_3O_8$
Exact Mass: 397.15

0.41 g of butanol (1 eq., 5.50 mmol) and 5 mol% tetradecane standard (70 µL) were stirred in 1.5 mL of dichloromethane (DCM) at room temperature for 1-2 min, after which a sample was collected for GC analysis (T_0). 10 mol.% triethylamine catalyst (80 µL) was added and the mixture was saturated with CO_2 (5 bar) for 15 min. Next, 1.08 g of 2,4-dinitrobenzaldehyde (1 eq., 5.50 mmol) added, allowed to solubilize in the butanol-DCM-CO_2 mixture and further saturated with 5 bar of CO_2 between 10-15 min. Furthermore, 0.46 g of *tert* butyl isocyanide (1 eq., 5.50 mmol, 0.63 mL) was added and the reaction performed under 10 bar of CO_2 for 48 h at room temperature (22-24 °C). After 48 h, a sample was collected for GC analysis (T_f) in order to calculate the conversion and relative ratio values between the P-4CR and its hydrolysis product. The crude mixture was concentrated *via* rotary evaporation and purified via column chromatography (gradient CH:EE starting from 15:1 to 2:1). The product was obtained as white powder. Conversion: 40 %, isolated yield: 22 %.

^{1}H NMR (500 MHz, CDCl$_3$) δ (ppm) = 8.86 (d, Ar-CH, 1H), 8,47 (dd, Ar-CH, 1H), 7.93 (d, Ar-CH, 1H), 6.63 (s, CH, 1H), 6.29 (br, NH, 1H), 4.21 (m, CH$_2$, 2H), 1.66 (m, CH$_2$, 2H), 1.42-1.36 (m, 3 CH$_3$, + CH$_2$, 11H), 0.94 (t, 3 CH$_3$, 9H).

^{13}C NMR (125 MHz, CDCl$_3$) δ (ppm) = 164.18 (o), 153.75 (n), 148.38 (m), 147.85 (l), 137.32 (k), 130.73 (g), 127.54 (h), 120.47 (i), 73.92 (f), 69.60 (d), 52.35 (j), 30.52 (c), 28.61, 18.88 (b), 13.67 (a).

ATR-IR: v(cm^{-1}) = 3415.4, 3113.2, 2969.0, 2932.2, 2862.5, 1755.1, 1668.2, 1532.3, 1345.6, 1248.8, 912.3, 735.5.

Exact mass: [C$_{17}$H$_{23}$N$_3$O$_8$Na]$^+$ *m/z* = 420.15, obtained (ESI-MS) = 420.13640
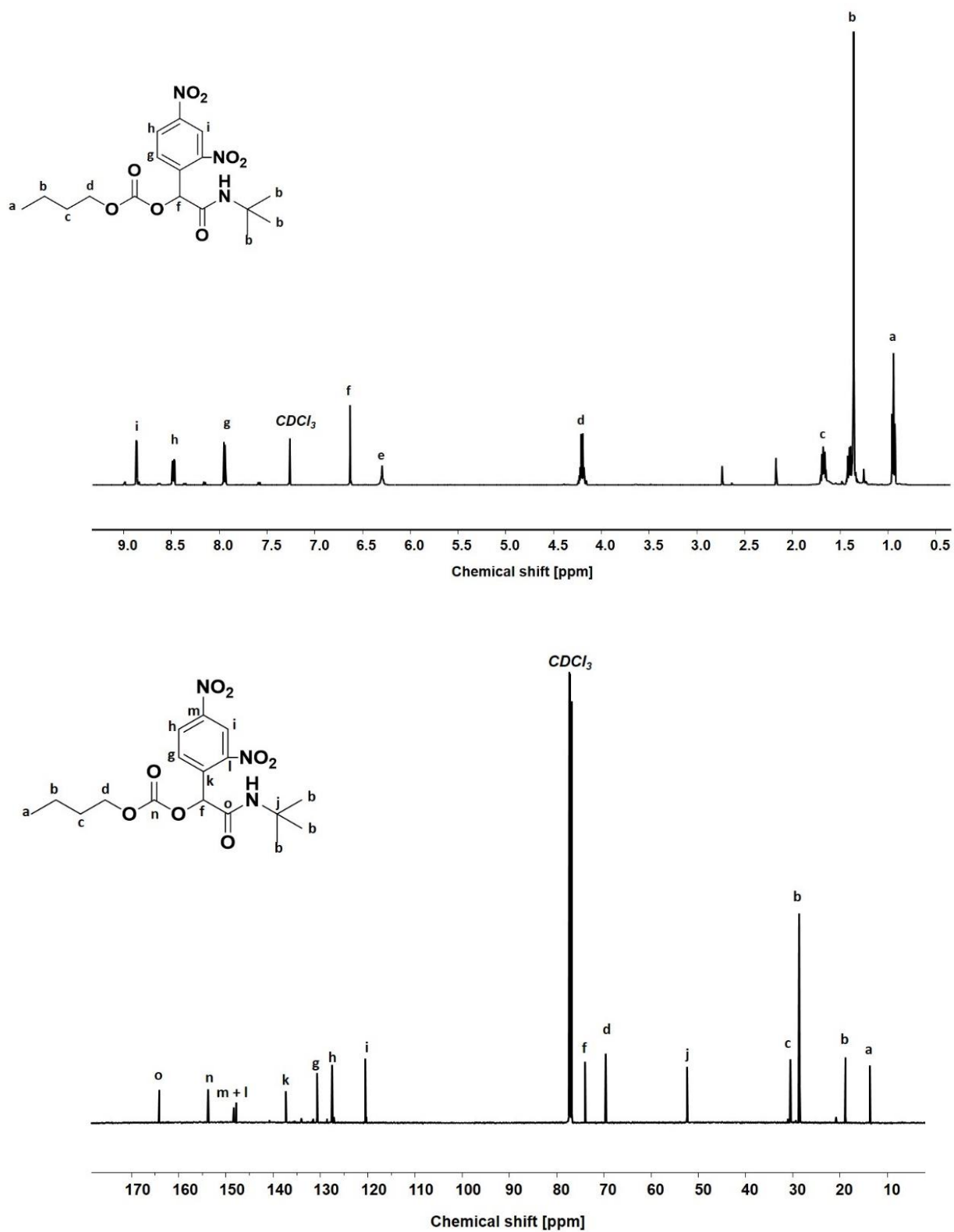
Figure 119: ^{1}H (top) and ^{13}C NMR (bottom) of P-4CR **19a**, measured in CDCl$_3$.

20a. 1-(tert-butylamino)-1-oxododec-11-en-2-yl cyclohexyl carbonate

Chemical Formula: $C_{23}H_{41}NO_4$
Exact Mass: 395.30
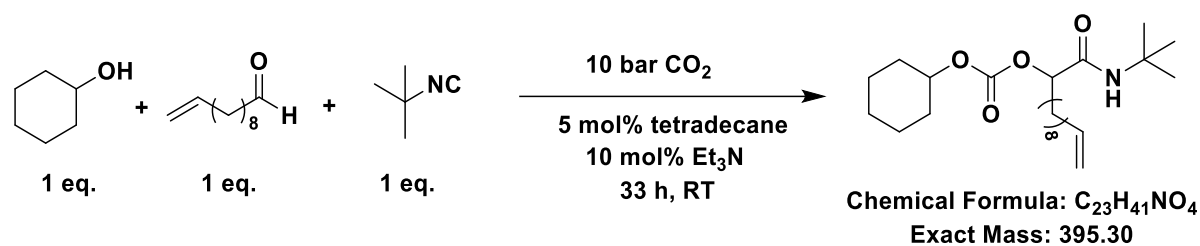
0.55 g of cyclohexanol (1 eq., 5.50 mmol) and 5 mol% tetradecane standard (70 µL) were stirred in 1.5 mL of dichloromethane (DCM) at room temperature for 1-2 min, after which a sample was collected for GC analysis (T_0). 10 mol.% triethylamine catalyst (80 µL) was added and the mixture was saturated with CO_2 (5 bar) for 15 minutes. Next, 0.93 g of undecylenic aldehyde (1 eq., 5.50 mmol, 1.14 mL) was added after which both solutions were mixed and further saturated with 5 bar of CO_2 between 10-15 min. Furthermore, 0.46 g of *tert* butyl isocyanide (1 eq., 5.50 mmol, 0.63 mL) was added and the reaction performed under 10 bar of CO_2 for 33 h at room temperature (22-24 °C). After 33 h, a sample was collected for GC analysis (T_f) in order to calculate the conversion and relative ratio values between observed products. The crude mixture was concentrated via rotary evaporation and purified via column chromatography (gradient CH:EE starting from 15:1 to 5:1). The product was obtained as sticky white powder. Conversion: 35 %, isolated yield: 18 %.

^{1}H NMR (500 MHz, CDCl$_3$) δ (ppm) = 5.92 (s, NH, 1H), 5.79 (m, CH, 1H), 4.98-4.88 (m, CH=CH$_2$, 3H), 4.61 (m, CH, 1H), 2.00-1.25 (m, 3 CH$_3$ + 13 CH$_2$, 35H).

^{13}C NMR (125 MHz, CDCl$_3$) δ (ppm) = 168.92 (h), 154.47 (g), 139.22 (c2), 114.16 (c1), 77.61 (b + d), 51.29 (f), 33.83, 31.89, 31.54, 29.35, 29.23, 29.09, 28.73, 26.94, 25.19, 24.52, 23.11 (a).

ATR-IR: v(cm^{-1}) = 3315.68, 3074.56, 2923.50, 2860.56, 1752.74, 1663.65, 1520.34, 1454.49, 1245.32, 1015.82, 900.58, 794.06.

Exact mass: [C$_{23}$H$_{41}$NO$_4$Na]$^+$ *m/z* = 418.30, obtained (ESI-MS) = 418.29147
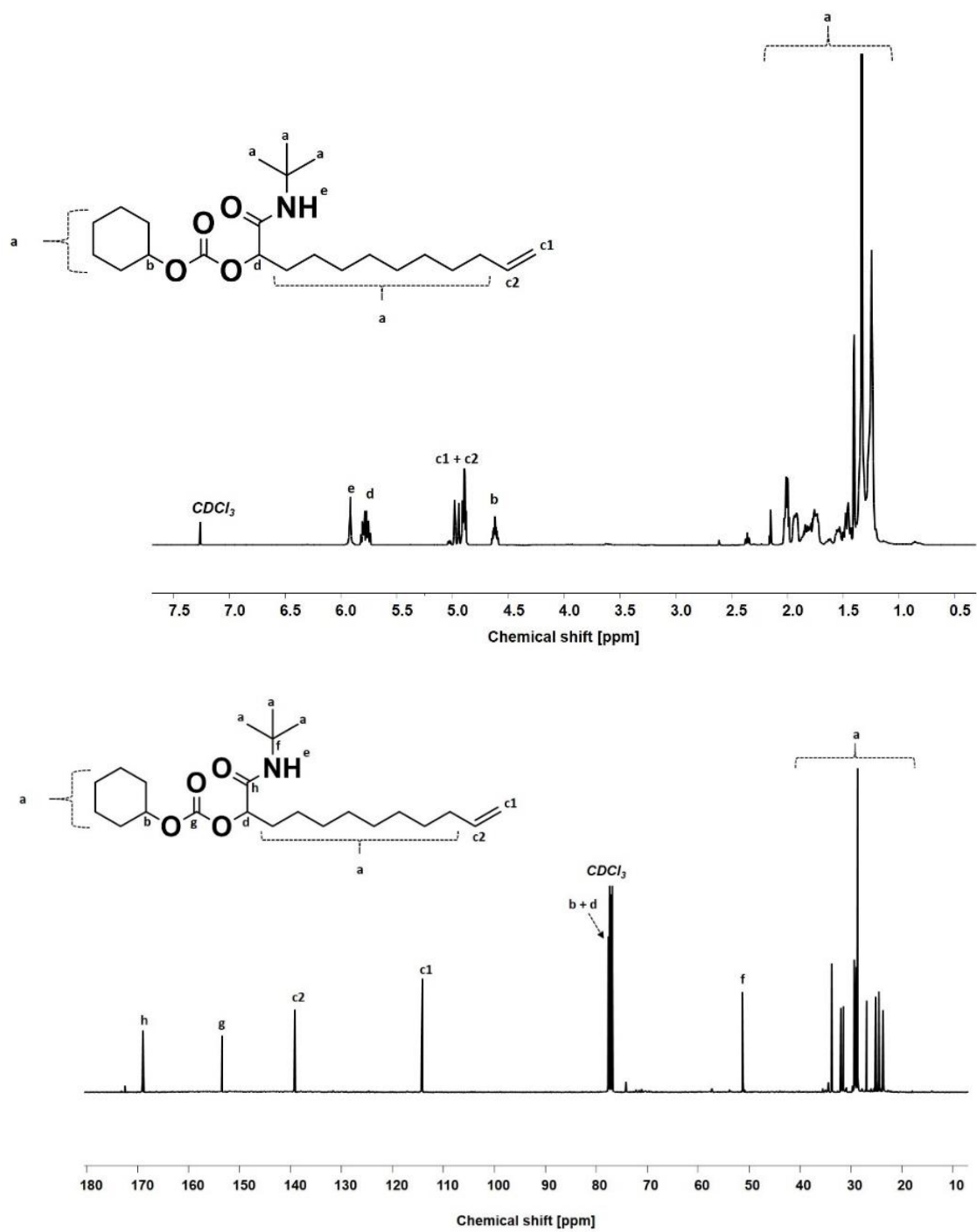
Figure 120: ^1H (top) and ^{13}C NMR (bottom) of P-4CR **20a**, measured in CDCl₃.

Hydrolysis product **11c***: N*-(tert-butyl)-2-hydroxy-3-methylbutanamide

Isolated yield: 30 %

^{1}H NMR (500 MHz, CDCl$_3$) δ (ppm) = 6.19 (s, NH, 1H), 3.94 (t, CH, 1H), 3.81 (m, CH, 1H), 2.45 (d, OH, 1H), 2.13 (m, CH, 1H), 1.91, 1.71, 1.62 (m, 3 CH$_2$, 6H), 1.37, 1.18 (m, 2 CH$_2$, 4H), 1.02, 0.85 (d, 2 CH$_3$, 6H).

^{13}C NMR (125 MHz, CDCl$_3$) δ (ppm) = 172.04 (i), 76.28 (g), 48.02 (f), 33.38, 33.24, 32.19 (d + c), 25.64, 24.94 (b), 19.26, 15.46 (a).

ATR-IR: v(cm^{-1}) = 3326.3, 3219.0, 2927.6, 2852.3, 1631.9, 1533.3, 1451.0, 1023.7, 750.3.

Exact mass: [C$_{11}$H$_{21}$NO$_2$Na]$^+$ *m/z* = 222.16, obtained (ESI-MS) = 222.150531
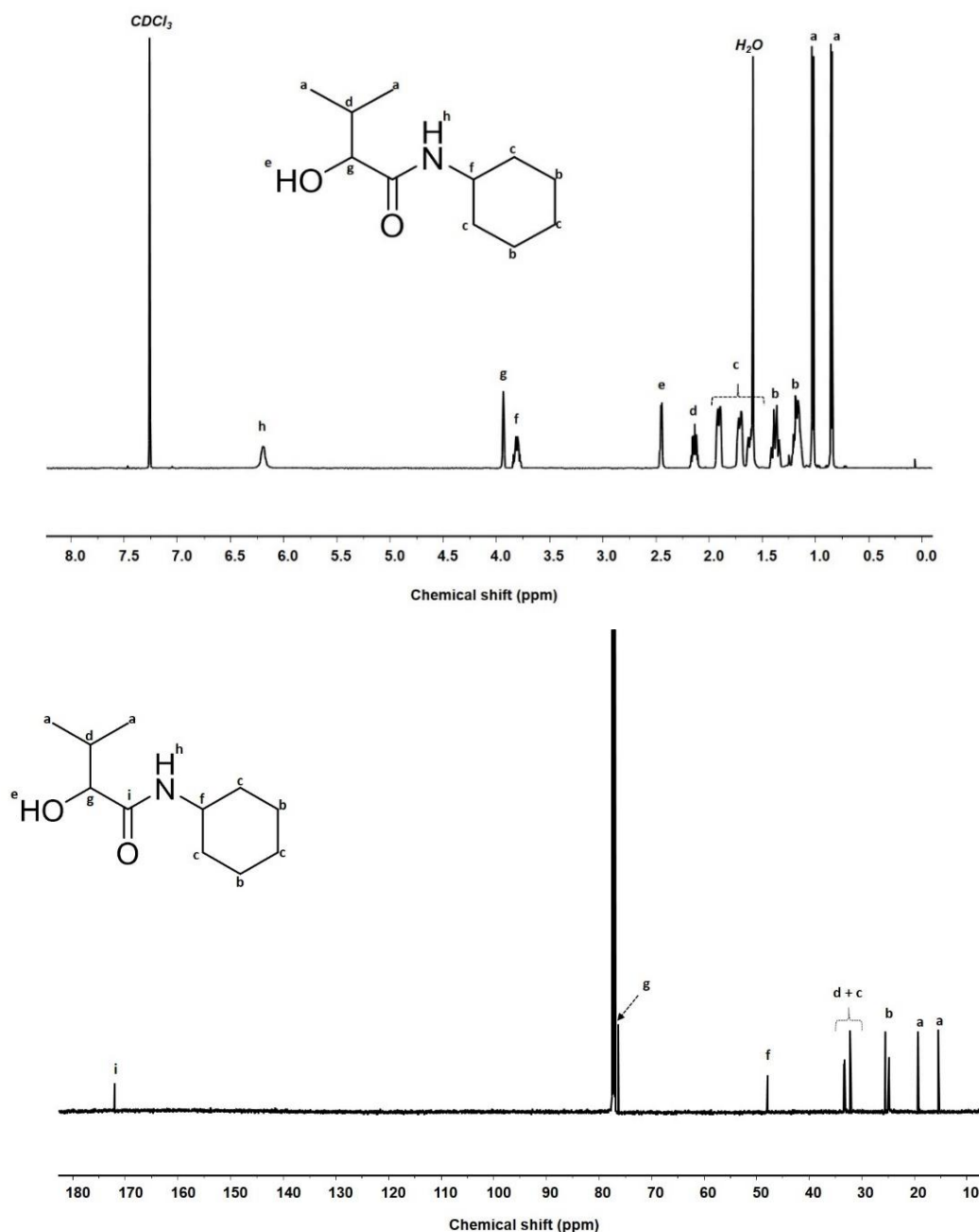
Figure 121: ^{1}H (top) and ^{13}C NMR (bottom) of the hydrolysis product **11c**, measured in CDCl$_3$.

Hydrolysis product **13a**: *N*-cyclohexyl-2-hydroxy-3-methylbutanamide

Isolated yield: 23 %

^{1}H NMR (500 MHz, CDCl$_3$) δ (ppm) = 6.31 (s, NH, 1H), 3.81 (d, CH, 1H), 3.05 (s, OH, 1H), 2.09 (m, CH, 1H), 1.35 (s, 3 CH$_3$, 9H), 1.00, 0.83 (d, 2 CH$_3$, 6H).

^{13}C NMR (125 MHz, CDCl$_3$) δ (ppm) = 172.81 (h), 76.21 (e), 51.15 (g), 32.06 (c), 28.87 (b), 19.32, 15.46 (a).

ATR-IR: v (cm⁻¹) = 3340.3, 3257.9, 2956.6, 2931.7, 2868.6, 1639.0, 1532.5, 1457.1, 1025.8, 709.9.

Exact mass: [C₉H₁₉NO₂Na]⁺ *m/z* = 196.14, obtained (ESI-MS) = 196.13054
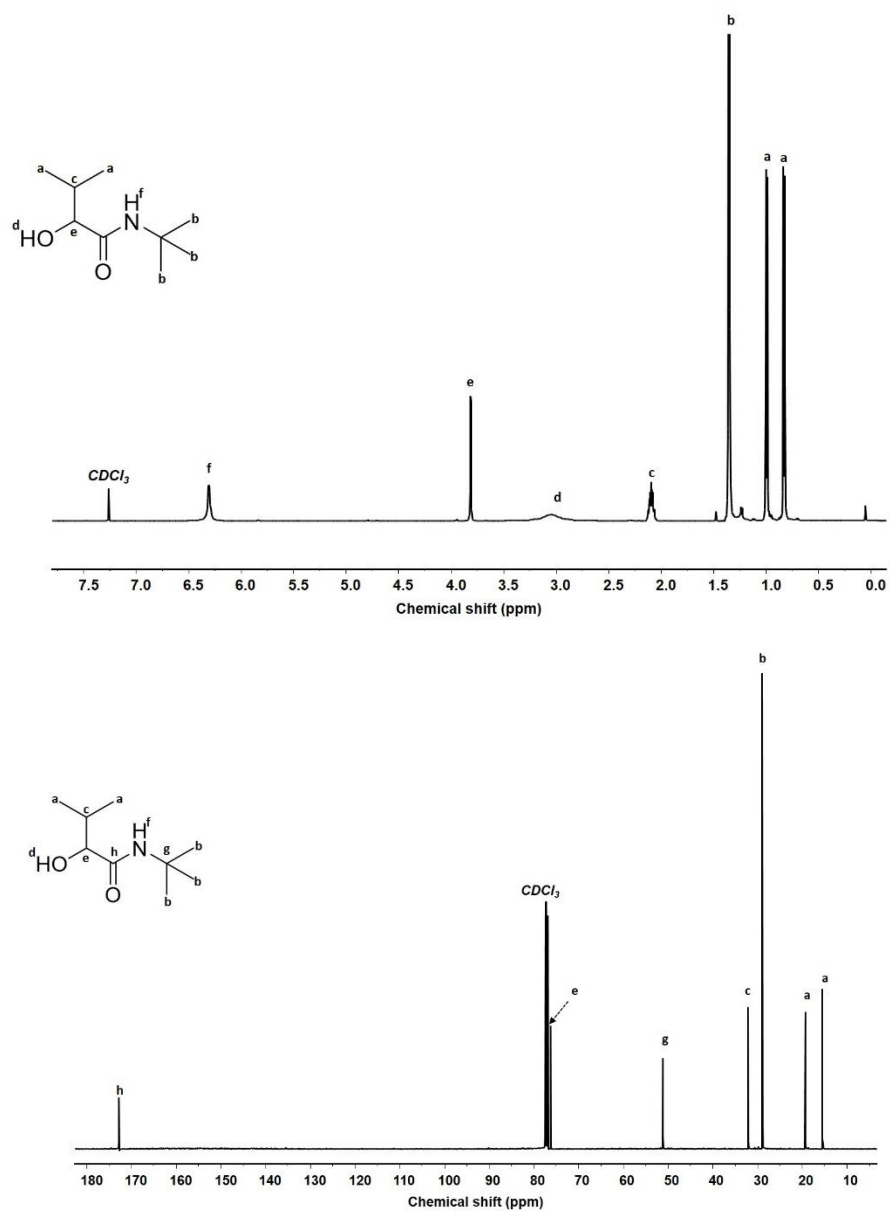
Figure 122: ¹H (top) and ¹³C NMR (bottom) of the hydrolysis product **13a**, measured in CDCl₃.

Hydrolysis product **19a**: N-(tert-butyl)-2-(2,4-dinitrophenyl)-2-hydroxyacetamide

Isolated yield: 63%

^{1}H NMR (500 MHz, CDCl$_3$) δ (ppm) = 8.77 (d, Ar-CH, 1H), 8.47 (dd, Ar-CH, 1H), 7.90 (d, Ar-CH, 1H), 6.72 (s, NH, 1H), 5.61 (s, CH, 1H), 4.63 (br, OH, 1H), 1.32 (s, 3 CH$_3$, 9H).

^{13}C NMR (125 MHz, CDCl$_3$) δ (ppm) = 168.19 (l), 148.72 (k), 147.40 (j), 142.23 (i), 130.95 (e), 127.87 (f), 120.16 (g), 68.29 (c), 52.21 (h), 28.59 (a).

ATR-IR: ν (cm^{-1}) = 3399.0, 3294.5, 3124.0, 2927.9, 2860.6, 1655.5, 1527.5, 1347.9, 1086.9, 1060.1, 914.6, 836.2, 733.1, 710.8, 569.8.

Exact mass: [C$_{12}$H$_{15}$N$_3$O$_6$Na]$^+$ *m/z* = 320.10, obtained (ESI-MS) *m/z* = 320.0842
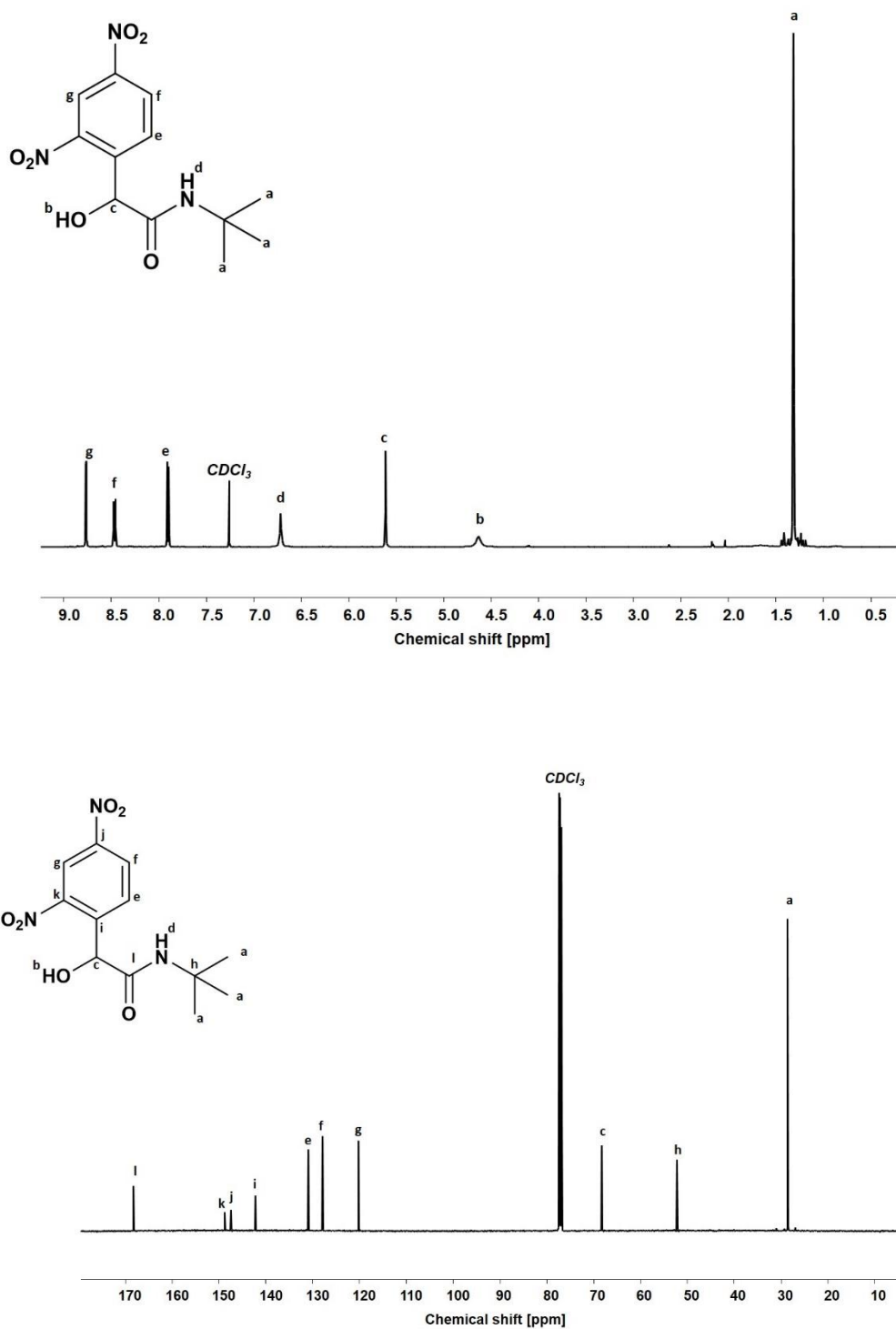
Figure 123: ^{1}H (top) and ^{13}C NMR (bottom) of the hydrolysis product **19a**, measured in CDCl$_3$.

9. Appendix

9.1 Bibliography

(1) *Petroleum; Encyclopædia Britannica;* Chisholm, H., Ed., 11th ed.; Cambridge University Press, **1911**.

(2) Russell, L. S. *A heritage of light: Lamps and lighting in the early Canadian home*; University of Toronto Press: Toronto, Buffalo, **2003**.

(3) Geyer, R.; Jambeck, J. R.; Law, K. L. Production, use, and fate of all plastics ever made. *Sci. Adv.* **2017**, *3*, e1700782.

(4) PlasticEurope. The Plastic Industry report Berlin **2016**.

(5) Thompson, R. C.; Moore, C. J.; Vom Saal, F. S.; Swan, S. H. Plastics, the environment and human health: current consensus and future trends. *Philos. Trans. R. Soc. London. Ser. B.* **2009**, *364*, 2153–2166.

(6) Thompson, R. C.; Swan, S. H.; Moore, C. J.; Vom Saal, F. S. Our plastic age. *Philos. Trans. R. Soc. London. Ser. B.* **2009**, *364*, 1973–1976.

(7) The price of oil - in context. *CBC News,* 18th April **2006**.

(8) United Nations Environment Programme. *Environmental assessment of Ogoniland*; United Nations Environment Programme: Nairobi Kenya, **2011**.

(9) World Economy Forum. The New Plastic Economy: Rethinking the future of plastics **2016**.

(10) Marc, L. What Is the Greenhouse Effect? *livescience.com*.

(11) Jancovici, J.-M. What is the greenhouse effect. In *jancovici.com*; Jancovici, J.-M., Ed.

(12) Umair, S.R. Global Warming: Causes, Effects and Solutions. *Dureeamin Journal* **2015**, *Aug vol. 1*.

(13) Brundtland, C. G. *Our Common Future, The World Commission on Environmental Development*; Oxford University Press: Oxford, 1987.

(14) *Paris 2015: Getting a global agreement on climate change;* Willis, R., Ed.; Green Alliance: London, 2014.

(15) European Comission. *Single-use plastics*; Brussels, May 2018.

(16) Sheldon, R. A. *Chem. Ind. (London)* **1992**, 903–906.

(17) Sheldon, R. A. The E Factor: fifteen years on. *Green Chem.* **2007**, *9*, 1273.

(18) Anastas, P. T.; Warner, J. C. *Green chemistry: Theory and practice*, 1st ed.; Oxford University Press: Oxford, 2000.

(19) Anastas, P. T.; Zimmerman, J. B. Twelve Principles of Green Engineering. *Env. Sci. Tech.* **2003**, *37*, 94A-101A.

(20) Röper, H. Renewable Raw Materials in Europe – Industrial Utilisation of Starch and Sugar. *Starch* **2002**, *54*, 89–99.

(21) Introduction: Green Chemistry and Catalysis. In *Green Chemistry and Catalysis*; Sheldon, R. A., Arends, I. W. C. E., Hanefeld, U., Eds.; Wiley-VCH Verlag GmbH & Co. KGaA: Weinheim, Germany, 2007; pp 1–47.

(22) Sheldon, R. A. Green and sustainable manufacture of chemicals from biomass: state of the art. *Green Chem.* **2014**, *16*, 950–963.

(23) Delidovich, I.; Hausoul, P. J. C.; Deng, L.; Pfützenreuter, R.; Rose, M.; Palkovits, R. Alternative Monomers Based on Lignocellulose and Their Use for Polymer Production. *Chem. Rev.* **2016**, *116*, 1540–1599.

(24) Rose, M.; Palkovits, R. Cellulose-based sustainable polymers: state of the art and future trends. *Macromol. Rapid. Comm.* **2011**, *32*, 1299–1311.

(25) Putro, J. N.; Soetaredjo, F. E.; Lin, S.-Y.; Ju, Y.-H.; Ismadji, S. Pretreatment and conversion of lignocellulose biomass into valuable chemicals. *RSC Adv.* **2016**, *6*, 46834–46852.

(26) Klemm, D.; Heublein, B.; Fink, H.-P.; Bohn, A. Cellulose: fascinating biopolymer and sustainable raw material. *Angew. Chem. Int. Ed. Engl.* **2005**, *44*, 3358–3393.

(27) Payen, A. *C. R. Hebd. Seances Acad. Sci.* **1838**, *7*, 1052.

(28) Payen, A. *C. R. Hebd. Seances Acad. Sci.* **1838**, *7*, 1125.

(29) Brogniartm, A. Pelonze, A. B. Dumas, R. *Comptes Rendus* **1839**, *8*, 51–53.

(30) Stevens, C. V.; Verhé, R. *Renewable bioresources: Scope and modification for non-food applications / editors Christian V. Stevens with Roland Verhé*; J. Wiley: Chichester, 2004.

(31) Cannon, R. E.; Anderson, S. M. Biogenesis of bacterial cellulose. *Crit. Rev. Microbiol.* **1991**, *17*, 435–447.

(32) Rainer, J.; Luiz, F.F. Production and application of microbial cellulose. *Polym. Degrad. Stab.* **1998**, *59*, 101–106.

(33) Vandamme, E. J.; Baets, S. de; Vanbaelen, A.; Joris, K.; Wulf, P. de. Improved production of bacterial cellulose and its application potential. *Polym. Degrad. Stab.* **1998**, *59*, 93–99.

(34) Moon, R. J.; Martini, A.; Nairn, J.; Simonsen, J.; Youngblood, J. Cellulose nanomaterials review: structure, properties and nanocomposites. *Chem. Soc. Rev.* **2011**, *40*, 3941–3994.

(35) Abdul Khalil, H.P.S.; Bhat, A. H.; Ireana Yusra, A. F. Green composites from sustainable cellulose nanofibrils: A review. *Carbohydr. Polym.* **2012**, *87*, 963–979.

(36) Isikgor, F. H.; Becer, C. R. Lignocellulosic biomass: a sustainable platform for the production of bio-based chemicals and polymers. *Polym. Chem.* **2015**, *6*, 4497–4559.

(37) Staudinger, H. Uber Polymerisation. *Ber. Dtsch. Chem. Ges.* **1920**, *53*, 1073–1085.

(38) Ferrier, W. G. The crystal and molecular structure of β-D-glucose. *Acta Cryst* **1963**, *16*, 1023–1031.

(39) Aburto, J.; Alric, I.; Thiebaud, S.; Borredon, E.; Bikiaris, D.; Prinos, J.; Panayiotou, C. Synthesis, Characterization, and Biodegradability of Fatty- Acid Esters of Amylose and Starch. *J. Appl. Polym. Sci.* **1999**, *74*, 1440–1451.

(40) Winkler, H.; Vorwerg, W.; Wetzel, H. Synthesis and properties of fatty acid starch esters. *Carbohydr. Polym.* **2013**, *98*, 208–216.

(41) Richter, A.; Klemm, D. Regioselective sulfation of trimethylsilyl cellulose using different SO_3-complexes. *Cellulose* **2003**, *10*, 133–138.

(42) Altaner, C.; Saake, B.; Puls, J. Mode of action of acetylesterases associated with endoglucanases towards water-soluble and -insoluble cellulose acetates. *Cellulose* **2001**, *8*, 259–265.

(43) Altaner, C.; Puls, J.; Saake, B. Enzymes aided analysis of the substituent distribution along the chain of cellulose acetates regioselectively modified by the action of Aspergillus niger acetylesterase. *Cellulose* **2003**, *10*, 391–395.

(44) Billès, E.; Onwukamike, K. N.; Coma, V.; Grelier, S.; Peruch, F. Cellulose oligomers production and separation for the synthesis of new fully bio-based amphiphilic compounds. *Carbohydr. Polym.* **2016**, *154*, 121–128.

(45) Habibi, Y.; Lucia, L. A.; Rojas, O. J. Cellulose nanocrystals: chemistry, self-assembly, and applications. *Chem. Rev.* **2010**, *110*, 3479–3500.

(46) Hindi, S.S. Microcrystalline Cellulose: The Inexhaustible Treasure for Pharmaceutical Industry. *Nanoscience and Nanotechnology Research* **2017**, *4*, 17–24.

(47) Klemm, D.; Kramer, F.; Moritz, S.; Lindström, T.; Ankerfors, M.; Gray, D.; Dorris, A. Nanocelluloses: a new family of nature-based materials. *Angew. Chem. Int. Ed. Engl.* **2011**, *50*, 5438–5466.

(48) Roller, S.; Jones, S. A. *Handbook of fat replacers*; CRC Press: Boca Raton, London, 1996.

(49) Lavoine, N.; Desloges, I.; Dufresne, A.; Bras, J. Microfibrillated cellulose - its barrier properties and applications in cellulosic materials: a review. *Carbohydr. Polym.* **2012**, *90*, 735–764.

(50) Golmohammadi, H.; Morales-Narváez, E.; Naghdi, T.; Merkoçi, A. Nanocellulose in Sensing and Biosensing. *Chem. Mater.* **2017**, *29*, 5426–5446.

(51) O'Sullivan, A. C. Cellulose: the structure slowly unravels. *Cellulose* **1997**, *4*, 173–207.

(52) Azizi Samir, M. A. S.; Alloin, F.; Dufresne, A. Review of recent research into cellulosic whiskers, their properties and their application in nanocomposite field. *Biomacromolecules* **2005**, *6*, 612–626.

(53) Nishiyama, Y. Structure and properties of the cellulose microfibril. *J Wood Sci* **2009**, *55*, 241–249.

(54) Yamamoto, H. In Situ crystallization of bacterial cellulose I. Influences of polymeric additives, stirring and temperature on the formation celluloses I-alpha and I-beta as revealed by cross polarization/magic angle spinning (CP/MAS) ^{13}C NMR spectroscopy. *Cellulose* **1994**, *1*, 57–66.

(55) Yamamoto, H.; Horii, F. CPMAS carbon-13 NMR analysis of the crystal transformation induced for Valonia cellulose by annealing at high temperatures. *Macromolecules* **1993**, *26*, 1313–1317.

(56) Ishikawa, A.; Okano, T. Fine structure and tensile properties of ramie fibres in the crystalline form of cellulose I, II, IllI and IV. *Polymer* **1997**, *38*, 463–468.

(57) Nishiyama, Y.; Langan, P.; Chanzy, H. Crystal Structure and Hydrogen-Bonding System in Cellulose Iβ from Synchrotron X-ray and Neutron Fiber Diffraction. *J. Am. Chem. Soc.* **2002**, *124*, 9074–9082.

(58) Nishiyama, Y.; Sugiyama, J.; Chanzy, H.; Langan, P. Crystal structure and hydrogen bonding system in cellulose I(alpha) from synchrotron X-ray and neutron fiber diffraction. *J. Am. Chem. Soc.* **2003**, *125*, 14300–14306.

(59) Langan, P.; Nishiyama, Y.; Chanzy, H. X-ray Structure of Mercerized Cellulose II at 1 Å Resolution. *Biomacromolecules* **2001**, *2*, 410–416.

(60) Ek, M.; Gellerstedt, G.; Henriksson, G. *Pulp and Paper Chemistry and Technology*; de Gruyter: Berlin, **2009**.

(61) Sjöström, E. *Wood chemistry: Fundamentals and applications / Eero Sjöström*, 2nd ed.; Academic Press: San Diego, London, **1993**.

(62) Botello, J. I.; Gilarranz, M. A.; Rodríguez, F.; Oliet, M. Preliminary study on products distribution in alcohol pulping of Eucalyptus globulus. *J. Chem. Technol. and Biot.* **1999**, *74*, 141–148.

(63) Schoenbein, C.F. *Pogg. Ann* **1846**, *70*, 220.

(64) Schoenbein, C.F. *Ber. Naturforsch. Ges. Basel* **1847**, *7*, 27.

(65) Wertz, J.-L.; Bédué, O.; Mercier, J.-P. *Cellulose Science and Technology*; EPFL Press: Lausanne, **2010**.

(66) Hyatt, J.W. US Patent 50,359, **1865**.

(67) Chardonnet, A. M. French Patent 165,349, **1884**.

(68) Schweizer, E. *J. Prakt. Chem* **1857**, *72*, 109.

(69) Despeissis, L.H. French patent 203,741, 1890.

(70) Cross, C. F.; Bevan, E. J.; Beadle, C. British Patent 8,700, 1892.

(71) Mueller, M. British Patent 10094, 1906.

(72) Ekman, K.; Turenen, O. T.; Huttunen, J. I. Finnish Patent 61,033, 1982.

(73) Hill, J. W.; Jacobson, R. A. U.S. Patent 2,134,825.

(74) Jacobson, R. A. Carbamic Esters from Urea. *J. Am. Chem. Soc.* **1938**, *60*, 1742–1744.

(75) Loth, F.; Schaaf, E.; Fink, H.-P.; Kunze, J.; Gensrich, H.-J. PCT Patent WO002004046198A1, **2004**.

(76) Johnson, D.L. US patent 3447956 A, **1969**.

(77) Swatloski, R. P.; Spear, S. K.; Holbrey, J. D.; Rogers, R. D. Dissolution of Cellose with Ionic Liquids. *J. Am. Chem. Soc.* **2002**, *124*, 4974–4975.

(78) Sixta, H.; Michud, A.; Hauru, L.; Asaadi, S.; Ma, Y. King, A.W.T. Kilpeläinen, I. Hummel, M. Ioncell-F: A High-strength regenerated cellulose fibre. *NPPRJ.* **2015**, *33*, 43–57.

(79) Heinze, T.; Liebert, T. *Celluloses and Polyoses/Hemicelluloses. In Polymer science: A comprehensive reference: Eds, Krzysztof Matyjaszewski, Martin Möller*; Elseiver: Amsterdam, **2012**.

(80) Schuetzenberger, J. *Compt. rend. Acad. Sciences* **1865**, *61*, 485.

(81) Cross, C. F.; Bevan, E. J. Fabrikation von celluloseacetat. *J. Soc. Chem. Ind. Bd.* **1895**, *14*, 435.

(82) Miles, G. W. AP 838,350, **1904**.

(83) Eichengruen.; Becker.; Guntrum. D.R.P 252,705, **1905**.

(84) Eichengruen, A. D.R.P 254,784, **1909**.

(85) Rustemeyer, P. 1. History of CA and evolution of the markets. *Macromol. Symp.* **2004**, *208*, 1–6.

(86) British Celanase Manufacturing Co. EP 165,519, **1920**.

(87) Clavel. D.R.P 355,533, **1920**.

(88) Suida, W. ber den Einflu\ der aktiven Atomgruppen in den Textilfasern auf das Zustandekommen von Frbungen. *Monatshefte fr Chemie* **1905**, *26*, 413–427.

(89) Dreyfus, H. French Patent 4,462,274, **1912**.

(90) Traill, D. *J. Soc. Chem. Ind. Trans*, *LIII*, 338T.

(91) Montonna, R. E. *Pap. Trade J. (Tappi Section)* **1936**, 35.

(92) McCormick, C. L.; Dawsey, T. R. Preparation of cellulose derivatives via ring-opening reactions with cyclic reagents in lithium chloride/N,N-dimethylacetamide. *Macromolecules* **1990**, *23*, 3606–3610.

(93) Heinze, T.; Dicke, R.; Koschella, A.; Kull, A. H.; Klohr, E.-A.; Koch, W. Effective preparation of cellulose derivatives in a new simple cellulose solvent. *Macromol. Chem. Phys.* **2000**, *201*, 627–631.

(94) Fink, H.-P.; Weigel, P.; Purz, H. J.; Ganster, J. Structure formation of regenerated cellulose materials from NMMO-solutions. *Prog. Polym. Sci.* **2001**, *26*, 1473–1524.

(95) Dorn, S.; Wendler, F.; Meister, F.; Heinze, T. Interactions of Ionic Liquids with Polysaccharides - 7: Thermal Stability of Cellulose in Ionic Liquids and N -Methylmorpholine-N -oxide. *Macromol. Mater. Eng.* **2008**, *293*, 907–913.

(96) T. Rosenau, A. Potthast, H. Sixta and P. Kosma. Review article The chemistry of side reactions and byproduct formation in the system NMMO/cellulose (Lyocell process). *Prog. Polym. Sci.* **2001**, *26*, 1763–1837.

(97) Kalia, S.; Kaith, B. S.; Kaur, I. *Cellulose Fibers: Bio- and Nano-Polymer Composites*; Springer Berlin Heidelberg: Berlin, Heidelberg, **2011**.

(98) Hindi, S.S.Z, Abohassan, R.A. Cellulose triacetate synthesis from cellulosic wastes by heterogenous reactions. *Bioresources* **2005**, *10*, 5030–5048.

(99) Varshney, V. K.; Gupta, P. K.; Naithani, S.; Khullar, R.; Bhatt, A.; Soni, P. L. Carboxymethylation of α-cellulose isolated from Lantana camara with respect to degree of substitution and rheological behavior. *Carbohydr. Polym.* **2006**, *63*, 40–45.

(100) Nasatto, P.; Pignon, F.; Silveira, J.; Duarte, M.; Noseda, M.; Rinaudo, M. Methylcellulose, a Cellulose Derivative with Original Physical Properties and Extended Applications. *Polymers* **2015**, *7*, 777–803.

(101) Mormann, W. Silylation of cellulose with hexamethyldisilazane in ammonia - activation, catalysis, mechanism, properties. *Cellulose* **2003**, *10*, 271–281.

(102) Mormann, W.; Demeter, J.; Wagner, T. Silylcellulose from silylation/desilylation of cellulose in ammonia. *Macromol. Symp.* **2001**, 49–57.

(103) Granja, P. L.; Pouységu, L.; Pétrand, M.; De-Jésu, B.; Baquey, C.; Barbosa, M. A. Cellulose Phosphates as Biomaterials. I. Synthesis and Characterization of Highly Phosphorylated Cellulose Gels. *J. Appl. Polym. Sci.* **2001**, *82*, 3341–3353.

(104) Saunders, C. W.; Taylor, L. T. A review of the synthesis, chemistry and analysis of nitrocellulose. *J. Energetic. Mater.* **1990**, *8*, 149–203.

(105) Law, R. C. 5. Applications of cellulose acetate— 5.1 Cellulose acetate in textile application. *Macromol. Symp.* **2004**, *208*, 255–266.

(106) Edgar, K.J, Buchanan, C.M, Debenham, J.S, Rundquist, Seiler, B.D, Shelton, M.C, Tindall, D. Advances in cellulose ester performance and application. *Prog. Polym. Sci.* **2000**, *26*, 1605–1688.

(107) Hummel, A. 3.2 Industrial processes. *Macromol. Symp.* **2004**, *208*, 61–80.

(108) Anastas, P.; Eghbali, N. Green chemistry: principles and practice. *Chem. Soc. Rev.* **2010**, *39*, 301–312.

(109) Curzons, A.D.; Constable, D.C.; Cunningham, V.L. Solvent selection guide: a guide to the integration of environmental, health and safety criteria into the selection of solvents. *Clean Products and Processes* **1999**, 82–90.

(110) Capello, C.; Fischer, U.; Hungerbühler, K. What is a green solvent? A comprehensive framework for the environmental assessment of solvents. *Green Chem.* **2007**, *9*, 927.

(111) Trost, B. The atom economy-a search for synthetic efficiency. *Science* **1991**, *254*, 1471–1477.

(112) Koller, G.; Fischer, U.; Hungerbühler, K. Assessing Safety, Health, and Environmental Impact Early during Process Development. *Ind. Eng. Chem. Res.* **2000**, *39*, 960–972.

(113) Jessop, P. G. Searching for green solvents. *Green Chem.* **2011**, *13*, 1391-1398.

(114) Chen, C.-Y.; Chen, M.-J.; Zhang, X.-Q.; Liu, C.-F.; Sun, R.-C. Per-O-acetylation of cellulose in dimethyl sulfoxide with catalyzed transesterification. *J. Agric. Food Chem.* **2014**, *62*, 3446–3452.

(115) Guo, Y.; Wang, X.; Shen, Z.; Shu, X.; Sun, R. Preparation of cellulose-graft-poly(ε-caprolactone) nanomicelles by homogeneous ROP in ionic liquid. *Carbohydr. Polym.* **2013**, *92*, 77–83.

(116) Barthel, S.; Heinze, T. Acylation and carbanilation of cellulose in ionic liquids. *Green Chem.* **2006**, *8*, 301–306.

(117) Kakko, T.; King, A. W. T.; Kilpeläinen, I. Homogenous esterification of cellulose pulp in [DBNH][OAc]. *Cellulose* **2017**, *24*, 5341–5354.

(118) Yang, Y.; Xie, H.; Liu, E. Acylation of cellulose in reversible ionic liquids. *Green Chem.* **2014**, *16*, 3018–3023.

(119) Yang, Y.; Song, L.; Peng, C.; Liu, E.; Xie, H. Activating cellulose *via* its reversible reaction with CO_2 in the presence of 1,8-diazabicyclo[5.4.0]undec-7-ene for the efficient synthesis of cellulose acetate. *Green Chem.* **2015**, *17*, 2758–2763.

(120) Onwukamike, K. N.; Grelier, S.; Grau, E.; Cramail, H.; Meier, M. A. R. Sustainable Transesterification of Cellulose with High Oleic Sunflower Oil in a DBU-CO_2 Switchable Solvent. *ACS Sustainable. Chem. Eng.* **2018**, *6*, 8826–8835.

(121) Llevot, A.; Dannecker, P.-K.; Czapiewski, M. von; Over, L. C.; Söyler, Z.; Meier, M. A. R. Renewability is not Enough: Recent Advances in the Sustainable Synthesis of Biomass-Derived Monomers and Polymers. *Chem. Eur. J.* **2016**, *22*, 11510–11521.

(122) Dwyer, R. W.; Abel, S. G. The Efficiencies of Cellulose Acetate Filters. *Beiträge zur Tabakforschung International/Contributions to Tobacco Research* **1986**, *13*, 243–253.

(123) Tang, L.-G.; Hon, D. N.-S.; Zhu, Y.-Q. An investigation in solution acetylation of cellulose by microscopic techniques. *J. Appl. Polym. Sci.* **1997**, *64*, 1953–1960.

(124) Welton, T. Room-Temperature Ionic Liquids. Solvents for Synthesis and Catalysis. *Chem. Rev.* **1999**, *99*, 2071–2084.

(125) Hallett, J. P.; Welton, T. Room-temperature ionic liquids: solvents for synthesis and catalysis. 2. *Chem. Rev.* **2011**, *111*, 3508–3576.

(126) Graenacher, C. US Patent 1,943,176, **1934**.

(127) los Ríos, A. P. de; Irabien, A.; Hollmann, F.; Fernández, F. J. H. Ionic Liquids: Green Solvents for Chemical Processing. *J. Chem.* **2013**, *2013*, 1–2.

(128) Mallakpour, S.; Dinari, M. Ionic Liquids as Green Solvents: Progress and Prospects. In *Green Solvents II*; Mohammad, A., Inamuddin, D., Eds.; Springer Netherlands: Dordrecht, **2012**; pp 1–32.

(129) Mäki-Arvela, P.; Anugwom, I.; Virtanen, P.; Sjöholm, R.; Mikkola, J. P. Dissolution of lignocellulosic materials and its constituents using ionic liquids—A review. *Ind. Crops. Prod.* **2010**, *32*, 175–201.

(130) El Seoud, O. A.; Koschella, A.; Fidale, L. C.; Dorn, S.; Heinze, T. Applications of ionic liquids in carbohydrate chemistry: A window of opportunities. *Biomacromolecules* **2007**, *8*, 2629–2647.

(131) Liebert, T.; Heinze. T. Interaction of ionic liquids with polysaccharides: Solvents and reaction media for the modification of cellulose. *bioresources* **2008**, *3*, 576–601.

(132) Isik, M.; Sardon, H.; Mecerreyes, D. Ionic liquids and cellulose: Dissolution, chemical modification and preparation of new cellulosic materials. *Int. J. Mol. Sci.* **2014**, *15*, 11922–11940.

(133) Kosan, B.; Michels, C.; Meister, F. Dissolution and forming of cellulose with ionic liquids. *Cellulose* **2008**, *15*, 59–66.

(134) Vitz, J.; Erdmenger, T.; Haensch, C.; Schubert, U. S. Extended dissolution studies of cellulose in imidazolium based ionic liquids. *Green Chem.* **2009**, *11*, 417.

(135) Clough, M. T.; Geyer, K.; Hunt, P. A.; Son, S.; Vagt, U.; Welton, T. Ionic liquids: not always innocent solvents for cellulose. *Green Chem.* **2015**, *17*, 231–243.

(136) Gericke, M.; Fardim, P.; Heinze, T. Ionic liquids--promising but challenging solvents for homogeneous derivatization of cellulose: Molecules (Basel, Switzerland) **2012**, *17*, 7458–7502.

(137) Aggarwal, V. K.; Emme, I.; Mereu, A. Unexpected side reactions of imidazolium-based ionic liquids in the base-catalysed Baylis–Hillman reaction. *Chem. Commun.* **2002**, 1612–1613.

(138) Zhang, H.; Wu, J.; Zhang, J.; He, J. 1-Allyl-3-methylimidazolium Chloride Room Temperature Ionic Liquid: A New and Powerful Non-derivatizing Solvent for Cellulose. *Macromolecules* **2005**, *38*, 8272–8277.

(139) Ebner, G.; Schiehser, S.; Potthast, A.; Rosenau, T. Side reaction of cellulose with common 1-alkyl-3-methylimidazolium-based ionic liquids. *Tetrahedron. Lett.* **2008**, *49*, 7322–7324.

(140) Massonne, K.; Siemer, W.; Mormann, W.; Leng. W. BASF, WO 027250, **2009**.

(141) Satria, H.; Kuroda, K.; Tsuge, Y.; Ninomiya, K.; Takahashi, K. Dimethyl sulfoxide enhances both the cellulose dissolution ability and biocompatibility of a carboxylate-type liquid zwitterion. *New J. Chem.* **2018**, *42*, 13225–13228.

(142) Wu, J.; Zhang, J.; Zhang, H.; He, J.; Ren, Q.; Guo, M. Homogeneous acetylation of cellulose in a new ionic liquid. *Biomacromolecules* **2004**, *5*, 266–268.

(143) Mormann, W.; Wezstein, M. Trimethylsilylation of cellulose in ionic liquids. *Macromol. Biosci.* **2009**, *9*, 369–375.

(144) Chowdhury, S. A.; Vijayaraghavan, R.; MacFarlane, D. R. Distillable ionic liquid extraction of tannins from plant materials. *Green Chem.* **2010**, *12*, 1023.

(145) King, A. W. T.; Asikkala, J.; Mutikainen, I.; Järvi, P.; Kilpeläinen, I. Distillable acid-base conjugate ionic liquids for cellulose dissolution and processing. *Angew. Chem. Int. Ed. Engl.* **2011**, *50*, 6301–6305.

(146) Parviainen, A.; King, A. W. T.; Mutikainen, I.; Hummel, M.; Selg, C.; Hauru, L. K. J.; Sixta, H.; Kilpeläinen, I. Predicting cellulose solvating capabilities of acid-base conjugate ionic liquids. *ChemSusChem.* **2013**, *6*, 2161–2169.

(147) Cetin, N. S.; Tingaut, P.; Ozmen, N.; Henry, N.; Harper, D.; Dadmun, M.; Sèbe, G. Acetylation of cellulose nanowhiskers with vinyl acetate under moderate conditions. *Macromol. Biosci.* **2009**, *9*, 997–1003.

(148) Jebrane, M.; Pichavant, F.; Sèbe, G. A comparative study on the acetylation of wood by reaction with vinyl acetate and acetic anhydride. *Carbohydr. Polym.* **2011**, *83*, 339–345.

(149) Jebrane, M.; Sèbe, G. A novel simple route to wood acetylation by transesterification with vinyl acetate. *Holzforschung* **2007**, *61*, 215.

(150) Chen, J.; Xu, J.; Wang, K.; Cao, X.; Sun, R. Cellulose acetate fibers prepared from different raw materials with rapid synthesis method. *Carbohydr. Polym.* **2016**, *137*, 685–692.

(151) Roscher, G. Vinyl Esters. *Ullmann's Encyclopedia of Industrial Chemistry*; Wiley-VCH Verlag GmbH & Co. KGaA: Weinheim, Germany, **2000**; p 149.

(152) Thümmler, K.; Fischer, S.; Peters, J.; Liebert, T.; Heinze, T. Evaluation of molten inorganic salt hydrates as reaction medium for the esterification of cellulose. *Cellulose* **2010**, *17*, 161–165.

(153) Jessop, P. G.; Heldebrant, D. J.; Li, X.; Eckert, C. A.; Liotta, C. L. Reversible Nonpolar-to-Polar Solvent. *Nature* **2005**, *436*, 1102.

(154) Zhang, Q.; Oztekin, N. S.; Barrault, J.; Oliveira Vigier, K. de; Jérôme, F. Activation of microcrystalline cellulose in a CO_2-based switchable system. *ChemSusChem.* **2013**, *6*, 593–596.

(155) Xie, H.; Yu, X.; Yang, Y.; Zhao, Z. K. Capturing CO_2 for cellulose dissolution. *Green Chem.* **2014**, *16*, 2422–2427.

(156) Onwukamike, K. N.; Tassaing, T.; Grelier, S.; Grau, E.; Cramail, H.; Meier, M. A. R. Detailed Understanding of the DBU/CO_2 Switchable Solvent System for Cellulose Solubilization and Derivatization. *ACS Sustainable. Chem. Eng.* **2018**, *6*, 1496–1503.

(157) Schenzel, A.; Hufendiek, A.; Barner-Kowollik, C.; Meier, M. A. R. Catalytic transesterification of cellulose in ionic liquids: sustainable access to cellulose esters. *Green Chem.* **2014**, *16*, 3266-3271.

(158) Carr, F. J.; Chill, D.; Maida, N. The lactic acid bacteria: a literature survey. *Crit. Rev. Microbiol.* **2002**, *28*, 281–370.

(159) Buntara, T.; Noel, S.; Phua, P. H.; Melián-Cabrera, I.; Vries, J. G. de; Heeres, H. J. Caprolactam from renewable resources: catalytic conversion of 5-hydroxymethylfurfural into caprolactone. *Angew. Chem. Int. Ed. Engl.* **2011**, *50*, 7083–7087.

(160) Winkler, M.; Raupp, Y. S.; Köhl, L. A. M.; Wagner, H. E.; Meier, M. A. R. Modified Poly(ε-caprolactone)s: An Efficient and Renewable Access via Thia-Michael Addition and Baeyer–Villiger Oxidation. *Macromolecules* **2014**, *47*, 2842–2846.

(161) Lowe, J. R.; Martello, M. T.; Tolman, W. B.; Hillmyer, M. A. Functional biorenewable polyesters from carvone-derived lactones. *Polym. Chem.* **2011**, *2*, 702–708.

(162) Lundberg, D. J.; Lundberg, D. J.; Hillmyer, M. A.; Dauenhauer, P. J. Techno-economic Analysis of a Chemical Process To Manufacture Methyl-ε-caprolactone from Cresols. *ACS Sustainable. Chem. Eng.* **2018**, *6*, 15316–15324.

(163) Song, L.; Yang, Y.; Xie, H.; Liu, E. Cellulose Dissolution and In Situ Grafting in a Reversible System using an Organocatalyst and Carbon Dioxide. *ChemSusChem.* **2015**, *8*, 3217–3221.

(164) Mayumi, A.; Kitaoka, T.; Wariishi, H. Partial substitution of cellulose by ring-opening esterification of cyclic esters in a homogeneous system. *J. Appl. Polym. Sci.* **2006**, *102*, 4358–4364.

(165) Dong, H.; Xu, Q.; Li, Y.; Mo, S.; Cai, S.; Liu, L. The synthesis of biodegradable graft copolymer cellulose-graft-poly(L-lactide) and the study of its controlled drug release. *Colloids Surf., B.* **2008**, *66*, 26–33.

(166) Xu, Q.; Song, L.; Zhang, L.; Hu, G.; Du, J.; Liu, E.; Zheng, Q.; Liu, Y.; Li, N.; Xie, H. Organocatalytic Cellulose Dissolution and In Situ Grafting of ε-Caprolactone via ROP in a Reversible DBU/DMSO/CO₂ System. *ChemistrySelect* **2017**, *2*, 7128–7134.

(167) Galbis, J. A.; García-Martín, M. d. G.; Paz, M. V. de; Galbis, E. Synthetic Polymers from Sugar-Based Monomers. *Chem. Rev.* **2016**, *116*, 1600–1636.

(168) Li, W. Y.; Jin, A. X.; Liu, C. F.; Sun, R. C.; Zhang, A. P.; Kennedy, J. F. Homogeneous modification of cellulose with succinic anhydride in ionic liquid using 4-dimethylaminopyridine as a catalyst. *Carbohydr. Polym.* **2009**, *78*, 389–395.

(169) Yin, X.; Yu, C.; Zhang, X.; Yang, J.; Lin, Q.; Wang, J.; Zhu, Q. Comparison of succinylation methods for bacterial cellulose and adsorption capacities of bacterial cellulose derivatives for Cu²⁺ ion. *Polym. Bull.* **2011**, *67*, 401–412.

(170) Chen, J.; Su, M.; Zhang, X.; Chen, R.; Hong, J.; Yang, L.; Yang, Z. The role of cations in homogeneous succinoylation of mulberry wood cellulose in salt-containing solvents under mild conditions. *Cellulose* **2014**, *21*, 4081–4091.

(171) Xin, P.-P.; Huang, Y.-B.; Hse, C.-Y.; Cheng, H. N.; Huang, C.; Pan, H. Modification of Cellulose with Succinic Anhydride in TBAA/DMSO Mixed Solvent under Catalyst-Free Conditions. *Materials (Basel, Switzerland)* **2017**, *10*.

(172) Söyler, Z.; Onwukamike, K. N.; Grelier, S.; Grau, E.; Cramail, H.; Meier, M. A. R. Sustainable succinylation of cellulose in a CO₂-based switchable solvent and subsequent Passerini 3-CR and Ugi 4-CR modification. *Green Chem.* **2018**, *20*, 214–224.

(173) Elschner, T.; Heinze, T. Cellulose carbonates: a platform for promising biopolymer derivatives with multifunctional capabilities. *Macromol. Biosci.* **2015**, *15*, 735–746.

(174) Labafzadeh, S. R.; Helminen, K. J.; Kilpeläinen, I.; King, A. W. T. Synthesis of cellulose methylcarbonate in ionic liquids using dimethylcarbonate. *ChemSusChem.* **2015**, *8*, 77–81.

(175) Tundo, P.; Musolino, M.; Aricò, F. The reactions of dimethyl carbonate and its derivatives. *Green Chem.* **2018**, *20*, 28–85.

(176) Mutlu, H.; Ruiz, J.; Solleder, S. C.; Meier, M. A. R. TBD catalysis with dimethyl carbonate: a fruitful and sustainable alliance. *Green Chem.* **2012**, *14*, 1728.

(177) Söyler, Z.; Meier, M. A. R. Sustainable functionalization of cellulose and starch with diallyl carbonate in ionic liquids. *Green Chem.* **2017**, *19*, 3899–3907.

(178) Kulicke, W.-M.; Clasen, C.; Lohman, C. Characterization of Water-Soluble Cellulose Derivatives in Terms of the Molar Mass and Particle Size as well as Their Distribution. *Macromol. Symp.* **2005**, *223*, 151–174.

(179) Heinze, T.; Schwikal, K.; Barthel, S. Ionic liquids as reaction medium in cellulose functionalization. *Macromol. Biosci.* **2005**, *5*, 520–525.

(180) Kostag, M.; Jedvert, K.; Achtel, C.; Heinze, T.; El Seoud, O. A. Recent Advances in Solvents for the Dissolution, Shaping and Derivatization of Cellulose: Quaternary Ammonium Electrolytes and their Solutions in Water and Molecular Solvents. *Molecules (Basel, Switzerland)* **2018**, *23*.

(181) Köhler, S.; Liebert, T.; Heinze, T. Ammonium-based cellulose solvents suitable for homogeneous etherification. *Macromol. Biosci.* **2009**, *9*, 836–841.

(182) Pourchez, J.; Grosseau, P.; Guyonnet, R.; Ruot, B. HEC influence on cement hydration measured by conductometry. *Cem. Conc. Res.* **2006**, *36*, 1777–1780.

(183) Singh, N.K.; Mishra, P.C.; Singh, V.K.; Narang, K.K. Effects of hydroxyethyl cellulose and oxalic acid on the properties of cement. *Cem. Conc. Res.* **2003**, *33*, 1319–1329.

(184) Köhler, S.; Liebert, T.; Heinze, T.; Vollmer, A.; Mischnick, P.; Möllmann, E.; Becker, W. Interactions of ionic liquids with polysaccharides 9. Hydroxyalkylation of cellulose without additional inorganic bases. *Cellulose* **2010**, *17*, 437–448.

(185) Evans, R.; Wearne, R. H.; Wallis, A. F. A. Molecular weight distribution of cellulose as its tricarbanilate by high performance size exclusion chromatography. *J. Appl. Polym. Sci.* **1989**, *37*, 3291–3303.

(186) Knölker, H.-J.; Braxmeier, T.; Schlechtingen, G. A Novel Method for the Synthesis of Isocyanates Under Mild Conditions. *Angew. Chem. Int. Ed. Engl.* **1995**, *34*, 2497–2500.

(187) Kreye, O.; Mutlu, H.; Meier, M. A. R. Sustainable routes to polyurethane precursors. *Green Chem.* **2013**, *15*, 1431.

(188) Maisonneuve, L.; Lamarzelle, O.; Rix, E.; Grau, E.; Cramail, H. Isocyanate-Free Routes to Polyurethanes and Poly(hydroxy Urethane)s. *Chem. Rev.* **2015**, *115*, 12407–12439.

(189) Erythropel, H. C.; Zimmerman, J. B.; Winter, T. M. de; Petitjean, L.; Melnikov, F.; Lam, C. H.; Lounsbury, A. W.; Mellor, K. E.; Janković, N. Z.; Tu, Q.; Pincus, L. N.; Falinski, M. M.; Shi, W.; Coish, P.; Plata, D. L.; Anastas, P. T. The Green ChemisTREE: 20 years after taking root with the 12 principles. *Green Chem.* 2018, *20*, 1929–1961.

(190) Dömling, A. Recent developments in isocyanide based multicomponent reactions in applied chemistry. *Chem. Rev.* **2006**, *106*, 17–89.

(191) Strecker, A. Ueber die künstliche Bildung der Milchsäure und einen neuen, dem Glycocoll homologen Körper;. *Ann. Chem. Pharm.* **1850**, *75*, 27–45.

(192) Théato, P. *Multi-Component and Sequential Reactions in Polymer Synthesis* 269; Springer International Publishing: Cham, **2015**.

(193) Gu, Y. Multicomponent reactions in unconventional solvents: state of the art. *Green Chem.* **2012**, *14*, 2091.

(194) Touré, B. B.; Hall, D. G. Natural product synthesis using multicomponent reaction strategies. *Chem. Rev.* **2009**, *109*, 4439–4486.

(195) Brauch, S.; van Berkel, S. S.; Westermann, B. Higher-order multicomponent reactions: beyond four reactants. *Chem. Soc. Rev.* **2013**, *42*, 4948–4962.

(196) Ganem, B. Strategies for innovation in multicomponent reaction design. *Acc. Chem. Res.* **2009**, *42*, 463–472.

(197) Ugi, I.; Dömling, A.; Hörl, W. Multicomponent reactions in organic chemistry. *Endeavour* **1994**, *18*, 115–122.

(198) Haven, J. J.; Baeten, E.; Claes, J.; Vandenbergh, J.; Junkers, T. High-throughput polymer screening in microreactors: boosting the Passerini three component reaction. *Polym. Chem.* **2017**, *8*, 2972–2978.

(199) Kakuchi, R. Multicomponent reactions in polymer synthesis. *Angew. Chem. Int. Ed. Engl.* **2014**, *53*, 46–48.

(200) Ugi, I.; Heck, S. The Multicomponent Reactions and their Libraries for Natural and Preparative Chemistry. *CCHTS* **1970**, *4*, 1–34.

(201) Mironov, M. A. Multicomponent reactions and combinatorial chemistry. *Russ. J .Gen. Chem.* **2010**, *80*, 2628–2646.

(202) D'Souza, D. M.; Müller, T. J. J. Multi-component syntheses of heterocycles by transition-metal catalysis. *Chem. Soc. Rev.* **2007**, *36*, 1095–1108.

(203) Sunderhaus, J. D.; Martin, S. F. Applications of multicomponent reactions to the synthesis of diverse heterocyclic scaffolds. *Chem. Eur. J.* **2009**, *15*, 1300–1308.

(204) Váradi, A.; Palmer, T. C.; Notis Dardashti, R.; Majumdar, S. Isocyanide-Based Multicomponent Reactions for the Synthesis of Heterocycles. *Molecules (Basel, Switzerland)* **2015**, *21*, E19.

(205) Kreye, O.; Tóth, T.; Meier, M. A. R. Introducing multicomponent reactions to polymer science: Passerini reactions of renewable monomers. *J. Am. Chem. Soc.* **2011**, *133*, 1790–1792.

(206) Sehlinger, A.; Kreye, O.; Meier, M. A. R. Tunable Polymers Obtained from Passerini Multicomponent Reaction Derived Acrylate Monomers. *Macromolecules* **2013**, *46*, 6031–6037.

(207) Solleder, S. C.; Meier, M. A. R. Sequence control in polymer chemistry through the Passerini three-component reaction. *Angew. Chem. Int. Ed. Engl.* **2014**, *53*, 711–714.

(208) Solleder, S. C.; Zengel, D.; Wetzel, K. S.; Meier, M. A. R. A Scalable and High-Yield Strategy for the Synthesis of Sequence-Defined Macromolecules. *Angew. Chem. Int. Ed. Engl.* **2016**, *55*, 1204–1207.

(209) Colquhoun, H.; Lutz, J.-F. Information-containing macromolecules. *Nat. Chem* **2014**, *6*, 455–456.

(210) Lutz, J.-F.; Ouchi, M.; Liu, D. R.; Sawamoto, M. Sequence-controlled Polymers. *Science* **2013**, *341*, 1238149.

(211) Oelmann, S.; Meier, M. A. R. Synthesis and unimolecular micellar behavior of amphiphilic star-shaped block copolymers obtained via the Passerini three component reaction. *RSC Adv.* **2017**, *7*, 45195–45199.

(212) Oelmann, S.; Travanut, A.; Barther, D.; Romero, M.; Howdle, S. M.; Alexander, C.; Meier, M. A. R. Biocompatible Unimolecular Micelles Obtained via the Passerini Reaction as Versatile Nanocarriers for Potential Medical Applications. *Biomacromolecules* **2018,** DOI: 10.1021/acs.biomac.8b00592.

(213) Boukis, A. C.; Reiter, K.; Frölich, M.; Hofheinz, D.; Meier, M. A. R. Multicomponent reactions provide key molecules for secret communication. *Nat. Commun.* **2018**, *9*, 1439.

(214) Dömling, A.; Ugi, I. Multicomponent reactions with Isocyanides. *Angew. Chem. Int. Ed. Engl.* **2000**, *39*, 3168–3210.

(215) Hantzsch, A. Condensationsprodukte aus Aldehydammoniak und ketonartigen Verbindungen. *Ber. Dtsch. Chem. Ges.* **1881**, *14*, 1637–1638.

(216) Atwal, K. S.; Swanson, B. N.; Unger, S. E.; Floyd, D. M.; Moreland, S.; Hedberg, A.; O'Reilly, B. C. Dihydropyrimidine calcium channel blockers. 3. 3-Carbamoyl-4-aryl-1,2,3,4-tetrahydro-6-methyl-5-pyrimidinecarboxylic acid esters as orally effective antihypertensive agents. *J. Med. Chem.* **1991**, *34*, 806–811.

(217) Miri, R.; Javidnia, K.; Hemmateenejad, B.; Tabarzad, M.; Jafarpour, M. Synthesis, evaluation of pharmacological activities and quantitative structure-activity relationship studies of a novel group of bis(4-nitroaryl-1,4-dihyropyridine). *Chem. Biol. Drug Des.* **2009**, *73*, 225–235.

(218) Kellogg, R. M.; van Bergen, T. J.; van Doren, H.; Hedstrand, D.; Kooi, J.; Kruizinga, W. H.; Troostwijk, C. B. The Hantzsch 1,4-Dihydropyridine Synthesis as a Route to Bridged Pyridine and Dihydropyridine Crown Ethers. *J. Org. Chem* **1980**, *45*, 2854–2861.

(219) Biginelli, P. *Ber. Dtsch. Chem. Ges.* **1893**, *26*, 447–450.

(220) Kappe, C.O. Biologically active dihydropyrimidones of the Biginelli-type-a literature survey. *Eur. J. Med. Chem* **2000**, *35*, 1043–1052.

(221) Lewis, R. W.; Mabry, J.; Polisar, J. G.; Eagen, K. P.; Ganem, B.; Hess, G. P. Dihydropyrimidinone positive modulation of delta-subunit-containing gamma-aminobutyric acid type A receptors, including an epilepsy-linked mutant variant. *Biochemistry* **2010**, *49*, 4841–4851.

(222) Nagarajaiah, H.; Mukhopadhyay, A.; Moorthy, J. N. Biginelli reaction: an overview. *Tetrahedron. Lett.* **2016**, *57*, 5135–5149.

(223) Mannich, C.; Krösche, W. Ueber ein Kondensationsprodukt aus Formaldehyd, Ammoniak und Antipyrin. *Arch. Pharm. Pharm. Med. Chem.* **1912**, *250*, 647–667.

(224) Passerini, M. *Gazz.Chim.Ital* **1921**, *51*, 126–129.

(225) Ugi, I.; Steinbrückner, C. Über ein neues Kondensations-Prinzip. *Angew. Chem.* **1960**, *72*, 267–268.

(226) Gautier, A. Ueber die Einwirkung des Chlorwasserstoffs u. a. auf das Aethyl- und Methylcyanür. *Ann. Chem. Pharm.* **1867**, *142*, 289–294.

(227) Scheuer, P. J. Isocyanides and cyanides as natural products. *Acc. Chem. Res.* **1992**, *25*, 433–439.

(228) Lieke, W. Ueber das Cyanallyl. *Ann. Chem. Pharm.* **1859**, *112*, 316–321.

(229) Hofmann, A. W. Beobachtungen vermischten Inhalts. *Ber. Dtsch. Chem. Ges.* **1870**, *3*, 761–772.

(230) Hofmann, A. W. Ueber eine neue Reihe von Homologen der Cyanwasserstoffsäure. *Ann. Chem. Pharm.* **1867**, *144*, 114–120.

(231) Ugi, I.; Meyr, R. Neue Darstellungsmethode für Isonitrile. *Angew. Chem.* **1958**, *70*, 702–703.

(232) Skorna, G.; Ugi, I. Isocyanide Synthesis with Diphosgene. *Angew. Chem. Int. Ed. Engl.* **1977**, *16*, 259–260.

(233) Eckert, H.; Forster, B. Triphosgene, a Crystalline Phosgene Substitute. *Angew. Chem. Int. Ed. Engl.* **1987**, *26*, 894–895.

(234) Rothe, W. Vorläufige Mitteilung über eine neues Antibiotikum. *Pharmazie.* **1950**, *5*, 190.

(235) Nobuhara, M.; Tazima, H.; Shudo, K.; Itai, A.; Okamoto, T.; Iitaka, Y. *Chem. Pharm. Bull* **1976**, *24*, 832–834.

(236) Ugi, I.; Dömling, A.; Werner, B. The Chemistry of Isocyanides, their MultiComponent Reactions and their Libraries. *Molecules* **2003**, *8*, 53–66.

(237) Baker, R. H.; Stanonis, D. The Passerini Reaction. III. Stereochemistry and Mechanism 1,2. *J. Am. Chem. Soc.* **1951**, *73*, 699–702.

(238) Ugi, I.; Meyr, R. Isonitrile, V. Erweiterter Anwendungsbereich der Passerini-Reaktion. *Chem. Ber.* **1961**, *94*, 2229–2233.

(239) Mumm, O. *Berichte der deutschen chemischen Gesellschaft* **1910**, *43*, 886.

(240) Bochek, A. M. Effect of Hydrogen Bonding on Cellulose Solubility in Aqueous and Nonaqueous Solvents. *Russ. J. Appl. Chem.* **2003**, *76*, 1711–1719.

(241) Nanta, P.; Skolpap, W.; Kasemwong, K.; Shimoyama, Y. Dissolution and modification of cellulose using high-pressure carbon dioxide switchable solution. *J. Supercrit. Fluids.* **2017**, *130*, 84–90.

(242) Wang, J.; Xue, Z.; Yan, C.; Li, Z.; Mu, T. Fine regulation of cellulose dissolution and regeneration by low pressure CO_2 in DMSO/organic base: dissolution behavior and mechanism. *PCCP* **2016**, *18*, 32772–32779.

(243) Carrera, G. V.S.M.; Jordão, N.; Branco, L. C.; Nunes da Ponte, M. CO_2 capture and reversible release using mono-saccharides and an organic superbase. *J. Supercrit. Fluids.* **2015**, *105*, 151–157.

(244) Heldebrant, D. J.; Jessop, P. G.; Thomas, C. A.; Eckert, C. A.; Liotta, C. L. The reaction of 1,8-diazabicyclo5.4.0undec-7-ene (DBU) with carbon dioxide. *J. Org. Chem.* **2005**, *70*, 5335–5338.

(245) Heldebrant, D. J.; Yonker, C. R.; Jessop, P. G.; Phan, L. Organic liquid CO_2 capture agents with high gravimetric CO_2 capacity. *Energy Environ. Sci.* **2008,** 1, 487-493.

(246) Andanson, J.-M.; Pádua, A. A. H.; Costa Gomes, M. F. Thermodynamics of cellulose dissolution in an imidazolium acetate ionic liquid. *Chem. Commun.* **2015**, *51*, 4485–4487.

(247) Shi, M.; Shen, Y.-M. Synthesis of Mixed Carbonates via a Three-Component Coupling of Alcohols, CO_2, and Alkyl Halides in the Presence of K_2CO_3 and Tetrabutylammonium Iodide. *Molecules (Basel, Switzerland)* **2002**, *7*, 386–393.

(248) King, A. W. T.; Jalomäki, J.; Granström, M.; Argyropoulos, D. S.; Heikkinen, S.; Kilpeläinen, I. A new method for rapid degree of substitution and purity determination of chloroform-soluble cellulose esters, using 31P NMR. *Anal. Methods* **2010**, *2*, 1499.

(249) Pang, J.-H.; Liu, X.; Wu, M.; Wu, Y.-Y.; Zhang, X.-M.; Sun, R.-C. Fabrication and Characterization of Regenerated Cellulose Films Using Different Ionic Liquids. *J. Spectro.* **2014**, *2014*, 1–8.

(250) Sescousse, R.; Gavillon, R.; Budtova, T. Wet and dry highly porous cellulose beads from cellulose–NaOH–water solutions: influence of the preparation conditions on beads shape and encapsulation of inorganic particles. *J Mater Sci* **2011**, *46*, 759–765.

(251) Trygg, J.; Fardim, P.; Gericke, M.; Mäkilä, E.; Salonen, J. Physicochemical design of the morphology and ultrastructure of cellulose beads. *Carbohydr. Polym.* **2013**, *93*, 291–299.

(252) Innerlohinger, J.; Weber, H. K.; Kraft, G. Aerocellulose: Aerogels and Aerogel-like Materials made from Cellulose. *Macromol. Symp.* **2006**, *244*, 126–135.

(253) Liebner, F.; Rosenau, T. *Functional materials from renewable sources*; ACS symposium series 1107; American Chemical Society: Washington, DC, **2012**.

(254) Pekala, R. W. Organic aerogels from the polycondensation of resorcinol with formaldehyde. *J. Mater. Sci.* **1989**, *24*, 3221–3227.

(255) Bock, V. Emmerling, A. Saliger, R. Fricke, J. Structural Investigation of Resorcinol Formaldehyde and Carbon Aerogels Using SAXS and BET. *J. Porous. Mater.* **1997**, *4*, 287–294.

(256) Thapliyal, P. C.; Singh, K. Aerogels as Promising Thermal Insulating Materials: An Overview. *Journal of Materials* **2014**, *2014*, 1–10.

(257) Wu, Z.-Y.; Li, C.; Liang, H.-W.; Chen, J.-F.; Yu, S.-H. Ultralight, flexible, and fire-resistant carbon nanofiber aerogels from bacterial cellulose. *Angew. Chem. Int. Ed. Engl.* **2013**, *52*, 2925–2929.

(258) García-González, C. A.; Alnaief, M.; Smirnova, I. Polysaccharide-based aerogels—Promising biodegradable carriers for drug delivery systems. *Carbohydr. Polym.* **2011**, *86*, 1425–1438.

(259) Ulker, Z.; Erkey, C. An emerging platform for drug delivery: aerogel based systems. *J. Controlled. Release.* **2014**, *177*, 51–63.

(260) Kistler, S. S. Coherent Expanded Aerogels and Jellies. *Nature* **1931**, *127*, 741.

(261) Kistler, S. S. Coherent Expanded-Aerogels. *J. Phys. Chem.* **1931**, *36*, 52–64.

(262) Liebner, F.; Haimer, E.; Wendland, M.; Neouze, M.-A.; Schlufter, K.; Miethe, P.; Heinze, T.; Potthast, A.; Rosenau, T. Aerogels from unaltered bacterial cellulose: application of scCO2 drying for the preparation of shaped, ultra-lightweight cellulosic aerogels. *Macromol. Biosci.* **2010**, *10*, 349–352.

(263) Pääkkö, M.; Vapaavuori, J.; Silvennoinen, R.; Kosonen, H.; Ankerfors, M.; Lindström, T.; Berglund, L. A.; Ikkala, O. Long and entangled native cellulose I nanofibers allow flexible aerogels and hierarchically porous templates for functionalities. *Soft Matter* **2008**, *4*, 2492.

(264) Zhang, Z.; Sèbe, G.; Rentsch, D.; Zimmermann, T.; Tingaut, P. Ultralightweight and Flexible Silylated Nanocellulose Sponges for the Selective Removal of Oil from Water. *Chem. Mater.* **2014**, *26*, 2659–2668.

(265) Wang, Z.; Liu, S.; Matsumoto, Y.; Kuga, S. Cellulose gel and aerogel from LiCl/DMSO solution. *Cellulose* **2012**, *19*, 393–399.

(266) Hoepfner, S.; Ratke, L.; Milow, B. Synthesis and characterisation of nanofibrillar cellulose aerogels. *Cellulose* **2008**, *15*, 121–129.

(267) Jin, H.; Nishiyama, Y.; Wada, M.; Kuga, S. Nanofibrillar cellulose aerogels. *Colloids. Surf., A.* **2004**, *240*, 63–67.

(268) Buchtová, N.; Budtova, T. Cellulose aero-, cryo- and xerogels: towards understanding of morphology control. *Cellulose* **2016**, *23*, 2585–2595.

(269) Sun, C. C. True density of microcrystalline cellulose. *J. Pharm. Sci.* **2005**, *94*, 2132–2134.

(270) Pircher, N.; Carbajal, L.; Schimper, C.; Bacher, M.; Rennhofer, H.; Nedelec, J.-M.; Lichtenegger, H. C.; Rosenau, T.; Liebner, F. Impact of selected solvent systems on the pore and solid structure of cellulose aerogels. *Cellulose* **2016**, *23*, 1949–1966.

(271) Alder, C. M.; Hayler, J. D.; Henderson, R. K.; Redman, A. M.; Shukla, L.; Shuster, L. E.; Sneddon, H. F. Updating and further expanding GSK's solvent sustainability guide. *Green Chem.* **2016**, *18*, 3879–3890.

(272) Du, M.; Mao, N.; Russell, S. J. Control of porous structure in flexible silicone aerogels produced from methyltrimethoxysilane (MTMS): the effect of precursor concentration in sol–gel solutions. *J Mater Sci.* **2016**, *51*, 719–731.

(273) Shinko, A.; Jana, S. C.; Meador, M. A. Crosslinked polyurea aerogels with controlled porosity. *RSC Adv.* **2015**, *5*, 105329–105338.

(274) Ciolacu, D.; Ciolacu, F.; Popa, V. I. Amorphous cellulose – Structure and Characterization. *Cellul. Chem. Technol.* **2011**, *45*, 13-21.

(275) Wang, P.; Tao, B. Y. Synthesis of cellulose-fatty acid esters for use as biodegradable plastics. *J. Environ. Polym. Degr.* **1995**, *3*, 115–119.

(276) Kulomaa, T.; Matikainen, J.; Karhunen, P.; Heikkilä, M.; Fiskari, J.; Kilpeläinen, I. Cellulose fatty acid esters as sustainable film materials – effect of side chain structure on barrier and mechanical properties. *RSC Adv.* **2015**, *5*, 80702–80708.

(277) Dankovich, T. A.; Hsieh, Y.-L. Surface modification of cellulose with plant triglycerides for hydrophobicity. *Cellulose* **2007**, *14*, 469–480.

(278) Villiers, C.; Dognon, J.-P.; Pollet, R.; Thuéry, P.; Ephritikhine, M. An isolated CO2 adduct of a nitrogen base: crystal and electronic structures. *Angew. Chem. Int. Ed. Engl.* **2010**, *49*, 3465–3468.

(279) Ugi, I.; Steinbrückner, C. *Chem. Ber.* **1961**, *94*, 2802–2814.

(280) Keating, T. A.; Armstrong, R. W. The Ugi Five-Component Condensation Using CO_2, CS_2, and COS as Oxidized Carbon Sources. *J. Org. Chem.* **1998**, *63*, 867–871.

(281) Sehlinger, A.; Schneider, R.; Meier, M. A. R. Ugi reactions with CO_2: access to functionalized polyurethanes, polycarbonates, polyamides, and polyhydantoins. *Macromol. Rapid Comm.* **2014**, *35*, 1866–1871.

(282) Gurau, G.; Rodríguez, H.; Kelley, S. P.; Janiczek, P.; Kalb, R. S.; Rogers, R. D. Demonstration of chemisorption of carbon dioxide in 1,3-dialkylimidazolium acetate ionic liquids. *Angew. Chem. Int. Ed. Engl.* **2011**, *50*, 12024–12026.

(283) Barber, P. S.; Griggs, C. S.; Gurau, G.; Liu, Z.; Li, S.; Li, Z.; Lu, X.; Zhang, S.; Rogers, R. D. Coagulation of chitin and cellulose from 1-ethyl-3-methylimidazolium acetate ionic-liquid solutions using carbon dioxide. *Angew. Chem. Int. Ed. Engl.* **2013**, *52*, 12350–12353.

(284) König, S.; Ugi, I. Crosslinking of Aqueous Alginic Acid by Four Component Condensation with Inclusion Immobilization of Enzymes. *Z. Naturforsch.* **1991**, *46b*, 1261.

(285) Nooy, A. E. J. de; Capitani, D.; Masci, G.; Crescenzi, V. Ionic Polysaccharide Hydrogels via the Passerini and Ugi Multicomponent Condensations: Synthesis, Behavior and Solid-State NMR Characterization. *Biomacromolecules* **2000**, *1*, 259–267.

(286) Nooy, A. E. J. de; Masci, G.; Crescenzi, V. Versatile Synthesis of Polysaccharide Hydrogels Using the Passerini and Ugi Multicomponent Condensations. *Macromolecules* **1999**, *32*, 1318–1320.

(287) Khine, Y. Y.; Ganda, S.; Stenzel, M. H. Covalent Tethering of Temperature Responsive pNIPAm onto TEMPO-Oxidized Cellulose Nanofibrils via Three-Component Passerini Reaction. *ACS Macro. Lett.* **2018**, *7*, 412–418.

(288) Sehlinger, A.; Dannecker, P.-K.; Kreye, O.; Meier, M. A. R. Diversely Substituted Polyamides: Macromolecular Design Using the Ugi Four-Component Reaction. *Macromolecules* **2014**, *47*, 2774–2783.

(289) Yanai, H.; Oguchi, T.; Taguchi, T. Direct alkylative Passerini reaction of aldehydes, isocyanides, and free aliphatic alcohols catalyzed by indium(III) triflate. *J. Org. Chem.* **2009**, *74*, 3927–3929.

(290) El Kaim, L.; Gizolme, M.; Grimaud, L. O-arylative Passerini reactions. *Org. lett.* **2006**, *8*, 5021–5023.

(291) Tobisu, M.; Kitajima, A.; Yoshioka, S.; Hyodo, I.; Oshita, M.; Chatani, N. Brønsted acid catalyzed formal insertion of isocyanides into a C-O bond of acetals. *J. Am. Chem. Soc.* **2007**, *129*, 11431–11437.

(292) Denmark, S. E.; Fan, Y. The first catalytic, asymmetric alpha-additions of isocyanides. Lewis-base-catalyzed, enantioselective Passerini-type reactions. *J. Am. Chem. Soc.* **2003**, *125*, 7825–7827.

(293) Jessop, P. G.; Phan, L.; Carrier, A.; Robinson, S.; Dürr, C. J.; Harjani, J. R. A solvent having switchable hydrophilicity. *Green Chem.* **2010**, *12*, 809.

(294) Phan, L.; Chiu, D.; Heldebrant, D. J.; Huttenhower, H.; John, E.; Li, X.; Pollet, P.; Wang, R.; Eckert, C. A.; Liotta, C. L. *et al.* Switchable Solvents Consisting of Amidine/Alcohol or Guanidine/Alcohol Mixtures. *Ind. Eng. Chem. Res.* **2008**, *47*, 539–545.

(295) Anugwom, I.; Mäki-Arvela, P.; Virtanen, P.; Willför, S.; Sjöholm, R.; Mikkola, J.-P. Selective extraction of hemicelluloses from spruce using switchable ionic liquids. *Carbohydr. Polym.* **2012**, *87*, 2005–2011.

(296) Söyler, Z.; Onwukamike, K. N.; Grelier, S.; Grau, E.; Cramail, H.; Meier, M. A. R. Sustainable succinylation of cellulose in a CO_2-based switchable solvent and subsequent Passerini 3-CR and Ugi 4-CR modification. *Green Chem.* **2018**, *20*, 214–224.

(297) Lang, S. B.; Locascio, T. M.; Tunge, J. A. Activation of alcohols with carbon dioxide: intermolecular allylation of weakly acidic pronucleophiles. *Org. lett.* **2014**, *16*, 4308–4311.

(298) Jackson, H. L.; McCormack, W. B.; Rondestvedt, C. S.; Smeltz, K. C.; Viele, I. E. Control of peroxidizable compounds. *J. Chem. Educ.* **1970**, *47*, A175.

(299) Kakei, H.; Nemoto, T.; Ohshima, T.; Shibasaki, M. Efficient synthesis of chiral alpha- and beta-hydroxy amides: application to the synthesis of (R)-fluoxetine. *Angew. Chem. Int. Ed. Engl.* **2004**, *43*, 317–320.

(300) Barnett, B. R.; Figueroa, J. S. Zero-valent isocyanides of nickel, palladium and platinum as transition metal σ-type Lewis bases. *Chem. Commun.* **2016**, *52*, 13829–13839.

(301) Bhattacharyya, M.; Prakash, R.; Jagan, R.; Ghosh, S. Synthesis and ligand substitution of tri-metallic triply bridging borylene complexes. *J. Organomet. Chem.* **2018**, *866*, 79–86.

(302) Tashkandi, N. Y.; Cook, E. E.; Bourque, J. L.; Baines, K. M. Addition of Isocyanides to Tetramesityldigermene: A Comparison of the Reactivity between Surface and Molecular Digermenes. *Chem. Eur. J.* **2016**, *22*, 14006–14012.

(303) Patschinski, P.; Zhang, C.; Zipse, H. The Lewis base-catalyzed silylation of alcohols-a mechanistic analysis. *J. Org. Chem.* **2014**, *79*, 8348–8357.

(304) Le-Thanh, H.; Vocelle, D. 1 H NMR studies of proton transfer in Schiff base and carboxylic acid systems. *Can. J. Chem.* **1990**, *68*, 1909–1916.

(305) Rospenk, M.; Sobczyk, L. 1H NMR studies of proton transfer inortho-mannich bases. *Magn. Reson. Chem.* **1989**, *27*, 445–450.

(306) Alves, M.; Grignard, B.; Gennen, S.; Detrembleur, C.; Jerome, C.; Tassaing, T. Organocatalytic synthesis of bio-based cyclic carbonates from CO_2 and vegetable oils. *RSC Adv.* **2015**, *5*, 53629–53636.

9.2 List of abbreviations

ATR-IR: Attenuated total reflectance infrared spectroscopy

[Admim]$^+$[Br$^-$]: 1-*N*-allyl-2,3-dimethylimidazolium bromide

[C$_2$mim]$^+$[Cl$^-$]: 1-*N*-ethyl-3-methylimidazolium chloride

[C$_4$dmim]$^+$[Cl$^-$]: 1-*N*-butyldimethylimidazolium chloride

([C$_4$mim]$^+$[Cl$^-$]: 1-*N*-butyl-3-methylimidazolium chloride

[P$_{8881}$]$^+$[OAc]$^-$: Trioctylphosphonium acetate

[C$_2$mim]$^+$[OAc$^-$]: 1-*N*-butyl-3-methylimidazolium acetate

AGU: Anhydroglucose unit

[Amim]$^+$[Cl$^-$]: 1-*N*-allyl-3-methylimidazolium chloride

CNC: Cellulose nanocrystals

CO$_2$: Carbon dioxide

CP: Cellulose pulp

CTMP: Chemothermomechanical pulping

CTO: Calcium thiocyanate octahydrate-lithium chloride

Đ: Dispersity

DBN: 1,5-diazabicyclo[4.3.0]non-5-ene

DBU: 1,8-diazabicyclo[5.4.0]undec-7-ene

DMAC-LiBr: Dimethylacetamide-Lithium bromide

DMAC-LiCl: *N,N*-dimethylacetamide-lithium chloride

DMSO: Dimethyl sulfoxide

DMSO-TBAF: Dimethyl sulfoxide-tetrabutyl ammonium fluoride

DS: Degree of substitution

E-factor: Environmental factor

ESH: Environmental, health and safety

FACEs: Fatty acid cellulose esters

FP: Whatman™ filter paper No. 5

GC: Gas chromatography

GC-MS: Gas chromatography-mass spectrometry

IL: Ionic liquid

IMCRs: Isocyanide-based multicomponent reactions

SFP: Succinylated filter

LCA: Life cycle analysis

MCC: Microcrystalline cellulose

MCRs: Multicomponent reactions

MP: Mechanical pulp

MS: Molecular degree of substitution

MTBD: 7-methyl-1,5,7-triazabicyclo[4.4.0]dec-5-ene

NFC: Nanofibrillated cellulose

NMMO: *N*-methylmorpholine-*N*-oxide

NMR: Nuclear magnetic resonance spectroscopy

P-3CR: Passerini three component reaction

P-4CR: Passerini four component reaction

PE: Polyethylene

PET: Polyethylene terephthalate

PHK: Pre-Hydrolysis Kraft

PMMA: Poly(methyl methacryate)

PP: Polypropylene

PS: Polystyrene

PVC: Polyvinyl chloride

SEC: Size exclusion chromatography

SEM: Scanning electron microscopy

TBD: 1,5,7-Triazabicyclo[4.4.0]dec-5-ene

T_g: Glass transition temperature

TGA: Thermogravimetric analysis

TMG: 1,1,3,3-tetramethylguanidine

TMP: Thermomechanical pulp

Ugi-4CR: Ugi four component reaction

Ugi-5CR: Ugi five component reaction

UNEP: United Nations Environment Program

WEF: World Economy forum

XRD: X-ray diffraction

9.3 List of Figures

Figure 1: Summary of crude oil/fossil resources global challenges/concerns.

Figure 2: Types of multicomponent reactions, adapted from Ugi and Dömling.[214]

Figure 3: Structure of first isolated natural occurring isocyanide (xanthocillin).[234]

Figure 4: Change of C=O absorbance (from in situ formed carbonate anion) during a temperature cycle study on cellulose solubilization using DBU, MTBD and TMG as super bases.

Figure 5: **a**) ATR-IR proof of *in-situ* carbonate formation during cellulose solubilization in DBU-CO_2 solvent, **b**): ATR-IR showing evolution of C=O, DBU (C=N) and DBUH$^+$ (C=NH$^+$) as function of time; **c**): Visual proof for solubilization of cellulose (3 wt.% MCC, 30 °C, 5 bar CO_2, 10 to 15 min).

Figure 6: Optimization study *via* online *in-situ* ATR-IR measurement: effect of temperature at 5 bar of CO_2, 3 wt.% MCC.

Figure 7: Optimization study *via* online *in-situ* ATR-IR measurement: effect of CO_2 pressure at 30 °C (3 wt.% MCC).

Figure 8: Optimization study *via* online *in-situ* ATR-IR measurement: effect of cellulose concentration (reaction conditions: 30 °C, 20 bar CO_2, 15 min)

Figure 9: ATR-IR spectra of synthesized cellulose carbonate (methyl and benzyl); spectra are normalized with the intensity of the glycopyranose oxygen absorption at 1020 cm^{-1}.

Figure 10: ^{1}H (top) and ^{13}C (bottom) NMR spectra of cellulose-benzyl-carbonate in DMSO (d$_6$).

Figure 11: X-ray diffraction patterns of cellulose (MCC) and regenerated cellulose for different solubilization time (15 and 60 min) and temperatures (30 and 60 °C).

Figure 12: Effect of cellulose concentration on the apparent density of the aerogel.

Figure 13:SEM images of cellulose (5 wt.% MCC) aerogels obtained *via* freeze-drying (cellulose solubilized in DBU-CO_2 solvent system and coagulated using water).

Figure 14: SEM images of cellulose (5 wt.% MCC) aerogels obtained *via* freeze-drying (cellulose solubilized in a DBU-CO_2 solvent system and coagulated without addition of an anti-solvent).

Figure 15: SEM images of cellulose (5 wt.% MCC) aerogels obtained *via* freeze-drying (cellulose solubilized in a TMG-CO_2 solvent system and coagulated using ethanol).

Figure 16: Effect of cellulose concentration on the pore size of cellulose aerogels using DBU as a super base.

Figure 17: XRD data of cellulose (5 wt.% MCC) aerogels obtained *via* freeze-drying under various processing conditions.

Figure 18: Typical ATR-IR spectra of a fatty acid cellulose ester, MCC-1c (5 wt.% MCC, 3 eq. high oleic sunflower oil/AGU, 115 °C, 24 h) in comparison to native MCC.

Figure 19: ATR-IR spectra of fatty acid cellulose esters (FACEs) obtained using high oleic sunflower oil at various MCC concentrations:3 wt.% (MCC-1a), 4 wt.% (MCC-1b), 5 wt.% (MCC-1c). Peaks were normalized to the C-O absorbance of the pyranose units at 1025 cm^{-1} (3 eq. high oleic sunflower oil/AGU, 115 °C, 24 h).

Figure 20: ^{1}H (top, 1024 scans, 400 MHz) and ^{13}C (bottom, 6000 scans, 100 MHz) NMR (DMSO,d$_6$) at 90 °C for fatty acid cellulose esters (FACE, MCC-1d, 5 wt.% cellulose, 3 eq. high oleic sunflower oil/AGU, 115 °C, 6 h).

Figure 21: SEC traces (THF) of fatty acid cellulose esters (FACEs) from microcrystalline cellulose (MCC-1c; DS 1.59), cellulose filter paper (FP-1b; DS 1.48) and cellulose pulp (CP-1b; DS 1.40).

Figure 22: X-ray diffraction pattern of microcrystalline cellulose (MCC), regenerated MCC and fatty acid cellulose esters (FACEs) resulting from microcrystalline cellulose (MCC-1c, MCC-1i).

Figure 23: Thermogravimetric analysis (TGA) of microcrystalline cellulose (MCC) and resulting fatty acid cellulose esters (FACEs) from MCC (MCC-1c, MCC-1i) (5 wt.% cellulose, 24 h, 115 °C.

Figure 24: a) Images of thin films of fatty acid cellulose esters from MCC-F-1c (right) and CP-F-1b (left). b) SEM surface images of MCC-F-1c (right), FP-F-1b (TS section with surface in view, middle) and CP-F-1b (left). (Films made *via* solvent cast from solubilized FACEs in THF).

Figure 25: Thermogravimetric analysis (TGA) of fatty acid cellulose esters (FACEs) films (MCC-F-1i, MCC-F-1c, FP-F-1a, FP-F-1b, CP-F-1a, CP-F-1b).

Figure 26: Tensile strength measurements of fatty acid cellulose esters (FACEs) films (initial speed at 5 mm/min).

Figure 27: ATR-IR spectra comparison between MCC and Ugi 5-CR modified cellulose.

Figure 28: ^{1}H NMR showing the reaction between [C$_2$mim]$^+$[OAc]$^-$ ionic liquid and CO$_2$.

Figure 29: ATR-IR spectra comparison between filter paper cellulose (SF), succinylated cellulose (SFP), and Ugi 4-CR modified succinylated cellulose (**U1**).

Figure 30: ^{1}H NMR (top) and ^{13}C NMR (bottom) of Ugi 4-CR modified succinylated cellulose (U1) in THF(d$_8$).

Figure 31: ^{31}P NMR of Ugi 4-CR modified succinylated cellulose (**U1**) in CDCl$_3$.

Figure 32: SEC traces of succinylated cellulose (SFP) and Ugi 4-CR modified cellulose (**U1, U2, U3**) measurement relative to poly(methyl methacrylate) calibration in DMAc-LiBr (1% w/w).

Figure 33: TGA of filter paper cellulose (FP) compared to Ugi 4-CR modified cellulose (**U1, U2, U3**).

Figure 34: DSC data (2nd heating cycle) of succinylated filter paper cellulose (SFP) compared to Ugi 4-CR modified cellulose (**U1, U2, U3**).

Figure 35: Conversion of butanol over time observed via GC-MS (1.84 M, 1 eq. isobutyraldehyde, 1 eq. *tert*-butylisocyanide, 10 bar CO$_2$, 48 h at room temperature).

Figure 36: Relative percentage of the formed compounds (P-4CR, P-3CR and hydrolysis of P-4CR products, compare **Scheme 27**) over time (results obtained from GC). Reaction conditions: one   equivalent each of butanol, isobutyraldehyde and *tert*-butylisocyanide at 10 bar CO_2 in DCM (1.84 M) at room temperature.

Figure 37: ^{1}H NMR verification of the Lewis behaviour of isocyanide, ^{1}H ($CDCl_3$) NMR comparison between butanol (**a**), butanol and *tert*-butylisocyanide (**b**), butanol and triethylamine (**c**).

Figure 38: Structures of the synthesized P-4CR products including their conversion and isolated yields.

Figure 39: ATR-IR spectrum of P-4CR product **11a.**

Figure 40: ^{1}H NMR (top) and ^{13}C NMR (bottom) of P-4CR **11a**, measured in $CDCl_3$.

Figure 41: Structures and isolated yields of the P-4CR hydrolysis products.

Figure 42: ATR-IR C=O absorbance at 1665cm^{-1} during stability study of *in-situ* carbonate of octanol with temperature using DBU, MTBD and TMG as super bases (conditions: 20 bar of CO_2, 30 °C)

Figure 43: ATR-IR C=O absorbance at 1665 cm^{-1} during cellulose (3 wt.%) solubilization with DBU as super base and 10 bar CO_2 at different temperatures observed over time

Figure 44: ATR-IR C=O absorbance at 1665 cm^{-1} during cellulose (3 wt.%) solubilization with DBU as super base and 20 bar CO_2 at different temperatures observed over time

Figure 45: ATR-IR C=O absorbance at 1665 cm^{-1} during cellulose (3 wt.%) solubilization with DBU as super base and 40 bar CO_2 at different temperatures observed over time.

Figure 46: ATR-IR C=O absorbance at 1665 cm^{-1} during cellulose (3 wt.%) solubilization with DBU as super base at 40 °C and different CO_2 pressures (in bar) observed over time.

Figure 47: ATR-IR C=O absorbance at 1665 cm^{-1} during cellulose (3 wt.%) solubilization with DBU as super base at 50 °C and different CO_2 pressures (in bar) observed over time.

Figure 48: ATR-IR C=O absorbance at 1665 cm^{-1} during cellulose (3 wt.%) solubilization with DBU as super base at 60 °C and different CO_2 pressures (in bar) observed over time.

Figure 49: ATR-IR C=O absorbance at 1665 cm^{-1} during variation in cellulose concentration using DBU as super base after 20 bar of CO_2 applied for 15 minutes at various temperatures (30, 35, 40, 50, 60 °C).

Figure 50: ATR-IR C=O absorbance at 1665 cm^{-1} during variation in octanol concentration using DBU as super base after 20 bar of CO_2 applied for 15 minutes at 30 °C.

Figure 51: Viscosity measurement comparison between octanol and cellulose in DBU-DMSO-CO_2 solvent at concentration of 30 mg/mL.

Figure 52: ATR-IR of octyl-benzyl-carbonate

Figure 53: ^{1}H (top) and ^{13}C (bottom) NMR of octyl-benzyl-carbonate.

Figure 54: ^{31}P NMR of cellulose- benzyl-carbonate for DS determination.

Figure 55: ^{1}H (top) and ^{13}C (bottom) NMR of cellulose- methyl-carbonate measured in DMSO (d$_6$) at 80 °C.

Figure 56: Effect of coagulating solvent on the apparent density of cellulose aerogel using 5 wt.% MC and DBU as a super base.

Figure 57: Effect of the super base on the apparent density of cellulose aerogel using 5 wt.% MCC and methanol coagulation.

Figure 58: SEM image of cellulose aerogel from freeze-drying (using 7 wt.% MCC, DBU as a super base and water coagulation.

Figure 59: SEM image of cellulose aerogel from freeze-drying (using 10 wt.% MCC, DBU as super base and water coagulation.

Figure 60: SEM image of cellulose aerogel from freeze-drying (using 5 wt.% MCC, DBU as super base and methanol coagulation.

Figure 61: SEM image of cellulose aerogel from freeze-drying (using 7 wt.% MCC, DBU as super base and methanol coagulation.

Figure 62: SEM image of cellulose aerogel from freeze-drying (using 10 wt.% MCC, DBU as super base and methanol coagulation.

Figure 63: SEM image of cellulose aerogel from freeze-drying (using 5 wt.% MCC, DBU as super base and ethanol coagulation.

Figure 64: SEM image of cellulose aerogel from freeze-drying (using 5 wt.% MCC, DBU as super base and isopropanol coagulation.

Figure 65: SEM image of cellulose aerogel from freeze-drying (using 5 wt.% MCC, TMG as super base and methanol coagulation.

Figure 66: SEM image of cellulose aerogel from freeze-drying (using 5 wt.% MCC, DBN as super base and methanol coagulation.

Figure 67: SEM image of cellulose aerogel from freeze-drying (using 3 wt.% CP, DBU as super base and water coagulation.

Figure 68: SEM image of cellulose aerogel from freeze-drying (using 3 wt.% CP, DBU as super base and ethanol coagulation.

Figure 69: Effect of coagulating solvent on the pore size of cellulose aerogel using 5 wt.% MCC and DBU as a super base.

Figure 70: Effect of cellulose type and coagulating solvent on the pore size of cellulose aerogel using DBU as a super base.

Figure 71: Effect of the super base on the pore size of cellulose aerogel using 5 wt.% MCC and methanol coagulation.

Figure 72: ATR-IR spectra comparison between MCC and cellulose aerogel from freeze-drying (using 5 wt.% MCC, DBU as super base and methanol coagulation.

Figure 73: ATR-IR spectra comparison between pure and recovered DBU (using 5 wt.% MCC, DBU as super base and methanol coagulation).

Figure 74: ATR-IR spectra comparison between pure and recovered DMSO (using 5 wt.% MCC, DBU as super base and methanol coagulation).

Figure 75: ATR-IR spectra of fatty acid cellulose esters (FACEs) at various reaction time: MCC-1d (6 h), MCC-1e (12 h), MCC-1c (24 h), MCC-1f (48 h). (5 wt.% MCC, 3 eq. high oleic sunflower oil/AGU cellulose, 115 °C).

Figure 76: ATR-IR spectra of fatty acid cellulose esters (FACEs) at various reaction temperature: MCC- 1g (90 °C), MCC-1h (100 °C), MCC-1c (115 °C). (5 wt.% MCC, 3eq. high oleic sunflower oil/AGU cellulose, 24 h).

Figure 77: ATR-IR spectra of fatty acid cellulose esters (FACEs) at various high oleic sunflower oil equivalents: MCC-1i (1.5 eq./AGU), MCC-1c (3 eq./AGU), MCC-1j (6 eq./AGU). (5 wt.% MCC, 115 °C, 24 h).

Figure 78: ^{31}P NMR (CDCl$_3$), 400 MHz, 1024 scans: determination of degree of substitution (DS) of fatty acid cellulose ester (MCC-1d). (5 wt.% MCC, 3 eq. high oleic sunflower oil/AGU, 115 °C, 6 h).

Figure 79: ^{31}P NMR (CDCl$_3$), 400 MHz, 1024 scans: determination of degree of substitution (DS) of fatty acid cellulose ester (MCC-1e). (5 wt.% MCC, 3 eq. high oleic sunflower oil/AGU, 115 °C, 12 h).

Figure 80: ^{31}P NMR (CDCl$_3$), 400 MHz, 1024 scans: determination of degree of substitution (DS) of fatty acid cellulose ester (MCC-1c). (5 wt.% MCC, 3 eq. high oleic sunflower oil/AGU, 115 °C, 24 h).

Figure 81: ^{31}P NMR (CDCl$_3$), 400 MHz, 1024 scans: determination of degree of substitution (DS) of fatty acid cellulose ester (MCC-1f). (5 wt.% MCC, 3 eq. high oleic sunflower oil/AGU, 115 °C, 48 h).

Figure 82: ^{31}P NMR (CDCl$_3$), 400 MHz, 1024 scans: determination of DS of fatty acid cellulose ester (MCC-1i). (5 wt. (%) MCC, 1.5 eq. high oleic sunflower oil/AGU, 115 °C, 24 h.

Figure 83: ATR-IR spectra of fatty acid cellulose esters (FACEs) at various high oleic sunflower oil equivalents: FP-1a (1.5 eq./AGU), FP-1b (3 eq./AGU, 5 wt.% FP, 115 °C, 24 h).

Figure 84: ATR-IR spectra of fatty acid cellulose esters (FACEs) at various high oleic sunflower oil equivalents: CP-1a (1.5 eq./AGU), CP-1b (3 eq./AGU, 5 wt.% CP, 115 °C, 24 h).

Figure 85: ^{1}H NMR (top, 400 MHz, 1024 scans at 50 °C) and ^{13}C NMR (bottom, 100 MHz, 6000 scans at 50 °C) for fatty acid cellulose esters (FACE): MCC-1c. (5 wt.%, MCC, 3 eq. high oleic sunflower oil/AGU, 115 °C, 24 h, measured in THF, d$_8$.

Figure 86: ^{1}H NMR (top, 400 MHz, 1024 scans at 50 °C) and ^{13}C NMR (bottom, 100 MHz, 6000 scans at 50 °C) for fatty acid cellulose esters (FACE): FP-1b. (5 wt.% FP, 3 eq. high oleic sunflower oil/AGU, 115 °C, 24 h, measured in THF, d$_8$.

Figure 87: ^1H NMR (top, 400 MHz, 1024 scans at 50 °C) and ^{13}C NMR (bottom, 100 MHz, 6000 scans at 50 °C) for fatty acid cellulose esters (FACE): CP-1b. (5 wt.% CP, 3 eq. high oleic sunflower oil/AGU, 115 °C, 24 h, measured in THF, d_8.

Figure 88: ^{31}P NMR ($CDCl_3$), 400 MHz, 1024 scans :determination of degree of substitution (DS) of fatty acid cellulose esters (FACE): FP-1a. (5 wt.% FP, 1.5 eq. high oleic sunflower oil/AGU, 115 °C, 24 h).

Figure 89: ^{31}P NMR ($CDCl_3$), 400 MHz, 1024 scans: determination of degree of substitution (DS) of fatty acid cellulose esters (FACE): FP-1b. (5 wt.% FP, 3 eq. high oleic sunflower oil/AGU, 115 °C, 24 h).

Figure 90: ^{31}P NMR ($CDCl_3$), 400 MHz, 1024 scans: determination of degree of substitution (DS) of fatty acid cellulose esters (FACE): CP-1a. (5 wt.% CP, 1.5 eq. high oleic sunflower oil/AGU, 115 °C, 24 h).

Figure 91: ^{31}P NMR ($CDCl_3$), 400 MHz, 1024 scans :determination of degree of substitution (DS) of fatty acid cellulose esters (FACE): CP-1b. (5 wt.% CP, 3 eq. high oleic sunflower oil/AGU, 115 °C, 24 h).

Figure 92: SEC traces (DMAc-LiBr) comparison of fatty acid cellulose esters (FACEs) from microcrystalline cellulose (MCC-1i; DS 1.06), cellulose filter paper (FP-1a; DS 1.02) and cellulose pulp (CP-1a; DS 1.08).

Figure 93: X-ray diffraction pattern of FP and resulting fatty acid cellulose esters (FACEs) (FP-1a, FP -1b) (5 wt.% FP, 24 h,115 °C).

Figure 94: X-ray diffraction pattern of CP and resulting fatty acid cellulose esters (FACEs) (CP-1a, CP-1b) (5 wt.% CP, 24 h, 115 °C).

Figure 95: Thermogravimetric analysis (TGA) of FP and resulting fatty acid cellulose esters (FACEs) (FP-1a, FP-1b) (5 wt.% FP, 24 h, 115 °C).

Figure 96: Thermogravimetric analysis (TGA) of CP and resulting fatty acid cellulose esters (FACEs) (CP-1a, CP-1b) (5 wt.% CP, 24 h, 115 °C).

Figure 97: ATR-IR spectra Ugi 4-CR modified succinylated cellulose (**U1**).

Figure 98: ATR-IR spectra Ugi 4-CR modified succinylated cellulose (**U2**).

Figure 99: ATR-IR spectra Ugi 4-CR modified succinylated cellulose (**U3**).

Figure 100: ^1H NMR (top) and ^{13}CN NMR (bottom) of Ugi 4-CR modified succinylated cellulose (**U2**) in THF(d_8).

Figure 101: ^1H NMR (top) and ^{13}C NMR (bottom) of Ugi 4-CR modified succinylated cellulose (**U3**) in THF(d_8).

Figure 102: ^{31}P NMR of Ugi 4-CR modified succinylated cellulose (**U2**) in $CDCl_3$.

Figure 103: ^{31}P NMR of Ugi 4-CR modified succinylated cellulose **(U3)** in $CDCl_3$.

Figure 104: Effect of solvent on the relative percentage between P-4CR, P-3CR and hydrolysis products (1.84 M, 2 eq. isobutyraldehyde, 2 eq. *tert*-butylisocyanide, 10 bar CO_2, 24 h at room   temperature). Values obtained through GC measurement using tetradecane as internal standard.

Figure 105: Results obtained by GC of: **a**). Influence of catalyst (10 mol.% Et$_3$N) on the conversion of butanol over time compared to the reaction without any catalyst (conditions: 3.68 M in DCM, 2 eq. isobutyraldehyde, 2 eq. *tert*-butylisocyanide, 10 bar CO$_2$, 45-48 h at room temperature). **b**). Relative percentage of respective products (P-4CR, P-3CR and hydrolysis of P-4CR) for the reaction performed without catalyst. **c**). Relative percentage of respective products (P-4CR, P-3CR and hydrolysis of P-4CR) for the reaction performed with 10 mol.% Et$_3$N as catalyst. (b and c; values are obtained after normalization using tetradecane).

Figure 106: Comparison between Et$_3$N and DBU as catalyst on the relative percentage between P-4CR, P-3CR and hydrolysis products (1.84 M, 2 eq. isobutyraldehyde, 2 eq. *tert*-butylisocyanide, 10 bar CO$_2$, 24 h at room temperature). Values obtained through GC measurement with tetradecane as internal standard.

Figure 107: Effect of catalyst concentration using Et$_3$N on the relative percentage between P-4CR, P-3CR and hydrolysis products (1.84 M, 2 eq. isobutyraldehyde, 2 eq. *tert*-butylisocyanide,10 bar CO$_2$, 24 h at room temperature). Values obtained through GC measurement with tetradecane as internal standard.

Figure 108: Effect of CO$_2$ pressure on the relative percentage between P-4CR, P-3CR and hydrolysis products (10 mol.% triethylamine, 1.84 M, 2 eq. isobutyraldehyde, 2 eq. *tert*-butylisocyanide, 10 bar CO$_2$, 24 h at room temperature). Values obtained through GC measurement with tetradecane as internal standard.

Figure 109: ^{1}H (top) and ^{13}C NMR (bottom) of P-4CR **11a**, measured in CDCl$_3$.

Figure 110: ^{1}H (top) and ^{13}C NMR (bottom) of P-4CR **11b**, measured in CDCl$_3$.

Figure 111: ^{1}H (top) and ^{13}C NMR (bottom) of P-4CR **11c**, measured in CDCl$_3$.

Figure 112: ^{1}H (top) and ^{13}C NMR (bottom) of P-4CR **12a**, measured in CDCl$_3$.

Figure 113: ^{1}H (top) and ^{13}C NMR (bottom) of P-4CR **13a**, measured in CDCl$_3$.

Figure 114: ^{1}H (top) and ^{13}C NMR (bottom) of P-4CR **14a**, measured in CDCl$_3$.

Figure 115: ^{1}H (top) and ^{13}C NMR (bottom) of P-4CR **15a**, measured in CDCl$_3$.

Figure 116: ^{1}H (top) and ^{13}C NMR (bottom) of P-4CR **16a**, measured in CDCl$_3$.

Figure 117: ^{1}H (top) and ^{13}C NMR (bottom) of P-4CR **17a**, measured in CDCl$_3$.

Figure 118: ^{1}H (top) and ^{13}C NMR (bottom) of P-4CR **18a**, measured in CDCl$_3$.

Figure 119: ^{1}H (top) and ^{13}C NMR (bottom) of P-4CR **19a**, measured in CDCl$_3$.

Figure 120: ^{1}H (top) and ^{13}C NMR (bottom) of P-4CR **20a**, measured in CDCl$_3$.

Figure 121: ^{1}H (top) and ^{13}C NMR (bottom) of the hydrolysis product **11c**, measured in CDCl$_3$.

Figure 122: ^{1}H (top) and ^{13}C NMR (bottom) of the hydrolysis product **13a**, measured in CDCl$_3$.

Figure 123: ^{1}H (top) and ^{13}C NMR (bottom) of the hydrolysis product **19a**, measured in CDCl$_3$.

9.4 List of Schemes

Scheme 1: Photosynthesis reaction

Scheme 2: Structure of cellulose

Scheme 3: Interconversion between different allomorphs of cellulose crystal structures, adapted from O'Sullivan.[51]

Scheme 4: *Intra-* and *inter-* molecular hydrogen bonding in cellulose I structure. O3-H···O5 intramolecular (purple), O-H2···O6-H intramolecular (red) and H-O2···H6-O intermolecular (green) hydrogen bonds.

Scheme 5: Cellulose derivatives *via* homogeneous modification in ionic liquids or CO_2 switchable solvent systems.

Scheme 6: Concept of a distillable ionic liquid from TMG and propanoic acid, adapted from Kilpeläinen *et al.*[145]

Scheme 7: Derivative (top) and non-derivative (bottom) approach of CO_2 switchable solvent system, adapted from Jerome *et al.*[154] and Xie *et al.*[155]

Scheme 8: Design approach towards sustainable cellulose modification

Scheme 9: Strecker synthesis of α-amino nitriles.[191]

Scheme 10: Hantzsch synthesis of 1,4 dihydropyridine (DHP).[215]

Scheme 11: The Biginelli synthesis of 3,4-dihydropyrimidin-2-(1H)-one (DHPM).[219]

Scheme 12: Mannich synthesis of β-amino carbonyl compounds.[223]

Scheme 13: Resonance structures of isocyanide.

Scheme 14: Lieke route for isocyanide synthesis.[228]

Scheme 15: Hofmann route for isocyanide synthesis.[230]

Scheme 16: Ugi route for isocyanide synthesis.[231]

Scheme 17: General reaction scheme for the Passerini 3-CR.

Scheme 18: Generally accepted mechanism for Passerini 3-CR.[224,237,238]

Scheme 19: General reaction scheme for the Ugi 4-CR.

Scheme 20: Mechanism for the Ugi 4-CR.[225,239]

Scheme 22: General procedure for cellulose aerogels preparation from the DBU- CO_2 switchable solvent system.

Scheme 23: Cellulose solubilization in DBU-CO_2 switchable solvent system and subsequent transesterification using high oleic sunflower oil.

Scheme 24: General reaction scheme of Ugi 5-CR, adapted from Armstrong and Keating.[280]

Scheme 25: General reaction scheme for Ugi 5-CR on cellulose in DBU-CO_2 switchable solvent system.

Scheme 26: The general reaction scheme for Ugi 4-CR modification of succinylated cellulose.

Scheme 27: Formation of P-4CR products in the absence (**a**) and presence (**b**) of a base catalyst.   **c**) Hydrolysis of the P-4CR product. (see **Figure 38** for synthesized structures).

9.5 List of Tables

Table 1: Various biomass sources and composition for lignocellulose, adapted from Khalil *et al.*[35]

Table 2: Names and dissolution ability of frequently employed ionic liquids for cellulose solubilization.

Table 3: Comparison between various approaches for the synthesis of cellulose esters including estimated E-factors.

Table 4: Summary of the processing conditions and properties of cellulose aerogels from the CO_2 switchable solvent system.

Table 5: Control of degree of substitution (DS) of fatty acid cellulose esters with reaction time.

Table 6: SEC data, degree of substitution (DS) values, degradation temperature (T_d) and XRD data of fatty acid cellulose esters (FACEs).

Table 7: Thermal and mechanical characterization of fatty acid cellulose esters (FACEs) cast films.

Table 8: Reaction conditions, yield and conversion of Ugi 4-CR of succinylated cellulose.

Table 9: Elemental analysis of Ugi 4-CR modified succinylated cellulose products.

Table 10: Molecular weight and distribution data for succinylated cellulose (SFP) and Ugi-4CR modified succinylated cellulose.

Curriculum Vitae

Name	Kelechukwu Nnabuike ONWUKAMIKE
Date of birth	23.05.1988
Nationality	Nigerian

EDUCATION

02.2016-02.2019 Marie Sklodowska-Curie European Joint Doctoral in Functional Materials (EJD-FunMat).
Thesis Title: Sustainable Cellulose Solubilization, Regeneration and Derivatization in a DBU-CO_2 Switchable Solvent System.
Supervisors: Prof. M.A.R Meier (Karlsruhe Institute of Technology, Germany), Prof. H. Cramail, Prof. S. Grelier, Dr. E. Grau (University Bordeaux, France).

10.2013-06.2015 Erasmus Mundus MSc. in Functional Advanced Materials & Engineering (FAME).
Thesis Title: Synthesis of Amphiphilic Block Copolymer from Cellulose Oligomers *via* Click Reactions.
Supervisors: Dr. F. Peruch, Prof. S. Grelier, Dr. V. Coma, Dr. E. Billès (LCPO, University of Bordeaux, France).
Augsburg University Germany (Av. 1.6), University of Bordeaux France (Av. 15.5/20) mention *bien*.
Rank: Top 5%.

11.2007-12.2011 Bachelor of Technology (B.Tech) in Chemistry (Industrial Chemistry Option).
Federal University of Technology Owerri, Imo state, Nigeria
Grade: CGPA 4.65/5.0 (First Class Honours).

Rank: Best Graduating Student, Department of Chemistry and Faculty of Sciences.

WORK EXPERIENCE

02.2016-date	Marie Sklodowska-Curie Early Stage Researcher (ESR)-PhD Candidate.
	Research on developing Sustainable approaches for Cellulose derivatization, towards making processable Cellulose-based materials.
	Supervision of Organic Chemistry Practical (KIT).
	Supervision of Bachelor thesis and Internship (KIT, UBx)
02.2018-02.2018	Visiting researcher to Aalto University, Finland (two weeks). Investigating the Spinning of Cellulose pulp from DBU-CO_2 Switchable Solvent System, with *Prof. H. Sixta.*
10.2018-10.2018	Visiting researcher to University of Bayreuth, Germany (two weeks). Investigating the Electrospinning of Cellulose from the DBU-CO_2 Switchable Solvent System, with *Prof. A. Greiner*.
02.2015-06.2015	MSc. Research work on Synthesis of Block Copolymer from Cellulose Oligomers *via* Click Reactions, with *Dr. F. Peruch*.
02.2014-04.2014	Internship on Controlling the Surface Properties of Block Copolymers, with *Prof. G. Hadziioannou*.
04.2013-09.2013	Graduate Assistant (GA), Department of Chemistry, Federal University of Technology Owerri, Imo state, Nigeria. Responsible for organizing undergraduates tutorial lessons, Supervision of Organic Chemistry Practical and Bachelor thesis.
06.2010-12.2010	Intern, Soulmate Industries Nig. Ltd, Lagos state, Nigeria. Responsible for Quality Control during the production process.

SKILLS

1. Good team player, and excellent communication skills.
2. Analytical and critical thinking skills.
3. Expertise in Cellulose chemistry: solvents, derivatization and Cellulose-based material (fibres, aerogels, films) processing techniques.
4. Proficiency to work with high pressure CO_2.
5. Proficiency in various polymer characterization techniques (NMR, GPC, FT-IR, GC-MS, GC, SEM, DSC, TGA, SEM), Electrospinning and Tensile strength measurements.
6. Excellent skills in MS Word, Excel, PowerPoint.
7. Excellent skills in ChemDraw and Origin software.

AWARDS

1. Among 30 selected Marie-Sklodowska-Curie Researchers, for the FallingWall Lab, Brussels, Belgium (09.2018).
2. Poster Award (Second position), 22nd ACS Green Chemistry Conference, Portland, Oregon, USA (06.2018).
3. Best Oral Presentation Award (among 48 presentations), Young Scientist Symposium, Bordeaux, France (05.2018).
4. Marie-Sklodowska-Curie ITN Fellowship from the European Commission for Ph.D. studies (02.2016-01.2019).
5. IDX-LabEx Fellowship for Erasmus Mundus FAME MSc. Program (10.2013-06.2015).
6. Best Graduating Student Award, Department of Chemistry, Federal University of Technology, Owerri, Nigeria (12.2011).
7. Dean's Award for Best Graduating Student, Faculty of Sciences, Federal University of Technology, Owerri, Nigeria (12.2011).

SCIENTIFIC COMMUNICATION

Publications

1. K.N. Onwukamike, S. Grelier, E. Grau, H. Cramail, M.A.R Meier, Sustainable Approach for Cellulose Aerogel preparation from the DBU-CO_2 Solvent, *ACS Sustainable. Chem. Eng*, **2019**, 7(3), 3329.

2. K.N. Onwukamike, S. Grelier, E. Grau, H. Cramail, M.A.R Meier, Critical Review on Sustainable Homogeneous Cellulose Modification: Why Renewability is not enough, *ACS Sustainable. Chem. Eng*, **2019**, 7(2), 1826.

3. K.N. Onwukamike, S. Grelier, E. Grau, H. Cramail, M.A.R Meier, On the direct use of CO_2 in multicomponent reactions: Introducing the Passerini four component reaction, *RSC Advances*, 2018, 8, 31490.

4. K.N. Onwukamike, S. Grelier, E. Grau, H. Cramail, M.A.R Meier, Sustainable Transesterification of Cellulose with High oleic sunflower in a DBU-CO_2 Solvent, *ACS Sustainable. Chem. Eng*. 2018, 6, 7, 8826.

5. K.N. Onwukamike, T. Tassaing, S. Grelier, E. Grau, H. Cramail, M.A.R Meier, Detailed understanding of the DBU-CO_2 Switchable Solvent System for Cellulose Solubilization and Derivatization, *ACS Sustainable. Chem. Eng*. 2018, 6, 1, 1496.

6. Z. Söyler, K.N. Onwukamike, S. Grelier, E. Grau, H. Cramail, M. A.R. Meier, Sustainable Succinylation of Cellulose in a CO_2-based Switchable Solvent and Subsequent Passerini 3-CR and Ugi 4-CR modification, *Green Chem*. 2018, 20, 214.

7. E. Billès, K.N. Onwukamike, V. Coma, S. Grelier, F. Peruch, Cellulose Oligomers Production and Separation for the Synthesis of new fully Bio-based Amphiphilic Compounds, *Carbohydr. Polym.* 2016, 154, 121.

Oral presentations

1. K.N. Onwukamike, Breaking the walls of Unsustainable Fossil-based Resources. *MSCA-Researchers FallingWall Lab*, Brussels, Belgium (09. 2018).
    https://www.linkedin.com/feed/update/urn:li:activity:6452869354655617024

2. K.N. Onwukamike, S. Grelier, E. Grau, H. Cramail, M.A.R Meier, Sustainable Cellulose Solubilization, Derivatization and Regeneration in a DBU-CO_2 Solvent. *Biennial Meeting of the GDCh-Division of Macromolecular Chemistry*. Karlsruhe, Germany (09.2018).

3. K.N. Onwukamike, S. Grelier, E. Grau, H. Cramail, M.A.R Meier, Sustainable Cellulose Solubilization, Derivatization and Regeneration in a DBU-CO_2 solvent. *Bio-Environmental Polymer Society (BEPS) 25th annual meeting 2018*. Albany, New York, USA (08.2018).

4. K.N. Onwukamike, S. Grelier, E. Grau, H. Cramail, M.A.R Meier, Sustainable Cellulose Solubilization, Derivatization and Regeneration in a DBU-CO_2 solvent, *11th Edition of Young Scientist Symposium (YSS)*, Bordeaux, France (05.2018).

5. K.N. Onwukamike, S. Grelier, E. Grau, H. Cramail, M.A.R Meier, Sustainable Cellulose Solubilization and Derivatization in a DBU-CO_2 solvent, *20th Edition of the University of Bordeaux Doctoral School Day*, Bordeaux, France (04.2018).

6. K.N. Onwukamike, S. Grelier, E. Grau, H. Cramail, M.A.R Meier, Update on research progress on Sustainable Cellulose Solubilization and Derivatization in a DBU-CO_2 solvent, *Solvay, Laboratory of the Future (LOF)*. Bordeaux, France (04.2018).

7. K.N. Onwukamike, S. Grelier, E. Grau, H. Cramail, M.A.R Meier, Sustainable Cellulose Solubilization, Regeneration and Derivatization in a DBU-CO_2 Solvent, *EJD-FunMat 3rd Summer School*. Luxembourg (03.2018).

8. K.N. Onwukamike, S. Grelier, E. Grau, H. Cramail, M.A.R Meier, Update on research progress on Sustainable Cellulose Solubilization and Derivatization in a DBU-CO_2 solvent, *Solvay, Laboratory of the Future (LOF)*. Bordeaux, France (11.2017).

9. K.N. Onwukamike, P. Scholten, G. Chantereau, Developing an interface for promoting Sustainability through Science Communication*, EJD-FunMat Entrepreneurship Summer School*. Aveiro, Portugal (10.2017).

10. K.N. Onwukamike, T. Tassaing, S. Grelier, E. Grau, H. Cramail, M.A.R Meier, DBU-CO_2 as a Switchable Solvent for Cellulose Solubilization and Derivatization. *Bio-Environmental Polymer Society (BEPS) 24th annual meeting 2017*. Albany, California, USA (09.2017).

11. K.N. Onwukamike, S. Grelier, E. Grau, H. Cramail, M.A.R Meier, Sustainable Cellulose Regeneration and Derivatization, *2nd EJD-FunMat Summer School*. Aveiro, Portugal (03.2017).

12. K.N. Onwukamike, S. Grelier, E. Grau, H. Cramail, M.A.R Meier, Fundamental discussions on Ph.D. thesis topic, *1st EJD-FunMat Summer School*. Bordeaux, France (03.2016).

Poster presentations

1. K.N. Onwukamike, S. Grelier, E. Grau, H. Cramail, M.A.R Meier, Sustainable Cellulose Solubilization, Derivatization and Regeneration in a DBU-CO_2 solvent, *22nd ACS Green Chemistry conference*, Portland, Oregon, USA (06.2018).

2. K.N. Onwukamike, S. Grelier, E. Grau, H. Cramail, M.A.R Meier, Sustainable Cellulose Solubilization, Derivatization and Regeneration in a DBU-CO_2 solvent, Bordeaux Polymer Conference (BPC), Bordeaux, France (05.2018).

3. K.N. Onwukamike, T. Tassaing, S. Grelier, E. Grau, H. Cramail, M.A.R Meier, Study of CO_2 Switchable Solvent for Cellulose Solubilization, *5th EPNEO International Polysaccharide Conference*, Jena, Germany (08.2017).

4. Z. Söyler, K.N. Onwukamike, S. Grelier, E. Grau, H. Cramail, M.A.R Meier, CO_2-based Solvent for Sustainable Succinylation of Cellulose and Subsequent Passerini 3-CR and Ugi 4-CR modification, *Advanced Polymers via Macromolecular Engineering (APME)*, Ghent, Belgium (05.2017).

5. K.N. Onwukamike, S. Grelier, E. Grau, H. Cramail, M.A.R Meier, Cellulose Modification *via* the Ugi 5-CR in a DBU-CO_2 Switchable Solvent System, *19th Edition of the University of Bordeaux Doctoral School Day*, Bordeaux, France (04.2017).

6. K.N. Onwukamike, S. Grelier, E. Grau, H. Cramail, M.A.R Meier, Cellulose Modification *via* the Ugi 5-CR in a DBU-CO_2 Switchable Solvent System, *9th Workshop on Fats and Oils as Renewable Feedstocks for the Chemical Industry*, Karlsruhe, Germany (03.2017).

7. K.N. Onwukamike, S. Grelier, E. Grau, H. Cramail, M.A.R Meier, Cellulose Modification *via* the Ugi 5-CR in an ionic liquid. *Jahrestagung der Fachgruppe Nachhaltige Chemie (GDCh) 2016*, Karlsruhe, Germany (09.2016).